

X-RAY STRUCTURAL STUDIES OF SOME BIOLOGICALLY  
SIGNIFICANT MOLECULES

---

A Thesis presented in part fulfilment of the  
regulations for the award of the degree of

DOCTOR OF PHILOSOPHY

in the Faculty of Science, University of London.

by

FRANK HARMSWORTH ALLEN B.Sc. A.R.C.S.

Chemistry Department

Imperial College

London S.W.7.

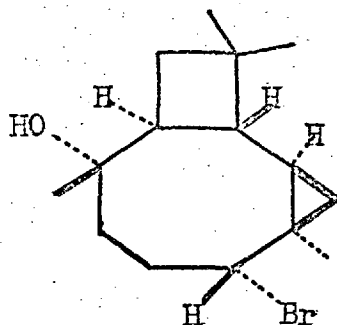
June 1968

Summary.

The crystal structures of derivatives of four biologically significant molecules have been determined using three-dimensional X-ray diffraction techniques, and the phase-determining heavy-atom method.

The structure of (+)-3-bromocamphor has been re-determined in order to establish unambiguously the absolute configuration of this key terpene. The assignment was made using the X-ray fluorescence technique, and its importance in the stereochemical correlation of the monoterpenes is discussed. The molecular geometry of the molecule is compared with data from other X-ray studies. In connection with this work a list has been prepared of organic molecules whose absolute configurations have been determined by X-ray methods, and the techniques involved have been reviewed.

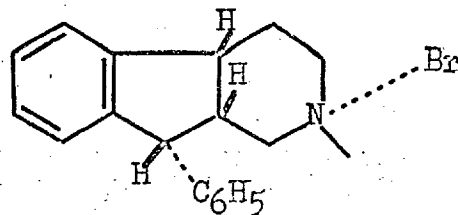
The monocyclic sesquiterpene humulene gives a tricyclic bromohydrin,  $C_{15}H_{25}OBr$ , which is monoclinic, space-group  $P2_1/n$ . The structure was elucidated using 1922 visually-estimated intensities, and refined to give a final  $R$  of 0.100. The proposed stereochemistry has been corrected to :



The geometry and conformation of the fused-ring system is discussed in some detail.

The biosynthetically important cyclodecatriene sesquiterpene germacatriene has recently been synthesized. The structure of the 1:1 adduct with silver nitrate,  $C_{15}H_{24}:AgNO_3$ , has been determined from visually-estimated intensity data, and refined to  $R = 0.097$ . The all-trans stereochemistry has been confirmed. The structure consists of chains of  $Ag^+$  ions and germacatriene units parallel to a, cross-linked by chains of  $Ag^+$  and  $NO_3^-$  ions parallel to b. The differences in reactivity between the double bonds is explained in terms of their torsional strain energies.

The synthetic pharmaceutical 2,3,4,4a,9,9a-hexahydro-2-methyl-9-phenyl-1H-indeno [2,1-c]pyridine, a possible anti-depressant, has been studied as the hydrobromide  $C_{19}H_{22}NBr$ . A Siemens automatic single-crystal diffractometer was used to collect the intensity data, which was absorption corrected. The final R-factor was 0.035. The all-cis stereochemistry :



was confirmed. The accuracy of the diffractometer experiment, and the geometry of the fused-ring system, are discussed.

A novel computer procedure, utilizing a 'bonding array', for the calculation of the geometrical characteristics of a molecule, is described.



### Acknowledgements.

I should like to thank Professor D. Rogers for his excellent supervision, and for the interest he has shown in this work; his enthusiasm is somewhat contagious. I should also like to thank Dr. J. K. Sutherland for much useful chemical discussion. The crystals were prepared by Dr. J.E. Baldwin, Dr. M. D. Solomon, Mr. E. D. Brown and Dr. P.R. Leeming, all of whom are thanked for their interest and help. Dr Leeming and his colleagues at Pfizer (U.K.) Ltd, Sandwich, Kent, are thanked for their generous hospitality.

I am indebted to other members of the Chemical Crystallography Laboratory, Imperial College, for their interest, and for useful discussion (not necessarily scientific); especially Drs Dave Hunt, Mike Drew, and Mick Hursthouse for initial day-to-day guidance during my first year, Peter Troughton for his help with the diffractometer experiment, Stephen Neidle, who collaborated in the preparation of the second absolute configuration list, and to Tom Keve, who has aided certain studies on the dynamics of a ping-pong ball. I am also indebted to those inmates of the structure factory not mentioned above, and to numerous other friends (especially Fred, Steve, Tony and Brian), for making the past six years at Imperial College a stimulating and wholly worthwhile

experience.

I should like to thank the staffs of both the University of London Institute of Computer Science, and the Imperial College Computer Unit, for carrying out the extensive calculations.

The Science Research Council is thanked for financial support in the form of a Research Studentship, during the tenure of which this work was performed.

I should like to express my sincere gratitude to my parents for their encouragement and help; to my wife, who has been wonderful throughout; and to our son Ashley, who arrived in the middle of chapter 7, and has given considerable vocal support.

" Fortunately science, like that nature to which it belongs, is neither limited by time nor by space. It belongs to the world, and is of no country and of no age. The more we know, the more we feel our ignorance; and in philosophy..  
..... there are always new worlds to conquer!

Sir Humphrey Davy 1825.

dedicated

to

the memory of my late father.

Contents.

<u>Chapter 1</u>	<u>Crystal Structure Analysis : An Historical</u>	
	<u>Introduction</u> . . . . .	12
1.1	Early Studies of the Crystalline State . . .	12
1.2	Developments in Physics . . . . .	17
1.3	The Diffraction of X-rays by a Crystal . . .	20
1.4	The Reciprocal Lattice and The Sphere of Reflection . . . . .	23
<u>Chapter 2</u>	<u>The Phase Problem and Some Methods of</u>	
	<u>Solution</u> . . . . .	26
2.1	Intensity Data and Their Correction . . .	26
2.2	The Phase Problem . . . . .	31
2.3	Patterson's Function and the Heavy-Atom Method . . . . .	32
2.4	The Refinement of Atomic Parameters : The Least-Squares Method . . . . .	40
<u>Chapter 3</u>	<u>Molecular Asymmetry : The Determination of</u>	
	<u>Absolute Configurations by X-rays</u> . . . . .	44
3.1	Normal Scattering : Friedel's Law . . . . .	46
3.2	Anomalous Scattering : The Bijvoet Technique	47
3.3	Some Extensions : Anomalous Dispersion Phasing and Hamilton's Method . . . . .	53

3.4	The Method of Internal Comparison . . . . .	55
3.5	Conclusion . . . . .	57
<u>Chapter 4</u>	<u>Data Collection and Treatment : Computer</u>	
	<u>Programs Used . . . . .</u>	58
4.1	Data Collection . . . . .	58
4.2	Data Treatment : Computer Programs Used . .	59
<u>Chapter 5</u>	<u>The Terpenes and Terpenoid Biosynthesis . .</u>	67
5.1	The Isoprene Rule . . . . .	67
5.2	The Basic Steps in Terpenoid Biosynthesis .	69
5.3	The Chemistry of (+)-camphor . . . . .	75
5.4	The Chemistry of Humulene . . . . .	80
5.5	The Chemistry of Germacatriene . . . . .	83
5.6	Note on Numbering Schemes . . . . .	87
<u>Chapter 6</u>	<u>The Absolute Configuration of (+)-Camphor :</u>	
	<u>The Crystal and Molecular Structure of</u>	
	<u>(+)-3-bromocamphor . . . . .</u>	88
6.1	Introduction . . . . .	88
6.2	Data Collection . . . . .	92
6.3	Two-Dimensional Work . . . . .	94
6.4	The Refinement of The Structure . . . . .	96
6.5	The Absolute Configuration of (+)-3bromo- camphor . . . . .	109
6.6	Discussion of the Absolute Configuration .	112
6.7	Discussion of the Structure . . . . .	119

<u>Chapter 7</u>	<u>The Crystal and Molecular Structure of</u>	
	<u>Humulene Bromohydrin : C<sub>15</sub>H<sub>25</sub>OBr</u>	129
7.1	Preliminary Work	129
7.2	Structure Solution	131
7.3	Refinement of the Structure	133
7.4	Discussion of the Structure	149
<u>Chapter 8</u>	<u>The Crystal and Molecular Structure of the</u>	
	<u>1:1 Adduct of Germacatriene with Silver</u>	
	<u>Nitrate : C<sub>15</sub>H<sub>24</sub>:AgNO<sub>3</sub></u>	173
8.1	Preliminary Work	173
8.2	Structure Solution	176
8.3	Refinement of the Structure	179
8.4	Discussion of the Structure	191
8.5	The Geometry about the Double Bonds and its Effect on their Reactivity	212
<u>Chapter 9</u>	<u>The Crystal and Molecular Structure of</u>	
	<u>2,3,4,4a,9,9a-hexahydro-2-methyl-9-phenyl-</u>	
	<u>1H-indeno [2,1-c] pyridine hydrobromide</u>	229
9.1	Chemical Introduction	229
9.2	Preliminary X-ray Studies	231
9.3	Experimental : The Siemens Automatic Single- Crystal Diffractometer	235
9.4	Structure Solution and Refinement	247
9.5	Discussion	275

<u>Appendix I</u>	<u>Reference Lists of Organic Structures</u> <u>whose Absolute Configurations have been</u> <u>determined by X-ray Methods . . . . .</u>	296
	(Reprinted from Chemical Communications)	
<u>Appendix II</u>	<u>The Uses of a 'Connectivity' or 'Bonding</u> <u>Array' in Molecular Geometry Calculations.</u>	297
II.1	Introduction . . . . .	297
II.2	The Connectivity or Bonding Array . . .	298
II.3	The Systematic Calculation of Bond Lengths Valence Angles, and Direction Cosines. .	302
II.4	The Systematic Calculation of Dihedral (Torsion) Angles . . . . .	304
II.5	The Program MOJO . . . . .	310
II.6	Further Uses of Bonding Array Theory . .	314
<u>Appendix III</u>	<u>Minimum-Energy Calculations . . . . .</u>	317
<u>References</u>	. . . . .	321

## CHAPTER 1.

### Crystal Structure Analysis : An Historical Introduction

Robert Bunsen is reported to have said : "Ein Chemiker, der kein Physiker ist, ist gar nichts"; in the present context this could be aptly 'translated' : "A Crystallographer who is not a Physicist, Mathematician, Chemist, Geologist, or even Artist, is worthless". It is the purpose of this chapter to amplify this plagiary by indicating briefly, and chronologically, the theories and observations from various disciplines which have become coalesced into the theoretical background of the science of crystal structure analysis.

#### 1.1. Early Studies of the Crystalline State.

Crystalline compounds have attracted man's attention since very early times, due to the beautiful facets and light effects exhibited by certain naturally occurring minerals, prized today as gemstones. The treatises of



the Alexandrian Greeks of ca. 250 A.D. contain the first references to practical topics, among them crystallization. The alchemists also knew these techniques, but it was not until the Renaissance brought the learning of the 'Old World' to the 'New' that further progress was made.

Speculation concerning the internal structure of crystals arose from the introduction of the microscope to scientific research by Malpighi (1628-94) and Leuwenhoek (1632-1723). In his 'Micrographia' (1667) Hooke explained their outward regularity as a consequence of the regular stacking of spheres (1). During his work on calcite and its effect on light, Huygens (1629-95) concluded that these spheres could be distorted into 'spheroids', and could be packed in a variety of ways (2). This was, no doubt, an analogy drawn from his explanation of the polarization of light.

Towards the end of the 18th century the Abbe René Haüy proposed (3) that crystals were composed of small cubic blocks, different stacking patterns accounting for observed morphological differences. Studies using the goniometer developed by Wollaston in 1809, put the 'Law of Constancy of Interfacial Angles', first proposed in 1669 by Steno (4), on a firm foundation. Haüy deduced that, if a compound crystallized with constant interfacial

angles, then the structure must consist of stacks of equidistant parallel planes, set at differing angles to each other. Further, each cube centre on his initial hypothesis may be regarded as a point on a lattice, which we may define as an abstraction of points, each having an exactly identical environment in parallel orientation in three dimensions.

W. H. Miller popularized these ideas in his book of 1839 <sup>(5)</sup>, in which he also introduced the term 'unitcell' to define the smallest indivisible unit of structure. His index notation for sets of lattice planes is based on three cell axes,  $\underline{a}$ ,  $\underline{b}$ ,  $\underline{c}$ , not necessarily orthogonal, but forming a right handed set, with interaxial angles  $\alpha$ ,  $\beta$ ,  $\gamma$ . If the zero'th plane of any stack passes through the origin, then the first plane makes intercepts  $\underline{a}/h$ ,  $\underline{b}/k$ ,  $\underline{c}/l$ , on the axes. The reciprocals of these intercepts, taken as multiples of  $1/\underline{a}$ ,  $1/\underline{b}$ ,  $1/\underline{c}$ , are  $h$ ,  $k$ ,  $l$ , the crystal plane indices. Intercepts on the negative directions of the axes are denoted  $\bar{h}$ ,  $\bar{k}$ ,  $\bar{l}$ .

The study of external morphology indicated that most crystals exhibited symmetry due to one or more of the following basic operations :

- i) centre of symmetry (inversion centre,  $\bar{1}$ )
- ii) axes of rotation (1-, 2-, 3-, 4-, or 6-fold)
- iii) mirror planes (m).

Two important propositions arise from this :

i) all crystals belong to one of seven systems, each displaying certain basic symmetry (see Table 1.1).

ii) there are 32 mathematically possible ways of combining symmetry operations acting through a point, these point groups or classes are distributed through the seven systems, each having the basic symmetry of that system, but some having higher symmetry. The class of highest symmetry in any system is designated holosymmetric. The classes are listed in Table 1.1.

In 1848 Bravais <sup>(6)</sup> deduced the 14 possible lattice types, distributed among the seven systems. The classification is based on the number of lattice points per cell, one denoting a primitive cell (P), and two or more denoting single-face-, body- or all-face-centred cells, (C, I, F). The rhombohedral type (R) is treated as trigonal (Table 1.1).

By 1860 it was obvious that the unitcell must be made up of molecules arranged according to symmetry operations acting throughout three dimensional space. In this case operations involving translation components must be considered :

i) screw axes,  $n_x$  : a rotation of  $2\pi/n$ , followed by a translation, parallel to the axis, of  $x/n$ .

ii) glide planes, reflection through a plane, followed by a translation parallel to it.

The complete mathematical analysis of the possible combinations of symmetry elements acting in three dimensions was

System.	Unitcell.	Bravais Lattices.	Crystal Classes.	Laue Symmetry.
(1) TRICLINIC.	$a \neq b \neq c,$ $\alpha \neq \beta \neq \gamma \neq 90^\circ$	P.	1, $\bar{1}$ .*	$\bar{1}$
(2) MONOCLINIC.	$a \neq b \neq c,$ $\alpha = \gamma = 90^\circ \neq \beta$	P, C.	2, m, $2/m$ .*	2/m
(3) ORTHORHOMBIC.	$a \neq b \neq c,$ $\alpha = \beta = \gamma = 90^\circ$	P, C, I, F.	222, mm2, mmm.*	mmm
(4) TETRAGONAL.	$a = b \neq c,$ $\alpha = \beta = \gamma = 90^\circ$	P, I.	a) 4, $\bar{4}$ , $4/m$ .* b) $4mm$ , $\bar{4}2m$ , $422$ , $4/mmm$ .*	$4/m$ $4/mmm$
(5) HEXAGONAL.	$a = b \neq c,$ $\alpha = \beta = 90^\circ; \gamma = 120^\circ$	P.	a) 6, $\bar{6}$ , $6/m$ .* b) $6mm$ , $\bar{6}m2$ , $622$ , $6/mmm$ .*	$6/m$ $6/mmm$
(6) TRIGONAL; (RHOMBOHEDRAL)	As (5) $(a = b = c,$ $\alpha = \beta = \gamma \neq 90^\circ)$	As (5) R.	a) 3, $\bar{3}$ .* b) $3m$ , $32$ , $\bar{3}m$ .*	$\bar{3}$ $\bar{3}m$
(7) CUBIC.	$a = b = c,$ $\alpha = \beta = \gamma = 90^\circ.$	P, I, F.	a) 23, $m\bar{3}$ .* b) $432$ , $\bar{4}3m$ , $m\bar{3}m$ .*	$m\bar{3}$ $m\bar{3}m$

TABLE 1.1. Subdivisions of the Seven Crystal Systems. (Holosymmetric Classes are marked \*)

completed, and simultaneously published, by three workers, Fedorov (7), Barlow (8), and Schoenflies (9). They all deduced the number of possible unique space-groups to be 230.

### 1.2. Developments in Physics.

The experimental method that was to prove and utilize the foregoing theories was introduced in Munich in 1912. This development was facilitated by the discovery of X-rays by Roentgen, at Wurtzburg, in 1895, and by considerable progress in the theory of wave motion, including diffraction. The latter phenomenon was first noted by Grimaldi (1613-63), and can be expressed in simple mathematical terms for monochromatic light of wavelength ( $\lambda$ ) incident upon a grating, with rulings of width (a) separated by a distance (b), as shown in Figure 1.1. Constructive interference of the diffracted wavelets can only occur when the path difference is a whole number (n) of wavelengths :

$$n\lambda = (a + b) \sin\theta \dots\dots\dots 1.1$$

where ( $\theta$ ) is the n'th order diffraction angle.

In 1912 Ewald presented his Thesis at Munich on : 'The Optical Properties of an Anisotropic Arrangement of Isotropic Resonators'. Von Laue seized upon an equation developed there, which showed the result of the superposition of all wavelets issuing from the resonators. He speculated on the

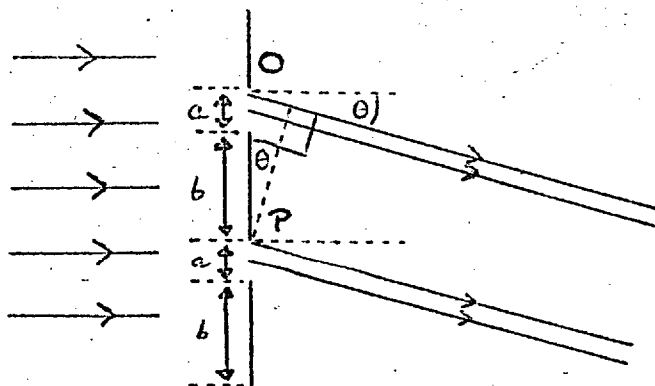


Figure 1.1 : Simple Diffraction Theory.

interaction of a very short wavelength radiation with a crystal lattice, which was thought to be such an arrangement. Sommerfeld <sup>(10)</sup> had estimated X-ray wavelengths to be of the order of  $10^{-8}$  cm. (  $1\text{\AA}$  ), and this radiation was chosen.

Working with Friedrich and Knipping, von Laue produced the first stationary-crystal X-ray diffraction photographs of  $\text{CuSO}_4$ ,  $\text{ZnS}$ ,  $\text{PbS}$ , and  $\text{NaCl}$ . The results were published together with an analysis of the diffraction theory pertinent to a three-dimensionally repeating unit. <sup>(11,12)</sup> Von Laue assumed that the pattern obtained was due to the diffraction of certain components of the polychromatic incident radiation, and refuted the idea that the observed

monochromaticity of the diffracted beam was due to a selective action by the crystal.

Late in 1912, W.L. Bragg deduced the first atomic crystal structure from Laue photographs of zinc blende. The paper (13) also contained three important conclusions :

- i) the 'Laue spots' could be explained by a reflection of the incident ray by the stacks of crystal planes;
- ii) if the incident beam was polychromatic, there was a selective action by the planes, reinforcing only those wavelengths which fitted their repeat distance;
- iii) the formulation of his Law concerning reflection from a stack of planes of spacing (d) :

$$n\lambda = 2d \sin\theta \quad \dots\dots\dots 1.2$$

similar to Eq. 1.1, where here :

$\theta$  is the glancing angle on the stack,

$\lambda$  is the wavelength 'selected',

and  $n$  is the order of reflection.

Using the X-ray spectrometer, developed with his father, Bragg deduced the alkali halide structures; many other determinations followed in the next decade.

It is interesting to note that the early structure determinations made minimal use of the elegant space-group theory mentioned above. Terada, working in Tokyo in 1913, was one of the first to realize its importance; but it was

not until Niggli <sup>(14)</sup> showed that the space-group could be determined from the systematic extinction of certain classes of diffracted spectra, that their determination became part of the routine preliminary study of crystals.

### 1.3. The Diffraction of X-Rays by a Crystal.

With reference to Fig. 1.1, we may note that if the phase of the wave scattered by point ( 0 ) is (  $\phi$  ), and that of the wave scattered by point ( P ) is (  $\phi + \psi$  ), then the phase of the wave scattered by the  $n$ 'th grating point from ( 0 ) is (  $\phi + n\psi$  ). Thus we may write the equation for the resultant wave from a one-dimensional grating of ( N ) similar scattering points as :

$$R = fe^{i\phi} \cdot \sum_{n=0}^{N-1} e^{in\psi} \dots\dots\dots 1.3$$

where ( f ) is the scattering power of each point.

Let us now consider a more general one-dimensional grating ( Figure 1.2 overleaf ). Each translation period ( a ) contains ( J ) points of differing scattering power (  $f_j$  ) at distances (  $X_j$  ) from the origin ( 0 ). Further, if we consider ( N ) such repeats, each of the ( J ) points is related to a similar point at distances :

$$X_j + a, X_j + 2a, \dots\dots X_j + ha, \dots$$

from the origin. We may represent the resultant wave



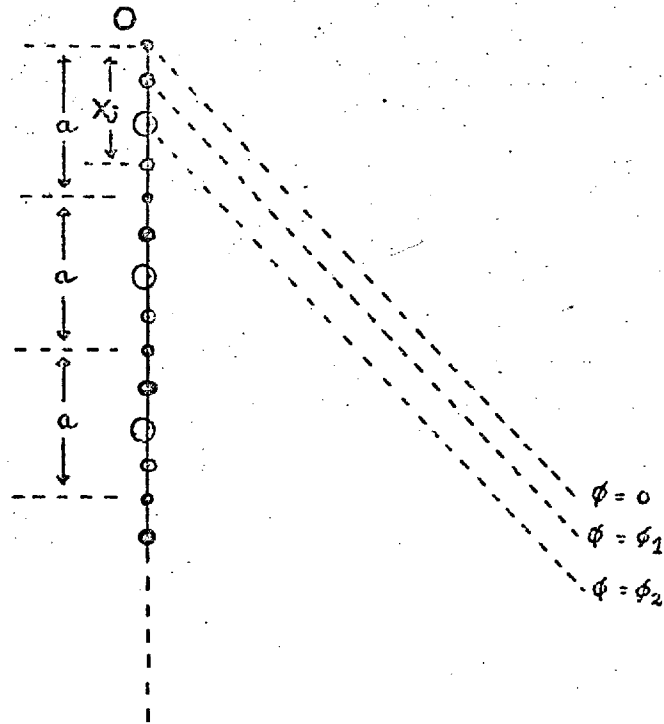


Figure 1.2 : A General One-Dimensional Grating.

from ( N ) repeats, by an equation analogous to 1.3 above :

$$R = ( f_1 e^{i\phi_1} + f_2 e^{i\phi_2} + \dots + f_j e^{i\phi_j} ) \sum_{n=0}^{N-1} e^{in\psi} \dots\dots 1.4$$

The expression in parentheses represents the resultant for one translation period ( a ). If we represent the h'th order maximum by ( F(h) ), and since it can be shown that the phase angle can be expressed :

$$\phi_j = h \frac{X_j}{a} 2\pi \dots\dots\dots 1.5,$$

we may write :

$$F(h) = \sum_{j=1}^J f_j e^{2\pi i h X_j} \dots\dots\dots 1.6$$

where :  $\underline{x}_j = X_j/a \dots\dots\dots 1.7,$   
 the fractional co-ordinate of the j'th scattering point.

This equation may be extended to treat a general three-dimensional lattice of points, referred to an axial set as previously defined, when the wave of order (hkℓ) may be represented :

$$F(hk\ell) = \sum_{j=1}^J f_j^0 e^{2\pi i (h\underline{x}_j + k\underline{y}_j + \ell\underline{z}_j)} \dots 1.8$$

This equation represents exactly the conditions for the diffraction of X-radiation by a crystal lattice, due to the interference of waves scattered by the electrons of the ( J ) atoms in the structure. F(hkℓ) is defined as the 'structure factor' for the plane with Miller indices h, k, ℓ. The factor ( $f_j^0$ ) is the 'atomic scattering factor', and represents the scattering power of the j'th atom; due to the finite size of the atomic electron cloud it is dependent on (  $\theta$  ) the scattering angle, for any particular wavelength; it is equal to ( Z ), the atomic number, at  $\sin\theta/\lambda = 0$  , but falls off rapidly at higher values. The terms  $\underline{x}_j, \underline{y}_j, \underline{z}_j$ , are the co-ordinates of the j'th atom as fractions of the unitcell edges a, b, c.

In the above discussion of the interaction of the electric vector (  $\vec{E}$  ) of the incident radiation with the atomic electrons, a static electron cloud has been assumed.

This is only approximately true at the absolute minimum temperature; at all other temperatures a correction term must be applied to the theoretical scattering factors ( $f_j^0$ ) :

$$f_j = f_j^0 e^{-(B \sin^2 \theta) / \lambda^2} \dots\dots\dots 1.9$$

The factor ( B ), due to Waller <sup>(15)</sup>, is known as the isotropic temperature factor, with units of  $\text{\AA}^2$ . However it is often more realistic to treat the atomic motion as ellipsoidal, rather than spherical, and the anisotropic correction is of the form :

$$f_j = f_j^0 e^{-(\beta_{11}h^2 + \beta_{22}k^2 + \beta_{33}l^2 + \beta_{12}hk + \beta_{13}hl + \beta_{23}kl)} \dots\dots 1.10.$$

In the discussion which follows these temperature correction terms must be borne in mind, but for simplicity of representation ( $f_j$ ) will be written for the corrected scattering factor.

#### 1.4. The Reciprocal Lattice and The Sphere of Reflection.

It is pertinent to introduce at this point the concept of the ( Gibbs-Ewald ) reciprocal lattice <sup>(16)</sup>, which has simplified the interpretation of all types of diffraction techniques based on moving crystals in monochromatic X-ray beams. If we imagine normals to the lattice plane stacks, on which are marked lengths proportional to the inverse of the repeat distance of the stack, then a second lattice is

produced in which a point represents a plane in the real-space lattice. This imaginary lattice is termed the reciprocal of the direct-space lattice, and the constant of proportionality is normally taken as ( $\lambda$ ), the wavelength of the incident radiation. The analogy between the reciprocal lattice and the diffraction pattern is simple, any spot on the pattern represents a reflection from a particular family of planes, which is associated with a specific reciprocal lattice point.

If we now construct a sphere of unit radius ( i.e. 1 reciprocal lattice unit ), with the incident beam as diameter, and place the origin of the reciprocal lattice at its point of emergence, then as the crystal rotates the reciprocal lattice rotates about a tangential axis. Reflection from a particular direct lattice plane ( $hkl$ ) occurs when the reciprocal point ( $hkl$ ) passes through the 'sphere of reflection'. ( Ewald sphere ).

The Bragg equation ( 1.2 ) sets the limiting value on the interplanar spacing (  $d$  ) that can be compassed by a wavelength ( $\lambda$ ); this is a consequence of the limit on  $\sin\theta$  of unity :

$$d = \frac{n\lambda}{2 \cdot \sin\theta} \dots\dots\dots 1.11$$

whence, for a first order reflection :

$$d_{\text{max}} = \frac{\lambda}{2} \dots\dots\dots 1.12$$

Min.

Thus, no information is obtained about the region of reciprocal space outside a sphere of radius 2 r.l.u., and this is called the limiting sphere.

We may rewrite Eq. 1.8 in vector notation :

$$G = \sum_{j=1}^J f_j \exp ( 2\pi i \vec{r}_j \cdot \vec{H} ) \dots\dots\dots 1.13$$

where the vector (  $\vec{r}_j$  ) defines the position of the j'th atom, and (  $\vec{H}$  ) defines a point in reciprocal space. ( G ) is thus the Fourier transform of one unitcell. Thus the structure factors (F) are the values of ( G ) at the reciprocal lattice points (hkℓ). We may thus construct a 'weighted' reciprocal lattice, with each point having an area proportional to the value of ( F(hkℓ) ). This lattice has the symmetry ( Laue symmetry ) of the diffraction pattern; this is the point group symmetry of the crystal plus a centre of symmetry<sup>‡</sup>, giving rise to 11 Laue groups listed in Table 1.1.

<sup>‡</sup> This is a consequence of Friedel's Law, which only holds under normal scattering conditions. For further discussion see Chapter 3.

## CHAPTER 2.

### The Phase Problem and some Methods of Solution.

#### 2.1. Intensity Data and Their Correction.

The only data available to the crystallographer are the relative positions and intensities of the diffracted spectra from the crystal lattice. The latter may be recorded photographically (chapter 4), or measured electronically (chapter 9). Photographic methods must necessarily be used for the former, from which the Laue symmetry, crystal system, and unit cell dimensions may be obtained. In 60 cases the systematically absent spectra define the space-group uniquely, otherwise the choice is reduced to a few; a knowledge of the optical rotatory properties of the crystals or their solutions can further restrict the choice (chapter 3).

A knowledge of the cell dimensions, density ( $\underline{D}_m$ ), and approximate molecular weight ( $\underline{M}$ ), enables the number

of molecules per cell (  $Z$  ) to be calculated; since this must be an integer, back-calculation reveals the accurate value of (  $M$  ). Large discrepancies between the calculated and expected values can reveal an inaccurate analysis or the presence of molecules of crystallization. Where (  $Z$  ) is lower than expected from a consideration of space-group symmetry, the molecules themselves must possess symmetry, these results are often of chemical significance in themselves. (17)

Once the intensity record has been collected, the data must be corrected for certain geometrical and physical factors, before further progress can be made :

i) The Polarization Factor. The incident X-ray beam ( received direct from the X-ray tube ) is non-polarized, the electric vector (  $\vec{E}$  ) assuming all directions with time. On reflection the component of (  $\vec{E}$  ) in the plane containing the incident and reflected beams is reduced in amplitude, whereas the component perpendicular to this plane is not; so the resultant is partially polarized. If we designate the measured intensity by (  $I^P(hkl)$  ), and the true value by (  $I^O(hkl)$  ), then :

$$I^O(hkl) = I^P(hkl) \cdot \left( \frac{1}{2} + \frac{1}{2} \cos^2 \theta \right)^{-1} = I^P(hkl) \cdot p^{-1}$$

..... 2.1

where (  $\theta$  ) is the Bragg angle and (  $p$  ) is the polarization factor.

ii) The Lorentz Factor (  $L$  ) is a measure of the rate at which the reciprocal lattice point (  $hk\bar{l}$  ) cuts the surface of the sphere of reflection. It is dependent on both (  $\theta$  ) and the radial cylindrical co-ordinate (  $\xi$  ), and takes the form :

$$L = 1 / \left\{ \left( \xi / 2 \right) \sqrt{4 \cos^2 \mu - \xi^2} \right\} \dots\dots\dots 2.2$$

for a Weissenberg photograph recorded at equi-inclination angle (  $\mu$  ). The above expression is usually combined with Eq. 2.1 for computational convenience, the observed intensity being multiplied by (  $L_p$  )<sup>-1</sup> to obtain (  $I^o(hk\bar{l})$  ).

iii) The Multiplicity Factor. In some methods of obtaining the intensity record it is impossible to separate certain reflections,  $h_1k_1\bar{l}_1$ ,  $h_2k_2\bar{l}_2$ , ...  $h_jk_j\bar{l}_j$ , and the value observed is the summation of the individual values. If the reflections are symmetry equivalent then :

$$I^{\text{total}} = m \cdot I(hk\bar{l}) \dots\dots\dots 2.3$$

however, for the recording methods used in the work to be described, the factor (  $m$  ) is unity.

iv) The Renninger Effect.<sup>(18)</sup> It is possible for X-rays, reflected from a set of planes  $h_1k_1\bar{l}_1$  to be reflected from a second set  $h_2k_2\bar{l}_2$ , which are, by chance, in the correct orientation. It can be shown that the doubly reflected ray adds to the intensity of the reflection  $h_1 + h_2$ ,  $k_1 + k_2$ ,  $\bar{l}_1 + \bar{l}_2$ , but obviously no correction



can be applied. The Renninger conditions can, however, be calculated, and the effect avoided by a very slight displacement of the data collection geometry. If large systematic errors can be attributed to this cause, the data so affected can be omitted from refinement; this has not proved necessary in the present work.

v) Absorption. All crystals absorb X-rays to some extent, depending on their size, shape, and the scattering matter present. The equation linking the incident and transmitted intensities ( $I^0$  &  $I^T$ ), is analogous to the Beer-Lambert law, viz :

$$I^T = I^0 \cdot e^{-\mu t} \dots\dots\dots 2.4$$

where ( t ) is the thickness of the specimen in cm., and (  $\mu$  ) is the linear absorption coefficient in  $cm^{-1}$ . This is given by :

$$\mu = \sum_{j=1}^J G_j \left\{ \frac{\mu}{\rho} \right\}_j \dots\dots\dots 2.5$$

for monochromatic radiation. (  $\rho$  ) is the density in  $g. cm.^{-3}$  (  $D_x$  ; the experimentally determined density is usually used ), and (  $\mu/\rho$  )<sub>j</sub> is the tabulated<sup>(19)</sup> mass absorption coefficient for the j'th atom, which comprises mass fraction (  $G_j$  ) of the total molecular weight.

Correction is only simple for spherical <sup>(20)</sup> and

cylindrical<sup>(21)</sup> specimens. The situation is more complex for irregular shapes, but solutions using a three-dimensional grid of sampling points, to obtain the path-length of the ray inside the crystal, give good results. A graphical method<sup>(22)</sup>, based on the work of Albrecht<sup>(23)</sup>, is one of the quickest for hand computation. A computer procedure is mentioned in chapter 9. If the value of ( $\mu$ ) is low, and the crystal dimensions are small, the correction can be ignored in all but the most precise work.

vi) Extinction. Most crystals behave as if they consisted of a number of tiny blocks, whose orientation varies over several minutes of arc, i.e. they are ideally imperfect. Primary extinction results from multiple reflection of rays from a given set of planes within one 'mosaic' block. The incident beam undergoes a phase change of  $\pi/2$  on reflection, so a doubly-reflected beam will be  $\pi$  out of phase with the main beam, and so reduces its intensity. The overall effect is that the intensity is now proportional to a power of ( $F(hkl)$ ) between 1 and 2. Secondary extinction is caused by the upper layers of the crystal reflecting an appreciable portion of the primary beam, this reduces the intensity incident on the lower layers (mosaic blocks) of the crystal, which are simultaneously oriented for reflection. Both effects reduce the the observed intensities, and this is

most acute for strong, low-order reflections .

Secondary extinction can be allowed for by defining a new linear absorption coefficient<sup>(24)</sup> as :

$$\mu' = \mu + gQ \dots\dots\dots 2.6$$

where ( Q ) is the energy diverted into the reflected beam, and ( g ) is a constant for a particular specimen. In this work corrections have not been applied, data so affected have simply been omitted from the final stages of refinement.

## 2.2. The Phase Problem.

The electron density (  $\rho$  ) at a point with fractional co-ordinates (  $x, y, z$  ) can be represented by a Fourier series in which the complex coefficients are the structure factors<sup>(25)</sup> (  $F(hkl)$  ) given by Eq. 1.8; thus :

$$\rho_{(xyz)} = \frac{1}{V} \sum_{h=-\infty}^{\infty} \sum_{k=-\infty}^{\infty} \sum_{l=-\infty}^{\infty} F(hkl) \exp\{-2\pi i( hx + ky + lz )\} \dots\dots\dots 2.7$$

This formula can be considerably simplified for machine computation by expressing the structure factor in the complex form :

$$F(hkl) = A + iB \dots\dots\dots 2.8$$

$$\text{where : } A(hkl) = \sum_j f_j \cos \phi_j = |F(hkl)| \cos \phi(hkl) \dots\dots\dots 2.9$$

$$\text{and : } B(hkl) = \sum_j f_j \sin \phi_j = |F(hkl)| \sin \phi(hkl) \dots\dots\dots 2.10$$

and by utilizing the space-group symmetry.

This, if the amplitudes and phases of the structure factors are known, a representation of the electron distribution within the crystal can be obtained, with spherically symmetrical peaks occurring at atomic centres. In practice the values of  $h, k, l$ , are limited by Eq. 1.12, and the maps suffer from series-termination errors. However the observed intensities are proportional to the square of the structure amplitude (  $F(hkl)$  ) ( for ideally imperfect mosaic crystals ) i.e. :

$$I^o(hkl) = k \cdot F(hkl)^2 = k [A(hkl)^2 + B(hkl)^2] \dots 2.11$$

since (  $F(hkl)$  ) is normally complex. Thus the experimental data give no direct information concerning the phases (  $\phi(hkl)$  ); this bare statement constitutes the phase problem of crystal structure analysis.

2.3. Patterson's Function and the Heavy Atom Method.

Patterson's function <sup>(26)</sup> represents a convolution of the electron density with itself, inverted at the origin. The function (  $P$  ) at a point (  $u, v, w$  ) in Patterson or vector space, referred to three axes (  $U, V, W$  ) parallel to the crystallographic axes, is :

$$P(uvw) = \int\int\int_{000}^{111} f(xyz) \cdot f\{x+u, y+v, z+w\} \underline{V} dx dy dz \dots\dots\dots 2.12$$

where (  $\underline{V}$  ) is the cell volume. It may be represented as

a Fourier series with  $|F(hkl)|^2$  as coefficients :

$$P(uvw) = \frac{1}{V} \sum_h \sum_{k=-\infty}^{+\infty} \sum_l |F(hkl)|^2 \exp\{-2\pi i(hu + kv + lw)\} \dots 2.13$$

We may rewrite this equation :

$$P(uvw) = \frac{1}{2V} \sum_h \sum_{k=-\infty}^{+\infty} \sum_l \left[ |F(hkl)|^2 \exp\{-2\pi i(hu + kv + lw)\} + |F(\bar{h}\bar{k}\bar{l})|^2 \exp\{+2\pi i(hu + kv + lw)\} \right] \dots 2.14$$

and, assuming that Friedel's Law holds ( see chapter 3 ),

we may now write :

$$P(uvw) = \frac{1}{V} \sum_h \sum_{k=-\infty}^{+\infty} \sum_l |F(hkl)|^2 \cos 2\pi ( hu + kv + lw ) \dots 2.15$$

This equation yields a function which is everywhere real, and exhibits a centre of symmetry .

Eq. 2.12 indicates that the Patterson will exhibit peaks when both  $\rho(xyz)$  and  $\rho(x+u, y+v, z+w)$  are large, i.e. they represent atomic centres in an electron-density map. Thus a peak will occur for each interatomic vector; if there are ( J ) atoms in the unit cell there will be (  $J^2$  ) peaks in the Patterson; of these ( J ) will coincide at the origin, the remaining (  $J(J-1)$  ) occurring in two centrosymmetrically related sets of (  $\frac{1}{2}J(J-1)$  ). Theoretically the origin peak should represent  $\sum_{j=1}^J Z_j^2$  electrons, while a peak representing a vector between the j'th and k'th atoms should contain  $Z_j \cdot Z_k$  electrons. In practice frequent overlap of peaks occurs, and the origin peak often obscures those of the second type.

The application of space-group symmetry to the Patterson by Harker (27) led to the first partial deconvolution method. Let us take, for example, a monoclinic crystal, space group P2; the general equivalent positions for the  $j$ 'th atom are :

$$1) \quad \underline{x}_j; \quad \underline{y}_j; \quad \underline{z}_j;$$

$$2) \quad -\underline{x}_j; \quad \underline{y}_j; \quad -\underline{z}_j;$$

and a peak of weight ( $Z_j^2$ ), representing the interatomic vector between two atoms related by the diad, will occur at co-ordinates :

$$u = 2\underline{x}_j; \quad v = 0; \quad w = 2\underline{z}_j;$$

obtained by subtraction of (2) from (1). This (uvw) section is referred to as the Harker section (xOz), since the co-ordinates  $\underline{x}_j, \underline{z}_j$ , are directly determined from the position of the peak maximum. Similar expressions can be worked out for other symmetry operations, and solution is sometimes simplified by the presence of atoms in special positions. Unfortunately, however, peaks arising between atoms not related by symmetry can blur the information contained in the Harker lines or sections; solution is facilitated if a small number of atoms in the structure have large ( $Z_j$ ), when vector peaks between symmetry related atoms will stand out against a low general background.

The determination of 'heavy-atom' co-ordinates in

this way has led to one of the most far-reaching methods of solving the phase problem; the development of the 'heavy-atom' method is largely due to Robertson and his school<sup>(28)</sup>. We can write the total structure factor ( $F(hkl)$ ) as ( $F^T$ ), and thence as a sum of the heavy- and light-atom contributions ( $F^H, F^L$ ):

$$F^T = F^H + F^L \dots\dots\dots 2.16.$$

In general the contribution ( $F^H$ ) will be large, usually sufficient to define the phase angles ( $0$  or  $\pi$ ) in the centrosymmetric case, for a large number of reflections. In the non-centrosymmetric case there is a similar probability that ( $\phi^H$ ) will approximate ( $\phi^T$ ) for a great proportion of the data. Thus a Fourier summation based only on the heavy-atom co-ordinates frequently gives a close approximation to the true electron-density distribution; at worst some chemically recognizable features will be shown, which enables the positions of some of the light atoms to be obtained. The use of successive Fourier syntheses then reveals the complete atomic arrangement. Lipson and Cochran<sup>(29)</sup> have suggested that the method works best when :

$$\sum (z^H)^2 \div \sum (z^L)^2 = 1 \dots\dots\dots 2.17$$

but, with the advent of more accurate data collection equipment, structures with a ratio greater than unity should be soluble. Cases where the ratio is less than

unity are often soluble by careful iterative Fourier techniques.

In the work to be described the heavy atom method has proved successful. In the initial stages a rejection test has been applied whereby (  $F(hkl)$  ) has been excluded from the Fourier series if :

$$|F^H| < x \cdot |F^T| \dots\dots\dots 2.18$$

where (  $x$  ) has been reduced from 0.33 in successive summations. Thus reflections of uncertain phase are excluded. A better procedure involves the use of Fourier coefficients of the form (  $w F(hkl)$  ), where (  $w$  ) is a weight ( from 0 to 1 ) based on the probability that the phase due to the heavy-atom is correct. Such functions have been described by Woolfson <sup>(30)</sup> for the centrosymmetric case, and by Sim <sup>(31)</sup> for the non-centrosymmetric case.

It is pertinent at this point to give a brief review of other methods of surmounting the phase problem. Early structure determinations relied on what are best termed 'trial and error' methods, comparing the observed structure amplitudes with those calculated from a structure model. The advent of the methods discussed above was one of the turning points, giving semi-direct information regarding the phases. A contemporary of the heavy-atom method was that of isomorphous replacement of one heavy-atom for another as utilized by Robertson <sup>(28)</sup> in the centré-



symmetric phthalocyanine derivatives. A method using double replacement was proposed in the acentric case (32). The method has recently been resurrected in connection with structural work on proteins (33), with remarkable results.

We may conveniently divide other methods of solving the phase problem into two classes :

i) Those which are directly related to the Patterson function, and

ii) Those which work, basically, with the weighted reciprocal lattice.

Each class may be further subdivided into two groups as follows :

( i (a) ) Methods which make chemical suppositions. In class ( i ) this involves the assumption that a fragment of known molecular geometry exists within the molecule. The best known of these are the Patterson searching techniques of Nordmann (34), and the fältmolekul or convolution molecule method of Hoppe (35), which uses a fragment together with others related by symmetry.

( i (b) ) Methods which make no chemical assumptions, but use crystal symmetry and the positions of some known heavier atoms ( which, in themselves are not sufficiently heavy to govern the phases of a large proportion of the data). Here we may list superposition methods and their corollaries : minimum functions and implication diagrams,

These methods may be classified as 'image seeking' and have been put on a rigorous theoretical basis by Buerger<sup>(36)</sup>. A more recent extension of these Patterson deconvolution methods is vector verification<sup>(37)</sup>.

We may also treat class (ii) in the same manner :

(ii (a)) One of the best known methods in this category involves the calculation of the Fourier transform (G) for one unit cell using Eq. 1.13. The transform is the reciprocal of this single unit, just as the reciprocal lattice is the reciprocal of a repeating pattern of many units. From the definition of (F(hkl)) arising from Eq. 1.13, we can compare the calculated transform with the weighted reciprocal lattice. The calculation of (G) is laborious, but can be avoided by the use of optical methods. Both approaches owe much to the work of Lipson and Taylor<sup>(38,39)</sup>.

(ii (b)) This group includes those methods which attempt to derive the phases directly from the observed structure amplitudes, and in which no chemical information is assumed in the derivation. The first major breakthrough was due to Harker and Kasper<sup>(40)</sup>, who applied the inequality relations of Schwartz and Cauchy to the unitary structure factors ( $U(hkl) \equiv U(\underline{h})$ )<sup>\*</sup>. The relationship :

---

\*  $U(\underline{h}) = F(\underline{h}) / \sum_j f_j$ , i.e. the structure<sup>factor</sup> as a fraction of the maximum possible value : obviously  $U(\underline{h})^2 \leq 1$ .

$$U(\underline{h}) \leq \frac{1}{2} + \frac{1}{2}U(2\underline{h}) \dots\dots\dots 2.19$$

was derived for a structure containing a symmetry centre, and can be extended to cover other symmetry operations.

Karle and Hauptmann <sup>(41)</sup> showed that restrictions were placed on the structure factors when it was assumed (quite validly) that the electron-density ( $\rho$ ) was non-negative. They derived some more general inequalities.

The development of relationships between the signs (s) of the structure factors in a centrosymmetric case was initiated by Sayre <sup>(42)</sup>. His work was extended by Cochran <sup>(43)</sup>, who showed that the relationship :

$$s(\underline{h}) = s(\underline{h}') \cdot s(\underline{h} + \underline{h}') \dots\dots\dots 2.20$$

was probably true if the corresponding values of (U) were large. The same result was independently obtained by Zachariasen <sup>(44)</sup> using a different method. Systematic methods for applying this type of relationship were developed by Grant, Howells and Rogers <sup>(45)</sup>, and by Woolfson <sup>(46)</sup>. The development of these methods in the last decade is largely due to Hauptmann and Karle and their co-workers. In 1953 <sup>(47)</sup> these authors derived a number of structure factor relationships which they designated ( $\Sigma_1 \rightarrow \Sigma_4$ ) and later obtained formulae assessing the probability that the sign of their sum was the sign of (U( $\underline{h}$ )). The use of symbols to represent unknown signs has led to the method being called 'sym-

bolic addition'. This type of approach has been extended to cover the non-centrosymmetric case<sup>(48)</sup>, with no mean success. Here, however the number of ambiguous sets of phases produced tends to be large. The theoretical background and practical procedures available in both cases have been reviewed by Karle and Karle<sup>(49)</sup>.

#### 2.4 The Refinement of Atomic Parameters : The Least-Squares Method.

If we have ( m ) linear equations of condition, involving ( n ) variables, (  $x_1, x_2, \dots, x_n$  ), of the form :

$$E_k + q_k = a_k x_1 + b_k x_2 + c_k x_3 + \dots \quad \dots 2.21$$

where each term (  $q_k$  ) can be determined experimentally with an error (  $E_k$  ), then if ( m ) exceeds ( n ) we may solve for the x's in  $p (= m!/n!(m-n)!)$  ways. Since the error terms are all different, ( p ) different solutions will be obtained. The theorem of Legendre<sup>(50)</sup> states that the best solution is obtained when  $\sum_{k=1}^n E_k^2$  is a minimum.

The crystallographic equation of condition is of the form :

$$q_k = f_k ( x_1, x_2, x_3, \dots, x_n ) \dots \dots \dots 2.22$$

where the (  $f_k$  ) terms are the structure factors, which

are functions of the positional and thermal parameters. As can be seen from Eqs. 1.8,9,10, these contain exponential terms, and do not supply the required linear conditions. However, if we assume that approximate solutions (  $x_i$  ) are known, and that an error (  $dx_i$  ) is associated with each variable (  $x_i$  ), we may expand Eq. 2.22 by Taylor's theorem :

$$q_k = f_k(x_n) + \sum_{i=1}^n \frac{\partial f_k}{\partial x_i} dx_i + \frac{1}{2} \sum_{i=1}^n \sum_{j=1}^n \frac{\partial^2 f_k}{\partial x_i \partial x_j} dx_i dx_j \dots\dots\dots 2.23.$$

If terms of order higher than one are ignored, since they involve the product of two small quantities, (  $m$  ) equations are obtained of the form :

$$\frac{\partial f_k}{\partial x_1} dx_1 + \frac{\partial f_k}{\partial x_2} dx_2 + \dots\dots\dots \frac{\partial f_k}{\partial x_n} dx_n = q_k - f_k(x_1 \dots x_n) \dots\dots\dots 2.24.$$

These may be expressed in matrix form :

$$( A ) dx = ( b ) \dots\dots\dots 2.25$$

where any element of (  $A$  ) may be written :

$$w_k^{\frac{1}{2}} \cdot \frac{\partial f_k}{\partial x_i} \dots\dots\dots 2.26$$

and of (  $b$  ) :

$$w_k^{\frac{1}{2}} \cdot \{ q_k - f_k(x_1, x_2, \dots x_n) \} \dots\dots 2.27$$

The terms (  $w_k$  ) are weights, expressing the estimated relative accuracy of (  $q_k$  ).

In this case minimisation of the sum of the squares of the errors involves finding :

$$\min \sum_{k=1}^m E_k^2 = \min \sum_{k=1}^m w_k \left\{ q_k - f_k(x_1, \dots, x_n) \right\} = \min \sum_{k=1}^m w_k \left( \left| |F_o| - |F_c| \right| \right)^2 \dots 2.28.$$

The process is cyclic, involving successive solution for the parameter shifts (  $dx_i$  ), until these are minimal. The value obtained is not a true minimum since higher terms in the expansion ( Eq. 2.23 ) have been ignored. In certain cases when high correlations, say between  $dx_i$ ,  $dx_j$ , occur, the convergence is slow or impossible; it is possible to overcome this by multiplying the shifts by a damping or enhancing factor.

In the work to be described weighting schemes have been used where all (  $w_k$  ) are unity, or one which makes the final summation of Eq. 2.28 approximately constant over ranges of  $|F_o|$ . In general the scheme described by Hughes<sup>(51)</sup>, in a paper which introduced the least-squares method to crystallography, has been found satisfactory :

$$\begin{aligned} w_k^{\frac{1}{2}} &= 1 & \text{for } F_o \leq F^{\#} \\ \text{and } w_k^{\frac{1}{2}} &= F^{\#}/F_o & \text{for } F_o > F^{\#} \end{aligned} \dots\dots\dots 2.29.$$

The constant (  $F^{\#}$  ) is chosen from an analysis of  $|F_o|$  &  $|F_c|$ .

A measure of the accuracy of the structure, and also of the rate of convergence is given by :

$$\underline{R} = \frac{\sum | |F_o| - |F_c| |}{\sum |F_o|} \dots\dots\dots 2.30.$$

although changes in the expression minimised ( i. e. in  $w_k (| |F_o| - |F_c| |)^2$  ) are often more significant. The weighted (  $\underline{R}$  )-factor (  $\underline{R}^w$  ) will be defined in the next chapter, and its significance discussed in another context.

### CHAPTER 3

#### Molecular Asymmetry :

##### The Determination of Absolute Configurations by X-Rays.

The study of molecular asymmetry has attracted the attention of chemists since the observations of Biot between 1815 and 1835. He noted that certain natural products, e.g. camphor, turpentine and some sugars, would rotate the plane of polarized light to the left, or to the right. The property was exhibited in solution, showing that it was a molecular, rather than a macroscopic, property. In 1848 Pasteur separated the enantiomorphic forms of tartaric acid by hand; the crystals differed only in the placement of one morphological facet. He noted that solutions of the two ~~two~~ types of crystals rotated the plane of polarization in opposite senses.

The explanation of the phenomenon arose from the proposition of the tetrahedral arrangement of the four bonds formed by carbon ( van't Hoff and Le Bel 1874). Previously the four bonds had been assumed coplanar, and



all compounds were their own mirror images. If, however, four different groups are bonded to a single carbon atom, only two tetrahedra are possible, one being the mirror image of the other. The conclusion was reached that all optically active compounds contained one or more of these asymmetric centres.

Although the measurement of the optical rotatory power is simple it does not give unequivocal information regarding the absolute configuration. Degradative chemical work can relate configurations to the arbitrary standards enunciated in the Fischer-Rosanoff convention; this, however, had an exactly even chance of being correct. It has become increasingly important to know the exact spatial relationships of atoms. Enzymic reaction in vivo frequently produces all-dextro or all-laevo products; conversely the in vivo system will frequently accept only one form, the other being either completely deleterious or just ignored. If the biochemist is to explain these phenomena, or the drug chemist is to synthesise the correct form, a knowledge of absolute configuration is of paramount importance. The X-ray methods to be described in this chapter have provided the key to the whole problem.

### 3.1. Normal Scattering : Friedel's Law.

We must first note that optically active compounds can only crystallize in space-groups which do not involve rotation-inversion axes ( $\bar{n}$ ) or mirror planes ( $m$ ), since these require the presence of the other enantiomorph. Thus all centrosymmetric space-groups are excluded ( $\bar{1}$ ), together with non-centrosymmetric ones involving mirror or glide planes. The only allowed space-groups are those involving pure rotation or screw axes, and there are only 65 possibilities; these are the 'regular point systems' of Sohncke (52).

The formulae derived in chapter 1 only apply under 'normal' scattering conditions : when the incident wavelength is very much less than any natural absorption wavelength of the atomic electrons in the structure. Under these conditions the wave scattered by any atom is  $\pi/2$  out of phase with the incident wave. This is true for all atoms, and the phase change can thus be ignored. We may now study the effect of this on the structure factors ( $F(hkl) \equiv F_N$ ) and the inverse ( $F(\overline{hkl}) \equiv \overline{F}_N$ ). Expansion of Eq. 1.5 to three dimensions gives :

$$\phi(hkl) = \sum_j 2\pi(hx_j + ky_j + lz_j) \dots\dots 3.1$$

$$\text{therefore : } \phi(hkl) = -\phi(\overline{hkl}) (= -\phi_N) \dots\dots\dots 3.2$$

Combining Eqs. 2.8,9,10, and using the present nomenclature,

we may write :  $F_N = |F_N| e^{i\theta_N}$  ..... 3.3.

and :  $\bar{F}_N = |F_N| e^{-i\theta_N}$  ..... 3.4

since the Bragg angles (  $\theta$  ) are equal for both reflections. However, Eq. 3.3 is the complex conjugate of Eq. 3.4, and vice versa, so that :

$|F_N|^2 = |\bar{F}_N|^2$  ..... 3.5

and :  $I_N = \bar{I}_N$  ..... 3.6

This is Friedel's Law <sup>(53)</sup>, a statement of the centrosymmetric nature of the intensities in reciprocal space. Thus, in the reconstitution of a structural image from the normal X-ray data, it is impossible to distinguish between a structure and its inverse, even though the atomic sequence 'seen' by the incident beam from the sides (hkl), ( $\bar{h}\bar{k}\bar{l}$ ) is different.

3.2. Anomalous Scattering : The Bijvoet Technique.

Von Laue <sup>(54)</sup> was the first to suggest that Friedel's Law should break down if the incident wavelength was slightly shorter than that of an atomic absorption edge ( e.g.  $\lambda_{Kabs}$  ) of one or more atoms in the structure. Theoretical calculations by Hönle <sup>(55)</sup> showed him to be correct; in this case the energy of the incident quanta is sufficient to excite the K-electrons, and the scattered wave from these atoms has a phase lead over those from

the normal scatterers. The scattering factor for the 'anomalous scatterers' is now a complex quantity :

$$f_j^A = f_j^{OA} + f_j'^A + if_j''^A \dots\dots\dots 3.7.$$

If we have a structure containing both normal and anomalous scatterers, we may write an expression analogous to Eq. 2.16 for the total structure factor (  $F(hk\ell)$  ) :

$$F_T = F_N + F_A \dots\dots\dots 3.8$$

We may now examine the effect of the presence of anomalous scatterers on the structure factors (  $F_T$  ) and (  $\bar{F}_T$  ), using the methods and nomenclature of Sect. 3.1, in which the real and imaginary parts of (  $F_A$  ) will be designated (  $F_A'$  ) and (  $F_A''$  ) respectively :

$$F_T = |F_N| e^{i\theta_N} + |F_A'| e^{i\theta_A} + i |F_A''| e^{i\theta_A} \dots\dots\dots 3.9$$

$$= |F_N| (\cos\theta_N + i\sin\theta_N) + |F_A'| (\cos\theta_A + i\sin\theta_A) + |F_A''| (i\cos\theta_A - \sin\theta_A) \dots\dots\dots 3.10$$

$$= ( |F_N| \cos\theta_N + |F_A'| \cos\theta_A - |F_A''| \sin\theta_A ) + i ( |F_N| \sin\theta_N + |F_A'| \sin\theta_A + |F_A''| \cos\theta_A ) \dots\dots\dots 3.11$$

We may also derive (  $\bar{F}_T$  ) in a similar manner to be :

$$\bar{F}_T = ( |F_N| \cos\theta_N + |F_A'| \cos\theta_A + |F_A''| \sin\theta_A ) + i ( |F_A''| \cos\theta_A - |F_A'| \sin\theta_A - |F_N| \sin\theta_N ) \dots\dots\dots 3.12$$

We can now obtain  $(|F_T|^2)$  and  $(|\bar{F}_T|^2)$  by multiplying Eqs. 3.11, 12, by their complex conjugates. When this is done they are not found equal, the difference being :

$$\Delta I \propto \left\{ |F_T|^2 - |\bar{F}_T|^2 \right\} = 4 |F_N| |F_A''| \sin(\phi_N - \phi_A) \dots 3.13.$$

Thus Friedel's Law is seen not to hold. The structure factors are best represented on an Argand diagram, such as Figure 3.1, which shows a quite general case. The difference in intensities will be a maximum when :

$$\phi_N = \phi_A \pm \pi/2 \dots\dots\dots 3.14$$

and a minimum when :

$$\phi_N = \phi_A \text{ or } \phi_A + \pi \dots\dots\dots 3.15$$

the first condition of Eq. 3.15 will always occur if the structure contains one type of anomalous scatterer only.

The effect was noted experimentally as early as 1930<sup>(56)</sup>, when zinc sulphide, which has an asymmetric crystal structure, was irradiated with  $Au(L\alpha)$ . The value of  $(\lambda_{Kabs})$  for Zn is 1.2805 Å, and the unequal intensities of the  $Au(L\alpha_1)$  ( $\lambda = 1.2738$  Å) component scattered from the planes (111) and ( $\bar{1}\bar{1}\bar{1}$ ) was demonstrated. The intensities due to the  $Au(L\alpha_2)$  component ( $\lambda = 1.2850$ ) were equal.

The further implications of this result were not fully realized until Bijvoet<sup>(57)</sup> proposed that the absolute configuration could be obtained by comparing the

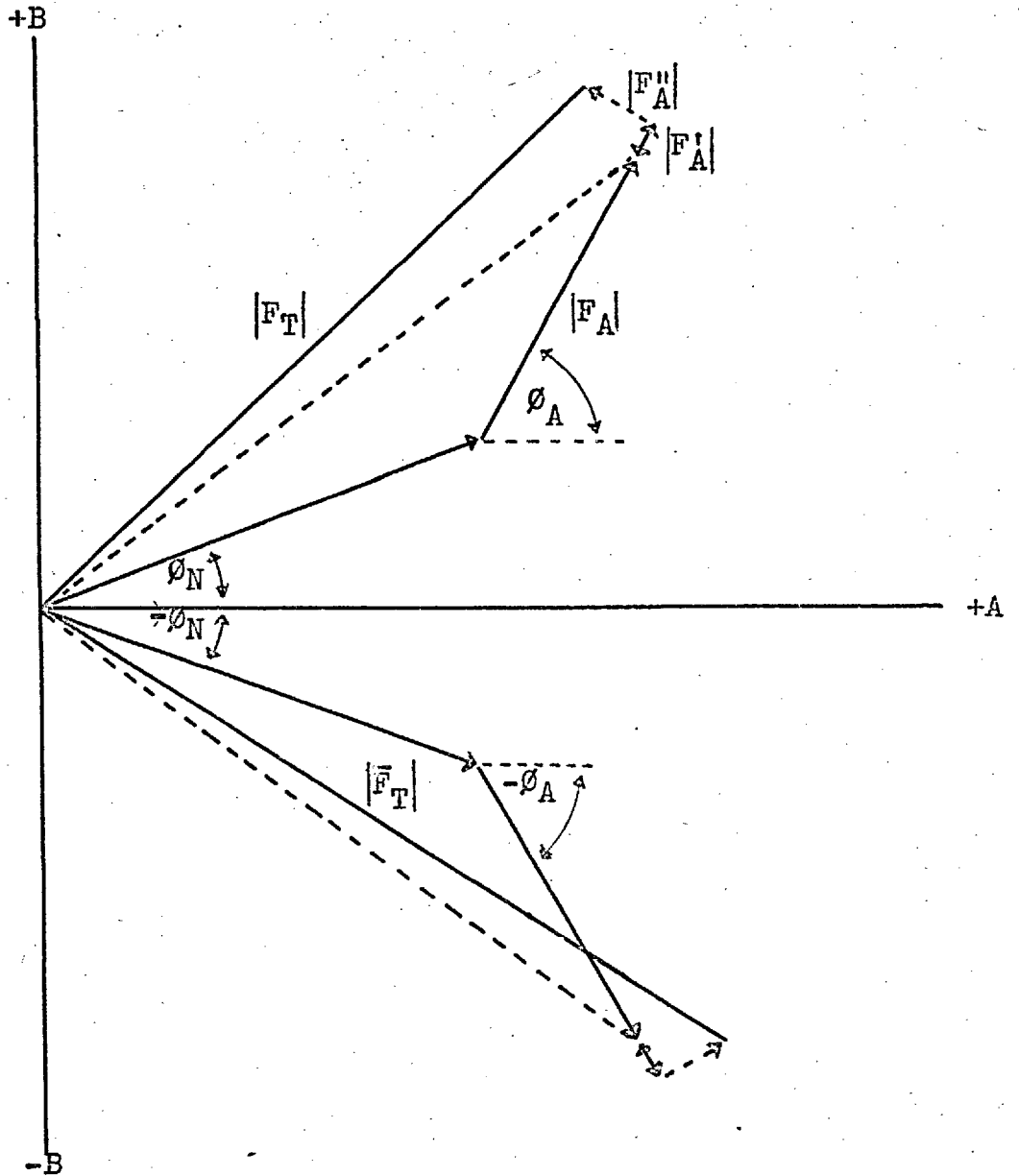


Figure 3.1. Argand Diagram showing the resultant amplitudes of the structure factors  $|F_T|$ ,  $|\bar{F}_T|$ , after correction for anomalous dispersion. In this perfectly general case  $|\bar{F}_T| > |F_T|$ .

observed inequalities, with those calculated from the known crystal structure. The intensities compared must be  $(hk\bar{l})$   $(\bar{h}k\bar{l})$  or their equivalents, and they have become known as 'Bijvoet pairs'. If good ( usually  $>85\%$  ) agreement is obtained, the structure, as determined, must represent the true spatial arrangement; a similar level of disagreement indicates that the inverse structure is 'absolutely' correct. For cases where the ' confidence level ' lies between these approximate limits, the experimental method may not have been applied with sufficient care, or the state of the refinement may not have given sufficiently accurate parameters for the calculation, ( which may be carried out by computer, or using Argand diagrams similar to Fig. 3.1. ).

We may now examine the requirements, both chemical and crystallographic, for a successful determination :

i) An anomalous scatterer, or scatterers, must be present in the structure, together with normal scatterers. Atoms of atomic number  $( Z ) \gg 16$  are required, and the condition is similar to the requirements for the heavy-atom method, which usually facilitates structure solution prior to an absolute configuration determination.

ii) The wavelength of the incident radiation must be sufficient to excite fluorescence, but the choice is not so restrictive as was initially thought. Hönle<sup>(55)</sup> had

predicted that where  $(\lambda_{inc}) > (\lambda_{Kabs})$  the energy was sufficient to excite L- or even M-electrons. This was shown experimentally by Peterson<sup>(58)</sup>, who excited the L-electrons of bromine ( $\lambda_{Labs} = 7.989 \text{ \AA}$ ) with Cu( $K_{\alpha}$ ) radiation ( $\lambda = 1.54178 \text{ \AA}$ ), and detected an average intensity difference of 8%. Dauben and Templeton<sup>(59)</sup> have calculated the correction terms ( $f'$ ) and ( $f''$ ) for atoms with  $Z \gg 20$  for the common wavelengths ( $K_{\alpha}$  lines of Mo, Cu, & Cr).

iii) The Bijvoet pairs must be indexed on a right-handed system of axes ( and the corresponding reciprocal lattice ) For photographic work the rotational sense of the goniometer axis must be correlated with the translational movement of the camera pot; the order in which the reciprocal lattice points pass through the sphere of reflection may then be analysed. This point has been dealt with by Peerdemann and Bijvoet<sup>(60)</sup>.

iv) Extreme care must be taken in the recording and measurement of the Bijvoet pairs. If photographic methods are used they must be recorded under identical conditions, i.e. on the same film. Usually the space-group symmetry allows pairs other than ( $hkl$ ), ( $\overline{hkl}$ ) to be compared; This is further discussed in chapter 6. Obviously electronic measurement has advantages, but photographic data may be measured best on a microdensitometer, and gives good results. If the discrepancies are expected to be



small, they will be most apparent among reflections with high ( $\theta$ ); this is because the normal scattering factor ( $f_j^0$ ) falls off rapidly with increasing ( $\theta$ ), while ( $f'$ ) and ( $f''$ ) are almost independent of ( $\theta$ ), since the electrons involved are confined to a small area close to the nucleus.

v) Care must be taken to avoid absorption errors which could reverse the assignment of absolute configuration in particularly adverse circumstances. For ( $\mu$ )  $> 100\text{cm}^{-1}$  it is wise to apply a systematic correction.

vi) The initial structure determination must be carried out to a good accuracy; the pitfalls in using inaccurate data will be mentioned in chapter 6.

The first assignment of absolute configuration was that of sodium rubidium-D-(+)-tartrate<sup>(61)</sup>; the rubidium atom ( $\lambda_{K_{\text{abs}}} = 0.81549 \text{ \AA}$ ) was excited by Zr( $K_{\alpha}$ ) radiation ( $\lambda_{K_{\alpha_1}} = 0.79010, \lambda_{K_{\alpha_2}} = 0.78588 \text{ \AA}$ ). The choice was historically apt: the results showed that ".... Fischer's arbitrary convention corresponds to reality" (62).

### 3.3. Some Extensions : Anomalous Dispersion Phasing and Hamilton's Method.

Reference to Eq. 3.13 shows that, if the positions of the anomalous scatterers can be found, the value of ( $\phi_N$ ) may be obtained, since all other terms in the equation may

be obtained experimentally. This method of solving the phase problem has been developed largely by Pepinsky et. al.<sup>(63)</sup> and by Ramachandran et. al.<sup>(64)</sup>. If the total structure is solved by this method, the solution automatically shows the absolute stereochemistry.

The use of linear hypothesis tests on the weighted crystallographic  $R$ -factor :

$$R^W = \left[ \frac{\sum_{i=1}^m w_i (|F_i|_o - |F_i|_c)^2}{\sum_{i=1}^m w_i |F_i|_o^2} \right]^{1/2} \dots\dots\dots 3.16$$

computed for (  $n$  ) parameters over (  $m$  ) observations (  $F_i$  ), was first suggested as a method for the determination of absolute configuration by Hamilton and Ibers<sup>(65)</sup>. The theory has been extended by Hamilton<sup>(66)</sup>, and he has published tables of the function :

$$\frac{R_1^W}{R_2^W} = \mathcal{R}_{b, m-n, \alpha} \dots\dots\dots 3.17$$

where (  $b$  ) is the dimension of the hypothesis, and (  $\alpha$  ) is the significance level. The terms (  $R_1^W$  ) and (  $R_2^W$  ) are the weighted  $R$ -factors for the structure and its enantiomorph, obtained from parallel refinements using data corrected for dispersion effects. The tables are computed at differing values of (  $\alpha$  ), and interpolation formulae are derived.

The statement : "the second configuration represents the true absolute stereochemistry", is a one-dimensional hypothesis. It is claimed that its validity may be accepted or rejected on a very small deviation of ( $\mathcal{R}$ ) from unity. However, Hamilton and Ibers have pointed out that the presence of systematic errors will invalidate the procedure. It appears to the present author that the procedure must be considered in the general context of  $\underline{R}$ -factor significance; for instance it is dubious to obtain results in this manner from  $\underline{R}^W$ - values higher than about 15%; it would be better to express the ratio ( $\mathcal{R}$ ) as a percentage of the mean value of  $\underline{R}_1^W$  and  $\underline{R}_2^W$ , this would obviously depend on the value of ( $f''$ ) and this should be quoted. The method has had only limited application, and the results (67,68) are so far unequivocal. The only advantage of the method is that extra photography and measurement is avoided; against this must be set the additional computer time required.

#### 3.4. The Method of Internal Comparison.

Although the techniques discussed above have produced many important results, it is not always possible to satisfy the required conditions. The method of internal comparison employs a known reference asymmetric centre, either within the molecule itself or :

i) introduced in the formation of a simple derivative, or ii) present in the solvent of crystallization.

In these cases the determination of the relative stereochemistry automatically leads to the absolute configuration at all other centres.

The method was suggested almost simultaneously by Pepinsky<sup>(69)</sup>, Mathieson<sup>(70)</sup>, and Hine and Rogers<sup>(71)</sup>.

The latter authors gave the first complete example : S-methyl-L-cysteine sulphoxide; the configuration of the L-cysteine was known with reference to the ( proven ) Fischer convention, and the structure determination established the configuration about optically-active sulphur for the first time.

Mathieson<sup>(70)</sup> has expounded some of the advantages :

i) no special precautions need be taken with regard to the radiation used;

ii) the method is equally applicable to light-atom structures where Patterson deconvolution or direct phasing techniques have been used;

iii) the addition of the reference<sup>centre</sup>/does not involve extra photography, but requires the positioning and refinement of a few extra atoms.

Additionally we may note that results can be obtained from two-dimensional studies, and, in any case, without recourse to very detailed refinement.

### 3.5. Conclusion.

The methods outlined above represent the only physical technique by which absolute configurations may be assigned in a completely unambiguous manner. In more complex molecules the detailed degradative chemical work can take much longer than an X-ray arbitration, although these have their limitations. It is pleasing to note that these assignments are being made as a standard part of the sequence of crystal structure analysis. As part of the experimental work on 3-bromo-(+)-camphor, the author performed an extensive literature search to assess the application of the Bijvoet technique; the results<sup>(72)</sup> showed that, between 1951 and 1966, 54 assignments had been made. The survey was extended to include determinations by other methods, and completed up to the end of 1967; 40 new entries were obtained<sup>(73)</sup>. Both lists are bound with this thesis as Appendix I.

Although this chapter has dwelt on the absolute configuration of organic molecules, the anomalous dispersion technique is capable of indicating the true absolute spatial atomic arrangement in an asymmetric structure, e.g. zinc sulphide or  $\alpha$ -quartz<sup>(74)</sup>. It is also finding application in the ever expanding field of asymmetric inorganic complexes.

## CHAPTER 4.

### Data Collection and Treatment : Computer Programs Used.

#### 4.1. Data Collection.

Both photographic and automatic electronic methods of data collection were employed in the work to be described. The Siemens automatic single-crystal diffractometer was used in only one case, and a discussion of its application will be delayed until chapter 9.

All photographic intensity data were collected using the equi-inclination Weissenberg technique and the multi-film pack method<sup>(75)</sup>. Two four-film packs were taken for each layer of the reciprocal lattice, with relative exposure times in the approximate ratio of 3:1; in this case, assuming a film-to-film attenuation of  $\sim 3.0$  for Ilford Industrial 'G' film, the intensities on the bottom film of the first pack approximate to those on the top film of the second.

All films were developed under similar conditions, i.e. immersed for 5 minutes at 60°F in Ilford Phenisol

developer, washed, and then fixed for 7 minutes in Kodak Unifix solution. The treated films were finally washed for about 2 hours.

Before the collection of accurate cell-dimensions and intensity data the camera pot radius was checked; using a suitable powder specimen enclosed in a Lindemann glass capillary tube, sets of powder lines were recorded on the edges of a full film, back calculation from the known d-spacings ( listed in the ASTM index ) gave the correct radius.

All intensities were measured visually using a graduated step-wedge ( except for the Bijvoet pairs (chapter 6 ) for which a Joyce-Loebl microdensitometer was used ). A strong reflection was chosen and exposed for a measured number of traverses of the camera pot, to produce a strip graduated in arbitrary units, usually from 1 to 40. To accomodate changes in spot shape on higher layers several wedges were made, at different equi-inclination angles, for each set of data. The intensities in each layer were then manually scaled-up to the level of the top ( most intense ) film.

#### 4.2. Data Treatment : Computer Programs Used.

Two distinct sets of crystallographic computer programs were used in this work :

X-RAY '63.

This is a completely homogeneous system, developed by Professor J. M. Stewart of the University of Maryland, and implemented on the Imperial College IBM 7090 in 1966. The program segments are written in FORTRAN II and stored in a compiled form on magnetic tape ( hereinafter magtape ), each may be called separately into store, and as many units as required may be used in one run, the linking routines are written in FAP. Intermediate computations are written to magtape ready for the next program, but permanent data, such as the reflection list, scattering factors, atomic positions and temperature factors, and weights, are stored on the user's magnetic tape and saved for future use.

ATSYS.

This is a set of single-program documents, with no linking routines, and does not constitute a system in the above sense. All programs are written in the EXCHLF extension of Mercury Autocode, and, as above, stored in a compiled form on magtape. The user's basic data is similarly stored, and input is cut to a minimum : only a short 'steering tape' indicating the file-number of the program, the locations of stored data, and the operations to be carried out. The formation of ATSYS is largely the



work of Dr. M. G. B. Drew<sup>(76)</sup>, who adapted and integrated programs from a number of different sources. As a 'home-grown' venture it has been amended and added to by a succession of students as the need arose.

The programs in both systems will be referred to only by their names in the text, since these names often give no indication of their function this will be indicated briefly below. There is also considerable overlap between the two systems, programs which cover the same ground will be listed together; programs unique to either system are listed separately. Name(s) of original author(s) are mentioned in as many cases as possible. The present writer is thankful to all those listed; he is more than aware of the frustrations involved !

<u>ATSYS</u>	<u>X-RAY '63</u>
CEDI, P.G.H.Troughton.	PARAM, R.A.Alden, H.L.Ammon.
<p>Least squares refinement of cell parameters from data input as : theta, <math>n\theta</math>, <math>\sin\theta</math>, or <math>\sin^2\theta</math>. Estimated standard deviations are produced for real and reciprocal cell dimensions.</p>	
FIFI, R.D.Diamand.	DATRDN, J.M.Stewart, M.A.Jarski, B.Morosin, R.Chastain.

Applies  $L_p^{-1}$  correction to raw intensities, and

in both systems is the initial means of magtape storage. All basic data required by X-ray '63 is read in, and stored for future use, at this stage, except, of course, the atomic parameters.

BOSS, M.M.Harding, M.G.B.Drew	FC, J.M.Stewart, R.Braun. FOURR, D.F.High et.al.
-------------------------------	---

Both programs will calculate 2D and 3D Patterson and Fourier maps at specified grid intervals. FOURR is completely general and takes precomputed structure factors from FC. BOSS contains its own structure factor routine, and is limited to triclinic, monoclinic, and some orthorhombic space-groups; others can be added as required. BOSS produces an agreement analysis in the form of a list of  $|F_o|$ ,  $|F_c|$ , and  $R$ , for reflections grouped in layers and by  $\sin^2\theta$  intervals, agreement is also assessed over ranges of  $|F_o|$  as fractions of  $|F_{max}|$ ; this latter enables a choice of weighting scheme to be made. These functions are covered in X-ray '63 by two programs : RLIST by W.Keefe and J.M.Stewart, and DELSIG by R. V. Chastain.

PAPA, M.G.B.Drew, F.H.Allen, P.Phavanantha.	PEKFIK, D.F.High.
--	-------------------

This program, basically the same in both systems, will read a Fourier map stored on magtape, and output fractional and grid co-ordinates of all electron-density maxima which exceed a set maximum. In PAPA Booth's parabolic method<sup>(77)</sup> is followed

BABA, R.D.Diamand, amended by Drew, Allen, Troughton	ORFLS, BLOKLS, DIAGLS, W.R.Busing, K.O.Martin, H.Levy, adapted by J.M.Stewart et.al.
---	--

Structure-factor least-squares refinement programs.

BABA uses a block-diagonal approximation, and follows the method outlined by Cruickshank<sup>(78)</sup>. The output parameters and structure-factors are stored on magtape ready for the next run. The agreement analysis from BOSS has recently been added to allow an appraisal of the weighting scheme to be made during refinement. The author has changed the input facilities to allow isotropic-anisotropic temperature factor conversion to be made at the user's discretion; also the scattering factors are now input direct from tables<sup>(19)</sup>, and converted internally to the values required by the program using Rollett's four-point interpolation<sup>(79)</sup>. Three separate routines are provided in X-ray '63. The standard version of ORFLS<sup>(80)</sup> has been amended to allow block-diagonal and diagonal-only approximations, as well as the full-matrix method.

ELSI, M.G.B.Drew.	BONDLA, D.F.High, J.M.Stewart, R.V.Chastain.
-------------------	---

Interatomic distances and angles programs. ELSI requires input of atomic positions ( $\underline{x}_r$ ) and their variances ( $V_{rr}$ ), these are converted to estimated standard deviations ( $\sigma_{rr}$ ) using Cruickshank's formula<sup>(81)</sup>:

$$\sigma_{rr}^2 = V_{rr} \sum_{i=1}^m w_i (|F_i|_o - |F_i|_c)^2 / (m-n) \dots 4.1$$

for (m) observations and (n) parameters. Standard deviations of lengths and angles are then computed using the formulae of Ahmed and Cruickshank<sup>(82)</sup> and Darlow<sup>(83)</sup>. Symmetry and translation operations are allowed for in both programs to obtain inter-molecular distances. BONDLA will also calculate hydrogen-atom positions, either tetrahedrally, trigonally, or linearly bonded, at a distance set by the user.

---

DIDO, R.A.Sparkes, D.J.Hunt.	LSQPL, R.V. Chastain.
------------------------------	-----------------------

Calculates the best plane through a set of input atoms, together with their mean distance from the plane. Other atoms may be re-positioned w.r.t. this plane, thus facilitating crystal drawing. DIDO uses the eigenvalue method outlined by Rollett<sup>(84)</sup>, while LSQPL follows the method of Schomaker et.al.<sup>(85)</sup>.

---

MATT, D.J.Hunt.	DATFIX, J.R. Holden.
-----------------	----------------------

Wilson's method<sup>(86)</sup> is applied to estimate the overall scale and temperature factor from two- or three-dimensional data. The programming method is similar to that outlined by Rogers<sup>(87)</sup> in the case of MATT. DATFIX also produces unitary structure factors, and is the initial program for application of direct methods via X-ray '63.

---

SFPO, F.H.Allen.

FCLIST, J.M.Stewart et. al.

Output of structure factor lists in a format suitable for reproduction in Theses and papers. The printing and paging formats are variable in both programs, and unobserved reflections can be suitably marked.

---

The following programs are unique to ATSYS :

POLO, M.G.B.Drew.

Reads in sets of data collected by rotation about two or three axes and initially corrected by FIFI. The common reflections are picked out to obtain inter-layer scale-factors, which are then refined by the method of Rollett, Hamilton and Sparkes<sup>(88)</sup>, to obtain the best fit. The final list, on an arbitrary unified scale, is written to magtape for further processing ( e.g. MATT ). The program also contains routines to sort the data to any order.

MOJO, F.H.Allen.

Produces : i) orthogonalized Angstrom co-ordinates, ii) bond lengths and direction cosines, iii) bond angles, iv) dihedral angles, for one asymmetric unit in a systematic manner, using a 'bonding array' or 'connectivity chart'. This obviates needless computation of unwanted information incurred in the full interatomic vector search programs. In addition other routines calculate specific

angles, distances, etc.; a specific routine to analyse the molecular geometry of cyclobutane rings was included to give the results listed in chapter 7. The programming scheme, relevant mathematics, and some examples of input and output, are shown in Appendix II.

Computer programs used specifically in connection with the Siemens diffractometer are briefly described in chapter 9.

## CHAPTER 5

### The Terpenes and Terpenoid Biosynthesis

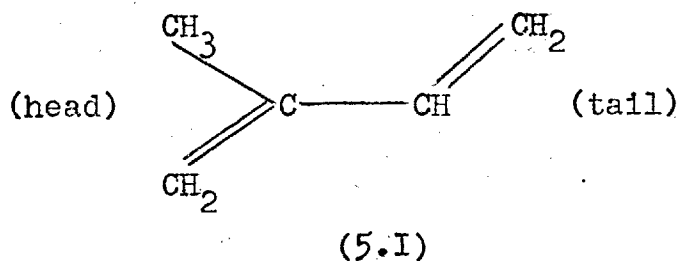
#### 5.1. The Isoprene Rule.

The production of isoprene (5.I) on the thermal decomposition of many naturally occurring hydrocarbons led Wallach<sup>(89)</sup> to propose that their structures were formed from a number (  $n$  ) of isoprene units (  $C_5H_8$  ). The name 'terpene' had originally been used for those hydrocarbons obtained from turpentine oil, but the classification became extended to include those substances which fitted the 'isoprene rule'. The natural diversity of the basic hydrocarbons, and their oxygenated derivatives, mainly from the plant kingdom, led to a sub-classification based on the number (  $n$  ) ( see Table 5.1, over page ). The group as a whole became known as the terpenoids, indicating that the molecular formula of the basic carbon skeleton could be written (  $C_5H_8$  ) <sub>$n$</sub> .

Later workers extended the isoprene rule<sup>(90)</sup>, and the

Table 5.1. Sub-Classification of the Terpenoids.

n	class ( common name ) ; molecular formula of basic hydrocarbon.
2	Monoterpenes; $C_{10}H_{16}$
3	Sesquiterpenes; $C_{15}H_{24}$
4	Diterpenes; $C_{20}H_{32}$
6	Triterpenes; $C_{30}H_{48}$
8	Tetraterpenes ( carotenoids ); $C_{40}H_{64}$
>10	Polyterpenes ( rubbers etc.); $(C_5 H_8)_n$



the basic hydrocarbons were regarded as being formed by :

- i) head to tail (regular) fusion,
  - or ii) head to head or tail to tail (irregular) fusion,
- followed by :

iii) cross-linking and cyclisation of these isoprene chains to give the observed diversity of carbon skeletons.

Recently the definition of 'terpenoid' has been extended by biosynthetic studies to include all compounds which follow the pathways described briefly in section 5.2. Thus the sterols and their derivatives must be regarded as



true terpenoids, while it has been suggested that other compounds which contain terpenoid elements in their molecules, together with fragments of different biosynthetic origin, should be called 'meroterpenoids' (91).

## 5.2. The Basic Steps in Terpenoid Biosynthesis.

In the early 1950's Ruzicka and his co-workers (92) recognized that geraniol (5.VII), farnesol (5.IX), and squalene (5.X), were key intermediates in the formation of mono-, sesqui-, and triterpenes respectively. In a series of brilliant rationalizations they derived schemes by which many of the known cyclic terpenoid skeletons could be obtained from these three compounds. This work has been confirmed by intensive biosynthetic studies in which the names of Cornforth, Popják, Bloch, and Lynen are prominent.

The isoprene rule formed a starting point for these studies, and many branched-chain five-carbon anions were used as biosynthetic precursors without total success. The breakthrough came with the discovery of mevalonic acid (5.III) (93), and its rapid incorporation into squalene and cholesterol. The mode of formation of mevalonate from acetate in plant cells, via the intermediacy of coenzyme-A (Co-A), has been studied by many groups, and two schemes appear to hold precedence (94). The ident-

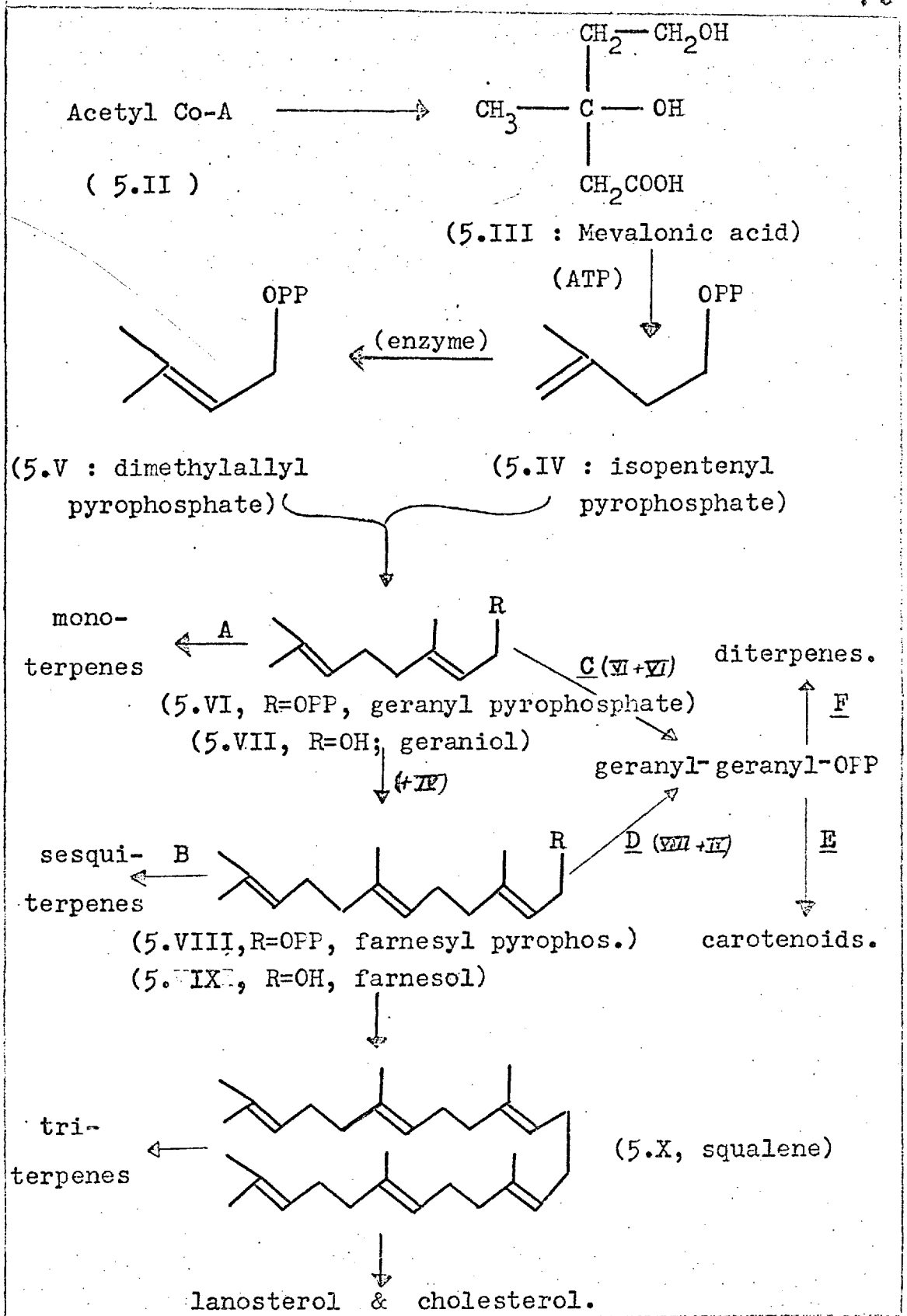


Figure 5.1, Outline of Terpenoid Biosynthesis.

ification of isopentenyl pyrophosphate (5.IV) as the final product of the phosphorylation of mevalonic acid in the presence of adenosine triphosphate (ATP)<sup>(95)</sup>, ended the search for the biological equivalent of isoprene.

The identification of farnesyl pyrophosphate (5.VIII) as a precursor of squalene, by Lynen and his co-workers<sup>(96)</sup>, was the next step in the chain. However they later showed that (5.VIII) was preceded in the biosynthetic sequence by geranyl pyrophosphate (5.VI)<sup>(97)</sup>, and showed that the latter was formed from mevalonate in two steps<sup>(98,99)</sup> :

i) the enzymic isomerization of (5.IV) to dimethylallyl pyrophosphate (5.V), followed by :

ii) the enzymic condensation or 'addition' of (5.IV) and (5.V).

A further 'addition' of (5.IV) to geranyl pyrophosphate gives the farnesyl precursor (5.VIII). We may express the final condensation of two units of (5.VIII) to form squalene (5.X) as being of the 'tail-to-tail' type. Much work has now been done on the biosynthesis of lanosterol and cholesterol from squalene, and this has recently been reviewed<sup>(100)</sup>.

The biosynthesis of the three major precursors suggested by Ruzicka forms the backbone of Fig 5.1. Much work is being conducted to discover the mechanisms of the enzymic condensations or 'additions' which must facilitate

the synthesis of the diterpenes and carotenoids from geraniol or farnesol, via routes C and/or D, and E, in Fig. 5.1. While the Figure only represents the bare bones of present knowledge, it does show how the terpenoids are related on what may be called the 'biogenetic isoprene rule'.

The structure determinations to which a large part of this thesis is devoted, concern derivatives of compounds which belong to the monoterpene ( (+)-camphor ) and sesquiterpene ( humulene and germ<sup>a</sup>cratriene ) classes. It is pertinent, therefore, to examine more closely the 'arms' A and B of the basic 'skeleton' of Fig. 5.1.

It now seems certain that the acyclic monoterpenes are biosynthesized by :

i) the enzymic condensation of two units of isopentenyl pyrophosphate (5.IV) ( or the condensation of this with some isomerization product, or the condensation of two of the latter), in the manner of the original isoprene rule, or ii) the enzymic hydrolysis or rearrangement of the geranyl precursor (5.VI).

The work of Ruzicka et al.<sup>(92)</sup> showed how some of the common mono- and bicyclic monoterpene skeletons could be formed from geraniol (5.VII). It is perhaps more exact to use the pyrophosphate (5.VI) as the precursor, since the  $\text{OPP}^-$  anion is a good leaving group, and facilitates

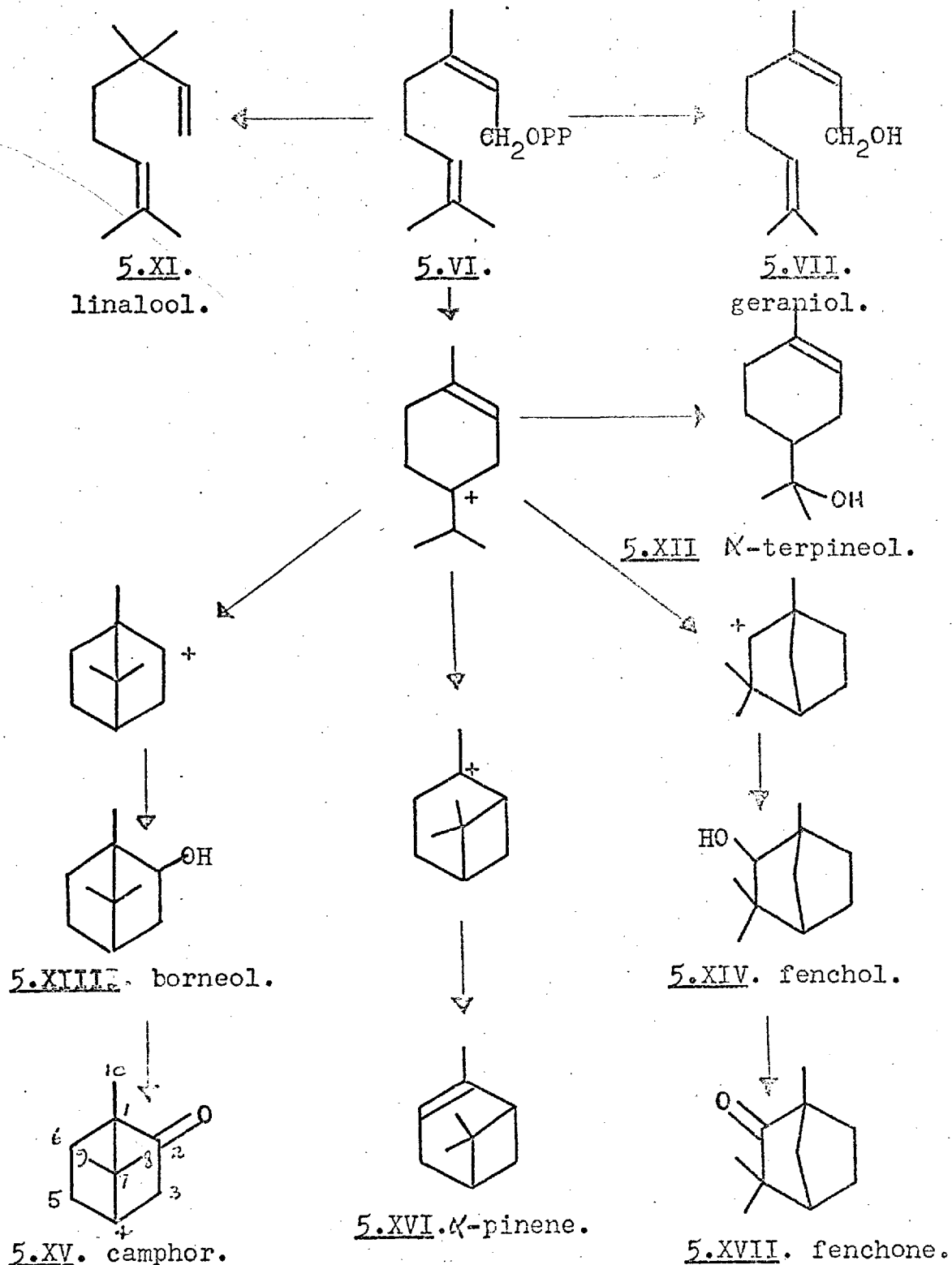


Figure 5.2. Possible Biosynthetic Route to the Cyclic Monoterpenes.

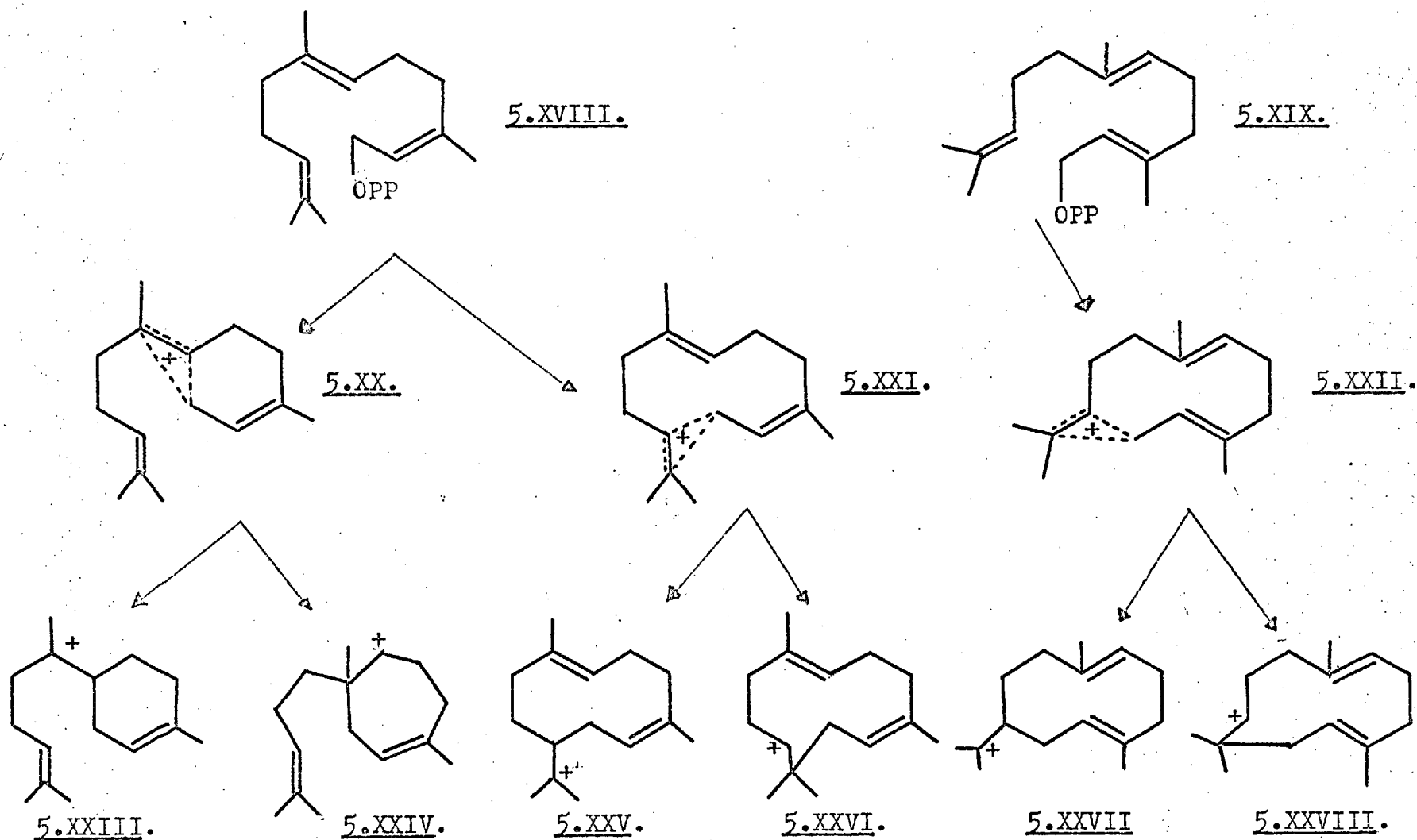


Figure 5.3. Possible cationic intermediates in sesuiterpene biosynthesis (102)

the required ionizations and cyclisations. The scheme shown in Figure 5.2. shows the probable route to camphor, and also indicates its relationship to some other cyclic monoterpenes.

The work of Ruzicka<sup>(92)</sup> on sesquiterpenes was extended by Hendrickson<sup>(101)</sup>, who showed that the carbon skeletons of virtually all known compounds could be derived by suitable cyclisations of either :

- i) cis-farnesyl pyrophosphate ( 5.XVIII),
- or ii) trans- farnesyl pyrophosphate (5.XIX).

Removal of the anion, followed by cyclization, gives rise to the cationic intermediates (5.XXIII-XXVIII), via the intermediacy of the non-classical cations (5.XX-XXII)<sup>(102)</sup>. The scheme is shown in Figure 5.3. While this scheme is probably not followed directly in nature, its utility as a means of classification cannot be disputed. The derivation of humulene and germacatriene from the farnesyl precursors will be traced in sections 5.4, and 5.5.

### 5.3. The chemistry of (+)-camphor.

The elucidation of the structure of camphor ( $C_{10}H_{16}O$ ) was one of the most fascinating pieces of early chemical research<sup>(103)</sup>. It occurs sparingly in nature, predominantly in the dextro-rotatory form, which is extracted from Cinnamonum camphora Nees, found in Southern China, Formosa,

and Japan. Its medicinal properties have been recognized since early times, while it was one of the substances used by Biot in his experiments on optical rotation. The vapour density and molecular weight were determined in 1833 by Dumas<sup>(104)</sup>, who gave the empirical formula shown above. Some thirty structures were suggested for the molecule, before Bredt<sup>(105)</sup> proposed the bicyclic ketone structure (5.XV) in 1893; this was later confirmed by synthesis<sup>(106)</sup>. The required cis-arrangement of the  $-CO-CH_2-$  bridge means that the two asymmetric centres ( $C_1$  &  $C_4$  in 5.XV) are not independent, a determination of the absolute configuration of (+)-camphor involves determining whether the gem-dimethyl bridge in 5.XV lies above or below the plane of the paper.

The reactions of (+)-camphor are numerous, and are well covered in standard texts<sup>(103,107)</sup>. Attention should be drawn to the simplicity of heavy-atom incorporation, chlorination and bromination at the 3- (or  $\alpha$ -) position being especially facile. The relationship of camphor to other mono- and bicyclic monoterpenes is suggested by Fig. 5.2. (+)-camphor gives (+)-borneol (5.XVIII) on reduction, while it can be prepared from (+)- $\alpha$ -pinene (5.XVI); the latter can also be converted into (+)- $\alpha$ -terpineol (5.XII). The essential similarity between the carbon skeletons of (+)-camphor and (+)-fenchone (5.XVII) has also been shown<sup>(108)</sup>. The configurational relationships are summarized in an excellent review by Birch<sup>(109)</sup>.



The difficulty of relating mono- and bicyclic mono-terpene configurations to the Fischer convention led Hückel<sup>(108)</sup> to propose a further arbitrary convention for these molecules based on (+)-camphor : if the molecule is drawn as in (5.XV), the gem-dimethyl bridge lies above the plane of the paper. The work of Fredga and Miettinen<sup>(110a)</sup>, and Porath<sup>(110b)</sup>, using the method of 'quasi-racemates'<sup>(111)</sup>, indicated, however, that the convention was incorrect. The experimental method may be summarized as follows<sup>(112)</sup> : if A and B form a compound, and A and the enantiomer of B form a mixture (or solid solution), then A and B are of the opposite configuration, and the converse. Determinations require the careful study of the melting point diagrams of mixtures of +A/+B, +A/-B (or of +A/+B, -A/+B).

Fredga and Miettinen<sup>(110a)</sup> applied the method to (+)-fenchone as follows : Wallach<sup>(113)</sup> had shown that this molecule could be degraded to (-)-~~X~~-isopropyl glutaric acid, and Fredga and Miettinen showed that the latter could be oxidised to (+)-isopropyl succinic acid. They went on to show that (-)-isopropyl succinic acid forms a 1:1 compound with (+)-methyl succinic acid, but not with the (-)-form; they therefore concluded that (+)-isopropyl succinic and (+)-methyl succinic acids have the same configuration. The latter has been

related<sup>(114)</sup> to the Fischer convention via malic acid; the correctness of this assignment has recently been shown<sup>(115)</sup> by the X-ray method. The stereochemical relationships (which are shown fully in Figure 6.4 on p. 116) gave the conclusion that (+)-fenchone, and hence (+)- $\alpha$ -pinene and (+)-camphor were represented by (5.XV-5.XVII) with the gem-dimethyl bridge below the plane of the paper.

The work of Porath<sup>(110b)</sup> followed a similar pattern; he converted (+)-camphor into (-)-camphoronic acid and thence into (-)- $\alpha$ -methyl- $\alpha$ -isopropyl succinic acid. The quasi-racemate technique was then used to determine the absolute stereochemistry of the latter. Again the gem-dimethyl bridge was shown to be below the plane in the conventional representation (5.XV). The stereochemical relationships involved here are also shown in Fig. 6.4 (p. 116); a full discussion of the implications of the above sets of results is deferred until section 6.6.

The method of quasi-racemates has some very serious restrictions however<sup>(112)</sup> : the compounds compared must be chemically very similar, and both enantiomers of at least one of the compounds must be obtainable. Even then great care must be exercised in the interpretation of the data, a recent example of this was the (incorrect) assignment of absolute configuration to (+)-2-isopropyl-

2-methyl glutaric acid<sup>(116)</sup>, and a consequent wrong assignment to its predecessor in the degradative chain (-)-methyl isopulegone. The correct assignment in the two cases was recently obtained using the X-ray method<sup>(117)</sup>. Thus the method does not guarantee success, results are best regarded as strong evidence in favour of a certain configuration, but not as absolute proof. If (+)-camphor is to be used as a starting point in stereospecific synthesis (as envisaged by Woodward<sup>(118)</sup>), or some salt is to be used as an internal reference centre (see sections 3.4, 6.5), the absolute configuration must be known unambiguously. For these reasons, and from its importance as a key terpene in the stereochemical schemes drawn up by Hückel<sup>(108)</sup> and Birch<sup>(109)</sup>, the X-ray arbitration was undertaken.

A description of this work, and a discussion of its relevance in the general field of terpene stereochemistry, forms the subject matter of chapter 6. It is sufficient to record here that the chemical work described above has been upheld; as has the lengthy stereochemical correlation published by Freudenburg and Lwowski<sup>(119)</sup>. The latter authors employed a rather complex scheme to arrive at a similar result in 1955; however the very length and complexity of the degradative

scheme used (some 18 compounds were synthesised in all) made the answer (although right) questionable.

#### 5.4. The Chemistry of Humulene.

The monocyclic sesquiterpene humulene was first isolated from oil of hops<sup>(120)</sup>. Degradative chemical work<sup>(121)</sup> showed it to be 1,1,4,8,-tetramethylcycloundecatriene ( $C_{15}H_{24}$ ), and this was confirmed by Sorm et. al.<sup>(122)</sup>, who synthesised 1,1,4,8,-tetramethylcycloundecane and showed it identical with hexahydrohumulene. Humulene has also been identified as the  $\alpha$ -caryophyllene constituent of clove oil<sup>(123)</sup>. Another constituent of clove oil, caryophyllene (5.XXIX, Fig.5.4.) (formerly known as  $\beta$ -caryophyllene), whose stereochemistry was elucidated by chemical<sup>(124)</sup> and X-ray<sup>(125)</sup> methods, was considered to be derived from the farnesyl precursor (5.XXVI)<sup>(101)</sup>. It was natural to suggest that its congener humulene had the same precursor, giving the trans-trans-cis-stereochemistry (5.XXX)<sup>(101)</sup> for humulene. The all-trans-stereochemistry (5.XXXI) was, however, proposed<sup>(126,127)</sup> on chemical, rather than biogenetic grounds, and has recently been shown correct by two independent X-ray analyses of the adduct  $C_{15}H_{24}:2AgNO_3$ <sup>(128,129)</sup>. Thus the farnesyl cation (5.XXVIII) is the probable biogenetic precursor of humulene (5.XXXI).

Recently Sutherland and his co-workers<sup>(130)</sup> have obtained the tricyclic bromohydrin (5.XXXII) by reaction of (5.XXXI) with N-bromosuccinimide. The relative stereochemistry shown was chemically defined at C(4) and C(5); at other points it was proposed on the basis of an apparently reasonable reaction mechanism (involving attack by hydroxyl at C(8) of (5.XXXI), followed by a concerted trans-cyclisation). The tricycle can be converted stereospecifically, and with equal facility, into ( $\pm$ )-caryophyllene (5.XXIX) or back to humulene, as shown in Figure 5.4, which sets out the whole series of relationships. Some derivative (probably cationic) analogous to compound (5.XXXII) thus appears to offer a possible alternative biosynthetic pathway from the farnesyl precursors (in this case from (5.XXVIII) ) to caryophyllene (5.XXIX).

In view of the possible biosynthetic relevance of humulene bromohydrin, and also to examine the geometry of the fused ring system, a full three-dimensional X-ray study was undertaken to establish the true stereochemistry of (5.XXXII). A description of the analysis<sup>(131)</sup> forms the subject matter of Chapter 7; it is sufficient to mention here that the results have shown the true relative stereochemistry of humulene bromohydrin to be as in (5.XXXIII), and not as proposed. The implications of this are discussed in Sect. 7.3.

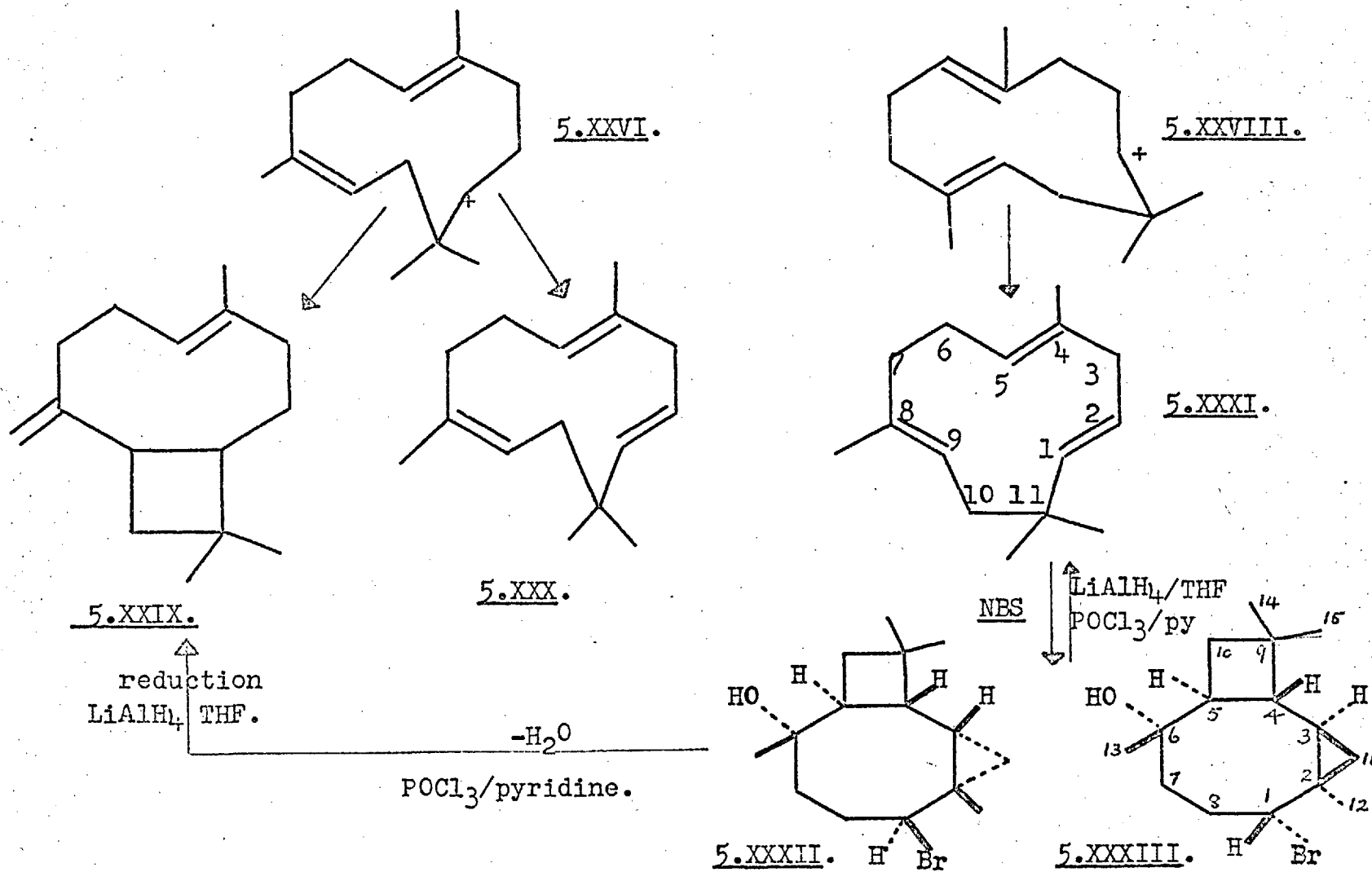


Figure 5.4. Derivation of Humulene from the Farnesyl Precursors: Formation of the Bromohydrin.

### 5.5 The Chemistry of Germacatriene.

Following the work of Ruzicka et.al.<sup>(92)</sup>, it was suggested by Barton and de Mayo<sup>(132)</sup> that ten-membered ring compounds could act as biosynthetic intermediates in certain cases. The suggestion was expanded by Hendrickson<sup>(101)</sup>, who used the triene (5.XXXIV, Figs.5.5,6), obtained by deprotonation of the farnesyl cation (5.XXVII), in a scheme for the biosynthesis of sesquiterpenes having the guiane (5.XXXVIII), elemene (5.XXXIX), selinane (5.XLI), and germacrane (cyclodecane) skeletons.

The cyclodecatriene (5.XXXIV) has recently been prepared by Sutherland and his co-workers<sup>(133)</sup> from the naturally occurring ketone germacrone (5.XXXV, obtained from zdravetz oil); it has been designated 'germacra-triene'<sup>(134)</sup>. The preparation, via the alcohol (5.XXXVI), and the acetate (5.XXXVII), is outlined in Fig. 5.5. The all-trans-stereochemistry was proposed<sup>(133)</sup> from degradative and spectroscopic evidence, and from the ready (and stereospecific) cyclisation to selinane derivatives (the bromohydrin (5.XLIII), obtained by reaction with N-bromosuccinimide, is typical); the cyclisation probably involves transannular  $\pi$ - $\pi$  interaction between the two endocyclic double bonds. Germacra-triene has also been converted<sup>(135)</sup> into the diol (5.XLII), having the guiane skeleton, by acid-induced

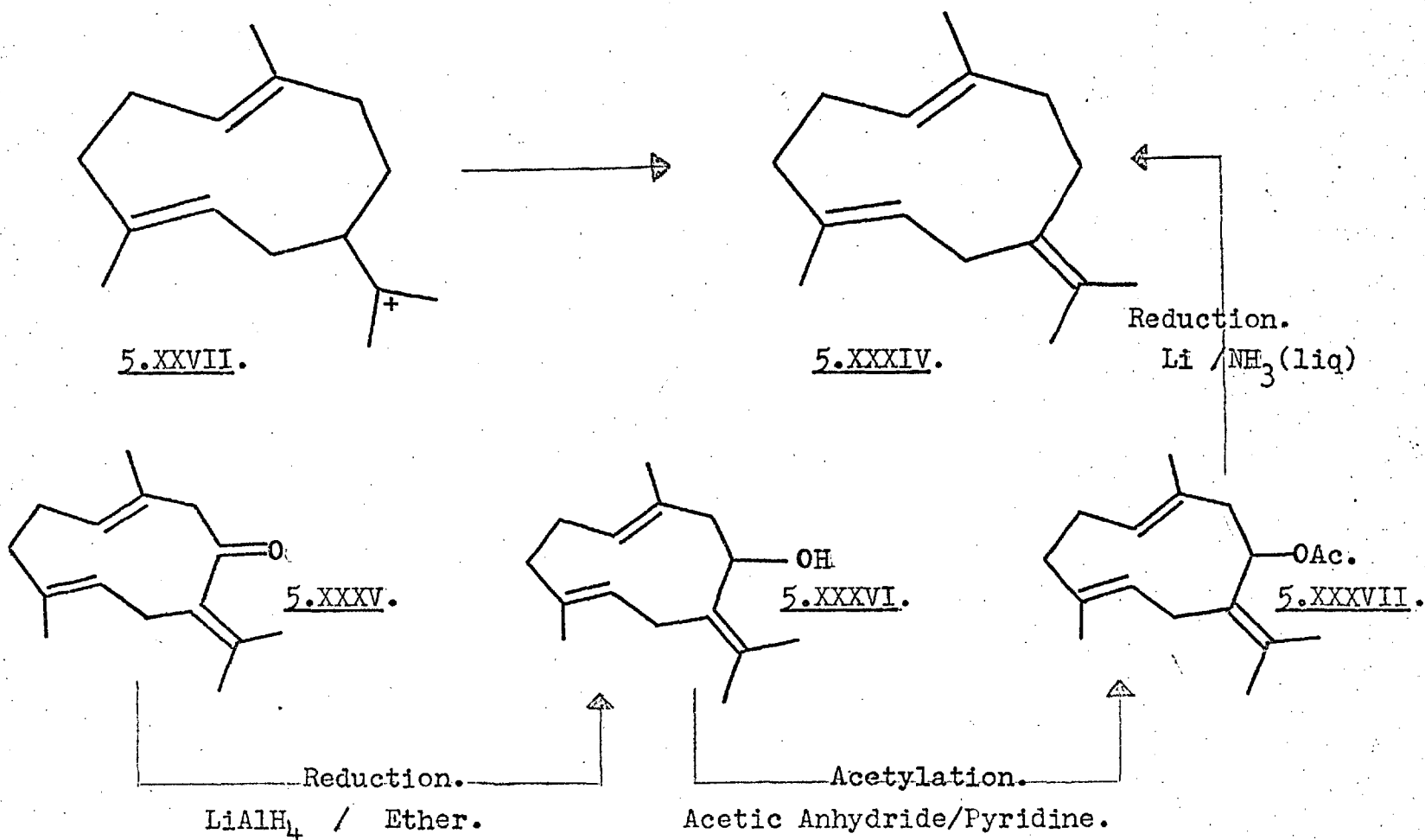


Figure 5.5. Probable Biogenesis of Germacatriene and its Preparation from Germacrone.



cyclisation of the epoxide (5.XLIV); and also into the previously undescribed elemene sesquiterpene  $\gamma$ -elemene (5.XL) via a Cope rearrangement at a temperature in excess of 120°.

A more inexplicable reaction of germacatriene is that with one mole of buffered peracetic acid, this gives a mixture of the three epoxides (5.XLIV-XLVI) with yields in the ratio 65:35: <1<sup>(136)</sup>. This implies great differences in the reactivities of the three double bonds. This must be a consequence of the geometry adopted just prior to reaction in solution, since  $\pi$ - $\pi$  transannular interactions should be unimportant in the case of epoxidation.

During the early experimental work it was discovered that germacatriene formed a crystalline adduct  $C_{15}H_{24}:AgNO_3$  on standing in a saturated solution of silver nitrate in ethanol<sup>(133)</sup>. In view of the obvious biosynthetic importance of the compound, a full three-dimensional X-ray study of the silver nitrate adduct was undertaken, both to check the stereochemistry, and to examine the molecular geometry about the double bonds. The X-ray work has confirmed the proposed stereochemistry, and also furnished an explanation<sup>(136)</sup> of the reactivity differences at the double bonds. A description of the X-ray study, and a discussion of the molecular geometry,

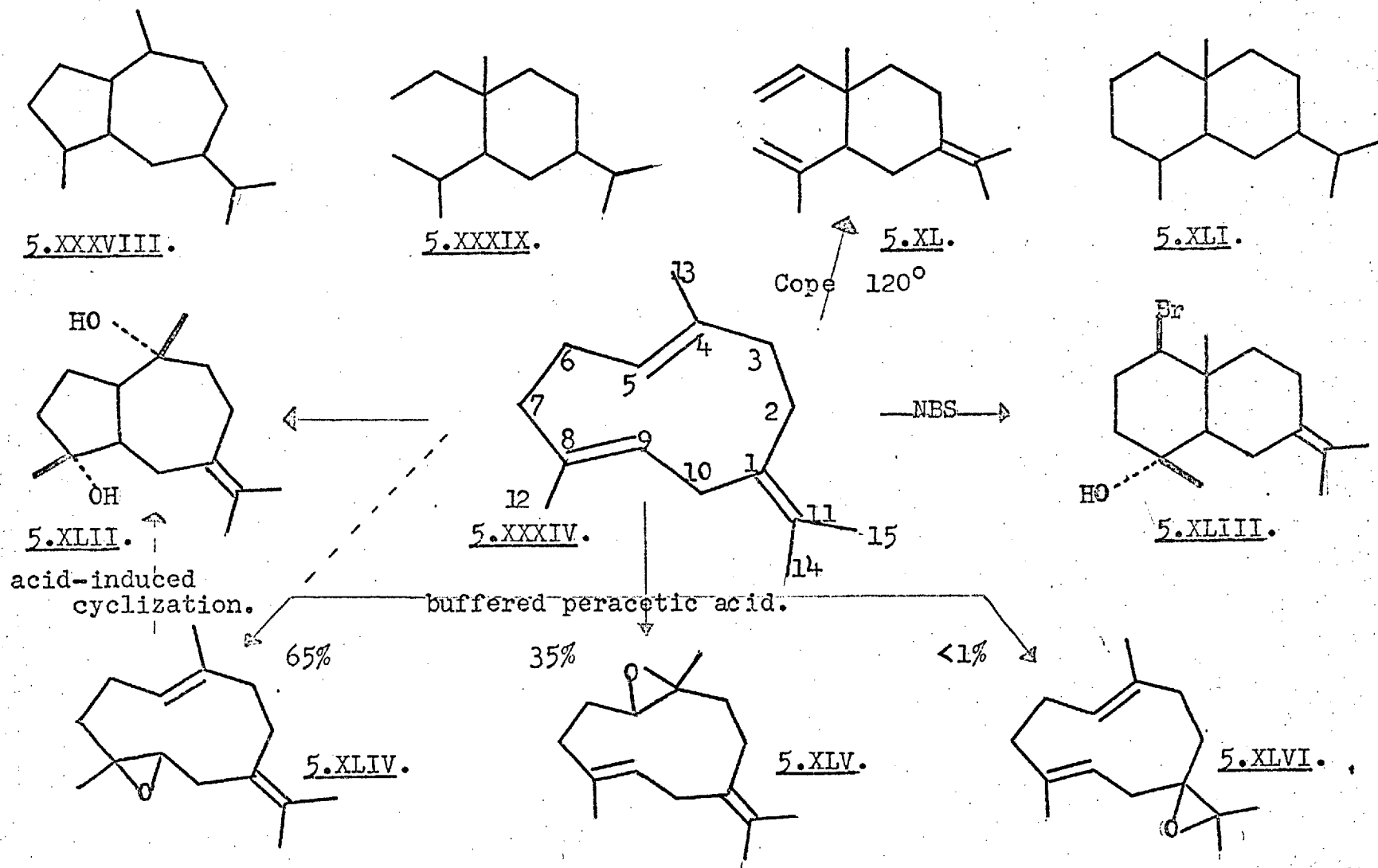


Figure 5.6. Some Reactions of Germacatriene, Showing its Relationship to other Sesquiterpenes

forms the subject matter of Chapter 8.

5.6. Note on Numbering Schemes.

The numbering schemes shown in this chapter, which have been chosen with some 'crystallographic licence', will be adhered to throughout this thesis. For ease of reference they are shown together in the pull-out diagram bound with the end-papers.

## CHAPTER 6

### The Absolute Configuration of (+)-Camphor :

### The Crystal and Molecular Structure of (+)-3-Bromocamphor

#### 6.1. Introduction.

The work to be described in this chapter began as a Research Exercise in Physical Chemistry performed by the Author during his final undergraduate year (1964-65) at Imperial College. The results obtained will be summarized below.

Initially attention was focussed on the compound : (-)-2-bromo-2-nitrocamphane; the crystal structure was known with good accuracy ( $R = 0.125$  for visually estimated data)<sup>(137)</sup>, while the identity of its configuration with that of (+)-camphor was known<sup>(103)</sup>. The compound was prepared by converting (+)-camphor to the oxime<sup>(138)</sup> which was treated with  $\text{Br}_2/\text{KOH}$  to give a pale yellow solid<sup>(139)</sup>. Recrystallization from aqueous methanol gave a white

feathery aggregate (m. pt. 218-221°(decomp) lit:220°(139)). Attempts to obtain single crystals suitable for X-ray work were unsuccessful.

Attention was now turned to (+)-3-bromocamphor, a compound first described by Keller<sup>(140)</sup>, which is known to have the same configuration as (+)-camphor<sup>(141)</sup>. The crystal structure had already been determined by Wiebenga and Krom<sup>(142)</sup> (hereinafter W & K), who studied the isomorphous series 3-bromo-, 3-chloro-, and 3-cyano-camphor. They determined the  $\underline{x}$ -,  $\underline{z}$ - co-ordinates of all atoms from the  $\left[010\right]$ -projections and refined them as far as was possible in 1946. The  $\underline{y}$ -co-ordinates for cyanocamphor were estimated from models and refined from the two other principal projections; no  $\underline{y}$ -co-ordinates were found for any atoms in the halides. The crystals were provided by Dr. J. E. Baldwin, then of the Organic Chemistry Dept., Imperial College; they are white prismatic needles, with an extinction direction parallel to the needle axis. The initial sample was too large for X-ray work, and smaller crystals were obtained by rapid cooling of saturated methanolic solutions.

The crystals were found to be unstable to X-irradiation, and numerous methods of protection were tried. It was found that a thin layer of pastel fixative sprayed uniformly, afforded sufficient protection for up to

70 hours exposure. The crystal data given by W & K were checked from oscillation and Weissenberg photographs taken about the a- and b-axes. The cell dimensions found showed good agreement; they were later refined by least-squares and are listed in Sect. 6.2. The crystals are monoclinic, space-group  $P2_1$ ; in this space-group, under normal conditions, the symmetry gives :

$$F(hk\bar{l}) = F(\overline{hk}l) = F(h\bar{k}l) \neq F(\bar{h}kl) \neq F(hk\bar{l}) \dots\dots\dots 6.1$$

Thus, to record the Bijvoet pairs photographically, the crystal must be mounted to rotate about either the a- or c-axes. The layers  $0k\bar{l}$ ,  $lk\bar{l}$ , were therefore recorded, using  $\text{CuK}\alpha$ -radiation and the multi-film pack method, and indexed on a rigidly right-handed system.<sup>(60)</sup> In this case a Stöbe Weissenberg goniometer was used, having the geometry shown in Figure 6.1(a) where the goniometer head rotates anti-clockwise (as seen by an observer at the open end of the camera), the translational movement of the pot is away from this observer; the direction chosen for  $+a^*$  is also shown. The direction of  $+c^*$  followed from a study of the  $lk\bar{l}$ -photograph superimposed upon  $0k\bar{l}$ , and was chosen to make an acute angle with  $+a^*$ . The direction of  $+b^*$  followed from the requirement that the system be right-handed. The chosen system (Fig. 6.1(b)) was then superimposed upon the crystal, and by utilizing the concept of the sphere of reflection in conjunction with the camera geometry, the correct cyclic sequence of axial rows was determined; the

correct indices were then assigned to all  $0k\bar{l}$  reflections.

The sign of the intensity difference  $I(0k\bar{l}) - I(0k\bar{l})$  was visually estimated for 18 Bijvoet pairs. The calculated differences were obtained using W & K's data for cyanocamphor, their  $x$ - and  $z$ -co-ordinates for Br, and an estimated  $y$ -co-ordinate for this atom. Structure factors ( $F_N$ ), ( $F_A$ ) ( $A=Br$ ) were computed using BABA; isotropic temperature factors ( $B$ ) of  $4.0 \text{ \AA}^2$  were allotted to C and O, and of  $3.0 \text{ \AA}^2$  to Br. The values were corrected for anomalous dispersion of  $\text{CuK}\alpha$  at Br using Argand diagrams (see Fig. 3.1); correction terms<sup>(59)</sup> :

$$f' = -0.9, \quad f'' = 1.5 \dots\dots\dots 6.2$$

were employed, and the sign of the difference  $F(0k\bar{l}) - F(0k\bar{l})$  obtained for all 18 pairs. The agreement between observed and calculated inequalities for this determination (A) is shown in Table 6.8 (p.110). The 77.7% vote obtained indicated that W & K's structure, if drawn on a right-handed set

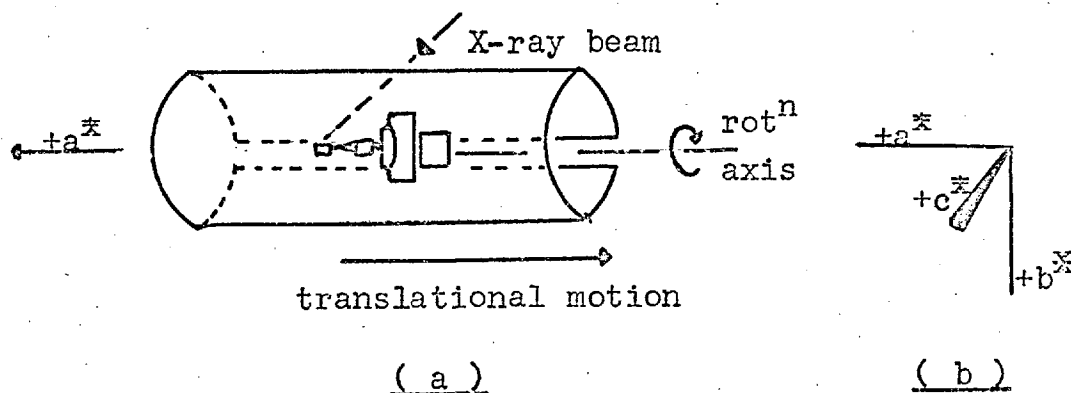


Figure 6.1 (a) Geometry of the Stöe Weissenberg Camera.  
(b) The chosen axial system.

of axes, represented the true absolute configuration. (110)  
 This confirmed the chemical work of Fredga and Miettinen, but with only about the same 'level of significance'. It was obvious that the positional data used was not sufficiently accurate to guarantee the result, and a redetermination of the crystal structure was undertaken. Apart from defining the absolute stereochemistry unambiguously, it has provided accurate data on the molecular geometry.

## 6.2. Data Collection.

The cell dimensions were obtained using CEDI, from some 25 theta values measured from equatorial Weissenberg photographs  $0k\bar{l}$ ,  $h0l$ . The values obtained, together with other relevant data, are listed below.

### Crystal Data.

(+)-3-bromocamphor:  $C_{10}H_{15}OBr$ ; Monoclinic; Laue symm.  $2/m$ .

$$\underline{a} = 7.36 \pm 0.01 \text{ \AA};$$

$$\underline{b} = 7.59 \pm 0.01 \text{ \AA};$$

$$\underline{c} = 9.12 \pm 0.01 \text{ \AA};$$

$$\underline{\beta} = 94.1^\circ \pm 0.4^\circ;$$

$$\underline{V} = 508 \text{ \AA}^3;$$

$$\underline{D}_x = 1.49 \pm 0.03 \text{ g.cm}^{-3}$$

( by flotation );

$$\underline{D}_c = 1.51 \text{ g.cm}^{-3}; \quad \text{for} \quad \underline{Z} = 2 \text{ molecules/cell};$$

$$\underline{M} = 231.03 \text{ (taking the standard } C^{12} = 12.00);$$

$$\underline{\mu} = 56.10 \text{ cm}^{-1} \text{ for CuK}\alpha (\lambda_{\text{mean}} = 1.54178 \text{ \AA}).$$

Absent spectra (only among  $0k0$  when  $k = 2n + 1$ ) defined



the space-group as  $P2_1$  (No.4.) or  $P2_1/m$  (No.11.)<sup>(143)</sup>.

The known optical activity of the compound ( $[\alpha]_D^{30} = +130^\circ$ ; in EtOH,  $c_{10}$ )<sup>(144)</sup> excludes the latter possibility (see sect. 3.1.) and leads to the unique definition as  $P2_1$ .

The previously described method of protecting the crystals proved unsuccessful over the long periods of X-irradiation required for the collection of the intensity record. A specimen of approximate dimensions : 0.4 x 0.2 x 0.13 mm. was therefore encapsulated in a Lindemann glass capillary tube, and set with the  $b$ -axis parallel to the axis of rotation of a Unicam Weissenberg goniometer. Using Ni-filtered  $CuK_{\alpha}$  radiation, the layers  $h0l$  -  $h5l$  were recorded. The reflections were indexed as described in sect.6.1. and 783 intensities were visually estimated using two graduated step wedges; a further 130 intensities were below the threshold value. No spot-shape correction was applied, but subjective weights were applied during the measurement. A further 50 intensities were similarly measured from the  $0kl$  photographs for correlating purposes; the  $lkl$  data was not measured, due to the very poor spot-shape.

### 6.3. Two-Dimensional Work.

A two-dimensional Patterson map for the [010] projection was computed using BOSS. It revealed the  $\underline{x}$ -,  $\underline{z}$ -co-ordinates of the bromine atom to be :

$$\underline{x} = 0.2628; \quad \underline{z} = 0.1663;$$

comparing well with W & K's values of :

$$\underline{x} = 0.2666; \quad \underline{z} = 0.1639.$$

A 2D Fourier map for the same projection, using only the phases given by the bromine atom position, yielded five well defined peaks;  $\underline{R}$  was 0.332. They were identified by comparison with W & K's positional parameters for cyanocamphor; the agreement is shown in Table 6.1. The map also showed that the co-ordinates of the bromine atom in the asymmetric unit were :

$$\underline{x} = 0.7372; \quad \underline{z} = -0.1663;$$

related to that obtained from the Patterson by a centre of

Table 6.1

Atom	W & K.		This Work.	
	$\underline{x}$	$\underline{z}$	$\underline{x}$	$\underline{z}$
O	0.403	0.061	0.409	0.068
C(2)	0.567	0.114	0.558	0.117
C(3)	0.728	0.031	0.751	0.039
C(10)	0.506	0.383	0.507	0.395
C(8)	0.933	0.419	0.920	0.406

symmetry in the  $[010]$ -projection (plane group P2) at  $\underline{x} = \frac{1}{2}$ ,  $\underline{z} = 0$ .

From the good agreement shown in Table 6.1, and from the overall similarity of the  $[010]$  Fourier projection for bromocamphor obtained here, with that for cyanocamphor obtained by W & K, it appeared that the co-ordinates of the atoms in the camphor framework of both derivatives were very similar<sup>(145)</sup>. It was felt that a three-dimensional refinement based on W & K's co-ordinates for C and O for cyanocamphor should be successful. A bead model was constructed, and the  $\underline{y}$ -co-ordinate of Br was estimated as 0.354, relative to the origin used by W & K. This value was then fixed as the arbitrary origin in the  $\underline{y}$ -direction in space-group P2<sub>1</sub>. The co-ordinates used to begin the refinement are shown in Table 6.2 overleaf.

#### 6.4. The Refinement of the Structure.

In this description, and similar ones in chapters 7, 8, & 9, refinement runs are designated I, A, or M :

I, indicates least-squares refinement with all atoms having isotropic temperature factors ( $B$ 's);

A, indicates that all atoms have anisotropic temperature factors ( $\beta_{ij}$ 's);

M, indicates that all non-hydrogen atoms are treated

TABLE 6.2.

(+)-3-Bromocamphor.Initial Co-ordinates in Least-Squares Refinement.

Atom	<u>x</u>	<u>y</u>	<u>z</u>
C(1)	0.631	0.333	0.267
C(2)	0.564	0.286	0.111
C(3)	0.731	0.214	0.033
C(4)	0.900	0.278	0.150
C(5)	0.894	0.478	0.167
C(6)	0.711	0.508	0.253
C(7)	0.817	0.200	0.278
C(8)	0.936	0.208	0.419
C(9)	0.767	0.014	0.292
C(10)	0.481	0.333	0.369
O	0.403	0.278	0.061
Br	0.7372	0.3540	-0.1663

as for A above, the hydrogen atoms being included in fixed positions, with fixed B-factors; the refinement may be loosely described as Mixed mode.

The main (b-) axis intensity data was  $I_p^{-1}$ -corrected using DATRDN and placed on a common arbitrary scale by comparison with intensities <sup>COMMON</sup> to  $0k1$ . The accidental absences were included at a value of  $\frac{2}{3}$  x the minimum observable intensity in the relevant part of the record.

No absorption correction was applied, since the cross-section of the crystal was fairly small and uniform, and ( $\mu$ ) was not large.

Refinement began with five cycles of unweighted full-matrix least-squares using ORFLS; the positional parameters from Table 6.2 were used, together with B-factors of  $4.0 \text{ \AA}^2$  for C and O, and  $3.0 \text{ \AA}^2$  for Br. Due to the paucity of correlating data the inter-layer scale factors were also made parameters in the refinement. The results of this run (I1) and of all subsequent runs will be found in Table 6.3 on page 101.

Before run I2 an analysis of the agreement between observed and calculated structure factors ( $|F_o|$  &  $|F_c|$ ) was made. A weighting scheme of the Hughes<sup>(51)</sup> type (Eq. 2.29) was devised to give reasonable constancy of  $\sum w(|F_o| - |F_c|)^2$  over ranges of  $|F_o|$ ; the constant  $F^*$  was 13.0 on the scale of the structure factors in Table 6.7. The scale factors were again refined and R fell to 0.184.

The isotropic temperature factors at the end of run I2 were converted into their anisotropic equivalents ( $\beta_{ij}$ ) and the refinement continued with runs A1-A4. During runs designated A or M the inter-layer scale factors were kept fixed, since their high correlations with the vibrational parameters makes this type of refinement formally invalid<sup>(145)</sup>. The only alterations made during

these runs were : after A1 five small high-order reflections were corrected for mis-indexing, and two others (1,1,0; 1,2,1;) removed for suspected extinction; after A3 a further reflection (0,2,1;) was removed for the same reason.

Molecular geometry calculations were performed, using BONDLA, after A1, A4, during the latter run the positions of the 15 hydrogen atoms were also computed, at bonding distances of 1.025 Å from carbon. In both cases the bond-lengths and angles made good chemical sense. Following run A4 a structure factor calculation was performed using FC to give values of  $F_N$  and  $F_{Br}$ ; the hydrogen atoms being included in their calculated positions. The results were used for an absolute configuration determination<sup>(147)</sup> which will be discussed in section 6.4.

An examination of the reflection data after A4 showed that some of the accidental absences were greater than the threshold values. A close examination of the photographs indicated that 57 were, in fact, marginally observable; Their intensity values were changed to the threshold value in the relevant part of the record.

It was decided to return to isotropic refinement to re-refine the inter-layer scale factors; no hydrogen atoms were included at this stage, and the weighting

was unchanged. The pertinent results (runs I3,A5, Table 6.3) show the large effect on  $R$  of the changes in scale-factors caused by relatively small corrections to the intensity data. It should be noted that this type of refinement has not had its more obvious pitfalls publicised : it appears advisable to return to the isotropic mode, after any change in data, weighting scheme etc., to re-refine the inter-layer scale factors. The experience gained here was used to make the (similar) refinement of germacatriene (chapter 8) a more efficient process.

A difference Fourier, with non-hydrogen atoms 'removed', revealed no spurious peaks; the six non-methyl hydrogens were discernible in positions close to those calculated by BONDLA. The methyl hydrogens were not shown. The final calculated hydrogen positions are shown in table 6.6 compared with those positions obtained from the difference map.

All fifteen hydrogen atoms were now included in structure factor calculations in their calculated positions, with  $B$ -factors  $0.5 \text{ \AA}^2$  greater than the value for the carbon atom to which they were bonded. A review of the weighting scheme was now carried out using DELSIG. Average values of  $(\|F_O\| - \|F_C\|)$  and  $\|F_O\|$  were output over ranges of  $\|F_C\|$ ; This showed that the bulk of

the data (749 terms) had structure factors in the range 0-20 on the scale of Table 6.7. It was found that a Hughes scheme with  $F^*$  set at 6.0 gave the best average of  $w(|F_o| - |F_c|)^2$  sums over the ranges chosen. This left 334 reflection intensities with unit weights.

Run I4 was performed to re-refine the scales to allow for the inclusion of hydrogen atoms, and the change in the weighting scheme. The refinement process was concluded with runs M1, M2, in which the scale factors were again fixed. There was no significant change in  $R$ , but the standard deviations of the atomic co-ordinates for C, O, Br, improved. The ratio of shift to standard deviation (S/E) on the final cycle was  $< 0.10$  for all parameters refined, and the least-squares process was concluded. The final positional and thermal parameters for C, O, Br, are shown in Tables 6.4 & 6.5 respectively. Final hydrogen atom positions were calculated from this data (Table 6.6) and were included in the final structure factor calculation, which gave an  $R$  value of 0.079 for the observed reflections. The final structure factor listing is shown in Table 6.7.

The estimated standard deviations in atomic co-ordinates shown in table 6.4 are significantly poor in the  $y$ -direction. This is due to the relatively low data cut-off at  $k=5$ . They are probably realistic estimates however, since full-matrix methods were used throughout.



TABLE 6.3.

(+)-3-Bromocamphor.The Refinement Process\*

Run	Cycles	<u>R</u>	Max S/E (scales)	Max S/E (all parameters)	Ave S/E
I1	5	0.256	-	-	-
I2	5	0.184	0.0300	-	-
A1	3	0.121	-	-	-
A2	3	0.102	-	-	-
A3	3	0.099	-	-	-
A4	3	0.098	-	-	-
I3	5	0.144	0.0009	0.0078	0.0020
A5	4	0.079	No ref	0.0538	0.0120
I4	3	0.145	0.0030	0.0100	0.0030
M1	3	0.080	No ref	0.8000	0.2230
M2	2	0.079	No ref	0.1000	0.0210

\* The full-matrix least-squares program ORFLS was used throughout.

TABLE 6.4.

(+)-3-Bromocamphor.Final Positional Parameters<sup>\*</sup> and Their Standard Deviations

Atom	$\bar{x}$	$\sigma_{\bar{x}}$	$\bar{y}$	$\sigma_{\bar{y}}$	$\bar{z}$	$\sigma_{\bar{z}}$
C(1)	0.6404	0.0016	0.3359	0.0031	0.2656	0.0012
C(2)	0.5665	0.0014	0.2949	0.0019	0.1097	0.0012
C(3)	0.7337	0.0016	0.2439	0.0027	0.0280	0.0011
C(4)	0.8838	0.0015	0.2795	0.0024	0.1382	0.0014
C(5)	0.8981	0.0021	0.4856	0.0025	0.1755	0.0015
C(6)	0.7204	0.0024	0.5151	0.0025	0.2555	0.0017
C(7)	0.8097	0.0015	0.2179	0.0029	0.2818	0.0012
C(8)	0.7605	0.0019	0.0174	0.0022	0.2773	0.0015
C(9)	0.9323	0.0020	0.2580	0.0029	0.4225	0.0013
C(10)	0.4928	0.0024	0.3226	0.0042	0.3734	0.0016
O	0.4128	0.0011	0.3090	0.0018	0.0570	0.0010
Br	0.7374	0.0002	0.3540	-	-0.1630	0.0001

Maximum and Average Positional Shifts on the Final Cycle:

	$\bar{x}$	$\bar{y}$	$\bar{z}$
Max shift (Å)	0.00036	0.00140	0.00067
Ave shift (Å)	0.00012	0.00050	0.00024

\* Positions are given as fractions of the cell edges  
(unless otherwise stated) throughout this Thesis.

TABLE 6.5.

(+)-3-Bromocamphor.

Final Anisotropic Thermal Parameters ( $\beta_{ij}$ 's)\* for the  
Non-Hydrogen Atoms

Atom	$\beta_{11}$	$\beta_{22}$	$\beta_{33}$	$\beta_{12}$	$\beta_{13}$	$\beta_{23}$
C(1)	0.02357	0.01211	0.01047	0.00061	-0.00073	0.00162
C(2)	0.01692	0.01164	0.01050	-0.00119	0.00213	0.00009
C(3)	0.02016	0.01715	0.00771	-0.00182	0.00085	0.00401
C(4)	0.01274	0.01704	0.01140	0.00138	-0.00057	0.00595
C(5)	0.02886	0.01148	0.01373	-0.01312	-0.00284	0.00683
C(6)	0.03056	0.00637	0.01606	0.00563	0.00194	-0.00431
C(7)	0.01543	0.02497	0.00873	0.00039	0.00028	0.00252
C(8)	0.02511	0.00273	0.01507	-0.00300	0.00318	0.00339
C(9)	0.02815	0.02288	0.00923	0.00154	-0.00333	0.00048
C(10)	0.03477	0.03606	0.01226	0.00531	0.00651	0.00437
O	0.01881	0.02073	0.01359	-0.00090	0.00067	-0.00100
Br	0.02900	0.02483	0.01037	0.00390	0.00388	0.00383

\* The temperature factors in the above table, which are all positive definite, are the parameters ( $\beta_{ij}$ ) in :

$$f = f^0 \exp(\beta_{11}h^2 + \beta_{22}k^2 + \beta_{33}l^2 + 2\beta_{12}hk + 2\beta_{13}hl + 2\beta_{23}kl)$$

TABLE 6.6.

(+)-3-Bromocamphor.Observed<sup>\*</sup> and Calculated<sup>^</sup> Hydrogen Positions

H Atom	Bonded to	Calculated			Observed		
		$\bar{x}$	$\bar{y}$	$\bar{z}$	$\bar{x}$	$\bar{y}$	$\bar{z}$
H(1)	C(3)	0.7003	0.1632	-0.0244	0.723	0.150	-0.079
H(2)	C(4)	0.9657	0.1868	0.1522	0.974	0.187	0.154
H(3)	C(5)	1.0174	0.5148	0.2462	1.090	0.505	0.223
H(4)	C(5)	0.8989	0.5683	0.0772	0.875	0.541	0.082
H(5)	C(6)	0.6288	0.6014	0.1930	0.635	0.609	0.206
H(6)	C(6)	0.7512	0.5696	0.3632	0.775	0.541	0.348
H(7)	C(8)	0.7084	-0.0260	0.3784			
H(8)	C(8)	0.8220	-0.0421	0.1404			
H(9)	C(8)	0.7180	0.0204	0.3069			
H(10)	C(9)	0.8801	0.2146	0.5236			
H(11)	C(9)	1.0315	0.1839	0.4307			
H(12)	C(9)	0.9815	0.4091	0.4108			
H(13)	C(10)	0.4349	0.1931	0.3807			
H(14)	C(10)	0.5051	0.2794	0.4340			
H(15)	C(10)	0.4311	0.4929	0.3858			

\* From a difference map following run A5.

^ Calculated from the final co-ordinates shown in Table 6.4. These parameters were not refined.

TABLE 6.7.(+)-3-Bromocamphor.Observed and Calculated Structure Amplitudes after  
Refinement.

The format of the table is :

h	k	l	$ F_o $	$ F_c $	$A_c$	$B_c$
---	---	---	---------	---------	-------	-------

Accidentally absent reflections are marked (L) (less-than).

The three reflections removed from refinement for suspected extinction were (in the same format) :

1	1	0	66.09	93.67	83.94	41.57
0	2	1	28.70	38.70	-18.10	34.20
1	2	1	42.87	57.48	32.36	42.51

The reflection 0 0 1 was obscured by the backstop.

0	0	2	43.40	43.35	-43.35	-0.01
0	0	3	41.09	43.78	-43.78	0.00
0	0	4	22.26	24.17	-24.17	0.00
0	0	5	11.51	12.51	12.51	-0.00
0	0	6	25.32	21.54	21.34	-0.00
0	0	7	27.09	25.01	25.01	0.00
0	0	8	4.09	3.89	-3.89	-0.00
0	0	9	19.58	21.19	-21.19	0.00
0	0	10	9.46	9.22	-9.22	-0.00
0	0	11	4.21	3.68	-3.68	-0.00
0	0	12	16.24	15.49	-15.49	0.00
1	0	1	11.18	10.34	-10.34	-0.00
1	0	2	46.67	52.47	-52.47	0.00
1	0	3	33.97	35.03	-35.03	0.00
1	0	4	35.23	37.98	-37.98	0.00
1	0	5	38.36	41.99	-41.99	0.00
1	0	6	2.25	1.86	-1.86	-0.00
1	0	7	14.65	14.57	-14.57	-0.00
1	0	8	14.23	12.38	-12.38	-0.00
1	0	9	1.78	1.57	-1.57	-0.00
1	0	10	8.62	8.47	-8.47	-0.00
1	0	11	8.70	7.46	-7.46	-0.00
1	0	-1	19.20	16.17	-16.17	0.00
1	0	-2	41.23	44.13	44.13	-0.00
1	0	-3	6.90	4.63	-4.63	-0.00
1	0	-4	38.47	37.86	-37.86	0.00
1	0	-5	37.52	38.41	38.41	0.00
1	0	-6	7.14	7.07	-7.07	0.00
1	0	-7	27.14	30.19	-30.19	0.00
1	0	-8	10.36	8.98	-8.98	-0.00
1	0	-9	4.12	2.37	-2.37	0.00
1	0	-10	8.17	7.82	-7.82	-0.00
1	0	-11	14.07	11.81	-11.81	0.00
2	0	1	15.23	16.06	-16.06	0.00
2	0	2	46.60	54.53	-54.53	0.00
2	0	3	39.73	44.81	-44.81	-0.00
2	0	4	8.91	8.42	-8.42	-0.00
2	0	5	13.83	13.28	-13.28	-0.00
2	0	6	24.22	23.31	-23.31	0.00
2	0	7	8.44	9.21	-9.21	0.00
2	0	8	10.86	9.50	-9.50	0.00
2	0	9	12.66	11.96	-11.96	0.00
2	0	10	5.94	5.32	-5.32	0.00
2	0	11	5.91	4.40	-4.40	0.00
2	0	-1	49.16	54.43	-54.43	-0.00
2	0	-2	29.41	25.95	-25.95	0.00
2	0	-3	19.08	19.86	-19.86	-0.00
2	0	-4	5.96	7.44	-7.44	-0.00
2	0	-5	1.17	1.40	-1.40	-0.00
2	0	-6	30.47	31.20	-31.20	-0.00
2	0	-7	27.38	29.28	-29.28	0.00
2	0	-8	1.84	1.44	-1.44	-0.00
2	0	-9	16.62	18.83	-18.83	0.00
2	0	-10	10.11	10.78	-10.78	-0.00
2	0	-11	0.95	0.88	-0.88	0.00
3	0	0	6.84	5.4	-5.4	0.00
3	0	1	33.46	37.65	-37.65	-0.00
3	0	2	34.41	35.98	-35.98	-0.00
3	0	3	2.33	2.38	-2.38	-0.00
3	0	4	31.98	33.40	-33.40	0.00
3	0	5	26.14	27.50	-27.50	0.00
3	0	6	7.89	7.23	-7.23	-0.00
3	0	7	10.39	10.57	-10.57	0.00
3	0	8	8.61	8.44	-8.44	-0.00
3	0	9	1.31	1.73	-1.73	0.00
3	0	10	8.05	5.4	-5.44	0.00
3	0	-1	28.16	27.37	-27.37	0.00
3	0	-2	45.17	46.84	-46.84	0.00
3	0	-3	18.33	15.63	-15.63	-0.00
3	0	-4	45.84	48.7	-48.7	-0.00
3	0	-5	42.66	45.79	-45.79	-0.00
3	0	-6	13.09	13.53	-13.53	0.00
3	0	-7	9.22	10.10	-10.10	-0.00
3	0	-8	15.13	16.29	-16.29	-0.00
3	0	-9	3.45	3.63	-3.63	-0.00
3	0	-10	3.87	3.34	-3.34	0.00
4	0	0	26.25	28.24	-28.24	-0.00
4	0	1	3.38	3.10	-3.10	-0.00
4	0	2	19.05	19.25	-19.25	0.00
4	0	3	7.72	8.4	-8.4	-0.00
4	0	4	4.97	4.96	-4.96	0.00
4	0	5	16.07	17.49	-17.49	0.00
4	0	6	17.77	18.71	-18.71	0.00
4	0	7	5.74	5.44	-5.44	-0.00
4	0	8	2.90	2.40	-2.40	0.00
4	0	9	6.86	5.76	-5.76	-0.00
4	0	10	0.76	0.13	-0.13	0.00
4	0	-1	15.67	13.41	-13.41	-0.00
4	0	-2	5.04	4.65	-4.65	-0.00
4	0	-3	22.99	22.70	-22.70	0.00
4	0	-4	16.46	15.10	-15.10	-0.00
4	0	-5	1.35	1.1	-1.1	0.00
4	0	-6	12.66	12.69	-12.69	-0.00
4	0	-7	11.33	12.14	-12.14	0.00
4	0	-8	1.46	0.16	-0.16	0.00
4	0	-9	11.94	11.02	-11.02	0.00
4	0	-10	8.65	8.44	-8.44	-0.00
5	0	0	10.76	9.68	-9.68	0.00
5	0	1	17.75	17.69	-17.69	-0.00
5	0	2	14.33	12.55	-12.55	-0.00
5	0	3	13.32	12.53	-12.53	0.00
5	0	4	17.64	17.00	-17.00	-0.00
5	0	5	4.11	4.40	-4.40	-0.00
5	0	6	6.53	5.46	-5.46	-0.00
5	0	7	9.53	8.53	-8.53	-0.00
5	0	8	6.13	5.22	-5.22	-0.00
5	0	9	0.86	0.74	-0.74	-0.00
5	0	-1	15.56	15.47	-15.47	-0.00

5	0	-2	22.93	22.88	22.88	0.00
5	0	-3	12.86	11.48	-11.48	-0.00
5	0	-4	7.19	6.86	-6.86	-0.00
5	0	-5	24.45	26.13	-26.13	-0.00
5	0	-6	10.56	11.27	-11.27	-0.00
5	0	-7	6.24	6.70	-6.70	-0.00
5	0	-8	9.41	9.52	-9.52	-0.00
5	0	-9	5.46	4.84	-4.84	-0.00
6	0	0	19.84	20.25	-20.25	0.00
6	0	1	7.9	7.48	-7.48	-0.00
6	0	2	1.49	0.44	-0.44	-0.00
6	0	3	7.58	7.35	-7.35	-0.00
6	0	4	3.17	3.24	-3.24	-0.00
6	0	5	4.33	3.99	-3.99	-0.00
6	0	6	6.73	6.29	-6.29	-0.00
6	0	7	1.99	2.29	-2.29	-0.00
6	0	8	6.78	4.47	-4.47	-0.00
6	0	-1	19.19	18.36	-18.36	0.00
6	0	-2	1.80	2.30	-2.30	-0.00
6	0	-3	16.96	17.15	-17.15	-0.00
6	0	-4	10.87	11.62	-11.62	0.00
6	0	-5	2.59	0.74	-0.74	-0.00
6	0	-6	7.93	7.96	-7.96	0.00
6	0	-7	8.38	9.44	-9.44	0.00
6	0	-8	1.16	0.88	-0.88	-0.00
7	0	0	6.34	6.39	-6.39	-0.00
7	0	1	12.49	12.19	-12.19	-0.00
7	0	2	5.69	5.27	-5.27	-0.00
7	0	3	4.28	3.80	-3.80	-0.00
7	0	4	4.8	5.14	-5.14	0.00
7	0	5	3.10	2.32	-2.32	0.00
7	0	6	1.08	1.14	-1.14	0.00
7	0	-1	3.17	2.30	-2.30	-0.00
7	0	-2	6.05	5.60	-5.60	0.00
7	0	-3	6.76	6.61	-6.61	-0.00
7	0	-4	1.44	0.79	-0.79	-0.00
7	0	-5	6.28	6.01	-6.01	0.00
7	0	-6	5.34	5.22	-5.22	0.00
7	0	-7	2.66	2.74	-2.74	-0.00
7	0	-8	5.33	4.61	-4.61	0.00
8	0	0	1.30	1.35	-1.35	-0.00
8	0	1	5.89	5.48	-5.48	0.00
8	0	2	3.98	4.08	-4.08	-0.00
8	0	3	1.01	0.62	-0.62	0.00
8	0	4	4.33	2.98	-2.98	0.00
8	0	5	6.72	7.22	-7.22	0.00
8	0	-1	1.31	1.33	-1.33	0.00
8	0	-2	4.11	4.44	-4.44	-0.00
8	0	-3	4.62	4.79	-4.79	-0.00
8	0	-4	1.08	0.46	-0.46	-0.00
8	0	-5	1.81	1.60	-1.60	-0.00
9	0	0	1.51	1.82	-1.82	-0.00
9	0	1	0.76	0.85	-0.85	-0.00
9	0	2	1.045	0.15	-0.15	-0.00
9	0	-1	1.62	1.97	-1.97	0.00
9	0	-2	1.76	1.77	-1.77	-0.00
9	0	-3	0.83	0.04	0.04	0.00
9	0	1	13.42	13.78	-13.78	-0.00
9	0	2	37.43	40.79	-40.79	-0.00
9	0	3	22.67	22.03	-22.03	-0.00
9	0	4	41.72	43.35	-43.35	-0.00
9	0	5	18.46	17.22	-17.22	-0.00
9	0	6	8.10	7.22	-7.22	-0.00
9	0	7	21.42	21.50	-21.50	-0.00
9	0	8	13.42	13.55	-13.55	-0.00
9	0	9	1.41	1.79	-1.79	-0.00
9	0	10	8.59	8.74	-8.74	-0.00
9	0	11	10.87	8.31	-7.69	-0.00
9	0	12	37.74	39.45	-39.45	-0.00
9	0	13	39.85	37.35	-37.35	-0.00
9	0	14	44.81	44.35	-44.35	-0.00
9	0	15	8.7	8.92	-8.92	-0.00
9	0	16	19.99	20.32	-20.32	-0.00
9	0	17	32.16	32.11	-32.11	-0.00
9	0	18	18.09	17.07	-17.07	-0.00
9	0	19	8.48	7.34	-7.34	-0.00
9	0	20	13.18	12.44	-12.44	-0.00
9	0	21	8.57	8.02	-8.02	-0.00
9	0	22	5.59	4.91	-4.91	-0.00
9	0	23	34.37	35.95	-35.95	-0.00
9	0	24	30.11	30.73	-30.73	-0.00
9	0	25	60.55	60.13	-60.13	-0.00
9	0	26	44.31	39.40	-39.40	-0.00
9	0	27	5.1	3.64	-3.64	-0.00
9	0	28	24.47	24.59	-24.59	-0.00
9	0	29	25.56	27.30	-27.30	-0.00
9	0	30	1.44	1.05	-1.05	-0.00
9	0	31	16.91	17.94	-17.94	-0.00
9	0	32	7.91	7.92	-7.92	-0.00
9	0	33	0.94	1.09	-1.09	-0.00
9	0	34	12.58	11.70	-11.70	-0.00
9	0	35	49.18	53.02	-53.02	-0.00
9	0	36	26.18	24.22	-24.22	-0.00
9	0	37	18.41	15.22	-15.22	-0.00
9	0	38	28.			

Table with multiple columns of numerical data, organized in rows and columns, likely representing a dataset or financial records. The data is arranged in a grid-like structure with varying column widths.

0	4	5	7.22	7.03	-6.64	3.56	6	4	5	2.79	2.36	2.84	-0.01	4	5	-5	6.57	5.00	-5.35
0	4	6	18.02	18.35	-17.68	4.92	6	4	6	3.33	4.24	4.21	0.55	4	5	-6	3.00	2.93	-2.70
0	4	7	5.86	4.90	-4.75	1.21	6	4	7	0.89	0.63	0.23	0.57	4	5	-7	5.72	6.35	-4.71
0	4	8	4.04	3.97	2.19	-3.21	6	4	8	10.41	9.05	7.29	-5.36	4	5	-8	10.54	8.15	-4.74
0	4	9	9.93	9.27	7.45	-6.07	6	4	9	3.37	2.73	2.56	0.94	4	5	-9	7.76	6.44	-4.34
0	4	10	6.16	5.99	5.42	-2.55	6	4	10	9.09	7.92	6.75	4.15	4	5	0	1.79	1.15	-6.14
1	4	0	25.71	28.99	16.43	-17.77	6	4	11	8.89	8.85	8.55	7.36	4	5	1	0.82	4.70	5.49
1	4	1	35.15	39.07	26.83	-15.27	6	4	12	1.78	2.00	-1.07	2.38	4	5	2	11.29	10.33	16.42
1	4	2	23.83	25.25	21.96	-12.49	6	4	13	6.88	6.11	5.96	-2.07	4	5	3	2.10	2.66	2.11
1	4	3	4.93	5.01	-3.50	-3.59	6	4	14	6.53	5.10	3.72	-3.27	4	5	4	3.38	3.78	-3.65
1	4	4	15.79	19.57	-15.91	11.39	7	4	0	4.35	4.32	-0.44	4.50	4	5	5	5.12	6.10	-5.15
1	4	5	11.71	15.06	-10.94	10.35	7	4	1	5.65	5.03	-4.38	3.54	4	5	6	3.17	2.14	6.75
1	4	6	5.19	4.97	4.27	-2.37	7	4	2	4.11	4.00	-4.44	1.20	4	5	7	7.29	7.07	-5.53
1	4	7	14.16	15.05	12.66	-8.69	7	4	3	1.57	1.70	0.69	-1.55	4	5	8	3.80	3.40	-1.46
1	4	8	13.20	14.77	12.91	-5.35	7	4	4	4.18	4.09	3.76	-2.63	4	5	9	10.29	9.74	2.29
1	4	9	4.48	4.22	2.45	3.80	7	4	5	1.11	2.09	2.07	-0.26	4	5	10	10.61	9.03	9.75
1	4	10	6.11	5.70	-3.37	4.60	7	4	6	7.55	7.21	6.29	3.53	4	5	11	1.73	0.04	0.36
1	4	11	35.85	40.08	-19.96	3.11	7	4	7	7.75	7.54	6.90	-3.04	4	5	12	8.41	6.04	-4.65
1	4	12	29.39	32.97	-30.12	13.48	7	4	8	6.24	5.94	2.94	-5.17	4	5	13	5.54	5.73	-4.53
1	4	13	5.97	5.48	-5.16	1.84	7	4	9	2.77	2.20	-2.45	-0.49	4	5	14	6.39	5.22	2.52
1	4	14	15.31	15.9	12.97	-8.55	7	4	10	5.29	5.15	-5.02	1.13	4	5	15	6.99	6.93	5.72
1	4	15	18.15	18.09	17.01	-7.49	8	4	0	2.85	3.10	-2.28	2.09	4	5	16	7.12	7.40	3.24
1	4	16	11.24	9.03	6.65	6.12	8	4	1	1.28	1.96	0.76	-1.85	4	5	17	4.33	5.01	-1.40
1	4	17	13.95	13.40	-6.47	11.73	8	4	2	3.16	4.43	1.90	-4.03	4	5	18	4.77	5.09	-5.05
1	4	18	16.79	17.19	-16.40	5.14	8	4	3	0.90	1.01	1.42	-1.21	4	5	19	1.75	1.87	-1.87
1	4	19	6.21	6.20	-6.50	-0.03	8	4	4	1.17	2.00	1.42	1.10	4	5	20	1.57	1.92	0.91
1	4	20	5.98	5.01	-4.38	4.12	8	4	5	1.33	0.20	0.20	-0.70	4	5	21	7.26	8.06	-6.73
2	4	0	20.40	18.82	-14.12	-9.24	8	4	6	1.22	2.20	2.15	-0.48	4	5	22	8.43	7.11	-7.66
2	4	1	20.90	17.25	16.61	-3.85	0	5	2	19.75	26.44	-22.35	-13.36	4	5	23	4.80	4.41	-4.39
2	4	2	20.46	18.01	-5.78	17.27	0	5	3	9.74	11.53	-6.28	-7.43	4	5	24	3.93	3.05	3.35
2	4	3	32.06	33.32	-26.73	19.90	0	5	4	13.52	16.03	15.96	1.51	4	5	25	7.02	6.95	6.66
2	4	4	19.22	19.12	-19.65	-1.58	0	5	5	14.92	17.02	16.50	4.16	4	5	26	2.72	3.08	2.96
2	4	5	10.03	11.01	7.33	-8.22	0	5	6	4.87	4.44	4.02	1.63	4	5	27	2.56	2.27	2.25
2	4	6	9.48	12.17	11.28	-4.55	0	5	7	11.93	12.47	-12.41	1.26	4	5	28	1.44	1.44	-1.52
2	4	7	5.82	5.98	5.69	1.86	0	5	8	13.53	12.13	-12.06	-1.27	4	5	29	3.51	4.07	-4.29
2	4	8	4.95	5.03	-5.69	5.28	0	5	9	4.10	3.07	-6.74	-3.50	4	5	30	2.10	2.08	-2.63
2	4	9	7.21	7.20	-5.65	4.12	0	5	10	2.25	2.07	3.56	-0.04	4	5	31	1.18	1.01	-7.62
2	4	10	10.90	8.72	-7.61	4.25	1	5	0	19.43	18.34	-18.22	-2.29	4	5	32	3.14	3.03	2.55
2	4	11	7.71	6.09	-5.68	-3.33	1	5	1	14.94	13.47	-13.39	1.47	4	5	33	2.51	2.6	-0.09
2	4	12	8.00	8.91	-3.38	8.25	1	5	2	16.46	17.00	17.07	-2.84	4	5	34	3.37	3.4	-3.37
2	4	13	28.24	29.99	-23.43	9.54	1	5	3	18.24	20.20	20.49	-0.85	4	5	35	3.07	3.21	-2.54
2	4	14	19.94	19.75	-19.47	3.30	1	5	4	10.59	11.42	8.62	7.49	4	5	36	1.07	1.44	-1.54
2	4	15	8.15	7.40	5.92	-4.44	1	5	5	8.86	11.40	-8.91	7.10	4	5	37	1.56	2.47	-1.54
2	4	16	21.79	22.12	17.67	-13.31	1	5	6	8.76	10.43	-10.38	-1.02	4	5	38	0.90	0.88	0.83
2	4	17	13.11	11.77	8.21	-8.44	1	5	7	6.48	6.91	-2.41	-6.47	4	5	39	7.81	6.83	6.55
2	4	18	6.88	6.02	-5.13	4.18	1	5	8	7.01	6.83	6.55	1.89	4	5	40	0.78	3.98	3.66
2	4	19	7.78	7.21	-4.69	5.99	1	5	9	10.19	9.78	3.98	3.66	4	5	41	6.19	5.03	-4.18
2	4	20	5.93	5.20	-4.75	2.11	1	5	10	12.50	12.35	12.11	-2.40	4	5	42	12.50	12.35	12.11
3	4	0	8.72	7.61	-4.25	4.25	1	5	11	20.93	25.1	24.34	-7.33	4	5	43	10.87	11.07	9.60
3	4	1	25.87	24.46	-22.16	11.22	1	5	12	3.83	5.78	-5.77	-0.43	4	5	44	5.78	5.77	-0.43
3	4	2	10.16	9.25	-7.71	2.93	1	5	13	12.14	13.17	-13.15	-0.74	4	5	45	6.53	6.79	-6.75
3	4	3	9.93	9.65	9.24	-2.81	1	5	14	3.49	3.93	3.90	-0.48	4	5	46	8.71	7.67	7.56
3	4	4	7.71	8.40	6.16	-6.29	1	5	15	10.19	11.47	4.17	4.73	4	5	47	12.52	9.91	9.86
3	4	5	10.77	11.77	8.24	-8.40	1	5	16	18.67	16.74	16.74	0.34	4	5	48	15.38	12.55	10.73
3	4	6	2.39	2.54	-0.92	-2.63	1	5	17	3.69	3.69	-2.96	-1.66	4	5	49	10.31	11.45	-9.88
3	4	7	7.64	9.71	-8.69	4.33	1	5	18	9.14	11.48	-11.48	0.12	4	5	50	1.79	0.99	0.28
3	4	8	7.10	8.20	-9.02	1.73	1	5	19	12.27	13.08	13.63	-1.21	4	5	51	12.27	13.08	13.63
3	4	9	4.24	3.25	-2.22	-2.60	1	5	20	8.71	7.67	7.56	0.71	4	5	52	10.33	8.98	8.91
3	4	10	25.94	18.22	16.46	-9.22	2	5	0	4.18	4.17	4.73	-1.52	4	5	53	1.15	1.07	0.14
3	4	11	27.82	23.07	-13.70	-14.52	2	5	1	18.67	16.74	16.74	0.34	4	5	54	22.37	18.00	-17.76
3	4	12	1.62	2.09	0.43	-2.04	2	5	2	15.38	12.55	10.73	6.67	4	5	55	23.45	22.34	-22.24
3	4	13	15.69	15.09	-3.64	15.27	2	5	3	3.69	3.69	-2.96	-1.66	4	5	56	7.55	6.46	-6.36
3	4	14	12.76	11.44	-6.18	9.63	2	5	4	10.31	11.45	-9.88	-7.79	4	5	57	9.42	7.04	7.62
3	4	15	5.84	6.44	-5.60	3.18	2	5	5	9.14	11.48	-11.48	0.12	4	5	58	15.97	14.36	12.15
3	4	16	3.80	4.01	4.65	-1.32	2	5	6	1.79	0.99	0.28	0.95	4	5	59	5.37	5.12	1.40
3	4	17	13.94	13.57	12.23	-5.41	2	5	7	12.27	13.08	13.63	-1.21	4	5	60	6.46	6.76	-6.70
3	4	18	7.47	7.38	7.09	-2.35	2	5	8	10.33	8.98	8.91	-1.15	4	5	61	11.27	10.99	-10.36
3	4	19	17.47	14.00	-13.06	5.27	2	5	9	6.19	5.40	-4.01	-3.45	4	5	62	6.19	5.40	-4.01
3	4	20	7.32	5.00	-4.73	-2.70	2	5	10	21.76	20.00	18.72	9.13	4	5	63	18.67	17.21	-17.16
4	4	0	14.19	12.48	6.66	-10.56	2	5	11	23.45	22.34	-22.24	2.09	4	5	64	4.35	3.08	2.62
4	4	1	22.73	21.09	20.79	-9.85	2	5	12	7.55	6.46	-6.36	-1.15	4	5	65	13.13	13.15	13.11
4	4	2	8.19	8.07	5.18	2.53	2	5	13	9.42	7.04	7.62	0.51	4	5	66	10.30	11.19	8.95
4	4	3	10.15	11.24	-5.42	9.85	2	5	14	5.69	6.33	5.60	3.92	4	5	67	5.69	6.33	5.60
4	4	4	7.34	9.37	-7.86	5.10	2	5	15	15.97	14.36	12.15	6.25	4	5	68	7.90	7.05	1.89
4	4	5	1.73	2.33	-1.97	-1.24	2	5	16	4.04	3.79	-3.28	1.91	4	5	69	4.04	3.79	-3.28
4	4	6	3.93	4.14	3.61	-2.02	2	5	17	6.19	5.40	-4.01	-3.45						



### 6.5. The Absolute Configuration of (+)-3-Bromocamphor.

It has been noted (Section 6.1) that the Bijvoet method, applied using the data of W & K (Table 6.2), failed to produce a conclusive consensus of anomalies. For the assignment of absolute configuration based on the refined structure the methods of both Bijvoet and Hamilton (see Chapter 3) were used.

#### i) The Bijvoet Method.

The Bijvoet pairs  $Ok\bar{l}$ ,  $Ok\bar{l}$ , used in the previous determination (A) were remeasured using a Joyce-Loebl integrating microdensitometer; the sign of the intensity difference was noted, and found to agree with the visual estimate in each case. Two additional pairs (035, 044) were included in the list, bringing the total to 20. The signs of the inequalities:  $F_T(Ok\bar{l}) - F_T(Ok\bar{l})$  were calculated exactly as described in section 6.1. Two determinations were made, one after refinement run A4 ( $R = 0.098$ ), and the other using the final parameters listed in Tables 6.4-6.6 ( $R = 0.079$ ); the agreement between observed and calculated inequalities is shown in Table 6.8, where the determinations are designated (B) and (C) respectively. Absorption effects were ignored throughout: the very regular shape of the crystal used meant that the correction for reflection and counter-reflection was virtually the same in this case.

TABLE 6.8.

(+)-3-Bromocamphor.Observed and Calculated Inequalities for the Bijvoet Pairs

hkl	s[I(Ok $\bar{l}$ ) - I(O $\bar{k}l$ )]	s[F(Ok $\bar{l}$ ) - F(O $\bar{k}l$ )]		
		A	B	C
011	+	+	+	+
012	-	+	-	-
013	-	+	-	-
014	-	+	-	-
015	-	+	-	-
016	+	+	+	+
017	-	-	-	-
022	+	+	+	+
023	+	+	+	+
024	-	-	-	-
025	+	+	+	+
026	+	+	+	+
027	-	-	-	-
029	+	+	+	+
033	+	+	+	+
034	-	-	-	-
035	-	-	-	-
036	+	+	+	+
043	+	+	+	+
044	-	-	-	-
		77.7%	100%	100%

ii) Hamilton's Method.

The data was corrected for anomalous dispersion (FC) using the scattering-factor correction terms given in Eq. 6.2. (p. 91 ). Four cycles of mixed-mode refinement was carried out using ORFLS; the parameters listed in Tables 6.4-6.6 were used, together with an overall scale-factor; the hydrogen parameters were not refined. The conventional R fell from 7.93% to 7.90%, and the weighted  $\underline{R}$  (  $\underline{R}_W^1$  ) was 11.449%; the maximum S/E was less than 0.10. A similar refinement of the enantiomorph (obtained by reversing all  $\underline{y}$ -co-ordinates) was carried out using the corrected data. Convergence was obtained after 5 cycles when the conventional R was 7.963% and the weighted  $\underline{R}$  (  $\underline{R}_W^2$  ) was 11.515%.

We may now test the one-dimensional hypothesis :

H : The second absolute configuration represents reality. The total number of parameters refined (n) was 108, and the number of observations (m) was 908; thus the number of degrees of freedom (m-n) is 800. Thus we have :

$$\mathcal{R}_{1,800,\infty} = \underline{R}_W^2 / \underline{R}_W^1 = 0.11515 / 0.11449 = 1.0057 \dots 6.3$$

From Table 1 of reference 66 we find :

$$\mathcal{R}_{1,120,0.005} = 1.034 \dots \dots \dots 6.4$$

and  $\mathcal{R}_{1,\infty,0.005} = 1.000 \dots \dots \dots 6.5$

The required value of  $\mathcal{R}$  may be obtained using the interpolation formulae quoted in the appendix to the paper, whence :

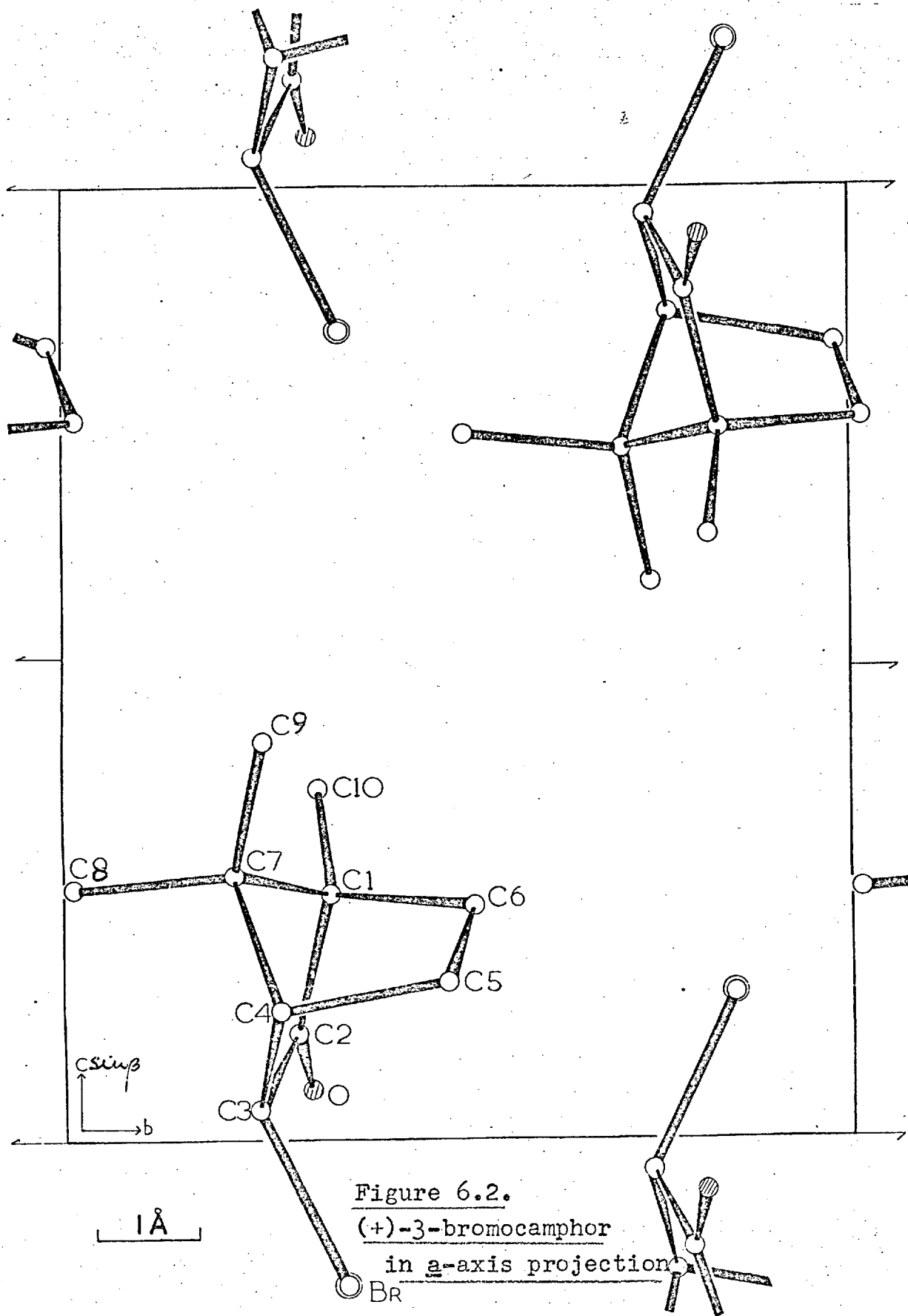
$$\mathcal{R}_{1,800,0.005} = 1.0051 \dots\dots\dots 6.6.$$

The hypothesis therefore has approximately 0.5% significance, and can be rejected.

The exceptionally small difference in weighted R-factors ( 0.07% ) is a consequence of the small value of  $f''$  (1.5); nevertheless the application of significance test theory has produced a remarkably high vote of confidence in the correct configuration. However it appears that only very slight systematic errors in the data could lead to erroneous results; assignments obtained solely by this method, and based on a very low R-factor difference, should be treated with caution.

#### 6.6. Discussion of the Absolute Configuration.

The results of both Bijvoet's and Hamilton's techniques show conclusively that the structure as determined, and drawn on a right-handed system of axes, represents the true absolute stereochemistry. Figure 6.2 shows the structure projected down the a-axis, and gives the conventional representation, shown in Figure 6.3 (cf. structural formula 5.XV) with the gem-dimethyl bridge



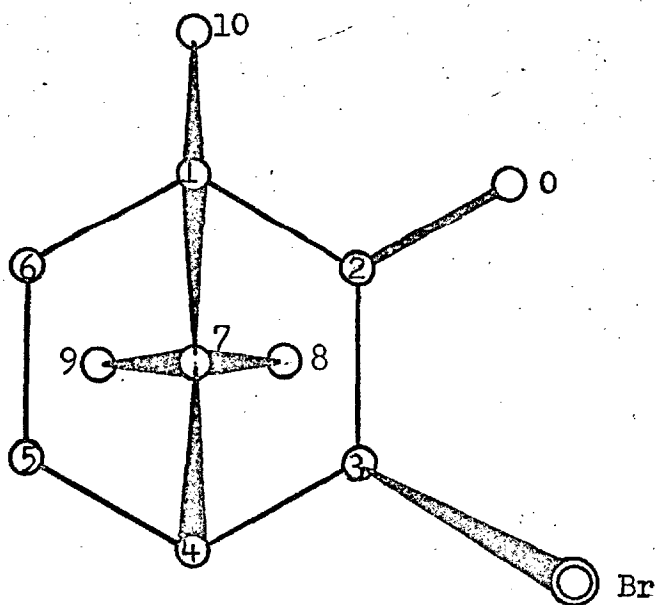


Figure 6.3. Absolute Configuration of (+)-3-Bromocamphor in the Conventional Chemical Representation.

below the plane of the paper. This confirms the degradative work of Fredga and Miettinen<sup>(110a)</sup>, Porath<sup>(110b)</sup> and Freudenburg and Lwowski<sup>(119)</sup>. Not only are the absolute configurations of (+)-fenchone (6.II Fig.6.4) and (+)- $\alpha$ -pinene confirmed by this work, but also those of the degradation products mentioned briefly in chapter 5. The next Figure (6.4) shows the stereochemical relationships between (+)-camphor (6.I), (-)-camphoronic acid (6.III), and (-)- $\alpha$ -methyl- $\alpha$ -isopropyl succinic acid (6.IV) after

Porath; it also shows the relationships between (+)-fenchone (6.II), (-)-~~X~~-isopropyl glutaric acid (6.V) and (+)-isopropyl succinic acid (6.VI) due to Fredga and Miettinen. Since the last mentioned compound occupies a key position in the stereochemical correlation chart for the monoterpenes drawn up by Birch<sup>(109)</sup>, the work described here, together with other X-ray work on substituted succinic acids<sup>(115,117)</sup>, has confirmed the absolute stereochemistry of a wide range of compounds. In particular the unequivocal definition of configuration of (6.IV) from the present work, and by other, more recent X-ray studies<sup>(117)</sup>, has confirmed the configurations assigned by Norin<sup>(148)</sup> to several members of the thujane group of monoterpenes. The time would seem right for an extensive review of monoterpene correlations, especially in the light of recent X-ray work; the brief outline given here and in chapter 5 does, however, show how the X-ray method, combined with known chemical data, can lead to extensive, and completely unequivocal assignments.

It was gratifying to note that, shortly after the completion of this work, two further determinations of the absolute configuration of (+)-camphor appeared in the literature : both agreed with the work described above. The first of these, by Northolt and Palm<sup>(149)</sup>, followed

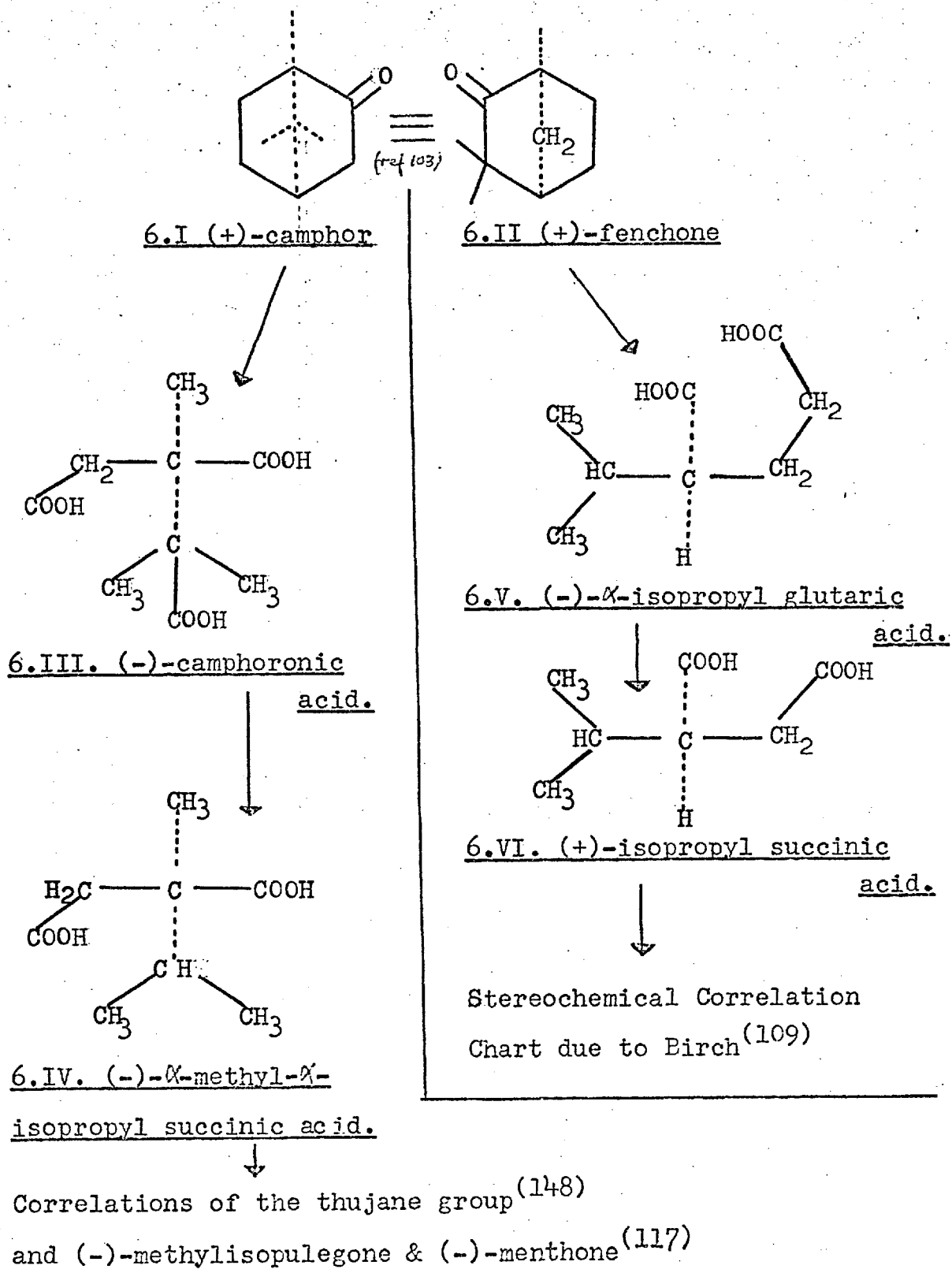


Figure 6.4.

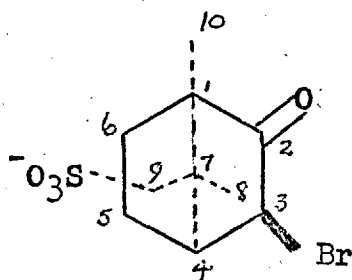


exactly the same scheme as described for determination A (section 6.1). The 3-bromo- compound was studied, and W & K's parameters used to obtain the calculated inequalities for only 9 Bijvoet pairs. We had much earlier rejected this method since it gave an inconclusive consensus of anomalies over 18 pairs. This case shows the danger of resurrecting old structures from the literature, in order to carry out configurational work; the accuracy of the parameters used is frequently not good enough to guarantee the result.

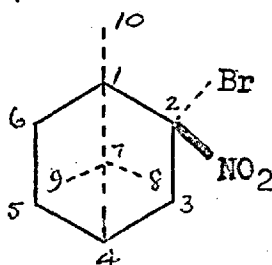
In their paper, Northolt and Palm cite the determination of the structure and absolute configuration of (+)-camphoroxime hydrobromide ( H.A.J. Oonk, Ph.D. Thesis, Utrecht 1965). To the author's knowledge this work has not yet appeared in the chemical literature, a surprising omission, considering it's relevance to the monoterpenes.

More recently the crystal structure of retusamine as the (+)-3-bromocamphor-9( $\alpha$ )-sulphonate monohydrate has been published<sup>(150)</sup>. Using Br excited by  $\text{CuK}\alpha$  radiation, the absolute configuration of both cation and anion have been established, that of the anion confirming the above assignments. This raises the possibility of using (+)-camphor- $\alpha$ -sulphonate salts (or their derivatives) as internal reference centres, to establish the absolute configuration of a complex organic cation.

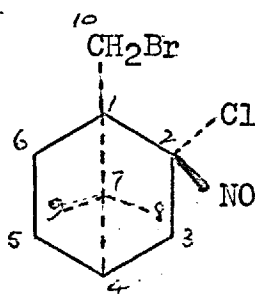
The substitution of bromine at C(3) in (+)-camphor gives rise to a third asymmetric centre. Figure 6.3 shows that the bromine is trans to the gem-dimethyl bridge (endo-configuration). The same configuration is found in the (+)-3-bromocamphor-trans-9( $\kappa$ )-sulphonate anion<sup>(150)</sup> (BCSO : 6.VII) and in bromo-isofenchone<sup>(151)</sup>; this contrasts with the cis-position adopted by the bulky halogen atom in (-)-2-bromo-2-nitrocamphane<sup>(137)</sup> (BNC : 6.VIII), and in (+)-10-bromo-2-chloro-2-nitroso-camphane<sup>(152)</sup> (BCNC : 6.IX).



6.VII. BCSO. (150)



6.VII. BNC. (137)\*



6.IX. BCNC. (152)\*

\* see footnote [ on page 125.

## 6.7. Discussion of the Structure.

### Molecular Geometry.

The bond lengths and valence angles within the asymmetric unit are given in Tables 6.9, 6.10, together with their estimated standard deviations; again these probably represent realistic estimates. The parameters are shown for clarity in Figure 6.5(a) and (b). Comparison with the values obtained by W & K is not significant, due to the lack of refinement in their determination.

The bond lengths are, in general, unremarkable. The short bond C(3)-C(4), and the long bond C(4)-C(5), are the only ones which differ by more than  $2.5\sigma$  from the accepted C-C single bond length of  $1.539 \text{ \AA}^{(153)}$ . This may not appear significant out of context, but is possibly a result of the strain due to the 'one-sided' substitution pattern. The overall average C-C distance ( $1.53\text{\AA}$ ) is close to the accepted average; however the average length on the substituted side of the six-membered ring, C(1)-C(4)<sup>‡</sup>, is  $1.50\text{\AA}$ , while on the unsubstituted side, C(4)-C(1)<sup>‡</sup>, it is  $1.55\text{\AA}$ . Comparable results have been found for BNC ( $1.52$  &  $1.58\text{\AA}$ ), and BCSO ( $1.53$  &  $1.56\text{\AA}$ ); the effect is not marked in BCNC ( $1.55$  &  $1.56\text{\AA}$ ), possibly due to the effect of the bulky Br atom at C(10).

---

‡ Numbering clockwise.

TABLE 6.9

(+)-3-Bromocamphor.

Intramolecular Bonded Distances (r) and their Estimated  
Standard Deviations ( $\sigma$ ) in Angstroms

	r	$\sigma$		r	$\sigma$
C(1) - C(2)	1.52	0.02	C(3) - C(4)	1.47	0.02
C(1) - C(6)	1.49	0.03	C(3) - Br	1.934	0.013
C(1) - C(10)	1.52	0.02	C(4) - C(5)	1.60	0.03
C(1) - C(7)	1.53	0.02	C(4) - C(7)	1.53	0.02
C(2) - C(3)	1.53	0.02	C(5) - C(6)	1.56	0.02
C(2) - O	1.20	0.01	C(7) - C(8)	1.56	0.03
C(7) - C(9)	1.55	0.02			

Average C - C single bond length :  $1.53 \pm 0.02 \text{ \AA}$

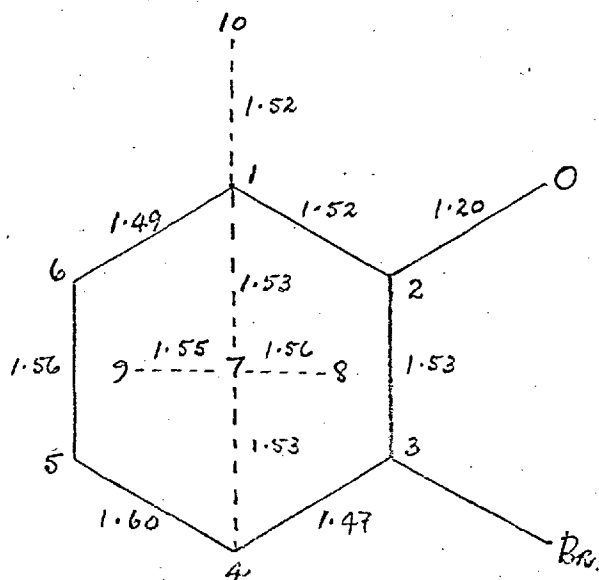


Figure 6.5 (a)

TABLE 6.10.

(+)-3-Bromocamphor.Valence Angles ( $\theta^\circ$ ) and their Estimated Standard Deviations ( $\sigma$ )

	$\theta^\circ$	$\sigma$		$\theta^\circ$	$\sigma$
C(1)-C(2)-C(3)	105.1	0.8	C(3)-C(2)-O	126.4	1.0
C(1)-C(2)-O	128.4	1.1	C(3)-C(4)-C(5)	111.1	1.3
C(1)-C(6)-C(5)	104.3	1.4	C(3)-C(4)-C(7)	103.5	1.0
C(1)-C(7)-C(4)	94.4	1.2	C(4)-C(3)-Br	118.7	1.1
C(1)-C(7)-C(8)	112.8	1.4	C(4)-C(5)-C(6)	101.2	1.3
C(1)-C(7)-C(9)	112.4	1.2	C(4)-C(7)-C(8)	115.4	1.2
C(2)-C(1)-C(6)	104.3	1.3	C(4)-C(7)-C(9)	111.8	1.3
C(2)-C(1)-C(7)	101.8	1.2	C(5)-C(4)-C(7)	98.0	1.2
C(2)-C(1)-C(10)	111.6	1.1	C(6)-C(1)-C(7)	102.6	1.3
C(2)-C(3)-C(4)	102.2	1.0	C(6)-C(1)-C(10)	113.9	1.8
C(2)-C(3)-Br	113.1	1.0	C(7)-C(1)-C(10)	120.8	1.6
C(8)-C(7)-C(9)	109.5	1.4			

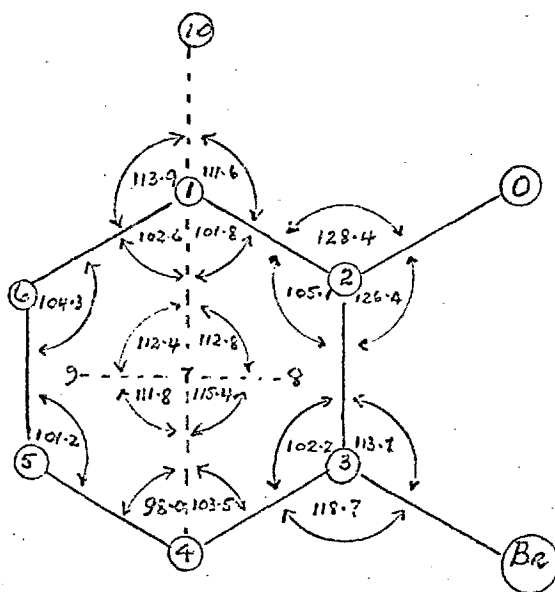


Figure 6.5 (b).

(For additional angles  
see above)

The C(3)-Br distance of 1.934 Å compares well with the average value for C-Br of 1.94 Å, quoted for the alkyl bromides<sup>(153)</sup>. The value in BCSO is, however, 0.05 Å longer. The C=O distance of 1.20 Å is exactly as determined for BCSO, and does not differ significantly from accepted averages<sup>(153)</sup>.

The most interesting feature of Table 6.10 is the negative deviation from the tetrahedral value (109.47°) of the valence angles in the norbornane skeleton, C(1)→C(7), in (+)-3-bromocamphor.(BC). Sim<sup>(154)</sup> has analysed this bicyclo[2,2,1]heptane system in terms of two fused cyclopentane rings having three corners in common, viz: C 2,3,4,7,1; C 5,6,4,7,1; (rings A & B). His theoretical analysis indicates that average values for the endocyclic valence angles should be approximately 100°; Table 6.11 shows the average values for rings A and B obtained here for BC, compared with the values for BCSO, BNC and BCNC. The results support Sim's work very well; in particular they show that the introduction of the ketonic oxygen at C(2) in BC and BCSO has little effect on the ring system.

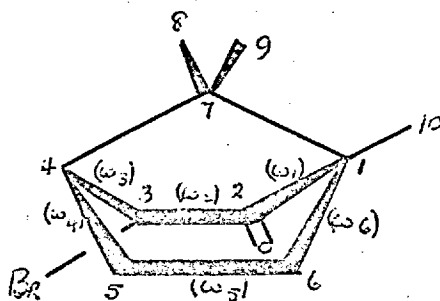
A noticeable feature of all compounds containing the norbornane skeleton is the consistently low value of the 'bridging' angle C(1)-C(7)-C(4). In the present structure it is 94.4°, comparing well with values of

93.1° in BCSO, 93.2° in BNC, and 95.0° & 91.2° in the two crystallographically independent molecules of BCNC. Sim<sup>(154)</sup> has ascribed this effect to the eclipsed interactions of groupings at C(2), C(3), C(5), C(6); this would appear reasonable since the interactions are relieved to some extent in anti-7-norbornenyl p-bromobenzoate<sup>(155)</sup>, anti-8-tricyclo-[3,2,1,0<sup>2,4</sup>]octyl p-bromobenzene sulphonate<sup>(156)</sup>, and p-bromobenzyl norbornamide<sup>(157)</sup>, and values for the 'bridge' angle of 96°, 97°, and 97°, respectively, are found.

The norbornane skeleton may also be regarded as a bridged cyclohexane ring, where the required cis-fusion of the bridge forces the ring into the boat conformation. This can be seen in Figure 6.2, and also in the perspective view of (+)-3-bromocamphor shown in 6.X below. The ideal conformation of the norbornane unit should consist of four four-atom planes, viz:

1,2,3,4; 1,6,5,4; 2,3,5,6; and 4,7,1,10;

table 6.12 shows the deviations (in Å) of the relevant atoms from the mean planes. The results for BC again compare well



6.X.

TABLE 6.11. Bicyclo[2,2,1]heptane system : average valence angles in the fused cyclopentane rings A & B.

	BC.	BCSO	BCNC		BNC
			1	2	
Ring A	101.4	99.7	101.1	100.4	101.3
Ring B	100.1	102.0	99.8	100.0	99.5

TABLE 6.12. Norbornane Skeleton : Deviations from mean planes (in  $\text{\AA}$ )

	BC.	BCSO	BCNC		BNC
			Mol 1.	Mol 2.	
C(1)	0.0241	-0.0124	-0.0287	0.0096	-0.0253
C(2)	-0.0354	0.0183	0.0421	-0.0139	0.0377
C(3)	0.0359	-0.0182	-0.0413	0.0143	-0.0384
C(4)	-0.0246	0.0123	0.0280	-0.0100	0.0261
C(1)	-0.0195	-0.0128	0.0030	-0.0021	0.0079
C(4)	0.0179	0.0119	-0.0030	0.0020	-0.0079
C(5)	-0.0261	-0.0174	0.0044	-0.0030	0.0113
C(6)	0.0277	0.0183	-0.0044	0.0031	-0.0113
C(2)	-0.0216	0.0105	-0.0259	-0.0234	0.0217
C(3)	0.0202	-0.0100	0.0250	0.0231	-0.0212
C(5)	-0.0199	0.0098	-0.0251	-0.0238	0.0206
C(6)	0.0212	-0.0103	0.0259	0.0241	-0.0211
C(4)	0.0293	-0.0050	0.0269	0.0055	0.0059
C(7)	-0.0140	0.0025	-0.0160	-0.0032	-0.0029
C(1)	-0.0495	0.0083	-0.0408	-0.0086	-0.0103
C(10)	0.0342	-0.0058	0.0299	0.0063	0.0073



with the values for BCSO, BNC, and BCNC; the deviations in all four compounds are small.

The strain-energy minimisation calculations\* of Hendrickson<sup>(158)</sup> have provided theoretical geometrical parameters for the most energetically stable cyclohexane conformations<sup>(159)</sup>. His optimum values of dihedral angles ( $\omega$ ) and valence angles ( $\theta$ ) for the boat-form, are compared with the values computed (MOJO)<sup>†</sup> for the cyclohexane ring in BC, BCSO, BNC, BCNC, in Table 6.13; The parameters involved are shown in 6.X, on the previous page. The results from the X-ray studies are very close, but differ significantly from the parameters for the minimum-energy form, showing the additional strain introduced by the presence of the gem-dimethyl bridge.

Table 6.14 shows the non-bonded intramolecular distances  $< 3.0 \text{ \AA}$  in BC. Robertson and his co-workers<sup>(152)</sup> cite the slightly longer distances from C(2) to C(7) and C(8)  $\sphericalangle$  (2.41 and 3.03  $\text{\AA}$ ) compared with those from C(6) to C(7) and C(9)  $\sphericalangle$  (2.39 and 2.88  $\text{\AA}$ ) in BCNC as indicative of the distorting effect of the bulky halogen atom cis to the gem-dimethyl bridge; a similar

---

\* see Appendix III for a brief discussion of this work.

† see Appendix II.  $\sphericalangle$  the numbering of C(8), C(9), has been reversed from that in the original papers to conform with chemical convention.

TABLE 6.13.

Comparison of Observed Dihedral Angles ( $\omega$ )<sup>o</sup> and Valence Angles ( $\theta$ )<sup>o</sup> for the Cyclohexane Ring with Values Obtained from Minimum Energy Calculations (159).

Param- eter	Theor. (159)	BC	BCSO	BCNC		BNC
				Mol 1	Mol 2	
$\omega_1$	52.1	77.8	73.8	73.9	67.6	72.7
$\omega_2$	0.0	6.1	3.0	6.9	2.3	6.5
$\omega_3$	52.1	65.1	69.3	65.9	71.5	68.9
$\omega_4$	52.1	68.2	68.7	71.8	71.7	71.2
$\omega_5$	0.0	4.4	2.9	0.7	0.5	1.8
$\omega_6$	52.1	73.1	73.3	67.2	68.5	68.3
$\theta_1$	112.0	104.3	104.2	107.6	108.4	105.2
$\theta_2$	112.5	105.1	104.3	106.9	101.9	105.8
$\theta_3$	112.5	102.2	103.7	100.2	104.4	102.5
$\theta_4$	112.0	111.1	108.4	113.5	112.2	113.9
$\theta_5$	112.5	101.2	100.1	103.7	98.2	100.0
$\theta_6$	112.5	104.3	106.2	104.2	109.6	105.3

TABLE 6.14.

(+)-3-Bromocamphor.Non-Bonded Intramolecular Distances (in Angstroms) < 3.0Å.

<u>Br</u> →		<u>C(3)</u> →		<u>C(7)</u> →	
C(2)	2.90	C(5)	2.53	C(10)	2.66
C(4)	2.93	C(6)	2.93		
		C(7)	2.35	<u>C(8)</u> →	
<u>C(1)</u> →		C(8)	2.85	C(9)	2.54
C(3)	2.42	0	2.45		
C(4)	2.25			<u>C(10)</u> →	
C(5)	2.40	<u>C(4)</u> →		0	2.91
C(8)	2.57	C(6)	2.44		
C(9)	2.56	C(8)	2.56		
0	2.45	C(9)	2.60		
<u>C(2)</u> →		<u>C(5)</u> →			
C(4)	2.33	C(7)	2.36		
C(5)	2.86	C(9)	2.84		
C(6)	2.37				
C(7)	2.37	<u>C(6)</u> →			
C(8)	2.91	C(7)	2.36		
C(10)	2.51	C(9)	2.87		
		C(10)	2.52		

pattern was noted for BNC. In the present case this distortion has been relieved due to a trans-substitution of Br at C(3). The table shows that the distances of C(2) and C(3) from C(7) and C(8) do not differ significantly from those of C(5) and C(6) to C(7) and C(9).

#### Intermolecular distances and Packing.

Figure 6.2 shows that the molecules pack in alternating layers parallel to the screw axes. This system is economical, but still allows clearances to be usually  $> 3.6 \text{ \AA}$ , as noted for BNC, and BCNC, which also crystallize in a space-group ( $P2_12_12_1$ ) involving only screw axes. Table 6.15. shows all intermolecular distances less than  $4.0 \text{ \AA}$ . Roman subscripts refer to atoms related to the set given in Table 6.4. by the following operations :

- (i)  $2-\underline{x}, \frac{1}{2}+\underline{y}, 1-\underline{z}$ ; (ii)  $2-\underline{x}, \frac{1}{2}+\underline{y}, -\underline{z}$ ; (iii)  $\underline{x}, 1+\underline{y}, \underline{z}$ ;  
 (iv)  $1-\underline{x}, \frac{1}{2}+\underline{y}, -\underline{z}$ .

TABLE 6.15. (+)-3-Bromocamphor : Intermolecular Distances

C(9) - C(8) <sub>i</sub>	3.95 Å	O - C(8) <sub>iv</sub>	3.59 Å
C(5) - Br <sub>ii</sub>	3.88	Br - C(8) <sub>iv</sub>	3.94
C(5) - C(3) <sub>ii</sub>	3.92	C(5) - O <sub>iv</sub>	3.88
C(6) - C(8) <sub>iii</sub>	3.83	C(6) - O <sub>iv</sub>	3.70
O - C(3) <sub>iv</sub>	3.54	Br - O <sub>iv</sub>	3.77

CHAPTER 7.The Crystal and Molecular Structure ofHumulene Bromohydrin :  $C_{15}H_{25}OBr$ .7.1. Preliminary Work.

The crystals were supplied by Dr. J. K. Sutherland and Dr. M. D. Solomon. They are colourless prisms with extinction directions transverse to the needle axis, possibly indicative of a monoclinic crystal with a non-unique axis (a- or c-) parallel to the needle direction. Oscillation and Weissenberg photographs confirmed this (Laue symmetry  $2/\underline{m}$ ), and showed that the crystals were stable to X-irradiation, giving excellent Weissenberg records after only 20 hours.

The photographs were indexed on a cell for which the absent spectra were :

$$h0l, \quad l \neq 2n; \quad 0k0 \quad k \neq 2n;$$

thus defining the space group uniquely as  $P2_1/\underline{c}$ .

Redefining  $\underline{c}$  reduced the  $\beta$ -angle by  $\approx 10^\circ$ , and changed the absence conditions to :

$$h0\bar{l}, \quad h + l \neq 2n; \quad 0k0 \quad k \neq 2n;$$

i.e. the space group was transformed to  $\underline{P}2_1/\underline{n}$ <sup>(160)</sup>. Cell parameters were obtained by a least-squares procedure (CEDI) applied to some 30 theta values measured from equatorial Weissenberg photographs.

### Crystal Data.

Humulene Bromohydrin:  $C_{15}H_{25}OBr$ ; Monoclinic  $\underline{P}2_1/\underline{n}$ :  $\underline{C}_{2h}^5$ : No. 14

$$\begin{aligned} \underline{a} &= 6.07 \pm 0.01 \text{ \AA}; & \underline{b} &= 19.54 \pm 0.02 \text{ \AA}; \\ \underline{c} &= 12.39 \pm 0.01 \text{ \AA}; & \beta &= 93.47^\circ \pm 0.25^\circ; \\ \underline{V} &= 1647 \text{ \AA}^3; & \underline{D}_x &= 1.36 \pm 0.03 \text{ g.cm}^{-3} \\ & & & \text{(by flotation)} \end{aligned}$$

$$\underline{D}_c = 1.37 \text{ g.cm}^{-3}; \quad \text{for } \underline{Z} = 4 \text{ molecules/cell};$$

$$\underline{M} = 301.27 \quad (\text{taking the standard } C^{12} = 12.00);$$

$$\underline{\mu} = 38.81 \text{ cm}^{-1} \quad \text{for } CuK\alpha \quad (\lambda_{\text{mean}} = 1.54178);$$

$$\underline{F}(000) = 632 \text{ electrons.} \quad \text{Needle axis : } \underline{a}.$$

The layers  $0k\bar{l}$ - $5k\bar{l}$  were photographed using Ni-filtered  $CuK\alpha$  radiation (see Chapter 4), using a crystal of approximate dimensions : 0.5 x 0.25 x 0.20 mm. A total of 1922 reflection intensities were visually estimated, and placed on a common (arbitrary) scale by comparison with 206 common data, from the (similarly recorded)  $h0\bar{l}$  and  $h\bar{l}\bar{l}$  layers, using the FOLIO program. A further 529

possible reflections in the Cu-sphere were treated as accidental absences, and included in the data list at a later stage. The absolute scale ( K ) was obtained during structure solution and refinement by comparing  $\sum |F_o|$  and  $\sum |F_c|$ .

## 7.2. Structure Solution.

The co-ordinates of the bromine atom were obtained from a 3D Patterson map. The symmetry equivalent positions in  $P2_1/n$  are :

1;	$\underline{x}$ ,	$\underline{y}$ ,	$\underline{z}$ ;	
2;	$-\underline{x}$ ,	$-\underline{y}$ ,	$-\underline{z}$ ;	
3;	$\frac{1}{2}-\underline{x}$ ,	$\frac{1}{2}+\underline{y}$ ,	$\frac{1}{2}-\underline{z}$ ;	..... 7.1
4;	$\frac{1}{2}+\underline{x}$ ,	$\frac{1}{2}-\underline{y}$ ,	$\frac{1}{2}+\underline{z}$ ;	

The resultant vector set for the four bromine atoms in the unit cell consists of six pairs of centrosymmetrically related peaks, whose co-ordinates, with respect to the bromine position :  $\underline{x}$ ,  $\underline{y}$ ,  $\underline{z}$ , are given by :

1;	$\pm$ (	$2\underline{x}$ ,	$2\underline{y}$ ,	$2\underline{z}$ ,	)	
2;	$\pm$ (	$-\frac{1}{2}+2\underline{x}$ ,	$-\frac{1}{2}$ ,	$-\frac{1}{2}+2\underline{z}$ ,	)	
3;	$\pm$ (	$-\frac{1}{2}$ ,	$-\frac{1}{2}+2\underline{y}$ ,	$-\frac{1}{2}$ ,	)	
4;	$\pm$ (	$-\frac{1}{2}$ ,	$-\frac{1}{2}-2\underline{y}$ ,	$-\frac{1}{2}$ ,	)	.... 7.2
5;	$\pm$ (	$-\frac{1}{2}-2\underline{x}$ ,	$-\frac{1}{2}$ ,	$-\frac{1}{2}-2\underline{z}$ ,	)	
6;	$\pm$ (	$-2\underline{x}$ ,	$2\underline{y}$ ,	$-2\underline{z}$ ,	)	

The full Patterson thus exhibits two Harker sections :

- 1:  $\underline{x}$ ,  $\frac{1}{2}$ ,  $\underline{z}$ , due to the  $2_1$  screw; ..... 7.3.  
 2:  $\frac{1}{2}$ ,  $\underline{y}$ ,  $\frac{1}{2}$ , due to the n-glide.

Use of the Harker sections gave the co-ordinates of bromine as :

$$\underline{x} = 0.093, \quad \underline{y} = 0.205 \quad \underline{z} = 0.247.$$

Using the phases given by the heavy atom ( $\underline{B} = 3.0\text{\AA}^2$ ) a 3D electron-density map was computed (BOSS); reflections for which  $|F_c| \leq 0.25 |F_o|$  were omitted from the Fourier summation;  $\underline{R}$  was 0.427. The nine atoms forming the macrocycle and fused cyclopropane ring\* were readily identified, and possible positions for C(9) and C(10) were also given. The resolution was, however, poor at the positions expected for the substituent methyl groups and hydroxyl.

Nine carbon atoms ( C(1)  $\rightarrow$  C(8) & C(11) ) were added to the structure factor calculation with  $\underline{B} = 4.0\text{\AA}^2$ ;  $\underline{R}$  fell to 0.338. The same rejection test was applied to the coefficients and the second map computed. This revealed all non-hydrogen atoms, but differentiation between C(13) and O was not possible from the electron-counts.

A third summation was performed to obtain optimum positions for the 17 atoms using Booth's method<sup>(161)</sup>. No observed structure amplitudes were rejected, and  $\underline{R}$  was

\* The numbering scheme is shown in full in the pull-out diagram bound with the end-papers.



0.251. Distinction between C(13) and O was still not possible.

### 7.3. Refinement of the Structure.

The conventions set up at the beginning of section 6.4, on page 95, will be used here. The progress of the refinement is shown in Table 7.1 on page 135. The block-diagonal least-squares program BABA was used throughout.

Initially the positional parameters and estimated B-factors were allowed to vary for 3 cycles, together with an overall scale factor (K), (run I1). A weighting scheme of the Hughes type (Eq. 2.29) was used, with  $F^*$  set at 850 on the scale of the structure factors in Table 7.5, this gave reasonably constant values of  $\sum w(|F_o| - |F_c|)^2$  over ranges of  $|F_o|$  and  $\sin^2\theta$ . The R-factor fell to 0.178, but C(13) and O showed anomalous B-factors of  $2.5\text{\AA}^2$  and  $7.5\text{\AA}^2$ , respectively lower and higher than the general level ( $\approx 4.1\text{\AA}^2$ ) for substituent atoms. The designation of the two peaks was interchanged and refinement continued (run I2) to 0.170. A bond-length calculation (ELSI) now showed sensible values for C(6)-C(13) and C(6)-O of 1.57 and 1.44  $\text{\AA}$  respectively; the B-factor shifts were minimal for the two atoms.

A difference map, with  $(F_o - F_c)$  as coefficients in the Fourier series, showed no spurious features, but

revealed some anisotropy in the structure. All B-factors were thus converted into their anisotropic equivalent  $\beta_{ij}$ 's (Eq. 1.10).  $R$  fell to 0.122 after runs A1, A2.

The accidental absences were now included in the structure factor calculation at an observed value of  $1/\sqrt{2} |F_o|_{\min}$  in the relevant part of the intensity record. Some misindexing was detected and corrected, and two reflections (2,1,0; 0,0,2;) were omitted for suspected extinction. Two further cycles (run A3) gave an  $R$ -value of 0.125 over all reflections.

A second difference map suggested positions for all but three of the non-methyl hydrogen atoms (see Table 7.4). These positions compared well with those calculated using BONDLA. The latter program also showed very sensible geometry at this stage. For the final stages of refinement all 25 hydrogen atoms were included in the structure factor calculations, using the calculated positions, together with a  $B$ -factor equal to that of the carbon or oxygen to which they were bonded, plus  $0.5\text{\AA}^2$ . The hydrogen parameters were not refined. After four further cycles of refinement (runs M1, M2) the ratio  $S/E$  (see p. 100) was less than 0.10 for all parameters; the maximum positional shift on the last cycle was  $0.0006\text{\AA}$ . The final parameters, together with estimated standard deviations where appropriate, are shown in Tables 7.2, 7.3. Hydrogen positions

calculated from the data of Table 7.2, are shown compared with the observed values in Table 7.4. The data from these three tables were used in a final structure factor calculation, with the overall  $|F_o|$  scale factor (K) from the final cycle. The overall R-factor was 0.114, but was 0.100 for the 1920 observed reflections not affected by extinction. The list is given in Table 7.5.

TABLE 7.1.

Humulene Bromohydrin : The Refinement Process.

Run.	Cycles.	-R-	Max.shift.Å.	$\sum w( F_o  -  F_c )^2$
I1	3	0.178	0.012	8380
I2	3	0.170	0.004	7725
A1	3	0.131	0.070	3476
A2	3	0.122	0.012	2256
A3	2	0.125*	0.0040	2236
M1	2	0.115*	0.0040	1842
M2	2	0.114*	0.0006	1831

\* Overall R-factor (including accidental absences).

Analysis of shifts on the final cycle.

	<u>X</u>	<u>Y</u>	<u>Z</u>
Max. shift Å.	0.00048	0.00060	0.00036
Ave. shift Å.	0.00025	0.00020	0.00020

TABLE 7.2.

Humulene Bromohydrin.

Final Positional Parameters for the Non-Hydrogen Atoms  
(in fractional co-ordinates) together with their Estimated  
Standard Deviations ( $\sigma$ ).

	$\bar{x}$	$\sigma_{\bar{x}}$	$\bar{y}$	$\sigma_{\bar{y}}$	$\bar{z}$	$\sigma_{\bar{z}}$
Br	0.08087	0.00015	0.20458	0.00004	0.25105	0.00008
C(1)	-0.10285	0.00134	0.28861	0.00036	0.25998	0.00056
C(2)	-0.17781	0.00127	0.31087	0.00033	0.14718	0.00055
C(3)	-0.19620	0.00125	0.38774	0.00035	0.12942	0.00052
C(4)	-0.15794	0.00111	0.43630	0.00031	0.22137	0.00048
C(5)	-0.35221	0.00124	0.44773	0.00033	0.29540	0.00053
C(6)	-0.38504	0.00111	0.40111	0.00036	0.39043	0.00050
C(7)	-0.45467	0.00115	0.32983	0.00036	0.35070	0.00058
C(8)	-0.28024	0.00130	0.27329	0.00036	0.33670	0.00058
C(9)	-0.27719	0.00118	0.52341	0.00033	0.30842	0.00052
C(10)	-0.15173	0.00113	0.51653	0.00033	0.20302	0.00050
C(11)	-0.00851	0.00139	0.34791	0.00037	0.08455	0.00055
C(12)	-0.34217	0.00156	0.26459	0.00037	0.08688	0.00061
C(13)	-0.19498	0.00140	0.40001	0.00043	0.47589	0.00057
C(14)	0.06909	0.00147	0.54889	0.00045	0.20561	0.00073
C(15)	-0.29349	0.00134	0.54110	0.00039	0.10552	0.00058
O	-0.57628	0.00095	0.43024	0.00030	0.44016	0.00046

TABLE 7.3.

Humulene Bromohydrin.

Final Anisotropic Thermal Parameters ( $\beta_{ij}$ 's) for the  
Non-Hydrogen Atoms.

Atom	$\beta_{11}$	$\beta_{22}$	$\beta_{33}$	$\beta_{23}$	$\beta_{13}$	$\beta_{12}$
Br	0.03613	0.00227	0.01151	-0.00020	0.00597	0.00254
C(1)	0.03333	0.00217	0.00577	0.00051	0.00181	-0.00137
C(2)	0.02976	0.00177	0.00606	-0.00132	-0.00647	-0.00203
C(3)	0.02973	0.00231	0.00508	-0.00164	0.00378	-0.00036
C(4)	0.02211	0.00205	0.00409	-0.00036	0.00038	-0.00020
C(5)	0.03022	0.00198	0.00514	-0.00013	0.00478	-0.00018
C(6)	0.02006	0.00289	0.00451	0.00136	0.00669	-0.00112
C(7)	0.01869	0.00248	0.00721	-0.00019	0.00344	-0.00372
C(8)	0.03020	0.00214	0.00654	0.00095	0.00422	-0.00007
C(9)	0.02733	0.00203	0.00514	-0.00090	0.00556	-0.00112
C(10)	0.02160	0.00226	0.00473	-0.00025	-0.00092	0.00180
C(11)	0.03841	0.00241	0.00554	-0.00041	0.01171	0.00178
C(12)	0.04194	0.00362	0.00555	-0.00276	-0.00341	-0.00482
C(13)	0.03318	0.00331	0.00519	-0.00095	-0.00097	-0.00063
C(14)	0.03259	0.00319	0.00865	-0.00056	0.00520	-0.00183
C(15)	0.03160	0.00277	0.00594	0.00116	-0.00452	0.00191
O	0.03315	0.00356	0.00850	-0.00048	0.01820	0.00495

The  $\beta_{ij}$ 's are parameters in Eq. 1.10.

TABLE 7.4.

Humulene Bromohydrin.

Observed<sup>\*</sup> and Calculated<sup>†</sup> Hydrogen Positions, given as  
Fractional Co-ordinates.

Atom Bonded		Calculated			Observed		
	to	$\bar{x}$	$\bar{y}$	$\bar{z}$	$\bar{x}$	$\bar{y}$	$\bar{z}$
H(1)	C(1)	-0.0012	0.3287	0.2954	-0.004	0.330	0.286
H(2)	C(3)	-0.3607	0.3973	0.0957	-0.374	0.389	0.053
H(3)	C(4)	-0.0013	0.4227	0.2607	-0.010	0.437	0.285
H(4)	C(5)	-0.5080	0.4490	0.2493	-	-	-
H(5)	C(7)	-0.5670	0.3104	0.4072	-0.510	0.270	0.360
H(6)	C(7)	-0.5407	0.3366	0.2730	-0.531	0.349	0.266
H(7)	C(8)	-0.2002	0.2633	0.4149	-0.165	0.281	0.440
H(8)	C(8)	-0.3660	0.2281	0.3079	-0.359	0.235	0.264
H(9)	C(9)	-0.4100	0.5599	0.3033	-	-	-
H(10)	C(9)	-0.1725	0.5333	0.3798	-0.167	0.534	0.398
H(11)	C(11)	-0.0042	0.3402	-0.0012	-0.017	0.340	-0.002
H(12)	C(11)	0.1569	0.3543	0.1192	0.138	0.356	0.091
H(13)	O	-0.7162	0.4511	0.4766	-	-	-
H(14)	C(12)	-0.3956	0.2805	0.0064	-	-	-
H(15)	C(12)	-0.4305	0.2260	0.1688	-	-	-
H(16)	C(12)	-0.3231	0.2500	0.0459	-	-	-
H(17)	C(13)	-0.1460	0.4501	0.5038	-	-	-
H(18)	C(13)	-0.0695	0.3974	0.4504	-	-	-
H(19)	C(13)	-0.2305	0.3492	0.5356	-	-	-
H(20)	C(14)	0.0733	0.6033	0.1932	-	-	-
H(21)	C(14)	0.1352	0.5415	0.1444	-	-	-
H(22)	C(14)	0.1747	0.5223	0.2826	-	-	-
H(23)	C(15)	-0.2893	0.5955	0.0931	-	-	-
H(24)	C(15)	-0.4685	0.5127	0.1096	-	-	-
H(25)	C(15)	-0.2296	0.5302	0.0413	-	-	-

\* From difference map following run A3. † Using BONDIA.

TABLE 7.5.Humulene Bromohydrin.Final Observed and Calculated Structure Factors.

The Format of the Table is :

<u>* l</u>	<u>h</u> 50  F <sub>o</sub>	<u>k</u> 50 F <sub>c</sub>
.	.	.

The accidental absences are marked -L- (less-than).  
The 2,0,0, reflection was partially obscured by the  
backstop. The two reflections omitted for suspected  
extinction were (in the same format) :

* 0	2 2010	1 3429	(sin <sup>2</sup> θ = 0.0663)
* 2	0 7520	0 -9391	(sin <sup>2</sup> θ = 0.0155)

4	3591	3625	15	380	-277	5	134	182	L	3	905	-859
6	4887	-4112	1	0	5	6	451	-365		4	7716	2375
8	2155	1970	2	2081	-2042	7	152	108	L	5	1692	1483
10	791	-654	3	2142	-1812	8	160	188		6	1833	-1643
12	406	421	4	538	508	9	406	371		7	1498	-1349
14	194	-170	5	388	342	10	167	168	L	8	407	367
	0	1	6	493	362	11	163	119	L	9	908	743
1	847	823	7	382	365	12	151	-148	L	10	900	-752
2	459	520	8	293	-290	13	132	60	L	11	734	-500
3	2292	1919	9	222	-189	14	105	-95	L	12	653	525
4	1719	-1354	10	165	-85		0	10			0	15
5	925	855	11	167	-155	L	3339	3237		1	157	-09
6	1136	1029	12	163	93	L	2638	-2599		2	159	60
7	253	209	13	150	159	L	3520	-3271		3	644	620
8	441	332	14	128	-169	L	1157	1046		4	164	-60
9	910	-818	15	97	35	L	3203	2895		5	814	-684
10	396	313		0	6		1009	-1000		6	410	-305
11	167	171	0	1634	-1295		1727	-1666		7	471	-372
12	166	57	L	6001	-5416		156	100	L	8	398	334
13	311	-234	L	2082	-1998		2373	2255		9	155	-25
14	137	27	L	3146	3144		167	35	L	10	253	244
15	109	-28	L	107	-57		1562	-1380		11	175	174
	0	2		3023	-2698	L	11	160	L	12	340	-269
0	2887	-2767	6	541	462		12	620			0	16
1	1432	1391	7	2968	2577		13	126	L	0	796	-663
2	3900	3666	8	150	157	L	14	557		1	3272	-2817
3	5900	5714	9	1193	-1154	L		0		2	164	09
4	2275	-2410	10	235	-227		1	1089		3	2242	1948
5	1713	-1725	11	167	-45	L	2	366		4	236	-186
6	3074	2588	12	228	199	L	3	535		5	1253	-1062
7	1142	1011	13	586	-511		4	395		6	408	341
8	2945	-2653	14	124	145	L	5	928		7	1008	851
9	305	-255	15	496	416	L	6	374		8	157	-175
10	2468	2265		0	7		7	227		9	775	-661
11	529	409	*	1886	-1550		8	907		10	131	-101
12	1670	-1598	1	882	-831		9	416		11	111	192
13	438	-350	2	392	-368		10	329			0	17
14	332	304	3	276	-335		11	155		1	166	18
15	456	358	4	386	379		12	140	L	2	668	-645
	0	3	5	132	-76	L	13	117	L	3	167	52
1	328	244	6	404	320	L		0		4	670	549
2	2455	2265	7	943	-745		0	3881		5	166	-48
3	611	476	8	323	294		1	2620		6	164	115
4	2816	2439	9	167	142	L	2	4043		7	158	30
5	784	-703	10	166	-98	L	3	1764		8	149	-149
6	721	695	11	159	-158	L	4	3195		9	334	-266
7	129	-129	12	143	73	L	5	1777		10	119	-179
8	449	-278	13	119	-175	L	6	2115		11	231	148
9	376	-363	14	82	-33	L	7	164			0	18
10	163	-101	15	0	6		8	1800			290	-164
11	167	202	*	0	4795		9	782		1	2009	1663
12	659	563	0	5329	854		10	790		2	579	445
13	154	72	1	710	4070		11	424		3	1415	-1215
14	134	-119	2	4583	-3576		12	458		4	810	-507
15	257	214	3	3863	-3095		13	107	L	5	1171	969
	0	4	4	3603	1987			0		6	630	503
0	3955	3924	5	2137	1975		1	404		7	1038	-857
1	2545	2671	6	1998	-1619		2	145	L	8	196	-144
2	5870	-5607	7	1837	-1053		3	784		9	744	660
3	4938	-4747	8	1252	977		4	306			0	19
4	2756	2727	9	1159	1030		5	158	L	1	155	35
5	5554	5439	10	1207	-1052		6	163	L	2	165	109
6	1291	-1207	11	-1190	-222		7	706	L	3	153	41
7	2404	-2103	12	311	109	L	8	167	L	4	150	-77
8	144	-81	13	138	-57	L	9	233		5	155	35
9	1836	1540	14	113	41	L	10	221		6	149	-32
10	164	-122	15	69	9	L	11	451		7	139	103
11	530	-407	*	0	119		12	123	L	8	356	324
12	518	444	1	156	-634			0			0	20
13	215	173	2	623	35	L	0	2761		1	1485	1305
14	132	-144	3	119	-1269	L	1	1792		1	598	-533
			4	1465			2	2175		2	1246	-904



3	762	621	13	396	-302	-11	138	-64	L	-3	82	138
4	1249	1018	14	216	-225	-10	1084	-1144		-2	4059	4026
5	356	-344	15	435	337	-9	1013	1621		-1	1220	1304
6	1239	-1011		1	2	-8	1320	1213		0	2197	2442
7	125	134	L	307	309	-7	1085	-1044		1	402	-307
8	908	684		112	-52	L	1654	-1756		2	3774	3641
	0	21	-13	128	-109	L	2111	2228		3	767	-746
1	151	-194	L	273	258	-4	953	-768		4	2226	-2475
2	210	-213		757	-761	-3	102	-196		5	702	-740
3	205	213	-10	502	490	-2	1445	-1471		6	1253	1349
4	140	-60	L	437	313	-1	2329	-2589		7	1038	948
5	132	98	L	1117	-1065	0	3914	3916		8	357	-340
6	299	252		653	-504	1	805	-915		9	327	-426
	0	22	-6	1137	1008	2	2080	-2338		10	995	977
0	1494	-1234	-5	690	-658	3	464	465		11	137	40
1	195	142	-4	2076	-1988	4	1396	1627		12	738	-645
2	1381	1168	-3	2579	2555	5	1184	901		13	117	-72
3	371	284	-2	901	-835	6	707	-872		14	97	-48
4	1487	-1081	-1	1934	-2213	7	777	799		15	64	-46
5	116	6	0	5770	-5532	8	299	210			1	7
6	103	811	L	4248	3876	9	1443	-1378		-15	265	-274
	0	23	L	5057	5076	10	864	-728		-14	278	171
1	122	144	L	3555	-3626	11	134	-49	L	-13	440	447
2	119	106	L	218	-208	12	731	642		-12	453	-409
3	161	-244		2643	3000	13	122	-161	L	-11	434	-305
4	212	-183		519	-372	14	327	-276		-10	872	740
	1	0		2139	-2435	15	75	178	L	-9	134	39
-15	90	-6	L	1315	-1392		1	5		-8	803	-646
-13	128	121	L	545	520	-15	80	-128	L	-7	1186	-1102
-11	1069	-1232		507	418	-14	106	-103	L	-6	2742	2802
-9	731	723		438	528	-13	123	266	L	-5	2053	2046
-7	1609	-1861		234	-164	-12	910	967		-4	3012	-3048
-5	3093	3358		124	-66	L	240	-190		-3	722	-740
-3	5939	-6663		107	-12	L	984	-963		-2	1707	1846
-1	1341	-1344		81	-115	L	921	899		-1	1447	1300
1	7881	7757		1	3		1909	1847		0	4461	-4647
3	488	630	-15	406	431	-7	1318	-1190		1	1191	-1246
5	1947	-2198	-14	383	377	-6	1994	-2052		2	1672	1822
7	456	473	-13	127	110	L	373	-248		3	563	503
9	866	-857	-12	272	-215		3818	4144		4	1321	-1337
11	938	924	-11	240	114	-3	1102	-989		5	293	-296
13	307	-201	-10	1061	1046	-2	4074	-4662		6	2230	2276
15	641	514	-9	1394	-1297	-1	932	-744		7	1628	1648
	1	1	-8	1817	-1751	0	3671	3788		8	911	-843
-15	90	37	L	1281	1366	1	680	607		9	662	-631
-14	276	-241		1542	1573	2	3760	-3487		10	391	349
-13	748	695	-5	2000	-2674	3	2493	2327		11	386	319
-12	193	-257	-4	1910	-2360	4	2270	2402		12	573	-553
-11	1015	-1084	-3	1934	1857	5	573	465		13	321	-324
-10	423	-383	-2	4027	4348	6	1805	-1967		14	92	148
-9	1759	1734	-1	5361	-5694	7	115	-30	L	15	52	24
-8	116	28	L	3477	-3377	8	1504	1577			1	8
-7	2711	-3049		3318	3342	9	896	-954		-15	158	151
-6	1611	-1760	1	5459	4624	10	1360	-1085		-14	542	-645
-5	2847	3315	2	4610	-4613	11	134	187	L	-13	455	-340
-4	1150	1102	3	3218	-3248	12	294	216		-12	405	347
-3	4849	-5547	4	3106	3300	13	120	28	L	-11	334	323
-2	869	852	5	1083	1071	14	284	-245		-10	138	33
-1	3923	5052	6	1330	-1363	15	74	-98	L	-9	136	46
0	694	1249	7	931	-957		1	6		-8	936	922
1	4362	-4549	8	317	360	-15	75	71	L	-7	829	770
2	710	-676	9	544	478	-14	102	-131	L	-6	849	-830
3	4614	4950	10	875	-843	-13	294	487		-5	1303	-1250
4	-1284	-1011	11	269	-259	-12	420	-468		-4	199	203
5	4534	-4429	12	349	326	-11	338	408		-3	544	534
6	336	-363	13	211	-60	-10	931	955		-2	1944	-2121
7	2049	2244	14	157	-192	-9	167	168		-1	2061	-2498
8	784	522	15	1	4	-8	1242	-1236		0	4548	4632
9	1513	-1488		84	58	L	254	-200		1	67	176
10	634	-602	-14	109	-73		1112	1140		2	1289	-1443
11	758	669	-13	125	-183	L	337	351		3	189	127
12	574	561	-12	635	727		2854	-2953		4	1186	1250

5	852	780	•12	282	-194	4	1519	-1371	•2	943	919
6	972	-1068	•11	808	-745	5	1336	1202	•1	135	-131
7	124	-77	L •10	271	-169	6	333	225	0	159	-43
6	788	819	•9	1355	1113	7	1381	-1310	1	142	223
9	335	326	•8	433	383	8	138	•117	L 2	795	640
10	240	-200	•7	862	-759	9	658	670	L 3	583	-441
11	135	-57	L •6	128	-5	L 10	124	111	L 4	586	-573
12	125	109	L •5	2233	2305	11	360	•296	5	309	287
13	109	104	L •4	1140	-1217	12	304	•235	6	1113	1044
14	86	-70	L •3	3278	-3154	13	238	207	7	327	-246
	1	9	•2	108	75	L 1	1	14	8	804	-751
-14	474	-456	•1	2859	3160	•12	259	•232	9	166	157
-13	308	-395	0	496	424	•11	246	224	10	416	318
-12	394	349	1	3874	-3655	•10	123	25	L 11	341	-261
-11	783	732	2	463	-365	•9	295	249	•10	1	17
-10	138	-130	L 3	1928	1863	•8	137	94	L 10	615	581
-9	1315	-1171	4	1066	969	•7	959	•933	•9	112	128
-8	593	512	5	2266	-2106	•6	137	28	L 8	1037	-905
-7	1511	1429	6	516	-430	•5	331	226	•7	130	20
-6	1528	-1491	7	1849	1805	•4	1106	933	•6	1059	931
-5	1871	-2056	8	138	-80	L •3	818	677	•5	137	-130
-4	877	922	9	1634	-1541	•2	1977	-1842	•4	1526	-1372
-3	4368	4446	10	134	65	L •1	1400	1428	•3	783	-714
-2	1905	-1775	11	731	722	0	1483	1423	•2	2077	1895
-1	3775	-3701	12	294	278	1	1008	•982	•1	1103	1024
0	1414	1455	13	385	-389	2	1804	-1788	0	1378	-1312
1	3469	3244	1	88	-71	L 3	318	276	1	138	66
2	1201	-1172	•13	109	-3	L 4	1342	1290	2	1526	1303
3	3492	-3464	•12	214	196	L 5	543	•458	3	138	101
4	1520	1538	•11	420	362	6	755	•626	4	1512	-1309
5	1920	1991	•10	477	-424	7	194	191	5	137	182
6	1217	-1264	•9	1015	-1031	8	385	252	6	944	856
7	1251	-1250	•8	744	657	9	521	•451	7	314	215
8	947	900	•7	1101	952	10	269	-189	8	449	-582
9	1136	1037	•6	1511	-1447	11	104	24	L 9	108	-121
10	138	83	L •5	598	525	12	84	-161	L 10	93	147
11	296	-200	•4	1635	1395	13	44	-85	L 1	18	18
12	420	354	•3	796	-682	•12	290	202	•10	84	-210
13	104	70	L •2	554	-641	•11	101	40	•9	191	-129
14	79	166	L •1	275	164	•10	570	-478	•8	114	-57
	1	10	0	1562	1465	•9	127	104	L 7	325	213
-14	78	116	L 1	833	-851	•8	1054	902	•6	775	-653
-13	103	-79	L 2	1292	-1313	•7	952	•847	•5	133	-82
-12	511	-579	3	174	195	•6	1089	-967	•4	1360	1142
-11	186	-252	4	810	769	•5	953	939	•3	137	-58
-10	644	576	5	650	-568	•4	1652	1504	•2	894	-714
-9	138	-37	L 6	546	-534	•3	757	-578	•1	517	-383
-8	573	-582	7	705	-728	•2	1295	-1096	0	1016	914
-7	317	-243	8	433	370	•1	1143	986	1	704	608
-6	1115	1101	9	614	596	0	1665	1590	2	955	-905
-5	738	730	10	481	-315	1	1427	-1339	3	613	-511
-4	156	-187	11	104	26	L 1	1854	-1731	4	939	904
-3	1940	-1762	12	382	330	2	1344	1248	5	419	325
-2	899	819	13	1	13	3	2280	2116	6	404	-309
-1	912	976	•13	363	-370	4	827	-797	7	341	-271
0	395	-353	•12	247	-181	5	1553	-1396	8	443	430
1	1701	-1802	•11	684	629	6	274	319	9	414	345
2	1368	-1159	•10	129	86	L 7	325	225	10	79	20
3	1891	1875	•9	1150	-1030	8	240	•168	•9	1	19
4	250	-251	•8	1252	-1146	9	619	-530	•8	88	-87
5	2006	-2032	•7	1898	1662	10	474	418	•5	616	528
6	125	113	L •6	2101	2034	11	204	230	•7	300	224
7	1584	1676	•5	1609	-1501	12	1	16	•6	687	-533
8	304	-249	•4	1168	-1098	•10	620	633	•5	1042	-876
9	138	-27	L •3	1779	1704	•9	170	•233	•4	765	650
10	546	559	•2	1111	1068	•8	774	-625	•3	845	719
11	518	412	•1	2768	-2720	•7	135	125	•2	208	•1156
12	117	-188	L 0	1238	-1161	•6	660	731	•1	1052	-876
13	392	-334	1	2385	2388	•5	277	286	0	816	714
14	69	5	L 1	1879	1880	•4	1499	-1404	1	1343	1103
	1	11	2	2412	-2336	•3	643	451	2	953	-854
-13	193	159	3						3	461	-366

4	824	727	-6	2248	-2332	-1	3018	-3476	-7	-1036	-1222		
5	471	366	-4	4981	5852	0	4777	4892	-6	935	-872		
6	379	-283	-2	2843	-3108	1	4486	3458	-5	656	607		
7	521	-416	2	1805	-1182	2	727	8788	-4	810	-733		
8	422	364	4	532	-258	3	1534	-1448	-3	1638	-1842		
9	567	466	6	2099	-2227	4	1308	1284	-2	714	-843		
	1	20	8	526	593	5	1233	1340	-1	1829	2185		
-8	488	-392	10	452	-422	6	1275	-1228	0	1419	1355		
-7	353	-240	12	554	358	7	1598	-1860	1	1644	-1900		
-6	569	452		2	1	8	586	721	2	930	779		
-5	119	83	L	-12	313	-304	9	1014	1170	3	2642	2623	
-4	700	-530	-11	944	-1024	10	523	-634	4	251	231		
-3	804	-706	-10	182	172	L	183	248	L	5	1553	-1706	
-2	448	395	-9	914	862	11	173	94	L	6	318	245	
-1	761	687	-8	1302	-1416	12	2	4	L	7	468	528	
0	555	-495	-7	146	80	L	-12	178	L	8	478	687	
1	714	-616	-6	2257	2371	-11	584	641	L	9	306	-408	
2	658	567	-5	843	672	-10	411	379		10	262	-378	
3	593	621	-4	1565	-1737	-9	1763	-1932		11	508	652	
4	425	-343	-3	1291	-1262	-8	661	747		12	106	182	
5	438	-313	-2	2378	2776	-7	1683	1885			2	7	
6	464	433	-1	1292	1548	-6	1702	-1736	-12	170	121		
7	98	-46	L	1	377	-419	-5	1569	-1700	-11	771	919	
8	467	-407	2	4469	3852	-4	2012	2234	-10	536	551		
	1	21	3	862	737	-3	2104	2176	-9	337	1631		
-7	722	-527	4	2288	-2296	-2	478	324	-8	1017	-1038		
-6	243	-180	5	2748	-2686	-1	1625	-1785	-7	2051	2339		
-5	859	697	6	1689	1797	0	878	-760	-6	306	-382		
-4	114	-134	L	7	434	416	1	2774	2446	-5	2237	2302	
-3	1069	-1023	L	8	972	-1056	2	1151	-1094	-4	673	-738	
-2	121	152	L	9	562	-535	3	302	232	-3	2196	2440	
-1	1353	1185	L	10	522	638	4	413	360	-2	772	861	
0	246	-282		11	184	29	L	916	930	-1	3540	-4005	
1	546	-1006		12	606	-785	6	849	701	0	499	-552	
2	120	39	L		2	2	7	159	-47	L	1	2439	2599
3	702	645	-12	312	-328	8	1082	1222	2	1433	1451		
4	159	-67	-11	185	172	L	571	525	3	3091	3156		
5	1013	-849	-10	182	-180	L	453	516	4	2532	-2582		
6	193	165	-9	347	403	L	182	362	L	5	2727	3133	
7	798	648	-8	161	20	L	171	-71	L	6	744	744	
	1	22	-7	933	-860		2	5	L	7	959	1004	
-7	473	310	-6	565	612	-12	176	163	L	8	253	219	
-6	83	-46	L	692	735	-11	521	629	9	1156	1233		
-5	324	-202	-4	1113	-1265	-10	184	142	L	10	369	401	
-4	101	132	L	253	232	-9	1127	1205	11	614	-877		
-3	106	140	L	2378	2618	-8	412	513	12	162	-42		
-2	110	-168	L	836	991	-7	2103	-2215		2	8		
-1	631	-530	0	2590	-2952	-6	1071	976	-12	238	-398		
0	317	-268	1	1565	-1275	-5	2260	2477	-11	311	375		
1	157	311	2	3184	2522	-4	768	799	-10	523	615		
2	109	-53	L	4543	4107	-3	3436	-3689	-9	368	-207		
3	235	255	3	2696	-2404	-2	685	708	-8	435	-415		
4	99	157	L	126	-93	L	3716	4288	-7	827	887		
5	532	363	6	1871	1975	0	291	-28	-6	594	738		
6	80	8	L	154	-27	L	4182	-4358	-5	728	-706		
7	243	-203	8	1590	-1760	2	146	40	-4	1647	-1699		
	1	23	9	1040	-1193	3	4294	4307	-3	131	-134		
-5	895	-784	10	185	129	L	725	563	-2	1417	1349		
-4	293	-254	11	184	116	L	1873	-1992	-1	1073	3340		
-3	990	926	12	174	89	L	871	857	0	2455	2517		
-2	95	58	L	2	3	6	2010	2234	1	2257	2240		
-1	1229	-1064	-12	507	621	7	490	587	2	1279	1212		
0	98	-69	L	740	832	8	772	878	3	875	-858		
1	389	809	10	633	-729	9	262	-274	4	643	-645		
2	500	359	-9	968	-1074	11	444	459	5	376	402		
3	879	-686	-8	461	437	12	169	102	L	6	518	559	
4	571	-402	-7	1036	1098		2	6	7	173	-118		
5	588	445	-6	1830	-1864	-12	388	433	8	256	-224		
	2	0	-5	2446	-2765	-11	580	694	9	292	206		
-12	626	685	-4	2765	3292	-10	185	210	L	10	133	213	
-10	1310	-1462	-3	4015	4728	-9	519	562	11	174	174		
-8	932	988	-2	2023	-2143	-8	171	143	L	12	157	-17	

-12	161	145	L	8	524	-709	7	685	6750	-8	143	-255	L		
-11	176	21	L	9	182	45	L	8	177	-7	157	-189	L		
-10	411	-435	L	10	245	302		9	166	-6	409	488			
-9	978	1113		11	157	-213	L	10	150	-5	737	-811			
-8	957	1098		2	238	12		2	15	-4	356	-311			
-7	981	-1042		*12	238	-237		-11	30A	*431	-3	677	782		
-6	1543	-1729		-11	224	-228		-10	14A	188	-2	258	102		
-5	792	825		-10	245	270		-9	32A	349	-1	449	-333		
-4	1737	1954		-9	681	799		-8	350	*383	0	367	-326		
-3	1993	-2251		-8	454	-379		-7	1089	-1238	1	776	740		
-2	1342	-1611		-7	1008	-1148		-6	185	116	L	2	446	433	
-1	173A	1856		-6	1050	1144		-5	1527	1637		3	763	-874	
0	1329	1316		-5	1694	1991		-4	36A	-377		4	352	-351	
1	2523	-2690		-4	1395	-1583		-3	1155	-1189		5	341	332	
2	2294	-2640		-3	164	121	L	-2	1145	1254		6	162	226	L
3	2459	2449		-2	1381	1411		-1	2190	2477		7	213	-274	
4	1088	1162		-1	388	-281		0	951	-1042		8	270	-325	
5	1152	-1156		0	670	-722		1	1926	-2156		2	19		
6	956	-1008		1	595	-529		2	363	377		-9	330	446	
7	177	162	L	2	1357	1397		3	1160	1247		-8	402	472	
8	1037	1158		3	408	-418		4	261	-318		-7	495	-592	
9	262	-383		4	1594	-1752		5	641	-708		-6	536	-672	
10	362	-381		5	532	625		6	367	412		-5	767	938	
11	170	72	L	6	631	678		7	750	902		-4	416	456	
12	369	458		7	185	8	L	8	417	*414		-3	920	-1043	
				8	451	-528		9	414	-514		-2	705	-855	
				9	252	-345		2	16	*		-1	615	730	
-12	154	127	L	10	236	341		-11	309	*475		0	562	628	
-11	343	-405		11	149	102	L	-10	135	*197	L	1	831	-924	
-10	257	-334		2	13	13		-9	614	759		2	350	-401	
-9	586	753		*11	212	358		-8	167	*294	L	3	544	670	
-8	898	962		-10	334	-398		-7	898	-1214		4	668	816	
-7	435	-402		-9	503	-647		-6	182	43	L	5	597	-733	
-6	538	-563		-8	520	597		-5	903	979		6	518	-666	
-5	648	601		-7	262	242		-4	370	426		7	470	609	
-4	1311	1305		-6	367	-336		-3	130A	-1531		8	287	317	
-3	296	-248		-5	160	252		-2	184	63	L	2	20		
-2	2454	-2666		-4	1629	1890	L	-1	901	965		-7	251	-274	
-1	444	472		-3	1001	1074		0	184	-38	L	-6	342	-367	
0	883	953		-2	1562	-1824		1	319	-259		-5	300	269	
1	400	-367		-1	1224	-1313		2	185	220	L	-4	316	207	
2	985	-919		0	1051	1105		3	321	152		-3	292	-294	
3	827	-988		1	529	506		4	185	*175	L	-2	706	-791	
4	1285	1494		2	832	-832		5	183	*272	L	-1.	238	205	
5	525	547		3	245	-304		6	350	323		0	631	750	
6	1651	-1854		4	1005	1066		7	344	464		1	158	-109	L
7	181	-222	L	5	771	817		8	161	*172	L	2	572	-697	
8	453	540		6	866	-1018		9	145	*245	L	3	161	147	L
9	184	-90	L	7	785	-859		2	17			4	535	575	
10	251	-279	L	8	514	626		-11	207	344		5	145	-150	L
11	164	338	L	9	490	564		-10	110	-10	L	6	298	-351	L
				10	503	-614		-9	39A	*477		7	293	206	
-12	293	-335		11	393	-430		-8	156	*183	L	2	21		
-11	166	134	L	2	14	14		-7	581	657		-7	291	403	
-10	564	640		*11	139	62	L	-6	174	78	L	-6	443	612	
-9	488	-490		-10	158	-106	L	-5	1142	-1281		-5	462	-556	
-8	523	-548		-9	172	-50	L	-4	440	*474		-4	533	-587	
-7	513	585		-8	442	523		-3	1197	1358		-3	298	345	
-6	2001	2183		-7	185	160	L	-2	165	*189	L	-2	684	737	
-5	239	159		-6	980	-1017		-1	1200	-1264		-1	659	-717	
-4	1804	-2088		-5	184	-69	L	0	185	59	L	0	661	-754	
-3	765	-544		-4	511	544		1	1571	1677		1	535	500	
-2	1848	2173		-3	712	700		2	523	490		2	566	892	
-1	871	731		-2	175	50	L	3	1221	-1516		3	336	-420	
0	2297	-2500		-1	1206	-1251		4	25A	*278		4	619	-703	
1	301	-268		0	1204	1350		5	97A	974		5	255	370	
2	2143	2439		1	1746	1866		6	172	189	L	6	276	422	
3	899	-920		2	612	-600		7	460	*635		2	22		
4	2024	-2440		3	1457	-1546		8	149	-61	L	-6	353	453	
5	243	295		4	258	274		9	262	410		-5	112	-47	L
6	1157	1415		5	865	1022		2	18			-4	426	-403	L
7	183	-274	L	6	370	-368		-9	177	*237		-3	131	18	L

-2	333	373		3	3	-5	16A	157	L	1	620	-526
-1	240	246	-10	560	510	-4	340A	-3507		2	419	-246
0	482	-560	-9	54A	-443	-3	1495	-1333		3	357	-378
1	337	-293	-8	440	-360	-2	3964	4065		4	917	757
2	268	271	-7	684	-665	-1	250	149		5	519	-438
3	127	216	L	669	-523	0	4174	-3984		6	2J4	-57
4	118	-190	L	151	-61	L	326	241		7	210	30
6	22A	216		190	-39	2	3667	3249		8	212	-222
	2	23		577	491	3	569	419		9	2J7	174
-4	360	457		1084	-1611	4	2602	-2544		10	195	408
-3	107	97	L	91	-65	5	562	458			3	10
-2	360	-440	0	522	-465	6	1572	1615	-10		230	136
-1	262	-328	1	998	839	7	571	567	-9		1026	1074
0	334	430	2	114	-55	L	114A	-1229	-8		367	351
1	32A	434	3	1299	1083	9	212	174	L	-7	1389	-1244
2	497	-609	4	879	707	10	292	332		-6	353	341
3	102	-149	L	565	411		3	7	-5	2222	7571	
4	413	600	6	506	-425	-10	514	455	-4	755	-743	
	3	0	7	387	-370	-9	590	508	-3	1629	1884	
-9	918	796	8	502	-516	-8	774	695	-2	560	451	
-7	1185	-1175	9	211	117	L	19A	-84	L	-1	1616	1410
-5	1411	1569	10	210	216	L	529	430	0	1179	1019	
-3	332	-570		3	4	-5	175	157	L	1	2466	2678
1	289A	-3466	-10	1236	-1372	-4	1202	-1142	2	676	540	
3	4964	4180	-9	589	523	-3	614	451	3	2523	2441	
5	353A	-3377	-8	487	432	-2	412	337	4	1402	1125	
7	1075	1044	-7	455	-447	-1	141	205	L	5	700	-544
9	988	-980	-6	2204	-2345	0	141	18	L	6	1443	1348
	3	1	-5	582	-503	1	381	296	7	599	5A6	
-10	992	-963	-4	2756	3025	2	151	19	L	8	557	-525
-9	1007	-1065	-3	671	-896	3	787	676	9	643	-746	
-8	623	720	-2	1483	-1642	4	172	157	L	10	189	49
-7	670	-640	-1	1776	1763	5	110A	-1687			3	11
-6	1339	1220	0	3059	3048	6	19A	141	L	-10	194	123
-5	938	834	1	1924	-1812	7	45A	414	-9	206	93	
-4	1337	1117	2	3086	-2838	8	29A	245	-8	211	-244	
-3	654	728	3	1220	1044	9	211	270	L	-7	473	418
-2	641	-738	4	2804	2663	10	204	32	L	-6	588	545
-1	226	266	5	1800	-1462		3	8	-5	273	142	
0	57A	625	6	1858	-1861	-10	465	449	-4	127	-77	
1	557	592	7	678	650	-9	212	-388	L	-3	468	-391
2	203	140	8	2001	1947	-8	1389	1507	-2	528	-542	
3	121	74	L	212	96	-7	810	778	-1	451	-349	
4	443	211	10	1109	-1244	-6	1900	-1828	0	1192	1102	
5	223	-217		3	5	-5	1904	-1747	1	644	-444	
6	350	-303	-10	212	-214	L	2563	2516	2	190	-51	
7	190	-77	L	210	-91	L	1325	1264	3	872	814	
8	203	-21	L	201	-21	L	2804	-2786	4	231	-190	
9	632	486	-7	536	448	-1	1805	-1750	5	207	-131	
10	211	-69	L	703	-657	0	1610	1372	6	211	-243	
	3	2	-5	1292	-1104	1	1835	1510	7	212	219	
-10	599	588	-4	590	-541	2	1643	-1494	8	2J8	162	
-9	1675	-1552	-3	380	-292	3	117A	-1115	9	198	-47	
-8	1535	-1403	-2	464	-410	4	1913	1452	10	181	-49	
-7	2603	2714	-1	1243	1104	5	1343	1667		3	12	
-6	1090	1016	0	466	321	6	189A	-1875	-10	187	57	
-5	2132	-2122	1	861	709	7	117A	-1154	-9	852	-874	
-4	2227	-2157	2	1663	-1118	8	103A	1067	-4	219	49	
-3	3241	3462	3	576	-532	9	416	446	-7	1405	1425	
-2	3261	3440	4	315	228	10	1059	593	-6	597	-554	
-1	2236	-2570	5	455	361		3	9	-5	1250	1047	
0	2064	-2379	6	186	238	L	205	249	L	-4	643	603
1	1561	1760	7	344	-223	-9	211	171	L	-3	1515	1521
2	2079	2114	8	208	153	L	211	171	L	-2	874	776
3	221A	-2089	9	212	-106	L	652	588	-1	2048	2027	
4	669	-519	10	208	90	L	199	112	L		947	-946
-5	1036	957		3	6	-5	464	472	1	2334	2475	
6	1617	1587	-10	845	716	-4	674	573	2	343	249	
7	271	-295	-9	211	166	L	173	74	L	3	2666	1670
8	455	-482	-8	1781	-1714	-2	472	341	4	969	-822	
9	517	451	-7	775	-717	-1	463	294	5	2630	948	
10	211	-163	L	2277	2408	0	163	69	L	6	203A	1040

7	840	-825		5	205	-66	L	2	802	757		10	324	-245
8	203	-116	L	4	1106	-1118	L	3	658	731			4	3
9	331	369		3	596	561		4	570	561			760	-876
10	172	354	L	2	1403	1286		5	490	498		-9	201	-140
	3	13	L	-1	560	-434		6	211	202		-8	138	10
-10	177	307	L	0	1405	-1327			3	21		-7	718	603
-9	194	-104	L	1	212	-109	L	-2	155	163	L	-6	1035	-1122
-8	204	-267	L	2	1765	1736	L	-1	15A	39	L	-5	1796	-1847
-7	210	-266	L	3	210	-153	L	0	15A	143	L	-4	1462	1516
-6	212	167	L	4	1306	-1542	L	1	15A	141	L	-3	2253	2158
-5	422	355		5	201	-49	L	2	151	187	L	-2	533	-502
-4	208	256	L	6	771	836		3	143	86	L	-1	1235	-1308
-3	411	369		7	180	136	L		3	22		3	889	908
-2	703	590		8	765	-796	L	-1	670	713		1	1252	1440
-1	349	-271			3	17		0	134	95	L	2	1824	-2018
0	636	-562		-8	162	-40	L	1	613	697		3	2107	-2043
1	701	-631		-7	178	-176	L	3	520	589		4	1335	1201
2	709	-698		-6	189	-41	L		4	0		5	1513	1734
3	830	779		-5	197	44	L	-10	197	163		6	614	-510
4	210	214	L	-4	203	-32	L	-8	862	802		7	953	-1056
5	212	-266	L	-3	206	-44	L	-6	210A	2140		8	141	114
6	211	57	L	-2	208	-14	L	-4	2172	-2431		9	176	319
7	206	334	L	-1	209	81	L	-2	2247	2305		10	131	-145
8	197	-43	L	0	209	183	L	0	1410	-1774			4	4
9	182	146	L	1	208	-118	L	2	883	980		-10	138	113
	3	14		2	207	146	L	4	213	248		-9	141	-00
-10	521	-523		3	204	257	L	6	445	388		-8	138	-102
-9	451	395		4	398	-365		8	281	-288		-7	839	-849
-8	791	859		5	383	-348		10	133	-58	L	-6	1140	1093
-7	583	-472		6	181	-30	L		4	1		-5	229	129
-6	1263	-1165		7	166	94	L	-10	837	912		-4	1353	-1377
-5	670	605			3	18		-9	281	260		-3	376	-347
-4	1842	1877		-8	670	708		-8	1851	-2020		-2	825	758
-3	891	-885		-7	458	-410		-7	365	343		-1	1516	1842
-2	2206	-2281		-6	930	-1018		-6	1103	1136		0	693	-770
-1	1210	1079		-5	455	-437		-5	1749	1819		1	1102	-1119
0	1606	1460		-4	945	969		-4	1080	-1215		2	651	403
1	1020	-980		-3	559	554		-3	373	-472		3	722	561
2	838	-738		-2	1446	-1248		-2	1993	2168		4	162	-130
3	731	645		-1	571	-564		-1	44	-81	L	5	979	-919
4	948	917		0	1617	1559		0	1983	-2366		6	133	-74
5	845	-815		1	636	602		1	434	-567		7	196	245
6	360	-430		2	1013	-1054		2	1630	1982		8	231	-302
7	491	473		3	476	-420		3	94	-147		9	138	40
8	188	246	L	4	881	775		4	146A	-1339	L	10	130	46
9	417	-406		5	399	404		5	110	114	L		4	5
	3	15		6	778	-830		6	604	596		-10	137	-120
-10	150	91	L		3	19		7	136	267	L	-9	889	914
-9	172	-164	L	-7	142	184	L	8	68A	801		-8	241	-274
-8	188	-21	L	-6	159	-129	L	9	130	16		-7	1546	-1409
-7	346	256		-5	296	-273		10	326	429		-6	742	728
-6	653	-610		-4	179	252	L		4	2		-5	1546	1727
-5	556	-505		-3	186	213	L	-10	482	-471		-4	941	-939
-4	423	386		-2	189	-136	L	-9	281	-264		-3	2320	-2608
-3	590	545		-1	331	-187	L	-8	274	204		-2	33	72
-2	212	-122	L	0	191	-106	L	-7	130	-68	L	-1	2485	2897
-1	366	335		1	190	108	L	-6	120	46	L	0	791	609
0	731	605		2	323	398		-5	576	538		1	1657	-1657
1	211	-143	L	3	181	-10	L	-4	747	680		2	225	224
2	599	-538		4	173	-160	L	-3	203	267		3	1433	1160
3	367	-343		5	162	83	L	-2	366	-346		4	158	173
4	211	-260	L	6	147	126	L	-1	90	-24		5	1399	-1402
5	208	88	L		3	20		0	434	602		6	134	80
6	202	-105	L	-7	540	-608		1	413	422		7	1005	902
7	192	247	L	-6	475	393		2	994	966		8	344	-346
8	177	54	L	-5	712	691		3	1010	712		9	513	-648
	3	16		-4	562	-545		4	1065	972		10	128	-138
-10	456	447		-3	830	-780		5	120	-73	L		4	6
-9	158	-156	L	-2	652	506		6	1409	-1409		-10	135	276
-8	558	-559		-1	628	817		7	137	113	L	-9	560	-570
-7	190	-44	L	0	707	-572		8	910	901		-8	140	-118
-6	798	794		1	742	-596		9	274	328		-7	432	449

-6	521	-504	0	1833	1797	7	131	193	L	2	378	-389
-5	576	-529	1	950	-861	8	273	379	L	3	131	-154
-4	324	-216	2	1491	-1516	9	100	-68	L	4	127	170
-3	831	915	3	1194	1116			13	L	5	295	343
-2	143	-106	4	1292	1406	-10	199	-217		6	273	-236
-1	259	-202	5	366	-275	-9	115	-45	L	7	242	-303
0	770	778	6	819	-940	-8	356	456			4	17
1	960	916	7	140	149	-7	652	740		-7	488	579
2	371	320	8	428	555	-6	892	-951		-6	110	138
3	688	-638	9	310	-357	-5	685	-662		-5	708	-702
4	347	-335	10	160	-288	-4	844	937		-4	302	-325
5	368	253		4	10	-3	819	813		-3	823	979
6	361	-358	-10	122	150	-2	840	-827		-2	448	555
7	443	-264	-9	132	-131	-1	484	-487		-1	940	-1024
8	140	25	L	437	-413	0	593	500		0	226	-169
9	428	423		562	689	1	594	587		1	984	1220
10	126	140	L	140	148	2	953	-1138		2	402	419
	4	7		585	-601	3	954	-1088		3	740	-793
-10	266	282	-4	330	-234	4	816	951		4	118	-141
-9	682	-653	-3	322	268	5	584	655		5	247	285
-8	562	-546	-2	834	817	6	653	-760		6	100	-25
-7	938	849	-1	649	-577	7	356	-408		7	292	-504
-6	1033	1050	0	1065	-1104	8	305	441		8	4	18
-5	1270	-1307	1	364	368			14		-5	338	451
-4	658	-668	2	347	272	-10	197	276		-4	113	-179
-3	1103	1195	3	503	-504	-9	106	39	L	-3	204	-224
-2	884	967	4	275	-351	-8	336	-290		-2	121	114
-1	1825	-2006	5	140	-90	-7	128	-201	L	-1	299	428
0	949	-978	6	1033	1115	-6	567	607		0	122	4
1	1940	1846	7	338	396	-5	137	251	L	1	121	-228
2	952	914	8	374	-411	-4	558	-533		2	118	30
3	1348	-1271	9	122	37	-3	140	-220	L	3	330	342
4	127	170	L	262	266	-2	911	893		4	107	-111
5	1207	1268	10	4	11	-1	422	-420		5	239	-247
6	138	-86	L	635	742	0	680	-655		6	4	19
7	744	-779	-9	128	-102	L	372	-396		-5	321	335
8	197	-192	-8	741	-763	2	525	453		-4	377	453
9	422	493	-7	139	-156	L	394	377		-3	336	-349
10	299	415	-6	1071	1242	4	583	-744		-2	438	-518
	4	8	-5	523	579	5	328	-311		-1	249	328
-10	130	-179	L	1308	-1616	6	256	221		0	445	618
-9	515	551	-3	384	-439	7	291	321		1	470	-610
-8	344	235	-2	1338	1361	8	106	-145	L	2	250	-285
-7	140	93	L	593	-538			15		3	552	677
-6	817	-834	0	1829	-1977	-9	737	849		4	293	394
-5	131	-34	L	328	349	-8	110	-142	L		4	20
-4	502	386	2	791	757	-7	511	-585		-3	128	147
-3	416	-460	3	365	400	-6	338	444		-2	301	321
-2	971	-926	4	395	-378	-5	704	766		-1	168	-273
-1	360	362	5	141	-163	L	630	-529		0	257	-343
0	1018	856	6	558	602	-3	731	-748		1	190	242
1	614	-553	7	135	-36	L	590	555		2	315	408
2	700	-589	8	286	-306	-1	882	927		3	4	21
3	1473	1456	9	116	141	L	140	-45	L	-3	264	287
4	642	738		4	12	0	736	-911		-2	643	726
5	577	-587	-10	344	-354	2	138	151	L	-1	159	-240
6	140	153	L	122	23	3	639	758		0	422	-520
7	141	19	L	294	315	4	461	-539			5	0
8	138	-53	L	336	324	5	627	-815		-9	162	71
9	130	-106	L	523	-416	6	121	157	L	-7	555	-459
10	118	-142	L	744	-807	7	270	353		-5	1923	1651
	4	9	-4	1066	1111			16		-3	1234	-1692
-10	537	-564	-3	393	376	-8	198	292		-1	794	1375
-9	135	221	L	1231	-1257	-7	352	381		1	334	-1655
-8	685	846	-1	237	-223	-6	294	-248		3	511	443
-7	688	-740	0	887	874	-5	438	-418		5	872	-741
-6	518	-516	1	238	-116	-4	321	327		7	518	548
-5	632	589	2	651	-624	-3	535	529		9	150	-143
-4	803	862	3	370	-322	-2	135	155	L		5	1
-3	1298	-1419	4	487	490	-1	360	-395		-9	634	-441
-2	1473	-1615	5	140	-178	L	136	-14	L	-8	401	-256
-1	1256	1336	6	363	-340	1	428	474		-7	453	349

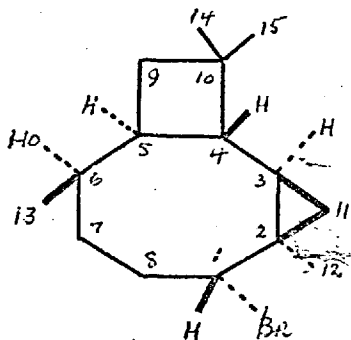
-6	430	258	6	516	-478	-2	851	806	-5	320	-325
-5	1269	-1047	7	163	132	L -1	840	751	-4	724	-645
-4	683	560	8	157	84	L L 0	149	180	L -3	633	559
-3	1985	2164	9	146	22	L 1	1171	948	-2	612	550
-2	221	-237		5	5	2	379	259	-1	897	-815
-1	1507	-1333	-9	446	-364	3	842	809	0	557	-448
0	720	-738	-8	652	-624	4	910	865	1	694	618
1	874	911	-7	163	175	L 5	518	445	2	231	276
2	222	137	-6	812	690	6	162	-242	L 3	604	-523
3	1501	-1233	-5	304	318	7	156	179	L L 4	354	-325
4	972	-799	-4	1107	-927	8	145	22	L L 5	153	149
5	1274	981	-3	133	-109	L 9	128	106	L 6	144	150
6	560	481	-2	750	696		5	9		5	13
7	802	-676	-1	120	13	L -9	285	209	-8	492	520
8	453	-356	0	541	-410	-8	614	-552	-7	550	-637
9	475	418	1	439	290	-7	819	861	-6	147	83
	5	2	2	1682	1628	-6	231	151	-5	689	672
-9	558	-450	3	411	-427	-5	1156	1099	-4	158	227
-8	463	-280	4	1270	-1110	-4	550	517	-3	737	-738
-7	683	672	5	454	388	-3	1539	-1453	-2	561	-515
-6	613	431	6	612	563	-2	494	389	-1	974	908
-5	402	-367	7	162	-86	L -1	980	900	0	513	346
-4	128	-60	L 8	156	-197	L L 0	821	597	1	1022	-954
-3	665	622	9	143	73	L 1	1064	837	2	320	-371
-2	321	340		5	6	2	552	448	3	589	582
-1	561	-658	-9	155	149	L 3	604	570	4	153	61
0	161	-212	-8	688	-611	4	164	-174	L 5	411	-325
1	274	-220	-7	284	-269	5	326	229		5	14
2	709	693	-6	559	535	6	504	408	-5	518	-441
3	131	-81	L -5	156	-121	L 7	372	345	-5	359	309
4	542	-463	-4	594	-543	8	440	-456	-4	456	403
5	582	531	-3	488	-401		5	10	-3	440	-317
6	162	-158	L -2	737	673	-9	508	484	-2	158	-100
7	518	-535	-1	321	356	-8	149	34	L -1	501	463
8	160	-208	L 0	588	-545	-7	545	557	0	158	09
9	149	162	L 1	815	626	-6	162	189	L 1	314	-220
	5	3	2	1009	801	-5	567	426	2	380	-377
-9	278	238	3	425	368	-4	517	508	3	370	249
-8	983	927	4	589	-532	-3	760	683	4	355	340
-7	1048	-895	5	162	-134	L -2	161	34	L	5	15
-6	1278	-1087	6	164	230	L -1	554	537	-6	358	353
-5	1603	988	7	161	-65	L 0	224	205	-4	497	-470
-4	723	639	8	306	-340	1	720	633	-3	363	346
-3	815	-687	9	139	-30	L 2	514	383	-2	769	825
-2	775	-650		5	7	3	164	102	L -1	568	-500
-1	1835	2164	-9	430	-419	4	164	142	L 0	743	-674
0	1304	1480	-8	507	407	5	161	219	L L 1	637	645
1	1198	-1171	-7	164	-61	L 6	156	-23	L 2	510	524
2	1056	-902	-6	977	-803	7	293	275	L 3	450	-479
3	270	164	-5	159	-63	L 8	132	23		5	16
4	361	237	-4	1020	921		5	11	-6	443	484
5	736	-617	-3	209	177	-9	127	-92	L -4	528	-574
6	163	-106	L -2	949	-938	-8	142	-169	L -2	631	687
7	462	432	-1	243	-233	-7	610	511	-1	451	302
8	159	59	L 0	1227	1053	-6	150	-123	L 0	423	-424
9	391	-368	1	249	233	-5	974	966	1	140	-229
	5	4	2	895	-733	-4	463	389		5	17
-9	159	-32	L 3	410	-273	-3	864	718	-4	484	502
-8	517	503	4	848	731	-2	163	119	-2	573	-515
-7	239	-208	5	653	614	-1	977	796		450	466
-6	666	-622	6	516	-412	0	610	-518			



## 7.4. Discussion of the Structure.

### Stereochemistry.

The structure is shown in a-axis projection in Figure 7.1; this shows that the proposed stereochemistry<sup>(130)</sup> (5.XXXII in Fig. 5.4) must be revised to 5.XXXIII, which is reproduced below as 7.I. The attack on the C(1)-C(2) double bond of humulene (5.XXXI) is thus revealed as cis-, but is trans- at the other two as proposed<sup>(130)</sup>. A possible alternative mechanism to the expected all-trans, concerted cyclisation of humulene involves intermediate formation of a bicyclobutonium ion<sup>(162)</sup>, which is attacked by hydroxyl.<sup>(163)</sup> Although the present study has furnished the complete stereochemistry of humulene bromohydrin, it will require careful biosynthetic studies to establish the pathway from the farnesyl precursor 5.XXVIII (Fig 5.4) to caryophyllene.



7.I. Humulene Bromohydrin : Representation of true Stereochemistry.

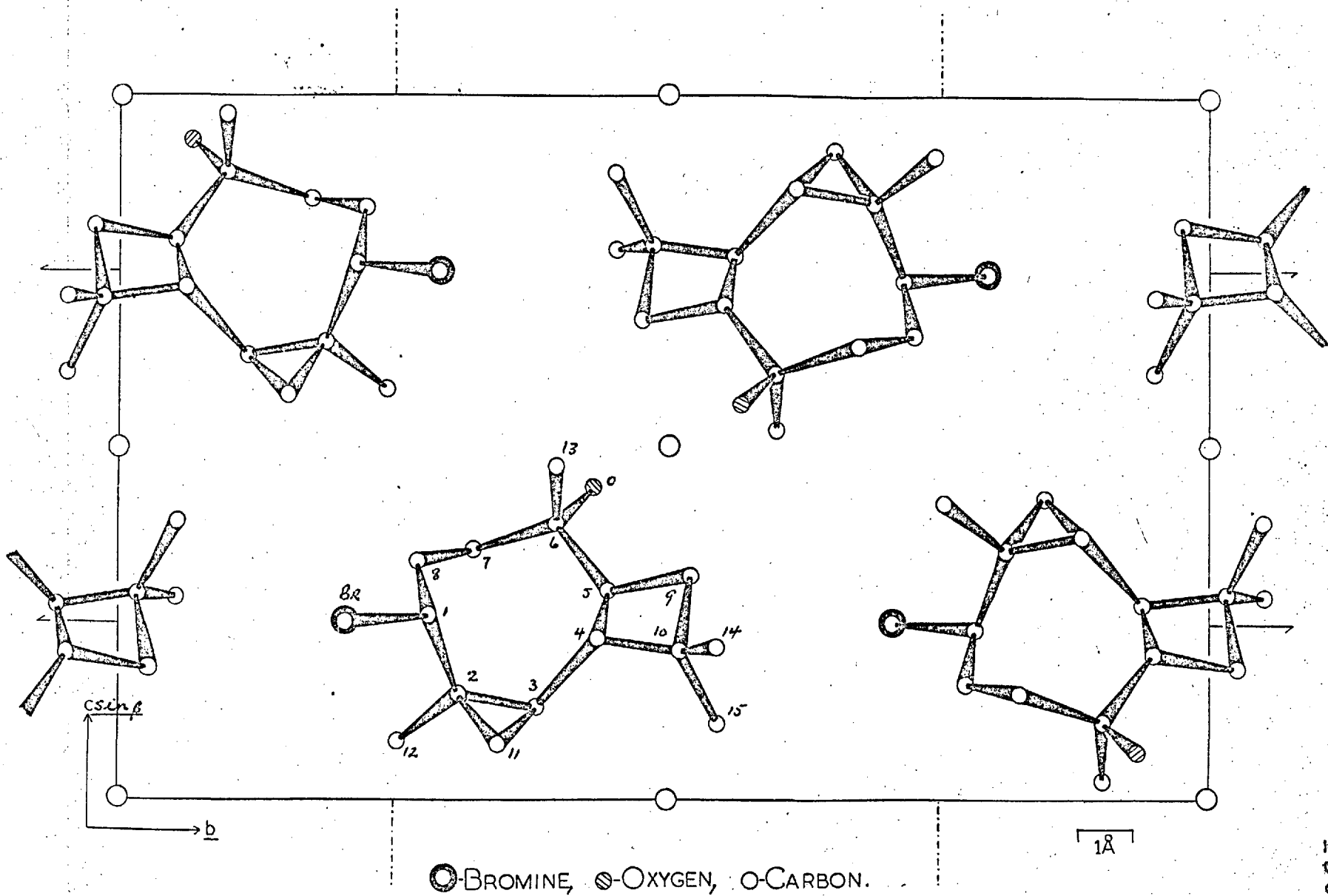
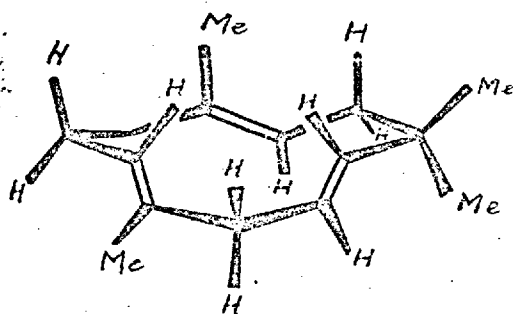


Figure 7.1. Humulene Bromohydrin in a-axis projection.

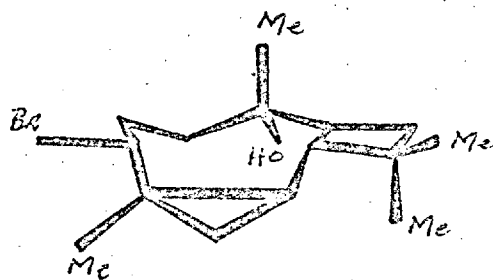
### Geometry and Conformation.

In view of the stereospecific reconstitution of the all-trans-triene ring of humulene from the bromohydrin, and the ease with which these reactions proceed in either direction<sup>(130)</sup> (see Sect. 5.4), it is instructive to note the close similarity between the conformation adopted by humulene in its silver nitrate adduct<sup>(128)</sup> (7.II, below), and that adopted by the bromohydrin (7.III). The perspective drawing shows that all three double bonds in humulene bis-silver nitrate are nearly perpendicular to the cycloundecatriene ring. This leaves the  $\pi$ -orbitals in 7.II ideally situated for cyclisation to form the cyclobutane ring of 7.III.

One might have expected such a large ring (7.II) to have a very mobile shape, especially in solution, and have ascribed the geometry found to the influence of  $\text{Ag}^+$ , and to packing requirements. However comparison of 7.II with 7.III indicates that the crystal conformation



7.II



7.III

adopted by humulene is no mere accident, and must have been present in solution immediately prior to cyclisation. Recent n.m.r. studies of the conformational equilibria of humulene in solution<sup>(164)</sup> have proved inconclusive in establishing 7.II as the preferred conformation. However there is some evidence that the conformations adopted by cyclic olefins in crystalline complexes are an accurate reflection of those adopted prior to reaction in solution : X-ray studies have shown that cis,cis,cis-1,4,7-cyclononatriene has, within experimental error, the same structure in both the free state<sup>(165)</sup> and in its silver nitrate adduct<sup>(166)</sup>; the same is also true of trans,trans,trans-1,5,9-cyclododecatriene<sup>(167)</sup> and germacatriene<sup>(136)</sup>, the latter compound will be discussed in section 8.4.

The interatomic distances and valence angles are shown in Tables 7.6, 7.7, respectively. They are also shown in Figure 7.2 for ease of reference. The standard deviations quoted are probably low estimates, since block-diagonal least-squares approximations were used to optimize the positional parameters.

The C(1)-Br distance of 1.992<sup>o</sup>Å is rather longer than the average value quoted for the alkyl bromides (1.94<sup>o</sup>Å<sup>(153)</sup>), but comparably long distances have been found in retusanine-(+)-3-bromocamphor-9(7 $\pi$ )-sulphonate<sup>(150)</sup>,

TABLE 7.6.Humulene Bromohydrin.

Intramolecular bonded distances (r), in Angstroms, together with their estimated standard deviations ( $\sigma$ ).

Atoms	<u>r</u>	<u><math>\sigma</math></u>	Atoms	<u>r</u>	<u><math>\sigma</math></u>
Br - C(1)	1.992	0.007	C(5) - C(6)	1.511	0.009
C(1) - C(2)	1.507	0.010	C(5) - C(9)	1.553	0.009
C(1) - C(8)	1.509	0.011	C(6) - C(7)	1.528	0.010
C(2) - C(3)	1.521	0.009	C(6) - C(13)	1.518	0.010
C(2) - C(11)	1.509	0.011	C(6) - O	1.462	0.009
C(2) - C(12)	1.510	0.011	C(7) - C(8)	1.547	0.010
C(3) - C(4)	1.490	0.009	C(9) - C(10)	1.557	0.009
C(3) - C(11)	1.513	0.011	C(10) - C(14)	1.480	0.010
C(4) - C(5)	1.553	0.010	C(10) - C(15)	1.518	0.010
C(4) - C(10)	1.585	0.009			

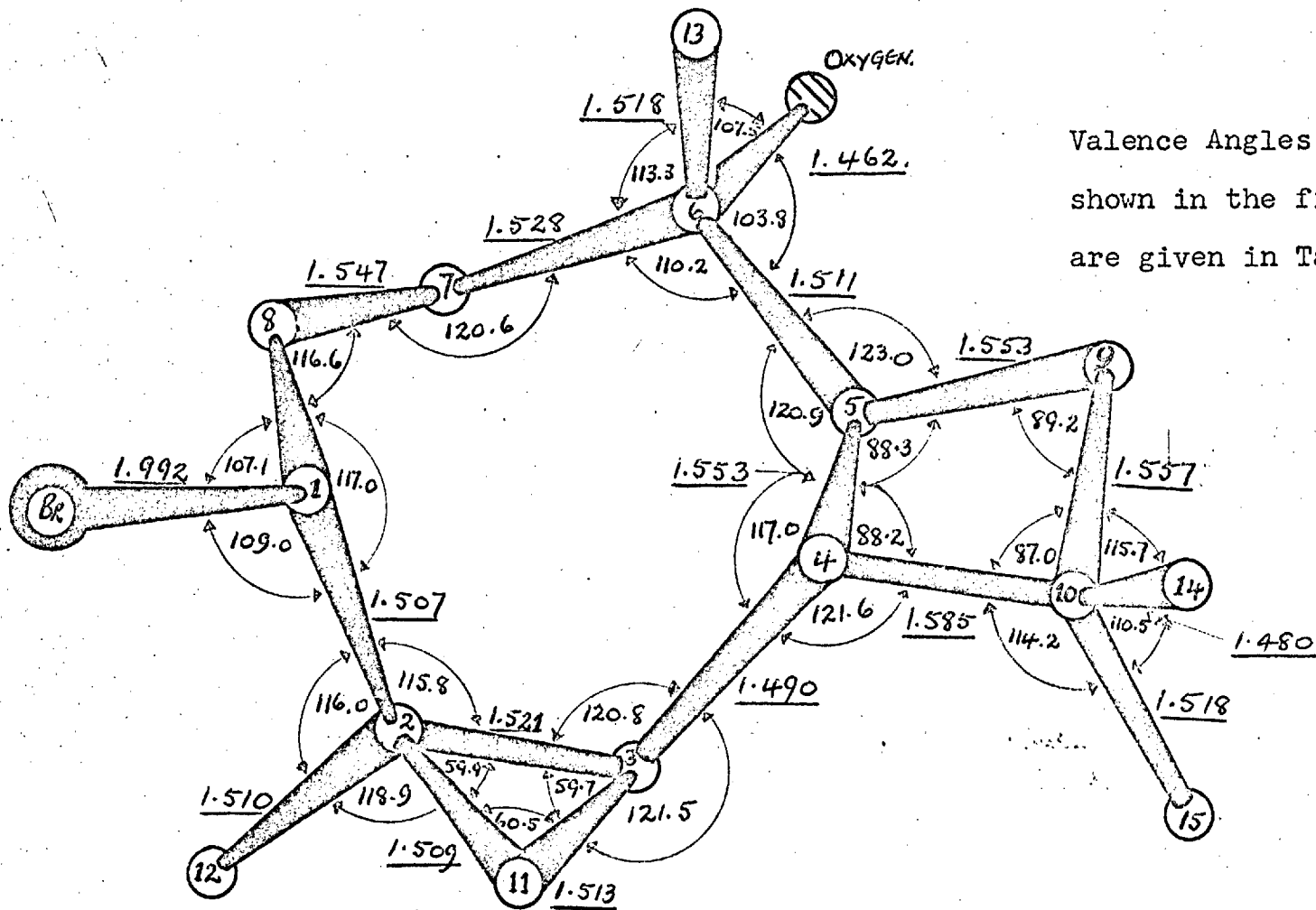


Figure 7.2. a-axis projection showing bondlengths (underlined) and valence angles.

TABLE 7.7.

Humulene Bromohydrin.

Valence Angles ( $\theta$ )<sup>o</sup> in the Asymmetric Unit, together with  
their Estimated Standard Deviations ( $\sigma$ )<sup>o</sup>.

Atoms	$\theta^{\circ}$	$\sigma^{\circ}$	Atoms	$\theta^{\circ}$	$\sigma^{\circ}$
Br-C(1)-C(2)	109.0	0.5	C(4)-C(10)-C(9)	87.0	0.5
Br-C(1)-C(8)	107.1	0.5	C(4)-C(10)-C(14)	116.7	0.6
C(1)-C(2)-C(3)	115.8	0.6	C(4)-C(10)-C(15)	114.2	0.5
C(1)-C(2)-C(11)	116.0	0.6	C(5)-C(4)-C(10)	88.2	0.5
C(1)-C(2)-C(12)	116.0	0.6	C(5)-C(6)-C(7)	110.2	0.5
C(1)-C(8)-C(7)	116.6	0.6	C(5)-C(6)-C(13)	114.9	0.6
C(2)-C(1)-C(8)	117.0	0.6	C(5)-C(6)-O	103.8	0.6
C(2)-C(3)-C(4)	120.8	0.5	C(5)-C(9)-C(10)	89.2	0.5
C(2)-C(3)-C(11)	59.7	0.5	C(6)-C(5)-C(9)	123.0	0.6
C(2)-C(11)-C(3)	60.5	0.5	C(6)-C(7)-C(8)	120.6	0.6
C(3)-C(2)-C(11)	59.9	0.5	C(7)-C(6)-C(13)	113.3	0.6
C(3)-C(2)-C(12)	118.6	0.6	C(7)-C(6)-O	106.2	0.6
C(3)-C(4)-C(5)	117.0	0.6	C(9)-C(10)-C(14)	115.7	0.6
C(3)-C(4)-C(10)	121.6	0.5	C(9)-C(10)-C(15)	111.0	0.6
C(4)-C(3)-C(11)	121.5	0.6	C(11)-C(2)-C(12)	118.9	0.6
C(4)-C(5)-C(6)	120.9	0.6	C(13)-C(6)-O	107.5	0.5
C(4)-C(5)-C(9)	88.3	0.5	C(14)-C(10)-C(15)	110.5	0.6

5'-bromo-5'-deoxythymidine<sup>(168)</sup>, and dibromomenthone<sup>(169)</sup>. Of the other exocyclic bonds the C(6)-O distance compares favourably with cited values<sup>(153)</sup>, while the C-Me distances, although shorter than the accepted C-C single bond value of 1.539 Å<sup>(153)</sup>, are not significantly so. The fused ring system presents some interesting geometrical and conformational points, and these are discussed separately below.

#### i) The Cyclo-octane Ring.

The assumption of the distorted crown as the preferred conformation<sup>(170)</sup>, from thermochemical and spectroscopic evidence, has recently been challenged. Hendrickson<sup>(158)</sup> has calculated the minimum strain-energy ( $E_{\min}$ ) (see Appendix III) for nine symmetrical conformers, as a function of the valence angles ( $\epsilon$ ), dihedral (torsion) angles ( $\omega$ ), and non-bonded H-H contacts ( $r$ ). He concluded that, when the valence angles are allowed to vary from the tetrahedral value ( $109.47^\circ$ ), the conformations with  $D_2$  and  $C_s$  symmetry are preferred, the latter being slightly less strained by ca. 0.3 kcal mole<sup>-1</sup>. In a later calculation<sup>(159)</sup> C-H and C-C non-bonded interactions were allowed for, and one other conformation included (symmetry  $S_4$ ). A value of  $112^\circ$  was now taken as that of minimum strain at saturated



carbon, from hybridization studies. In this case the  $\underline{C}_s$  form was preferred by 0.9 kcal mole<sup>-1</sup> over the  $\underline{S}_4$ , and by 1.7 kcal mole<sup>-1</sup> over the  $\underline{D}_2$ . Similar calculations by Wiberg<sup>(171)</sup>, and by Bixon and Lifson<sup>(172)</sup> have given comparable results. The latter workers have lifted the symmetry requirements, and conclude that their are four forms of comparable  $\underline{E}_{\min}$ ; the boat-chair (Hendrickson  $\underline{C}_s$  form), and the twisted crown ( not considered by Hendrickson, since it is not symmetric ), have the lowest values.

The occurrence of the boat-chair form has recently been shown by several X-ray determinations. Dunitz et.al.<sup>(173)</sup> have studied the cis- and trans-cycloöctane dicarboxylic acids, and Groth<sup>(174)</sup> has studied the cycloöctane peroxide dimer. The structural parameters in both cases have agreed well with the theoretical values. In the structure of taxinol<sup>(175)</sup> the cycloöctane ring is fused to two cyclohexane rings, but preserves approximate  $\underline{C}_s$  symmetry. Evidence for the distorted crown form, from a study of a salt of azacycloöctane<sup>(176)</sup> has been shown inconclusive<sup>(173)</sup> due to structural disorder. More recently 1,2,5,6-tetrabromocycloöctane<sup>(177)</sup> has been found to exist in this conformation in the crystal, and possibly in solution.

The ring in the present study ( C(1)→C(8) ) is

boat-chair, but is distorted from  $\underline{C}_s$  symmetry by the ring fusion. Figure 7.3 shows the ideal conformation, and the parameters involved; it is numbered as in the present study. Atoms C(2), C(4), C(6), C(8), show an average deviation from planarity (required by  $\underline{C}_s$  symmetry) of 0.19Å. Table 7.8(a) shows the values of ( $\underline{\omega}$ ) and ( $\underline{\theta}$ ) obtained in this work, compared with those of Hendrickson<sup>(159)</sup> and Bixon and Lifson<sup>(172)</sup>. The latter authors have also predicted the deviation from the mean plane ( C(1)-C(8) ) of all eight atoms in the ring, these figures are compared with those from the present study in Table 7.8(b). It can be seen that the largest deviations from the theoretical values are caused by the cyclopropane ring fusion, i.e.  $\underline{\omega}_2$  differs by  $\approx 48^\circ$ , and C(2) and C(3) show the largest discrepancies in the comparison of planarity.

The angular strain energy ( $\underline{E}_\theta$ ), involved in the variation of valence angles from  $112^\circ$ , is 7.33 kcal mole<sup>-1</sup> for the present structure, while the torsional strain ( $\underline{E}_\omega$ ) is 7.8 kcal mole<sup>-1</sup> \*. The non-bonded interactions are difficult to estimate, due to lack of resolution of hydrogen atoms; however the contribution from this source to  $\underline{E}_{\text{total}}$  is usually small. Comparison with

---

\* see Appendix III for formulae used.

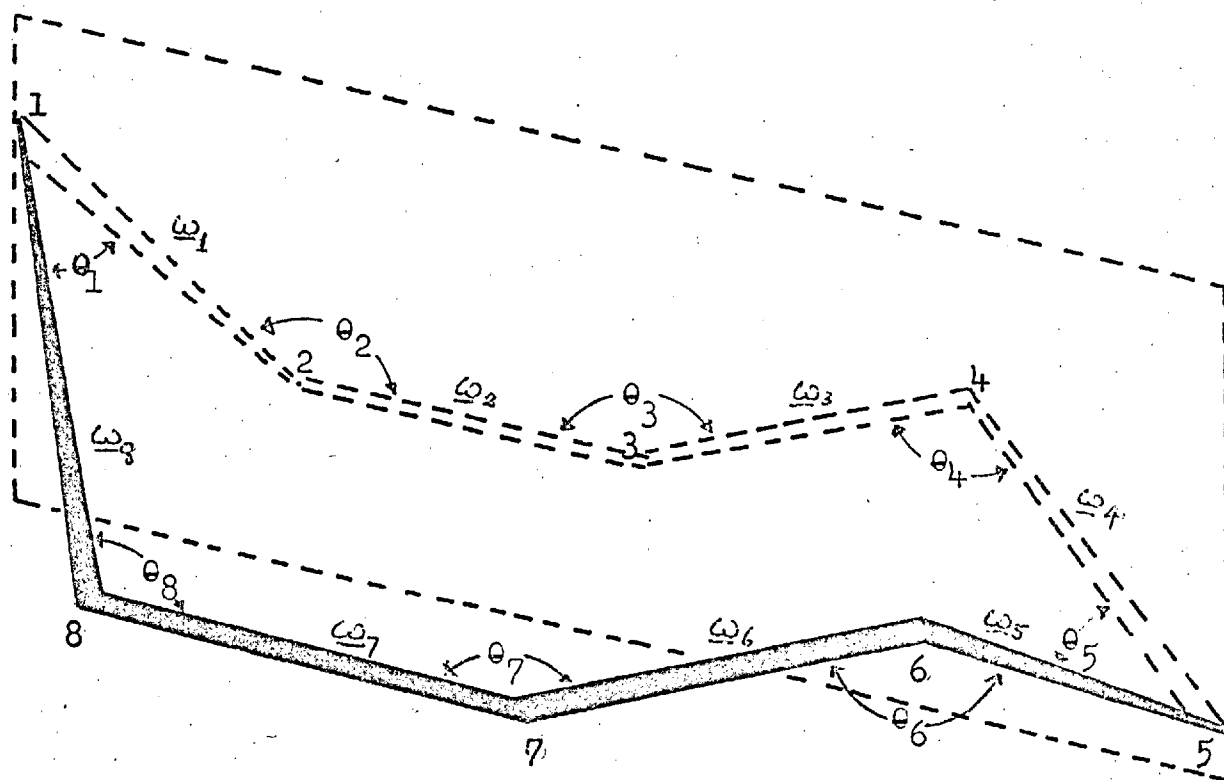


Figure 7.3. Ideal  $C_s$  (boat-chair) conformation for cyclooctane ring after Hendrickson<sup>(158)</sup>. The atomic numbering corresponds to the present study. For the minimum-energy form  $E_{\min} = E_{\theta} + E_{\omega} + E_{NB} = 11.1$  kcal/mol

TABLE 7.8(a).

Values of  $\theta_1-\theta_8$  and  $\omega_1-\omega_8^*$  for Humulene Bromohydrin, in comparison with the theoretical values from minimum - energy calculations (159,172).

Parameter	This work	Bixon & Lifson <sup>(172)</sup>	Hendrickson <sup>(159)</sup>
$\theta_1$	117.0°	116°	117°
$\theta_2$	115.7	116	116
$\theta_3$	120.8	114	116
$\theta_4$	117.0	114	116
$\theta_5$	120.9	115	117
$\theta_6$	110.2	113	116
$\theta_7$	120.6	115	116
$\theta_8$	116.6	116	116
$\omega_1$	-92.9°	-64°	-65.0°
$\omega_2$	4.4	-44	-44.7
$\omega_3$	80.7	106	102.2
$\omega_4$	-86.7	-72	-65.0
$\omega_5$	68.6	70	65.0
$\omega_6$	-93.0	-105	-102.2
$\omega_7$	58.7	46	44.7
$\omega_8$	53.3	64	65.0

\* Calculated using MOJO (Appendix II).

TABLE 7.8(b).

Displacement ( $d^*$  in Angstroms of C(1)-C(8) from the mean plane through the cyclooctane ring of Humulene Bromohydrin, compared with the theoretical values of Bixon and Lifson<sup>(172)</sup>.

Atom	$d_{\text{obs}}$	$d_{\text{theor}}$
C(1)	0.62	0.71
C(2)	-0.37	-0.08
C(3)	-0.38	-0.65
C(4)	0.47	0.35
C(5)	-0.08	0.06
C(6)	0.19	0.34
C(7)	-0.56	-0.65
C(8)	0.11	-0.08

\* Calculated using the program DIDO (chapter 4).

Hendrickson's data<sup>(159)</sup> shows that the value of  $\underline{E}_\theta + \underline{E}_\omega$  here, exceeds that for the ideal  $\underline{C}_S$  conformation by 6.55 kcal mole<sup>-1</sup>. This must reflect fairly accurately the additional strain introduced by the fusion with two (highly strained) small rings. It is surprising, therefore, how closely the conformation observed here tallies with that from minimum-energy calculations, despite the effects of what may be termed 'fusion strain'. It would be interesting to perform similar calculations with the parameters of taxinol<sup>(175)</sup>, when the full details are published.

On the limited evidence available it would appear that the X-ray results quoted above support the theoretical concepts. No one conformation appears to be preferred, and although spectroscopic results<sup>(177,178)</sup> indicate the occurrence of only one conformation in solution, there is no evidence that this is the same one in each case.

The overall average valence angle ( $\theta$ ) in the ring is  $117.4^\circ \pm 0.6^\circ$ , and compares well with values for 7-, 9-, and 10-membered saturated carbocycles, viz :  $116^\circ$  in the cycloheptane rings of bromogeigerin acetate<sup>(179)</sup>, and caryophyllene chlorohydrin<sup>(180)</sup>;  $117^\circ$  in cyclononylamine hydrobromide<sup>(181)</sup>;  $116^\circ$  in 1,6-cis-diaminocyclodecane<sup>(182)</sup>, and  $117^\circ$  in 1,6-trans-diaminocyclodecane<sup>(183)</sup>. The

general increase in  $\theta_{ave}$  over the tetrahedral value obtained from the X-ray results is also borne out by the theoretical minimum-energy calculations.

The average bond length in the cyclooctane ring is 1.521 Å ( average e.s.d. 0.010 Å ), which does not differ significantly from the accepted average. The short C(3)-C(4) distance is probably a reflection of the 'fusion strain'.

#### ii) The Cyclobutane Ring.

The proposed trans-fusion<sup>(130)</sup> has been confirmed, and its feasibility on conformational and geometrical grounds has been discussed above. Figure 7.4 shows that the ring is buckled, the average deviation of the atoms from the mean plane is 0.14 Å. In Table 7.9 the distortion observed here is compared with results of other studies, by both X-ray and electron diffraction, in terms of :

- (a) the average valence angle ( $\theta^p$ ) in the ring,
  - (b) the average bond-length ( $r$ ) in Å,
  - (c) the perpendicular distance ( $h$ ), in Å, between ring diagonals,
- and (d) the average dihedral fold about the diagonals,

$$\text{i.e. } \frac{\theta_{13} + \theta_{24}}{2} .$$

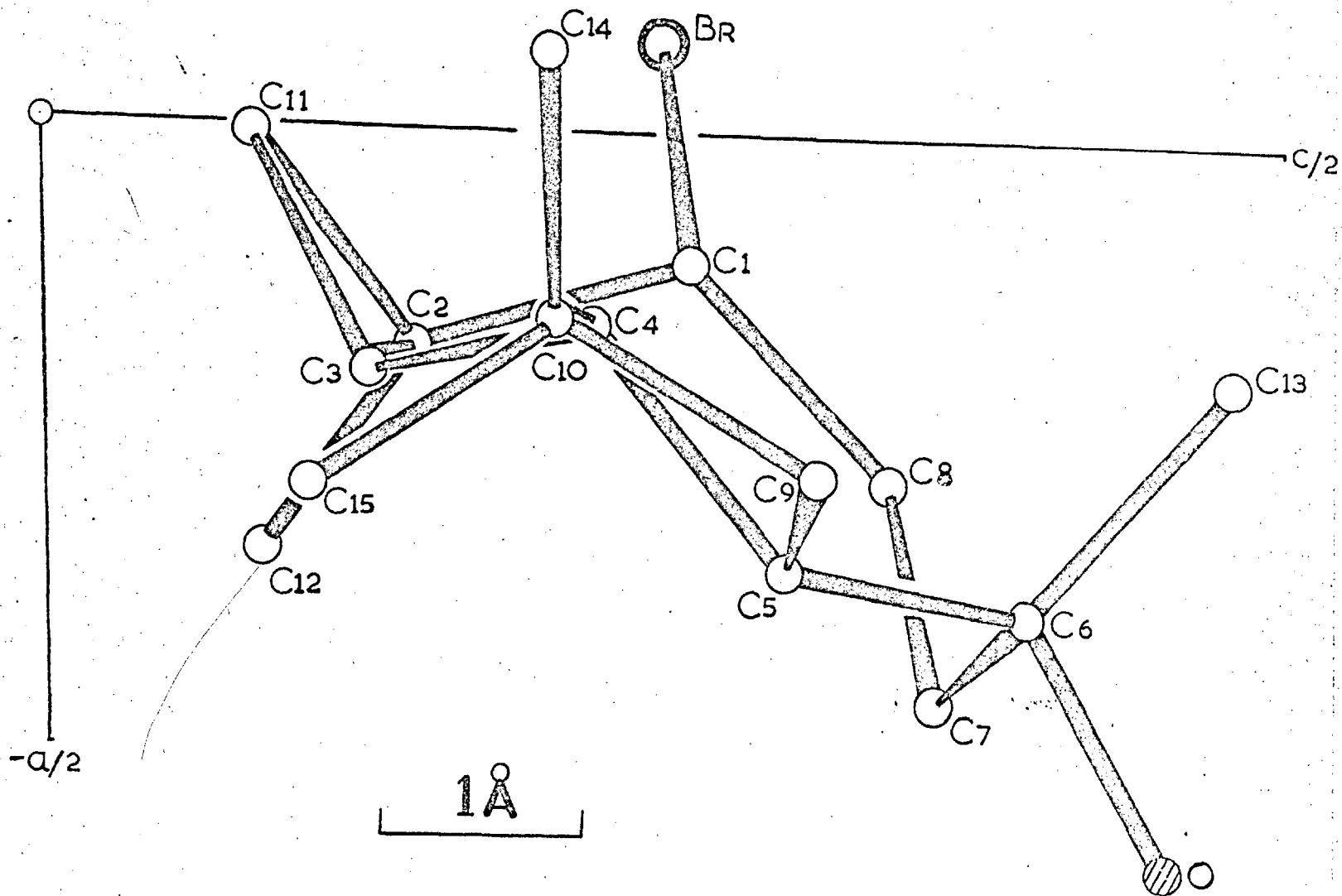


Figure 7.4. Humulene Bromohydrin in 010 projection, showing the buckling of the cyclobutane ring.



Criteria (c) and (d) are illustrated in Figure 7.5 below.

The results show that the ring is generally non-planar, even in cases of simple substitution, as predicted by theoretical work<sup>(186,193,194)</sup>. The effect is enhanced by trans-fusion to larger ring systems (entries 1,2,3, in Table 7.9). In the former case values of  $\phi_{ave}$  lie between  $152^\circ$  and  $160^\circ$ , but are as low as  $139^\circ$  in the latter. Relatively few idealized planar rings are found; where the X-ray method has been used the centres of such rings coincide with inversion centres ( $\bar{1}$ ).

A notable feature in all cases, except entry 4, is the increase of C-C bondlengths over the accepted value, an average of  $1.57\text{\AA}$  is given by the X-ray data, agreeing well with the electron-diffraction results. The effect occurs in both buckled and planar rings, and has been

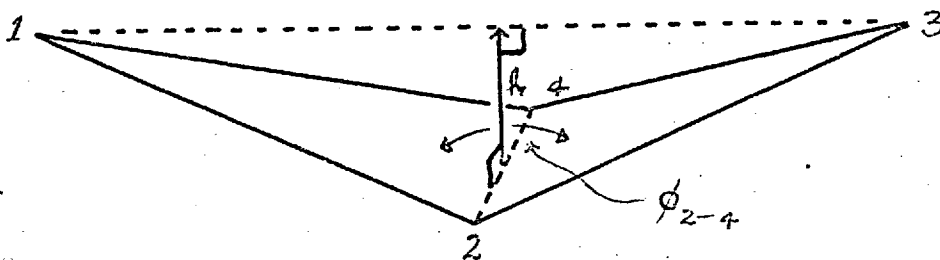


Figure 7.5. Criteria (c) & (d) in cyclobutane ring analysis.

TABLE 7.9.

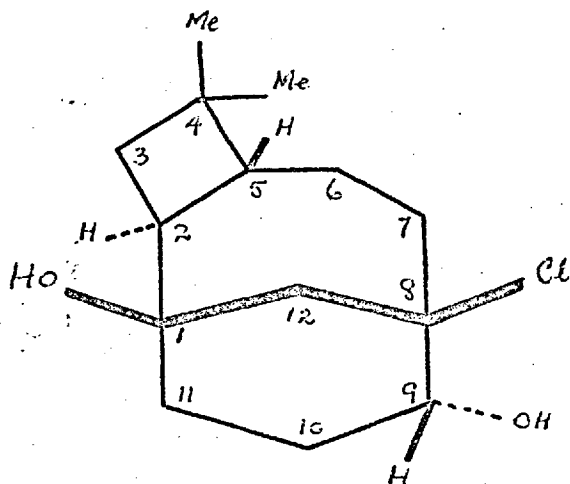
Analysis of Cyclobutane Ring Distortion (Criteria a - d)

Compound & Reference	Ave $\theta^{\circ}$	Ave $r$ Å	$h$ Å	Ave $\theta^{\circ}$
1. Humulene Bromohydrin	88.2	1.562	0.28	151
2. Caryophyllene (180) Chlorohydrin	87.0	1.556	0.36	143
3. Caryophyllene (125) Alcohol Chloride	86.3	1.573	0.40	139
4. Anemonin (184)	88.2	1.537	0.26	152
5. Octachloro- cyclobutane (185)	87.7	1.59	-	158
6. Cyclobutane (186) (⊗)	-	1.57	-	160
7. Cyclopentanone (187) (photodimer)	90.0	1.57	0.00	Planar
8. Methylene cyclobutane (188) (⊗)	90.0	1.56	0.00	Planar
9. Methylene cyclobutane (189) (⊗)	92.5	1.55	-	-
10. Methyl cyclobutane (190) (⊗)	-	1.56 <sub>5</sub>	-	-
11. Octafluoro- cyclobutane (190) (⊗)	89.0	1.60	-	160
12. Dimethyl keten dimer (191) (⊗)	93.0	1.56	-	-
13. Tetraphenyl cyclobutane (192)	90.0	1.57	0.00	Planar

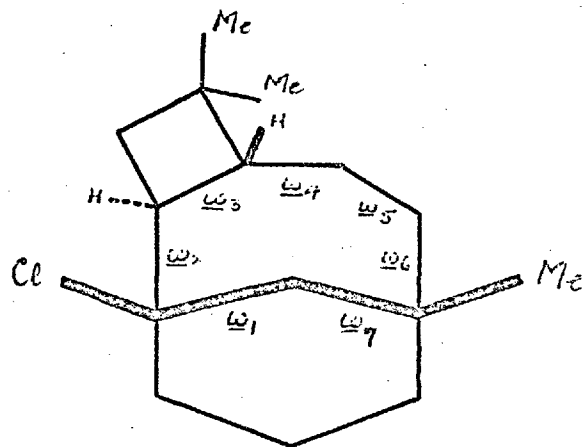
(⊗) Electron-Diffraction Study. / Where values have not been quoted in the cited reference they have been calculated using MOJO (Appendix II).

ascribed<sup>(186)</sup> to trans annular non-bonded repulsions between carbon atoms. The interactions involved across the diagonals are ca. 2.2 Å; in the present study 2.183 Å for C(5)-C(10), and 2.163 for C(4)-C(9). The C-C bond stretching from this source has been calculated<sup>(186)</sup> to be of the order of 0.038 Å; this estimate is borne out by the data of Table 7.9.

Caryophyllene chlorohydrin (CC)<sup>(180)</sup> (entry 2 of Table 7.9) and caryophyllene alcohol chloride (CAC)<sup>(125)</sup> (entry 3), are the most relevant to the present study; their structural formulae are shown in 7.IV, 7.V. The cyclobutane ring is trans-fused to a seven- (rather than eight- ) membered ring, and the distortion is considerably greater. In both cases the cycloheptane ring adopts the boat conformation, which is one of the



7.IV. Caryophyllene Chloro-  
hydrin (CC)



7.V. Caryophyllene Alcohol  
Chloride (CAC)

TABLE 7.10.

Values of  $\theta_{\text{ave}}^{\circ}$  and  $\omega_1 - \omega_7^{\neq}$  for CC and CAC compared with values from minimum-energy calculations<sup>(159)</sup>. The values of  $E_{\theta}$  and  $E_{\omega}$  are also given.<sup>\*</sup>

Parameter	Theoretical	Observed	
		CC(180)	CAC(125)
$\langle \theta \rangle$	115°	116°	112°
$\omega_1$	57.5	62	64
$\omega_2$	30.9	27	34
$\omega_3$	-69.9	-77	-83
$\omega_4$	0.0	13	8
$\omega_5$	69.9	52	70
$\omega_6$	-30.9	-20	-33
$\omega_7$	-57.5	-67	-63
$E_{\theta}$	1.77	4.07	1.07
$E_{\omega}$	5.55	6.58	5.90

$\neq$  Values calculated using MOJO (Appendix II).

$*$  Values given in kcal mole<sup>-1</sup>, the method of calculation follows that due to Hendrickson<sup>(159)</sup> and is set out in Appendix III.

minimum-energy preferred forms (159,195). The optimum values for  $\theta_{ave}$  and  $\omega_{1 \rightarrow 7}$  (the latter are shown in 7.IV) for this conformation are given in Table 7.10, together with the corresponding values for CC and CAC. The values of  $E_{\theta}$  and  $E_{\omega}$  are also listed. The agreement is reasonable, considering the strain due to fusion, and is better than in the cyclooctane ring discussed above. Although non-bonded interactions have been omitted it is possible to explain the increased distortion of the cyclobutane rings in CC and CAC in terms of the sums of  $E_{\theta}$  and  $E_{\omega}$  for the cycloheptane rings. The increased distortion of the macrocycles on fusion to smaller rings is reflected in the increase of this sum over that for the minimum-energy form; thus in the cyclooctane ring of humulene bromohydrin it was 6.55 kcal mole<sup>-1</sup>, in CC it is 3.33 kcal mole<sup>-1</sup>, while in CAC there is actually a decrease of 0.35 kcal mole<sup>-1</sup>. Thus it would appear that the trans-fused cyclobutane ring has been able to transfer some of its strain energy to the cyclooctane ring in humulene bromohydrin, and its geometry is approaching that given by non-fused rings (see Table 7.9). This has not happened to such a great extent in CC, and hardly at all in CAC, resulting in increased distortion of the cyclobutane rings. The inability of the cycloheptane rings in CC and CAC to

distort, and thus to relieve the strain in the cyclobutane rings, is almost certainly due to the 'stiffening' effect of the fused chair-form cyclohexane rings, which share the atoms C(1), C(12), C(8), (see 7.IV, 7.V).

The calculations are by no means rigorous, but they do tend to show the distribution of strain energy in the fused-ring systems considered. It is pleasing to note that the extent of distortion exhibited by the cyclobutane rings does follow in the order predicted by the energy calculations, as shown by Table 7.9. Thus the ring in the present study is least distorted, followed by the rings in CC and CAC in that order.

### iii) The Cyclopropane Ring.

A noticeable feature here is the slight contraction of the C-C distances (average  $\bar{r} = 1.514 \pm 0.010 \text{ \AA}$ ), which compares well with the cited average for cyclopropane rings of  $1.52 \text{ \AA}$  (153). This has been attributed<sup>(186,196)</sup> to bent-bonding, which brings the atomic nuclei into closer proximity. The distorting effect of the three-membered ring on the cyclooctane ring has been mentioned in (i) above.

TABLE 7.11.Humulene Bromohydrin.Non-bonded Intermolecular Contacts less than 4.0 Å.

Roman suffices refer to atoms related to the asymmetric unit given in Table 7.2 by the following symmetry operations :

- i)  $1 + x, y, z$ ;      ii)  $\frac{1}{2} - x, \frac{1}{2} + y, \frac{1}{2} - z$ ;  
 iii)  $-x, 1 - y, -z$ ;      iv)  $-1 - x, 1 - y, 1 - z$ ;  
 v)  $-1 - x, 1 - y, -z$ .

---

Br -	C(7) <sub>i</sub>	3.878	0 -	C(6) <sub>iv</sub>	3.992
C(13)-	O <sub>i</sub>	3.853	0 -	C(9) <sub>iv</sub>	3.413
C(14)-	Br <sub>ii</sub>	3.731	0 -	C(13) <sub>iv</sub>	3.767
C(15)-	C(11) <sub>iii</sub>	3.759	0 -	O <sub>iv</sub>	3.213
	C(15)	-	C(15) <sub>v</sub>	3.861.	

---

### Intermolecular Distances and Packing.

Figure 7.1 shows the molecular packing projected down the  $a$ -axis. The molecules pack in rows parallel to the  $2_1$  screw axes, but keep well clear of the centres of symmetry ( $\bar{1}$ ). The closest intermolecular contacts  $< 4.0 \text{ \AA}$  are shown in Table 7.11; they are all greater than the required van der Waals clearances. The closest contact ( $3.21 \text{ \AA}$ ) is between two oxygen atoms across a symmetry centre, but the directions of the O-H bonds preclude any possibility of hydrogen bonding.



CHAPTER 8.The Crystal and Molecular Structure of the 1:1 Adduct of  
Germacatriene with Silver Nitrate,  $C_{15}H_{24} \cdot AgNO_3$ .8.1. Preliminary Work.

The crystals were supplied by Dr. J. K. Sutherland and Mr. E. D. Brown; they were small white prisms. Examination under the polarizing microscope, with the aid of a quartz wedge, showed them to be uniaxial. The extinction directions, transverse to the needle axis, were indicative of a monoclinic crystal, with a non-unique (a- or c-) axis parallel to the needle direction. Oscillation and Weissenberg photographs exhibited Laue symmetry  $2/m$ , and confirmed the above indication. The conditions for absent spectra were shown to be :

$$h0l, \quad l \neq 2n; \quad 0k0, \quad k \neq 2n;$$

defining the spacegroup uniquely as  $P2_1/c$ . The cell parameters were obtained by the least-squares procedure (CEDI), applied to some 20 theta values measured from



by taking two equatorial ( $0k\bar{l}$ ) Weissenberg photographs, two weeks being allowed between each 45hr. exposure. The level of the intensities on the second film was reduced by about 25-30%, but no changes in the relative values could be detected visually. This indicated that no photo-sensitized structural changes were taking place.

A compromise had to be made between the size of crystal required for speedy data collection, and the size required to minimize absorption errors. Several crystals were tried, and one of approximate dimensions : 0.25 x 0.12 x 0.15 mm. was chosen and encapsulated. The layers  $0k\bar{l}$  -  $5k\bar{l}$  were recorded as described in section 4.1, using Ni-filtered  $\text{CuK}\alpha$  radiation. The average exposure time was  $\sim 50$ hr. per layer, and the oscillation range was reduced slightly to obtain as much high- $\theta$  data as possible, in order to reduce the Fourier series termination errors. A total of 1198 independent reflection intensities, out of some 2000 in the Cu-sphere, were visually estimated using step-wedges made at  $0k\bar{l}$ ,  $2k\bar{l}$ ,  $4k\bar{l}$ . The layers  $h0\bar{l}$ ,  $h1\bar{l}$ , were similarly recorded and yielded 228 common data for correlation.

The two data lists were corrected for Lorentz and polarization effects (FIFI), and placed on a common, arbitrary scale using the POLO program. The absolute scale-factor (K) was obtained during structure solution

by comparing  $\sum |F_o|$  and  $\sum |F_c|$ . A systematic absorption correction, although desirable, was impossible due to the gradual decay of the crystals.

## 8.2. Structure Solution.

Two-dimensional Patterson maps were computed for the [100]- and [010]-projections, using BOSS. With respect to silver co-ordinates  $\underline{x}$ ,  $\underline{y}$ ,  $\underline{z}$ , vector peaks between centrosymmetrically related atoms occur at  $0, 2\underline{y}, 2\underline{z}$ ; and  $2\underline{x}, 0, 2\underline{z}$ ; respectively in these maps. The silver co-ordinates were given as :

$$\underline{x} = 0.052, \quad \underline{y} = 0.318, \quad \underline{z} = 0.319.$$

A two-dimensional electron-density map (BOSS) for the [010]-projection, using phases given by the above position (together with an estimated B-factor of  $3.0 \text{ \AA}^2$ ), showed the general shape and packing of the molecules; R was 0.356. The map is shown in Figure 8.1, which indicates that the molecules lie between symmetry elements at  $\underline{z} = 0, \frac{1}{4}, \frac{1}{2}, \frac{3}{4}, 1$ . This map may be compared with Figure 8.2 (p.192) which shows the final structure in b-axis projection.

Using the full, correlated, three-dimensional data list, a 3D Patterson map was computed (BOSS). Equations

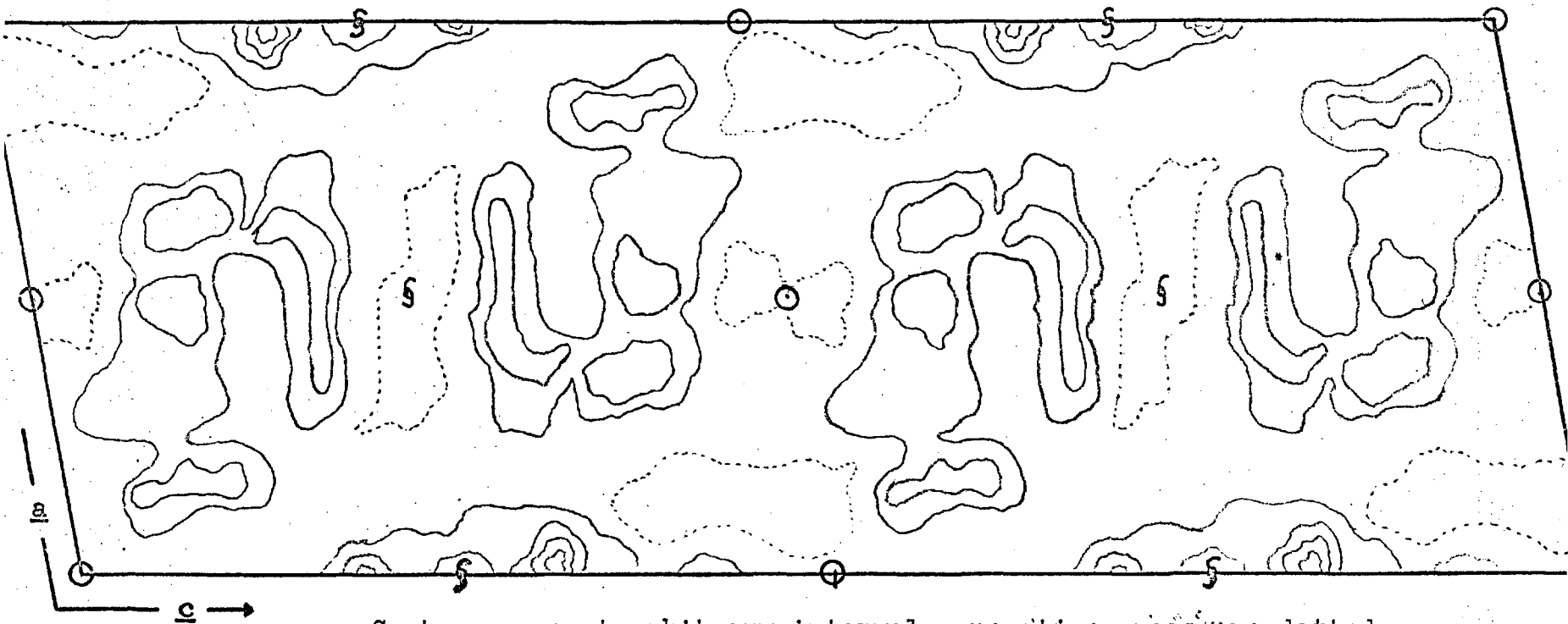


Figure 8.1. Germacatriene:AgNO<sub>3</sub> [010]-Fourier, which should be compared  
with Figure 8.2.

similar to 7.1, 7.2, (p. 131) give the Harker sections :

1.  $\underline{x}$ ,  $\frac{1}{2}$ ,  $\underline{z}$ ; due to the  $2_1$  screw,
- and 2.  $0$ ,  $\underline{y}$ ,  $\frac{1}{2}$ ; due to the  $\underline{c}$ -glide. .... 8.1.

The Patterson was solved uniquely for silver, giving the co-ordinates :

$$\underline{x} = 0.0541, \quad \underline{y} = 0.3182, \quad \underline{z} = 0.3177,$$

in excellent agreement with those obtained above.

A structure factor calculation using this position, with estimated B-factor as before, gave  $\underline{R} = 0.346$ . These values were then used to compute the first 3D electron-density map; reflections for which  $|F_c| \leq 0.25 |F_o|$  were omitted from the Fourier summation. The nitrate ion was immediately discernible in the  $\underline{x} = 0$  section; nine other peaks appeared to form the basis of the carbon skeleton, but their resolution was not good. Two further maps were computed (using the same rejection test for the structure factors) :

(i) included silver, nitrogen ( $\underline{B} = 4.0 \text{ \AA}^2$ ), and the three oxygens ( $\underline{B} = 4.0 \text{ \AA}^2$ ) in the structure-factor calculations, all as neutral atoms;  $\underline{R}$  was 0.327;

(ii) as above, plus the nine possible carbon sites ( $\underline{B} = 4.0 \text{ \AA}^2$ ),  $\underline{R}$  was 0.284.

The latter map confirmed the nine carbons, and revealed

the positions of all other non-hydrogen atoms. A bead model of the structure at this stage showed chemically sensible geometry.

A fourth map, including all atoms (except hydrogens) in the structure factor calculation ( $\underline{R} = 0.233$ ), showed no spurious features, but exhibited some series termination ripple; no reflections were rejected. Optimum atomic positions were obtained from the map using Booth's method<sup>(161)</sup>.

### 8.3. Refinement of the Structure.

The structure was initially refined using the block-diagonal method of BABA. The designation of Run Nos. follows the scheme outlined in Sect. 6.4. (p. 95). Positional parameters,  $\underline{B}$ -factors, and an overall scale factor ( $K$ ), were varied for four cycles; no weighting scheme was employed, but scattering factors<sup>(14)</sup> appropriate to the normal resonance hybrid nitrate ion, i.e.  $N^+$ ,  $O^{\frac{2}{3}-*}$ , and to  $Ag^+$ , were used.  $\underline{R}$  fell to 0.199 (run I1, see Table 8.1, p. 183).

A weighting scheme of the Hughes type<sup>(51)</sup> was then introduced, with  $F^*$  (Eq. 2.29) set to 450 on the scale of the structure factors of Table 8.4; four more cycles reduced  $\underline{R}$  by only 0.005 (run I2). An analysis of the

---

\* Obtained by linear interpolation between  $0^0$  and  $0^{-1}$

agreement within the individual layers showed considerable errors in the inter-layer scales. This was probably due to uncorrected absorption errors (see above), especially in the correlating data. This was collected with the crystal rotating about the  $b$ -axis, perpendicular to the needle. The X-ray path-lengths within the crystal were thus more variable in this case, compared with the main axis, where the cross-section presented to the beam was far more uniform.

It was therefore decided to include the inter-layer scale-factors as parameters in the isotropic refinement; as already noted, this procedure is invalid in the anisotropic case<sup>(146)</sup>. All further refinement was performed using the full-matrix program ORFLS. Four cycles of unweighted refinement, varying the parameters noted above, reduced  $R$  to 0.159 (run I3). The value of  $F^2$  was reset to 45, and a small number of misindexed reflections corrected. Eight strong, low-order, reflections ( $10\bar{2}$ , 200,  $20\bar{2}$ , 202, 212, 310, 312,  $30\bar{4}$ ) were removed for suspected extinction, and  $R$  fell to 0.104 (runs I4, I5, I6).

An analysis of the observed and calculated structure factors (DELSIG) showed that the average  $\left| |F_o| - |F_c| \right|$  increased linearly with increasing  $|F_o|$ , and the Hughes



weighting scheme was no longer applicable. A scheme was devised from the plot to give reasonably constant values of  $\sum w(|F_o| - |F_c|)^2$  over ranges of  $|F_o|$ , it took the form :

$$w = \frac{1}{1 + a|F_o|} \dots\dots\dots 8.2.$$

where the constant (a) was derived from the slope and intercept of the plot. Convergence was now slower, and four cycles reduced  $R$  to 0.100.

A noticeable feature of these later runs was the oscillatory motion of the nitrogen atom  $N^+$ , and  $O(2)$ . A bond-length calculation showed that the  $N^+ - O(2)$  distance was 1.15 Å, compared with  $N^+ - O(1)$  and  $N^+ - O(3)$  distances of 1.23 and 1.26 Å respectively. The stronger bonding of  $O(2)$  indicated that the charge distribution in the nitrate ion should be changed to  $N^+$ ,  $O(3)^{-1}$ ,  $O(1)^{-1}$ , and  $O(2)^0$ . Correction terms were also included to allow for dispersion effects at  $Ag^+$  using the values  $\Delta f' = -0.5$ ,  $\Delta f'' = 4.7$  (59).  $R$  fell to 0.099 (run 18), and parameter shifts for the nitrate ion became minimal.

A difference map was now computed using  $(F_o - F_c)$  as Fourier coefficients; although it revealed no spurious features, it was not possible to estimate hydrogen atom positions. They were therefore included in the final

stages of refinement in calculated positions (BONDLA), with B-factors equal to that of the carbon to which they were bonded, plus  $0.5 \text{ \AA}^2$ ; these parameters were not refined. The refinement was concluded with runs I9, I10; the ratio of shift to standard deviation was less than 0.10 for all parameters on the final cycle, the maximum positional shift was  $0.0004 \text{ \AA}$ .

Some cycles of refinement using anisotropic temperature factors were performed, but these parameters became non-positive-definite for some atoms (i.e. they were physically meaningless), and the process was not pursued. The failure was probably due to :

i) uncorrected absorption effects,  
and ii) the paucity of data, in the anisotropic case the ratio of observations to parameters was only 6, hardly high enough to guarantee a valid refinement.

The final parameters from the isotropic refinement (Tables 8.2, 8.3) together with the refined scale-factors, to obtain the structure factors shown in Table 8.4; the hydrogen atoms were included in the calculation in their calculated positions. The final R factor was 0.097, for 1190 reflections not affected by extinction. No attempt was made to assess the accidentally absent data, since the number of such terms was large, and the absorption errors would probably have made a comparison

of  $|F_o|$  and  $|F_c|$  rather meaningless. It should be noted that the standard deviations quoted in the following tables are probably realistic estimates, since full-matrix methods were used throughout.

TABLE 8.1.

Germacratriene:AgNO<sub>3</sub>.The Refinement Process.

Run.	Cycles	<u>R.</u>	$\sum w( F_o  -  F_c )^2.$	Max. Pos <sup>n</sup> Shift Å
I1*	4	0.199	50995	0.080
I2*	3	0.194	22595	0.032
I3	4	0.159	76940	0.040
I4	4	0.116	23920	0.021
I5	4	0.110	17630	0.008
I6	4	0.104	15310	0.005
I7	4	0.100	5265	0.0006
I8	4	0.099	5131	0.0006
I9	4	0.097	5065	0.0005
I10	2	0.097	5031	0.0004

\* Block-diagonal approximations (BABA), inter-layer scales not refined.

TABLE 8.2.

Germacatriene:AgNO<sub>3</sub> : Final Positional Parameters as Fractions of the Cell Edges, together with their Estimated Standard Deviations ( $\sigma$ )

Atom	$\underline{x}$	$\underline{\sigma}_x$	$\underline{y}$	$\underline{\sigma}_y$	$\underline{z}$	$\underline{\sigma}_z$
Ag	0.05644	0.00021	0.31799	0.00013	0.31868	0.00007
N	-0.00403	0.00267	0.12024	0.00177	0.20051	0.00098
O(1)	-0.01204	0.00245	0.05989	0.00166	0.25124	0.00091
O(2)	-0.04393	0.00218	0.07619	0.00144	0.14878	0.00081
O(3)	0.04615	0.00200	0.24235	0.00135	0.21058	0.00072
C(1)	0.54685	0.00263	0.02501	0.00160	0.41691	0.00087
C(2)	0.72512	0.00317	0.09135	0.00203	0.45475	0.00115
C(3)	0.86681	0.00303	0.12768	0.00201	0.41241	0.00104
C(4)	0.83943	0.00278	0.27082	0.00166	0.39279	0.00094
C(5)	0.73228	0.00329	0.30357	0.00178	0.33495	0.00109
C(6)	0.65552	0.00318	0.44262	0.00198	0.31070	0.00107
C(7)	0.44453	0.00274	0.42075	0.00160	0.30339	0.00089
C(8)	0.38674	0.00283	0.35095	0.00164	0.35987	0.00098
C(9)	0.37276	0.00281	0.21385	0.00163	0.35561	0.00096
C(10)	0.37644	0.00319	0.12054	0.00213	0.41520	0.00111
C(11)	0.53184	0.00283	-0.09788	0.00169	0.39702	0.00095
C(12)	0.41214	0.00332	0.42417	0.00219	0.42425	0.00121
C(13)	0.88903	0.00311	0.36882	0.00208	0.44878	0.00108
C(14)	0.70867	0.00432	-0.18730	0.00289	0.40367	0.00168
C(15)	0.36347	0.00433	-0.16495	0.00280	0.36365	0.00165

TABLE 8.3.

Germacratriene:AgNO<sub>3</sub>.

Final Isotropic Thermal Parameters (B), and their Estimated  
Standard Deviations ( $\sigma_B$ ).

Atom	<u>B</u>	<u><math>\sigma_B</math></u>	Atom	<u>B</u>	<u><math>\sigma_B</math></u>
Ag	2.91 Å <sup>2</sup>	0.05	C(6)	3.55 Å <sup>2</sup>	0.42
N	3.51	0.36	C(7)	2.34	0.34
O(1)	5.66	0.39	C(8)	2.60	0.36
O(2)	4.27	0.32	C(9)	2.64	0.36
O(3)	3.65	0.29	C(10)	3.83	0.44
			C(11)	2.71	0.36
C(1)	2.37	0.34	C(12)	4.18	0.47
C(2)	3.82	0.45	C(13)	3.62	0.42
C(3)	3.37	0.41	C(14)	6.79	0.71
C(4)	2.42	0.32	C(15)	6.64	0.70
C(5)	3.02	0.39			

TABLE 8.4.

Germacatriene : AgNO<sub>3</sub>.Final Observed and Calculated Structure Factors.

The format is :

	h	,	k	
↓	10  F <sub>o</sub>		10 F <sub>c</sub>	
•	•		•	

The following reflections were omitted for suspected extinction :

h	k	l	10  F <sub>o</sub>	10 F <sub>c</sub>	sinθ / λ
1	0	-2	1268	-1861	0.07512
2	0	0	1376	1981	0.13562
2	0	-2	1002	-1492	0.13451
2	0	2	983	-1342	0.15321
2	1	2	936	1316	0.16117
3	1	0	1042	-1381	0.20949
3	1	2	768	1088	0.22430
3	0	-4	1056	1434	0.20707







0	649	-673	-7	221	-236	13	243	-234		3,7,L		
1	243	-195				15	492	471	0	467	-457	
2	799	923	-1	2,12,L	284	-286	17	383	-330	2	610	639
3	207	145	-2		179	-167	-1	656	772	4	439	-365
4	274	-298	-3		270	236	-2	392	-392	6	316	-296
5	160	100					-3	128	74	8	493	475
8	353	408		3,0,L			-4	390	-381	9	265	132
10	460	-524	0		1205	1425	-5	1137	-1272	16	333	-308
12	248	155	2		309	311	-6	501	495	-1	190	146
14	248	207	4		1192	-1191	-7	1140	1037	-4	558	589
16	331	-312	6		1042	1089	-9	313	-249	-5	215	-114
-2	342	-340	8		166	141	-10	245	-234	-6	823	-867
-4	692	703	10		618	-789	-11	461	-432	-8	442	387
-5	259	-244	12		445	521	-13	819	788	-12	513	-466
-6	632	-620	14		313	-265				-14	575	522
-7	277	230	18		287	229	0	179	-142			
-8	512	460	20		335	-355	1	195	-152	0	361	-364
-9	272	245	22		169	155	2	284	-243	2	348	-359
-10	234	155	-6		406	501	3	747	-809	4	533	555
-12	582	-641					4	214	263	6	425	-431
-14	498	429		3,1,L			5	748	890	10	351	322
			1		953	1033	7	241	-239	12	387	-399
0	435	-386	3		485	-589	9	389	-324	14	238	256
2	233	-158	4		275	-329	11	534	566	-1	400	-392
4	353	396	5		183	-159	13	493	-521	-2	584	654
5	313	-290	6		519	-651	-1	988	1103	-4	425	-376
6	503	-516	8		957	1133	-2	284	225	-6	201	123
7	222	224	9		394	-418	-3	1086	-1194	-8	318	306
8	221	211	10		613	-647	-5	562	465	-10	489	-433
10	259	225	11		236	184	-6	144	84			
12	412	-414	14		397	377	-7	449	456			
14	300	303	16		376	-428	-9	731	-721	0	488	425
-2	667	723	18		269	277	-11	552	493	1	421	-354
-3	232	169	22		199	-217	-15	522	-498	2	342	-342
-4	309	-295	-1		441	-530				3	219	210
-6	166	-110	-2		573	680	0	426	366	7	262	-276
-8	346	361	-3		453	-504	1	529	521	8	360	-324
-10	393	-379	-4		592	646	2	482	-498	9	245	224
-14	272	266	-5		654	699	1	482	-498	-1	199	201
-16	431	-403	-6		1154	-1243	3	385	-352	-4	243	-184
			-7		368	-317	6	356	314	-5	262	-239
			-8		516	537	7	515	524	-6	341	346
			-9		351	308	8	282	-225	-7	259	237
			-10		206	177	9	579	-618	-8	433	-397
				3,2,L			11	200	142	-12	374	297
0	265	245			401	-502	13	284	215	-13	224	171
1	356	-356	0		165	-134	15	430	-376	-14	321	-272
2	265	-274	1		419	-441	-1	501	-466			
3	354	334	2		165	-134	-4	400	-404			
4	322	299	3		708	897	-5	685	664	3	281	-264
7	256	-216	4		635	747	-6	563	442	5	361	362
9	311	256	5		734	-950	-7	799	-880	-1	368	341
11	250	-262	6		406	-407	-8	296	-205	-3	411	-355
15	210	256	7		392	441	-11	437	369	-9	374	-322
-3	205	159	10		302	344	-12	469	382	-11	379	300
-4	410	-419	11		533	-648	-13	570	-536			
-5	289	-202	12		445	-425	-14	314	-265			
-6	441	425	13		366	401	-15	471	431			
-7	262	198	18		167	-202	-16	201	125	1	354	376
-8	273	-221	-1		398	-465				7	286	269
-10	226	-161	-2		799	884				-1	243	-215
-11	247	-163	-3		916	1040				-5	317	229
-12	304	331	-4		447	-322				-7	333	-263
-13	231	230	-5		274	-226	0	349	275			
-14	278	-329	-6		342	-313	2	309	266			
			-7		347	-268	3	350	274			
			-8		749	712	4	689	-812	-1	239	-203
			-9		739	666	5	296	-312	-3	257	220
			-10		813	-823	6	468	411			
			-11		696	-700	7	456	455			
			-12		474	389	12	468	405	0	134	93
				3,3,L			14	299	-272	2	390	399
			0		392	347	-1	476	-456	4	445	-518
			1		739	-850	-2	576	-566	6	251	220
			2		411	-457	-3	426	356	10	477	-529
			3		698	881	-4	511	480	12	477	569
			4		288	253	-5	266	-225	16	251	-247
			5		175	127	-8	395	-306	18	318	407
			6		251	294	-9	585	597	-4	1151	1226
			7		603	-723	-10	563	535	-6	137	72
			8		407	-366	-11	529	-423			
			9		615	675	-12	372	-337			
			11		340	-305	-14	246	-202	0	857	-911
							-15	317	255	1	159	156
							-16	483	386	2	341	371



#### 8.4. Discussion of the Structure.

##### i) Accuracy of the Determination.

The final  $R$ -factor of 0.097 is one of the lowest so far obtained for a silver adduct, despite the inapplicability of anisotropic temperature factors. In retrospect it may have been better to use a different crystal for the collection of each layer, to obtain a maximum of reflection data. The decay in each crystal would then have been small enough to allow an absorption correction to be made for each layer. The failure of anisotropic refinement would then have been overcome on both counts. The effects of light on the crystal could have been minimized by blackening the tube; however this would be difficult to achieve after setting the crystal on the camera. The additional time required to set the crystal in this case gives little advantage over the method employed, since, with a clear Lindemann tube the crystal could be partially set by eye, and was easily located and realigned when slipping occurred during data collection.

Maximum accuracy with rapidly decaying crystals can only be achieved by a careful appraisal of the photographic method; this gives a time-averaged record

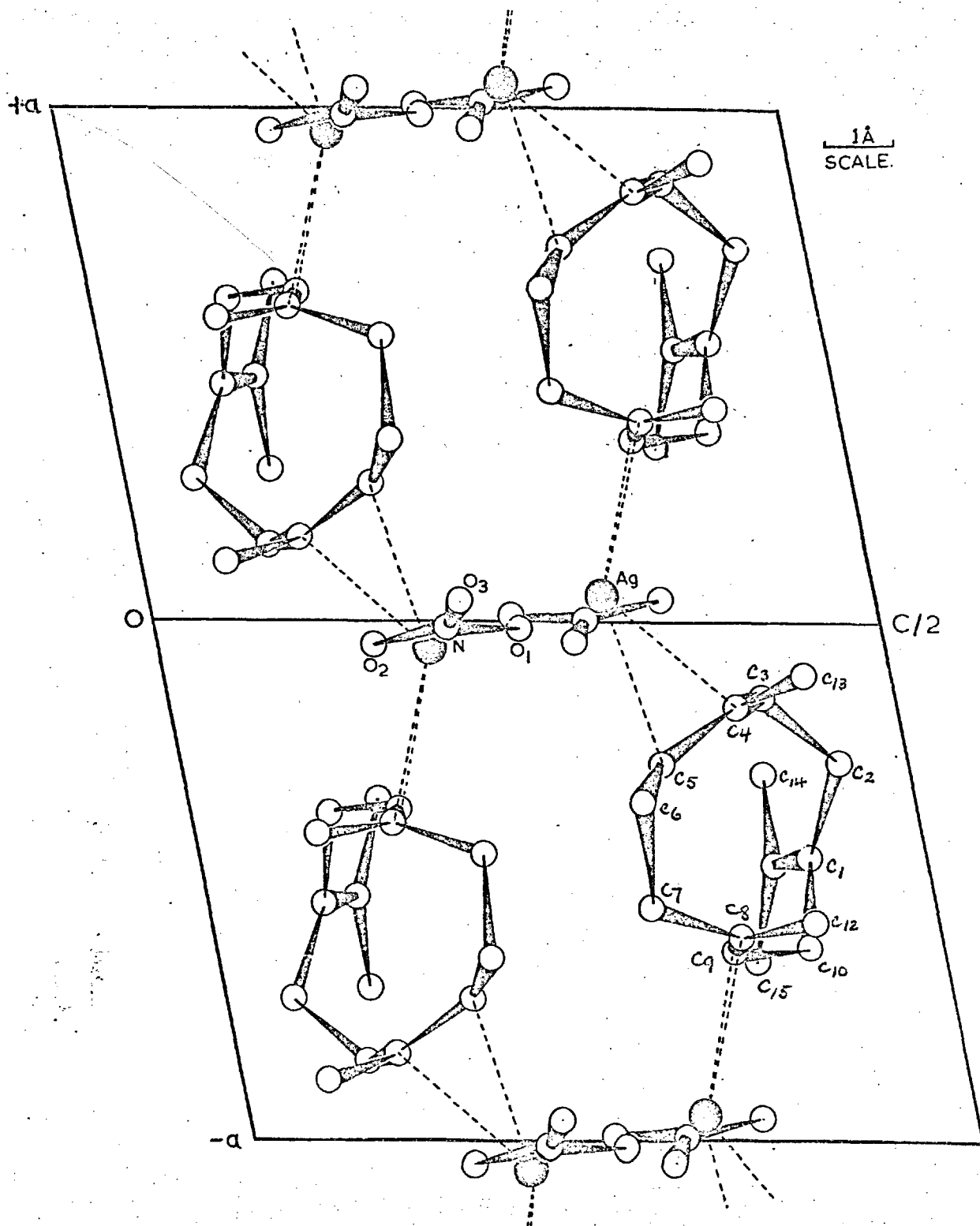


Figure 8.2. Germacatriene in  $b$ -axis projection.

of the individual intensities. The use of an automatic diffractometer, although more accurate in actual measurement, is debatable in these cases; each reflection is measured once only, and the rate of decay governs the precision with which the data can be put on a common scale.

Nevertheless the accuracy obtained certainly warrants the full discussion given below.

### ii) Stereochemistry and Conformation.

The cell contains two L and two D molecules; Figure 8.2 shows the  $[010]$ -projection of the structure. The silver and nitrate ions form infinite chains along the screw axes parallel to b (see also Figure 8.4) at  $z = \frac{1}{4}, \frac{3}{4}$ , and are cross-linked at any one level in z by germacatriene units. Each silver ion is co-ordinated to the C(4)-C(5) double bond of one molecule, and to the C(8)-C(9) double bond of another, giving rise to further chains parallel to a. There are no close contacts ( $< 3.5 \text{ \AA}$ ) between centrosymmetrically related chains, and the packing in the c-direction is relatively loose. The mode of packing is reflected in the elongation of the crystal habit along a.

The all-trans stereochemistry proposed<sup>(133)</sup> for germacatriene has been confirmed. Figure 8.3 (a) and

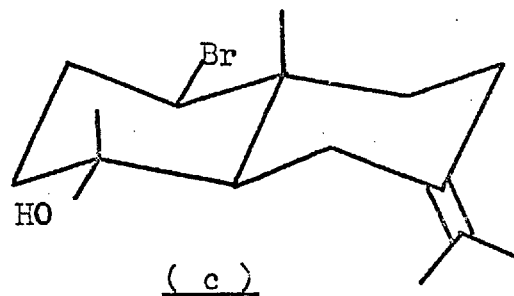
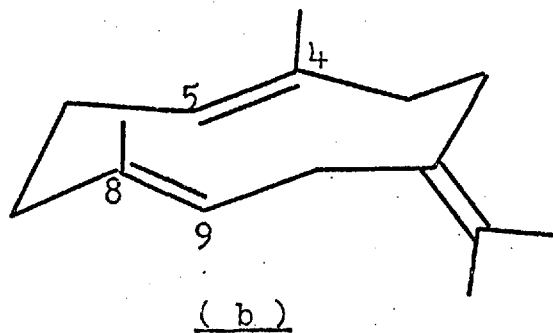
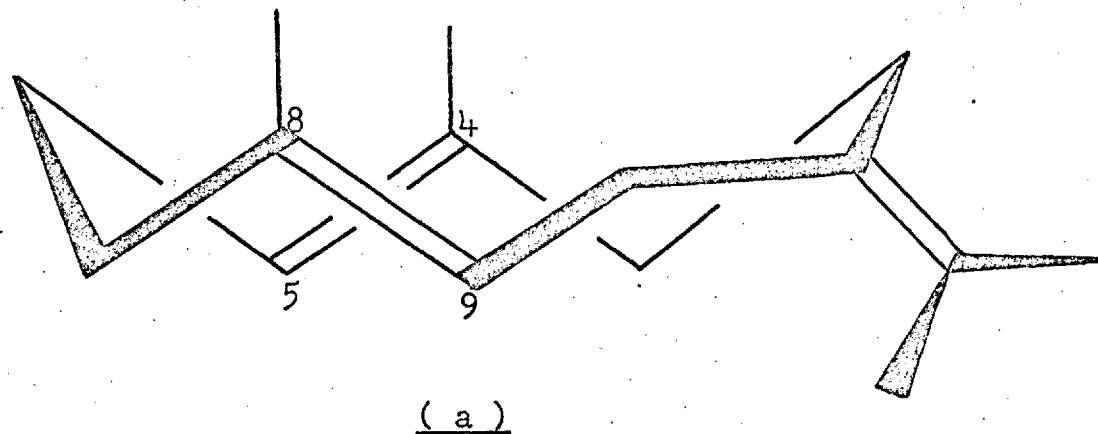


Figure 8.3. (a) Perspective view of the conformation of germacatriene in the crystals of its  $\text{AgNO}_3$  adduct. (b) Schematic view of conformation. (c) Schematic view of the conformation of the selinane derivative formed as a cyclisation product of germacatriene.

(b), show two views of the conformation adopted by the molecule in the crystal; as in the case of humulene and its bromohydrin 7.II, 7.III (p.157), there is an obvious chemical similarity between germacatriene and its cyclisation product Figure 8.3 (c). Again the planes of the endocyclic double bonds are roughly perpendicular to the plane of the macrocycle, leaving the  $\pi$ -orbitals ideally situated for the transannular cyclisation to the selinane derivative.

### iii) Molecular Geometry.

The bond distances and valence angles are shown in Tables 8.5, 8.6 respectively; the standard deviations given are probably realistic estimates, but have suffered due to the paucity of data. Non-bonded contacts within the ionic layer are shown in Table 8.7, while ionic layer-germacatriene contacts are shown in Table 8.8.

The average  $C_{sp^3}-C_{sp^3}$  and  $C_{sp^3}-C_{sp^2}$  distances are  $1.57 \pm 0.03 \text{ \AA}$  and  $1.53_5 \pm 0.03_0 \text{ \AA}$  respectively, while the average  $C_{sp^2}-C_{sp^2}$  distance is  $1.34_0 \pm 0.02_5 \text{ \AA}$ . These values do not differ significantly from those found for humulene<sup>(128)</sup> ( 1.54, 1.52, and 1.34  $\text{\AA}$  ), or from the accepted averages<sup>(153)</sup>. The discrepancy between the two C-Me distances in the isopropylidene group is curious, but could be due to crystal-packing forces, since

TABLE 8.5.

Germacatriene:AgNO<sub>3</sub>.

Intramolecular Bonded Distances (r) in Angstroms, together  
with their Estimated Standard Deviations (σ).

Atoms	<u>r</u>	<u>σ</u>	Atoms	<u>r</u>	<u>σ</u>
C(1) - C(2)	1.56	0.03	C(6) - C(7)	1.58	0.03
C(1) - C(10)	1.60	0.03	C(7) - C(8)	1.51	0.03
C(1) - C(11)	1.30	0.02	C(8) - C(9)	1.38	0.02
C(2) - C(3)	1.56	0.03	C(8) - C(12)	1.51	0.03
C(3) - C(4)	1.49	0.03	C(9) - C(10)	1.55	0.03
C(4) - C(5)	1.35	0.03	C(11) - C(14)	1.59	0.04
C(4) - C(13)	1.51	0.03	C(11) - C(15)	1.48	0.04
C(5) - C(6)	1.55	0.03	N - O(1)	1.23	0.03
N - O(2)	1.15	0.03	N - O(3)	1.28	0.02



TABLE 8.6.

Germacratriene:AgNO<sub>3</sub>.

Valence Angles ( $\theta^\circ$ ) in the Asymmetric Unit, together  
with their Estimated Standard Deviations ( $\delta^\circ$ ).

Atoms	$\theta^\circ$	$\delta^\circ$	Atoms	$\theta^\circ$	$\delta^\circ$
C(1)-C(2)-C(3)	115.4	1.8	C(5)-C(4)-C(13)	122.9	1.6
C(1)-C(10)-C(9)	105.2	1.8	C(5)-C(6)-C(7)	102.0	1.6
C(1)-C(11)-C(14)	119.4	1.9	C(6)-C(7)-C(8)	115.6	1.5
C(1)-C(11)-C(15)	126.4	2.0	C(7)-C(8)-C(9)	116.1	1.8
C(2)-C(1)-C(10)	111.2	1.5	C(7)-C(8)-C(12)	117.9	1.6
C(2)-C(1)-C(11)	125.2	1.8	C(8)-C(9)-C(10)	124.0	1.8
C(2)-C(3)-C(4)	107.9	1.8	C(9)-C(8)-C(12)	122.4	1.8
C(3)-C(4)-C(5)	120.2	1.6	C(10)-C(1)-C(11)	123.0	1.8
C(3)-C(4)-C(13)	114.3	1.6	C(14)-C(11)-C(15)	114.2	1.9
C(4)-C(5)-C(6)	128.7	1.7	O(1) -N - O(2)	124.9	1.9
O(1) - N - O(3)	113.0	1.8	O(2) -N - O(3)	122.1	1.9

TABLE 8.7.

Germacratriene:AgNO<sub>3</sub>.Non-bonded Contacts within the Ionic Layer <4.5Å.

Superscripted atoms (') are related to those in Table 8.2 by the symmetry operation :

$$-x, \quad \frac{1}{2} + y, \quad \frac{1}{2} - z.$$

Ag - O(1)	2.94 Å	Ag - N'	3.07 Å
Ag - O(2)	4.24	Ag - O(1)'	2.81
Ag - O(3)	2.37	Ag - O(2)'	2.68
Ag - N	3.13	O(3)-N'	4.26
		O(3)-O(1)'	3.30
		O(3)-O(2)'	4.45
		Ag - O(3)'	4.34

TABLE 8.8.

Germacratriene:AgNO<sub>3</sub>.Germacratriene - Ionic Layer Contacts <4.5 Å.

Roman subscripts indicate atomic positions related to those in Table 8.2 by the following operations :

- (I)  $1 + x, y, z;$  (II)  $1 + x, \frac{1}{2} - y, \frac{1}{2} + z;$   
 (III)  $1 - x, \frac{1}{2} - y, \frac{1}{2} - z;$  (IV)  $1 - x, -\frac{1}{2} + y, \frac{1}{2} - z;$   
 (V)  $-x, \frac{1}{2} + y, \frac{1}{2} - z;$  (VI)  $-x, -\frac{1}{2} + y, \frac{1}{2} - z.$

C(7) - Ag	3.18 Å	C(3) - Ag <sub>I</sub>	3.26 Å
C(8) - Ag	2.48	C(4) - Ag <sub>I</sub>	2.52
C(9) - Ag	2.57	C(5) - Ag <sub>I</sub>	2.54
C(10) - Ag	3.44	C(6) - Ag <sub>I</sub>	3.24
C(12) - Ag	3.28	C(13) - Ag <sub>I</sub>	3.26
C(9) - N	3.96	C(5) - N <sub>I</sub>	4.18
C(9) - O(1)	3.60	C(3) - O(1) <sub>I</sub>	3.73
C(10) - O(1)	4.08	C(4) - O(1) <sub>I</sub>	3.98
C(15) - O(1)	3.99	C(5) - O(1) <sub>I</sub>	3.75
C(7) - O(3)	3.69	C(5) - O(3) <sub>I</sub>	3.90
C(8) - O(3)	3.77	C(6) - O(3) <sub>I</sub>	4.42
C(9) - O(3)	3.51		
		C(13) - O(2) <sub>II</sub>	4.15

contd.

Table 8.8 Continued :

C(4) - N <sub>III</sub>	4.31 Å	C(7) - N <sub>V</sub>	3.86 Å
C(5) - N <sub>III</sub>	3.93	C(8) - N <sub>V</sub>	3.96
C(6) - N <sub>III</sub>	3.22	C(12) - N <sub>V</sub>	4.10
C(13) - N <sub>III</sub>	4.23	C(7) - O(1) <sub>V</sub>	3.51
C(5) - O(1) <sub>III</sub>	3.98	C(8) - O(1) <sub>V</sub>	3.88
C(6) - O(1) <sub>III</sub>	3.42	C(12) - O(1) <sub>V</sub>	4.46
C(4) - O(2) <sub>III</sub>	3.61	C(7) - O(2) <sub>V</sub>	3.71
C(5) - O(2) <sub>III</sub>	3.57	C(8) - O(2) <sub>V</sub>	3.41
C(6) - O(2) <sub>III</sub>	3.17	C(9) - O(2) <sub>V</sub>	4.38
C(13) - O(2) <sub>III</sub>	3.29	C(12) - O(2) <sub>V</sub>	3.26
C(6) - O(3) <sub>III</sub>	3.83	C(7) - O(3) <sub>V</sub>	4.87
C(14) - N <sub>IV</sub>	3.92	C(15) - Ag <sub>VI</sub>	4.43
C(14) - O(2) <sub>IV</sub>	3.78	C(15) - N <sub>VI</sub>	3.50
C(14) - O(3) <sub>IV</sub>	3.38	C(15) - O(1) <sub>VI</sub>	4.21
		C(15) - O(2) <sub>VI</sub>	3.51
		C(15) - O(3) <sub>VI</sub>	3.29

---

C(15) is closer to the ionic layer than C(14). The asymmetric position of the isopropylidene group with respect to the ionic layer can be seen in Figure 8.4.

It was noted in Chapter 7 (p. 162) that there is appreciable angular strain in medium-sized saturated carbocycles; average C-C<sub>sp3</sub>-C angles as high as 117° have been found experimentally (refs 179-183), confirming results from minimum-energy calculations<sup>(159)</sup>. The presence of five C<sub>sp2</sub> atoms in the cyclodecadiene ring of germacatriene has relieved this strain. Although the C-C<sub>sp3</sub>-C angles show a fairly wide spread (102° → 115.6°), the average value in the ring is now 109.2° ± 1.7°, close to the tetrahedral value. The comparable average in humulene is 111° (128).

The germacatriene molecule is distorted much past what can be achieved with a Dreiding model. Most of the distortion is at the endocyclic double bonds, and the two substituent methyl groups C(12), and C(13), are pushed in towards the centre of the ring (see Figure 8.4). Although the average C-C<sub>sp2</sub>-C angle for these bonds is 120.8°, there is a very wide spread (114.3° → 128.7°), and substantial out-of-plane twisting (sp<sub>2</sub>-sp<sub>2</sub> torsional strain) compared with the exocyclic isopropylidene double bond. The geometry about the double bonds is

further discussed in the next section (8.5), in relation to their observed reactivity differences.

iv) The Ionic Layer.

Figure 8.4 illustrates some interesting features of the ionic layer and its interaction with the organic moiety. It shows that the  $\text{Ag}^+$  ion is close to two oxygen atoms (O(1) and O(3)) of one  $\text{NO}_3^-$  ion, and to two more (O(1)' and O(2)'\*) of another, at distances ranging from 2.37 to 2.94 Å (see Table 8.7). The arrangement of the five atoms is nearly planar. The short contact ( $\text{Ag}^+ - \text{O}(3)$ ) is significantly shorter than the sum of the ionic radii of  $\text{Ag}^+$  and  $\text{O}^-$  given as 2.46 Å (200), and similar distances have been found in the silver nitrate complexes of cyclooctatetraene<sup>(198)</sup>, humulene<sup>(128)</sup>, and norbornadiene<sup>(201)</sup>; distances of 2.32 and 2.42 Å have recently been found between  $\text{Ag}^+$  and the oxygen atoms of water molecules in the bis-bullvalene :  $\text{AgBF}_4 \cdot \text{H}_2\text{O}$  complex<sup>(202)</sup>. The mode of chain formation is very similar to that found in the cyclooctatetraene complex<sup>(198)</sup>, and the average  $\text{Ag}^+ - \text{O}$  distance there (2.65 Å) compares well with the value of 2.70 Å in the present study.

The atoms of the nitrate ion are, as expected, closely coplanar, but the  $\text{N}^+$  is very slightly above the plane

\* The superscripts (') are explained in Table 8.7.

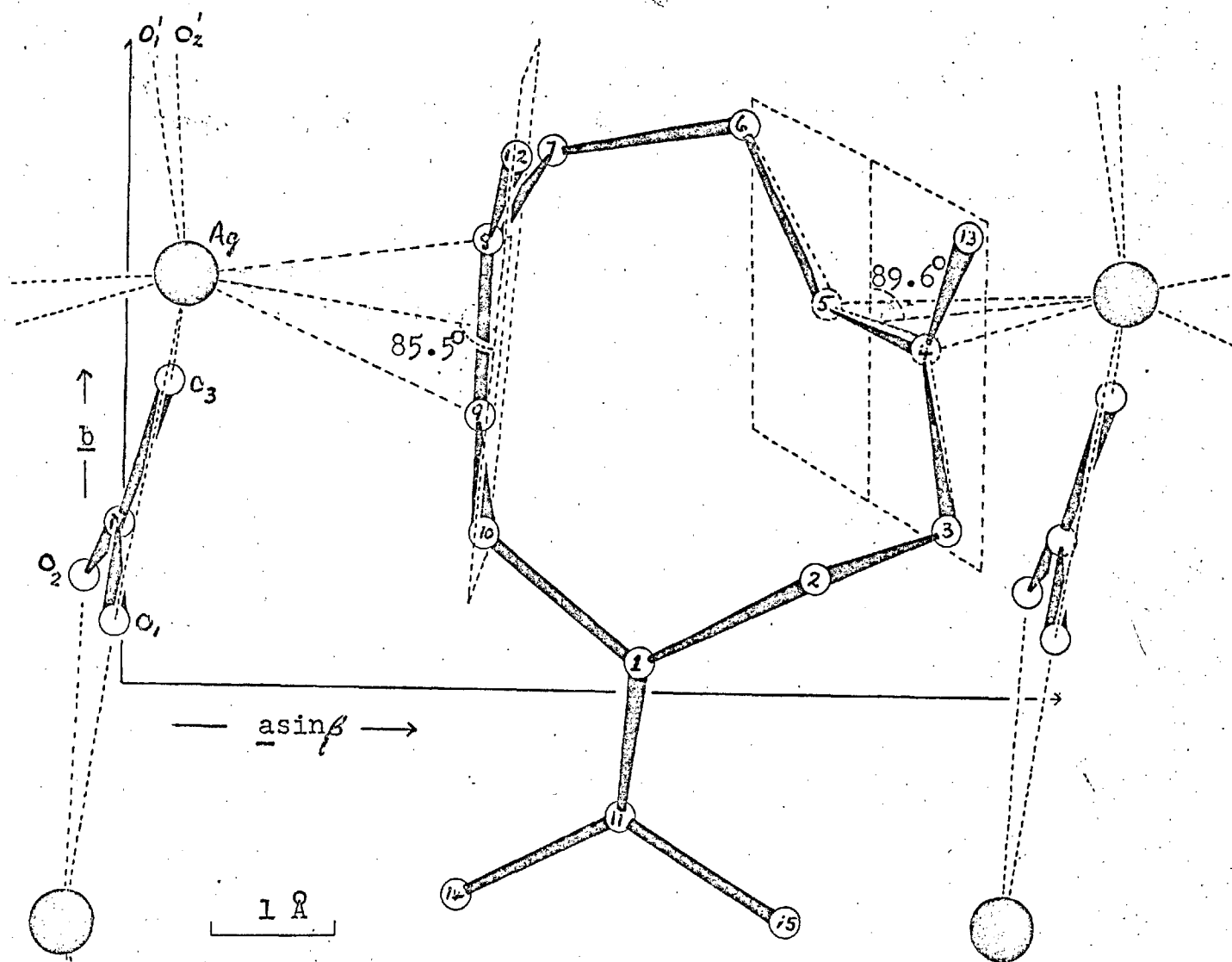


Figure 8.4 Germacatriene:AgNO<sub>3</sub> in  $c$ -axis projection showing modes of chain-formation, and the angles involved in the silver-ethylenic bond. (mean planes are  $ag\bar{o}$  dotted, the Ag - C=C planes are lightly shaded).

of the oxygens by  $\sim 0.02 \text{ \AA}$ . The variation of  $\text{N}^+ - \text{O}$  distances, from 1.15 to 1.28  $\text{ \AA}$ , is explicable in terms of the silver ion co-ordination. O(3) is the most strongly co-ordinated to  $\text{Ag}^+$  and has the longest  $\text{N}^+ - \text{O}$  distance, O(1) is weakly co-ordinated to two  $\text{Ag}^+$  ions and has a slightly stronger (and therefore shorter) bond to nitrogen, while O(2) is co-ordinated only weakly to one  $\text{Ag}^+$  and has an  $\text{N}^+ - \text{O}$  distance consistent with double-bond formation<sup>(153)</sup>. A similar argument could explain the significant deviation of valence angles  $\text{O}-\text{N}^+-\text{O}$ , involving O(1), from the expected value of  $120^\circ$ , since this atom has to satisfy the co-ordination requirements of two silver ions.

Figure 8.4 shows that the co-ordination polyhedron of the silver ion consists of eight atoms; the four oxygens noted above, and four  $\text{C}_{\text{sp}2}$  atoms from two germacatriene units. The arrangement may best be described by noting that the vectors from  $\text{Ag}^+$  to the midpoints of the double bonds, and to the nitrogen atoms of the nitrate ions, form a distorted tetrahedron. The angles involved are shown in Figure 8.5. The apparently bidentate  $\text{NO}_3^-$  ligand must be regarded as occupying only one co-ordination position, as in the ionic layer of the humulene adduct<sup>(128)</sup>, where the overall co-ordination is distorted trigonal bipyramidal,



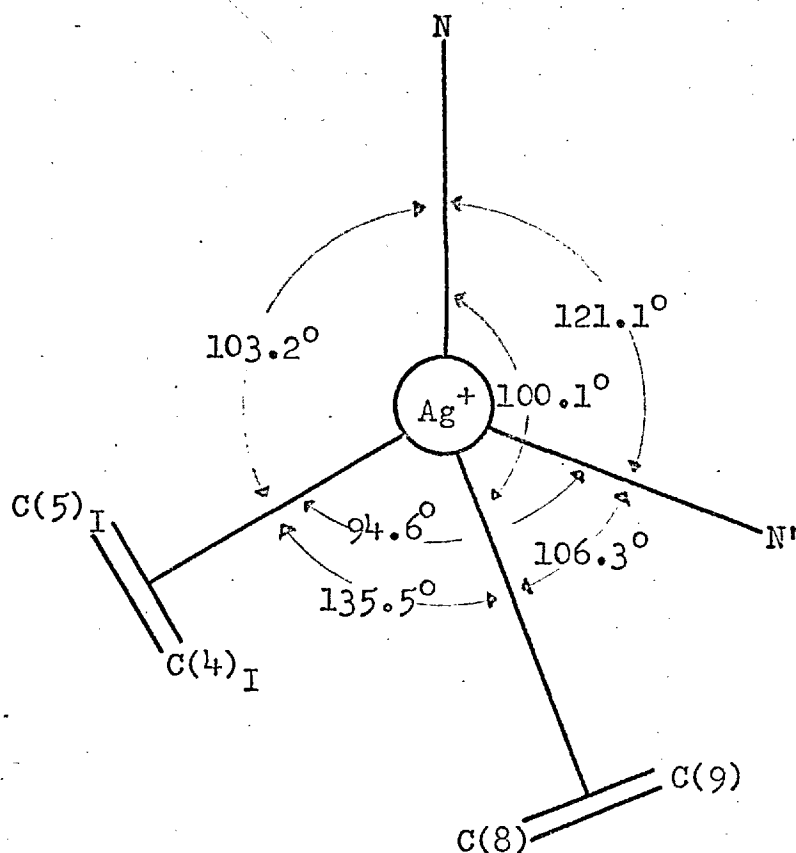


Figure 8.5. The distorted tetrahedral co-ordination of  $\text{Ag}^+$  in germacatriene. (The meanings of the subscripts and superscripts (I), (') are given in Tables 8.8, 8.7, respectively).

or in the tetranitritocobaltate(II) ion<sup>(203)</sup>, where the ligand field is effectively tetrahedral. Distorted tetrahedral co-ordination has been found in several mercury complexes<sup>(204)</sup>, where angles range from 92° to 155°.

v) Germacatriene - Ionic Layer Interactions.

The complexes of silver salts with molecules containing ethylenic linkages, studied so far by the X-ray method, show ratios of organic : inorganic moieties ranging from 3:1 to 1:2. An interesting comparison of the relative bond strengths is afforded by a study of the distances of  $\text{Ag}^+$  from the midpoints of the complexed double bonds. The results from this study are shown in Table 8.9, together with the relevant data for five other compounds. In a comparison of the distances given it is more meaningful to describe each compound by the ratio of complexed double bonds to  $\text{Ag}^+$  ions; furthermore the  $\text{Ag}^+$  - midpoint distances appear to fall into groups by which we may define the  $\text{Ag}^+$  - olefin  $\pi$ -bond 'order'. Bonds of the first 'order' occur when a single double-bond is complexed by a single  $\text{Ag}^+$  ion, and distances range from 2.26 to 2.29 Å; bonds of the second 'order' are exemplified by the present work, where one  $\text{Ag}^+$  ion is complexed to two ethylenic bonds only,

TABLE 8.9.

Silver Salt : Olefin Complexes, Comparison of  $\text{Ag}^+$  -  $\text{C}=\text{C}$  midpoint distances ( $\text{m}$ ) in  $\text{\AA}$ .

Compound	Organic : Inorganic.	Complexed double bonds : $\text{Ag}^+$	'Order'	No.	$\text{m}$ in $\text{\AA}$ .
Norbornadiene: $2\text{AgNO}_3$ (201)	1 : 2	1 : 1	1	2	2.26, 2.26.
Humulene: $2\text{AgNO}_3$ (128)	1 : 2	1 : 1	1	2	2.29, 2.29.
Germacratriene: $\text{AgNO}_3$	1 : 1	2 : 1	2	2	2.43, 2.43.
Cyclooctatetraene: $\text{AgNO}_3$ (198)	1 : 1	2 : 1	2	1	2.38.
			3(?)	1	2.73.
			-	1	ca. 3.0 $\text{\AA}$ .
<u>Tris</u> -bullvalene: $\text{AgBF}_4$ (199)	3 : 1	4 : 1	2	2	2.42, 2.43.
			3	2	2.63, 2.69.
<u>Bis</u> -bullvalene: $\text{AgBF}_4$ (202)	2 : 1	2 : 1	2	4*	2.36, 2.37,
					2.42, 2.46.
			-	4*	ca. 3.0 $\text{\AA}$ .

\* Two crystallographically independent molecules per asymmetric unit.

at midpoint distances of ca. 2.43 Å. By a simple linear extrapolation it would appear that a single  $\text{Ag}^+$  ion should be complexed to three equi-distant double bonds (i.e. pure third 'order'), at  $\text{Ag}^+$ -midpoint separations of ca. 2.6 Å. It is doubtful if the long contacts of ca. 3.0 Å, noted in Table 8.9. represent very strong interactions, but they do have some effect in stabilizing the crystal packing.

Thus, from the arguments above, it has been possible to break down the number of  $\text{Ag}^+$ -olefin bonds into their respective 'orders'. Although the data at present available is admittedly rather sparse, this break-down appears viable in an attempt at a meaningful classification of these complexes. It is unfortunate that comparison with the silver perchlorate : benzene complex<sup>(197)</sup>, and the complex of silver nitrate with the cyclooctatetraene dimer<sup>(205)</sup>, are not meaningful, due to a disordered  $\text{Ag}^+$  position in the former, and lack of definition in the latter. The full details of the structure determination of cis,cis,cis-1,4,7-cyclononatriene: $\text{AgNO}_3$ <sup>(166)</sup> have not yet appeared in the literature. Nevertheless, from the information given in the references cited in Table 8.9, it appears that the chemical stability and the number of 'bonds' formed by silver are correlated.

The individual  $\text{Ag}^+$ - $\text{C}_{\text{sp}^2}$  distances at the C(8)-C(9) double bond are significantly unequal (see Table 8.8), but

this is not true at the C(4)-C(5) bond. The asymmetric orientation of  $\text{Ag}^+$  with respect to the complexed double bond has been found in many of the compounds mentioned above, and was initially ascribed to crystal packing forces.<sup>(128)</sup> A molecular-orbital approach, applied to metal-olefin complexes in general<sup>(206,207)</sup>, has afforded a better explanation. Overlap is required between the symmetrical donor  $\pi$ -orbital of the olefin with a vacant metal orbital ( $\pi$ -bond), and also between a filled metal orbital and the antibonding  $\pi^*$ -orbital of the olefin ( $\mu$ -bond). It has been suggested that the asymmetric position adopted affords the best compromise between the two requirements<sup>(199)</sup>.

The strength of the  $\pi$ -bond in silver-olefin complexes is, however, weak, since the ion does not possess vacant orbitals of the correct symmetry to act as acceptors. This is reflected in the C=C bond lengths, which should be elongated in the case of strong  $\pi$ -bonding (which reduces the electron-density in the double bond, and thus reduces the bond-order). This has not been found in previous X-ray studies, nor in the present work, where the double-bond lengths (C(4)-C(5), C(8)-C(9)) are not significantly longer than the uncomplexed bond C(1)-C(11). However in the crystal structures of the complexes  $\text{K}^+(\text{C}_2\text{H}_4\text{PtCl}_3)^-$ <sup>(208)</sup>, and  $\text{Pt}(\text{C}_2\text{H}_4)(\text{NH}(\text{CH}_3)_2)\text{Cl}_2$ <sup>(209)</sup>, the ethylenic bond is elongated to 1.5 Å and 1.47 Å respectively; this is because the

platinous ion possesses a vacant (acceptor) d-orbital. One can only conclude that, in silver-olefin complexes, the  $\mu$ -bond is predominant; this would not, of course, increase the electron density between the olefinic carbon atoms to any great extent, and no cases of C=C distances less than ca. 1.30 Å have been reported. The lack of asymmetry at the C(4)-C(5) double bond in the present study is probably not explicable on a molecular orbital approach. While this has provided a good general picture of metal-olefin bonding, other factors, such as crystal-packing forces, and the presence of other atoms in the co-ordination polyhedron, must have some effect, and will differ from complex to complex.

In any event maximum overlap should occur when the  $\text{Ag}^+ - \text{C}_{\text{sp}^2} - \text{C}_{\text{sp}^2}$  plane is perpendicular to the mean plane through the olefinic linkage. In the present study the angle between the planes Ag, C(4), C(5), and C(3), C(4), C(5), C(6), C(13), is  $89.6^\circ$ , and the angle between the planes Ag, C(8), C(9), and C(7), C(8), C(9), C(10), C(12), is  $85.5^\circ$ . The planes are shown dotted in Figure 8.4. The values agree well with comparable angles in the tris-bullvalene adduct<sup>(199)</sup> ( $91.5^\circ$  &  $91.1^\circ$ ), and in the humulene adduct<sup>(128)</sup> ( $85^\circ$  &  $87^\circ$ ). Where  $\text{Ag}^+$  is asymmetric to two double bonds (e.g. cyclooctatetraene: $\text{AgNO}_3$ ), or complexed to only one cis-double bond (norbornadiene: $2\text{AgNO}_3$ ), there are substantial

deviations from  $90^\circ$ . Thus the substitution pattern at the complexed double bond also appears to affect the bonding to the metal ion.

On a more empirical scale it is interesting to note that the shortest 'first-order'  $\text{Ag}^+$ -olefin bond (2.26 Å) is still longer than the sum (2.03 Å) of the  $\text{Ag}^+$  ionic radius (1.26 Å<sup>(210)</sup>) and the covalent radius of carbon (0.77 Å). This indicates that the distance of closest approach of  $\text{Ag}^+$  to the olefinic bond is ca. 1.0 Å. A similar result can be obtained for  $\text{Cu}^+$  in the complexes norbornadiene: $\text{CuCl}$ <sup>(211)</sup> and catena- $\mu$ -chloro-cyclooctatetraene  $\text{Cu(I)}$ <sup>(212)</sup>; the  $\text{Cu}^+$ -midpoint distances are 1.97 and 1.98 Å respectively, and the ionic radius of  $\text{Cu}^+$  is 0.96 Å. The comparison is interesting since both  $\text{Ag}^+$  and  $\text{Cu}^+$  have filled d-orbitals, and do not readily form  $\pi$ -bonds. The value 1.0 Å could thus be termed the ' $\mu$ -bonding radius' of carbon. In the case of platinum, which is a ready acceptor of  $\pi$ -electrons (see above), a similar study shows a ' $\pi$ -bonding radius' of ca. 0.75 Å, indicative of stronger bonding.

A single uniform theory of bonding in metal-olefin complexes is still far from clear. The numerous factors involved make structural predictions difficult, and many further X-ray studies of high precision will be required to clarify the situation. However the very great chemical

interest in these compounds, both from the organic and inorganic points of view, makes them ideal 'targets' for crystallographic investigation.

### 8.5. The Geometry about the Double Bonds and its Effect on their Reactivity.

#### i) The Molecular Geometry about the Double Bonds.

The increased distortion of the endocyclic double bonds in germacatriene, compared with that of the exocyclic isopropylidene group, has been mentioned briefly above (see Sect. 8.4 (iii) ). The distortion is analysed in Figure 8.6 (for all three bonds) in terms of :

- |  |   |              |
|--|---|--------------|
| i) Valence Angles ( $\theta^\circ$ ),  | } | Fig. 8.6 (a) |
| ii) $sp^3 - sp^2$ torsion angles ( $\delta^\circ$ ) <sup>‡</sup> ,   |   |              |
| and iii) $sp^2 - sp^2$ torsion angles ( $\tau^\circ$ ) <sup>‡</sup> , shown in Fig. 8.6 (b) in the form of Newman diagrams <sup>‡</sup> (213). |   |              |

It can be seen that criteria (i) and (ii) match closely for both endocyclic bonds, and that most of the distortion is due to out-of-plane twisting about the axis of the bond, so that the planes of the pairs of substituents are no

---

<sup>‡</sup> To preserve clarity in the discussion which follows; the symbol ( $\omega$ ) will be reserved for  $sp^3-sp^3$  torsion angles, as in Chaps. 6 & 7.

<sup>‡</sup> See also Appendix II, Figure II.2, for further examples.



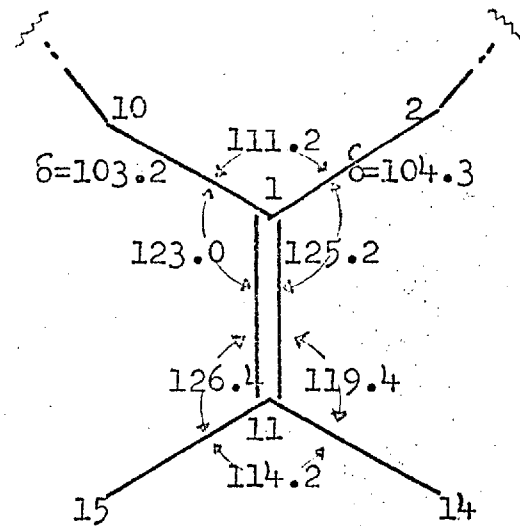
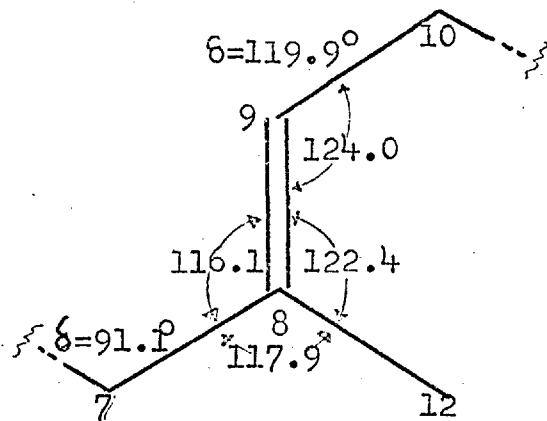
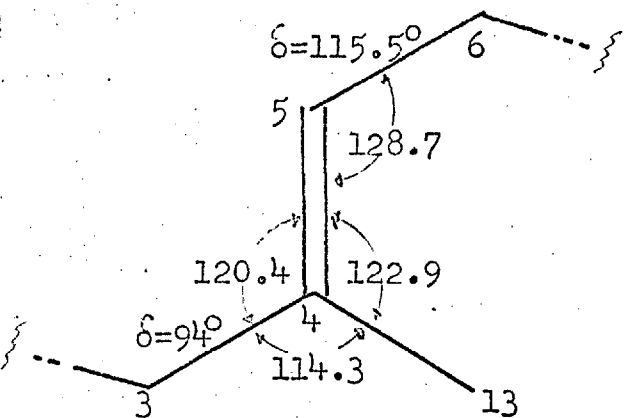


Figure 8.6 (a) Germacatriene:AgNO<sub>3</sub>, Valence angles and sp<sup>3</sup>-sp<sup>2</sup> torsion angles ( $\delta$ ) about the double bonds.

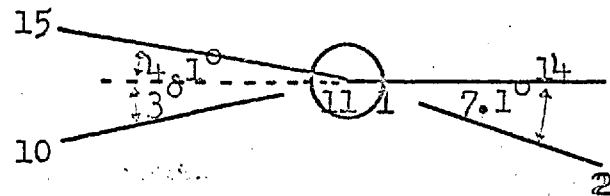
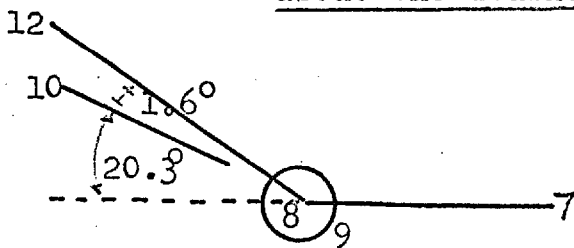
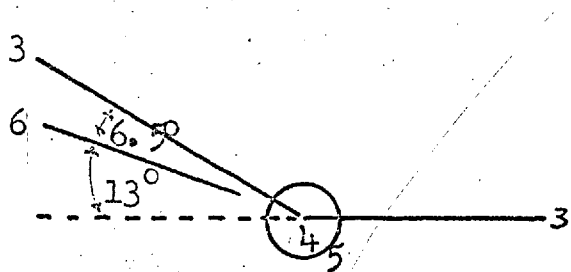
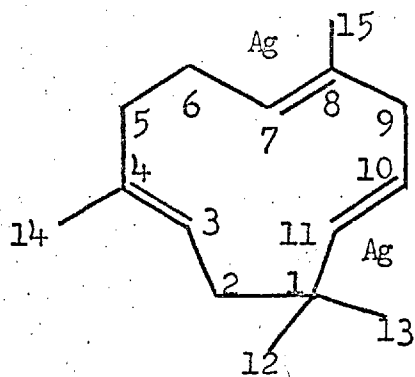
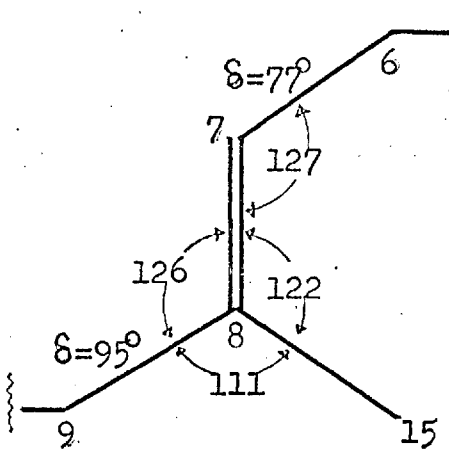
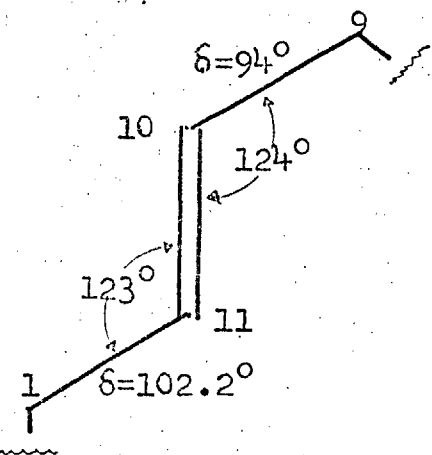


Figure 8.6 (b) Germacatriene:AgNO<sub>3</sub>, Newman projections down each double bond showing the sp<sup>2</sup>-sp<sup>2</sup> torsion angles ( $\tau$ )

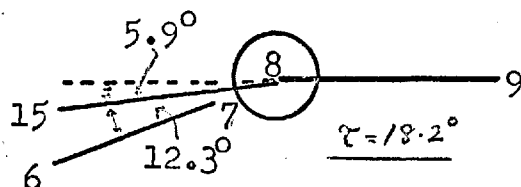
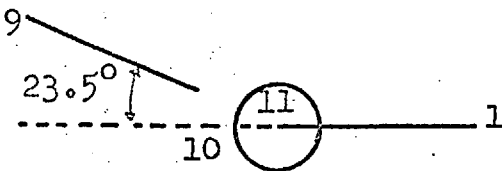
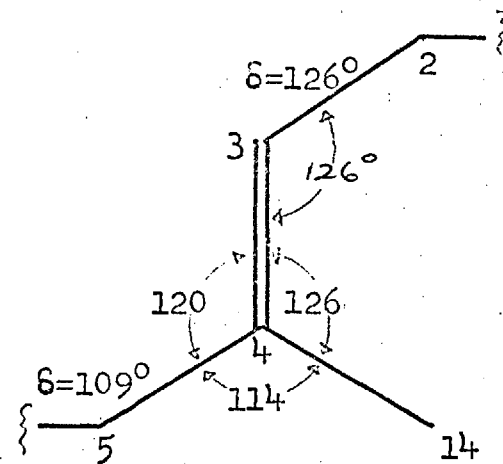


(a)

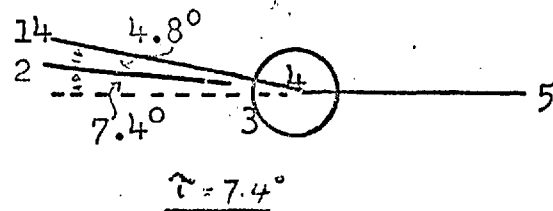
Figure 8.7. (a) Structure and numbering scheme for humulene.  
 (b) Valence angles and  $sp^3-sp^2$  torsion angles ( $\delta$ ) about the three double bonds.  
 (c) Newman diagrams showing the  $sp^2-sp^2$  torsion angles ( $\tau$ ).



(b)



(c)



longer parallel ( criterion (iii) ). This  $sp^2 - sp^2$  torsional strain is greater for the C(8)-C(9) bond than for the C(4)-C(5) bond; it is almost negligible for the C(1)-C(11) bond. The data of Table 8.10, which shows the deviations ( $d$ , in Å) of the relevant atoms from the mean plane through each double bond, also reflects this sequence; thus  $\langle d \rangle_{8-9} > \langle d \rangle_{4-5} > \langle d \rangle_{1-11}$ . The results explain, in a purely qualitative manner, the observed differences in reactivity of the three bonds; however it has been possible to obtain some more quantitative results from strain-energy calculations; these will be discussed below.

It is possible that a small amount of the observed distortion at the endocyclic double bonds is due to  $Ag^+ - C$  non-bonded repulsions. This may well account for the positions adopted by the two methyls ( C(12) & C(13) ), pushed in towards the centre of the ring, and towards one another, by angles of  $19.5^\circ$  and  $22.0^\circ$  (Fig. 8.6 (b)). Their distances from  $Ag^+$  (3.26 and 3.28 Å respectively) are almost equal. Even after this deformation the Me-Me separation is still large (3.57 Å), and the positions adopted may be a compromise between Me-Me and  $Ag^+ - Me$  repulsions.

It is doubtful whether the  $Ag^+$  ion has much effect on the ring geometry and conformation. The distances of  $Ag^+$  from C(3), C(6), C(7), C(10), are all  $> 3.18$  Å (Table 8.8), i.e. longer than any distance quoted in Table 8.9, and much

TABLE 8.10.

Germacratriene:AgNO<sub>3</sub>.

Deviations (d) in Angstroms of Constituent Atoms from the  
Mean Plane through each Double Bond \*.

Bond	Atom	<u>d</u>	<u>⟨d⟩</u>
C(4)=C(5)	C(3)	-0.080	
	C(4)	0.120	
	C(5)	0.042	<u>0.065.</u>
	C(6)	-0.059	
	C(13)	-0.023	
C(8)=C(9)	C(7)	-0.122	
	C(8)	0.151	
	C(9)	0.098	<u>0.100.</u>
	C(10)	-0.105	
	C(12)	-0.022	
C(1)=C(11)	C(2)	-0.018	
	C(10)	-0.016	
	C(1)	0.053	
	C(11)	-0.011	<u>0.018.</u>
	C(14)	-0.002	
	C(15)	-0.005	

\* Calculated using LSQPL.

longer than the sum of the  $\text{Ag}^+$  ionic radius and the covalent radius of carbon (2.03 Å, see p. 211). Furthermore none of the atoms in the ring are as mobile as the methyl carbons mentioned above.

In the case of the humulene: $2\text{AgNO}_3$  adduct<sup>(128)</sup> the three double bonds are all endocyclic; the two complexed bonds C(10)-C(11), C(7)-C(8), (see Fig. 8.7 (a)) show marked, but unequal, distortion; the uncomplexed bond C(3)-C(4) is again almost planar. An analysis of the distortion, similar to that given for germacatriene, is shown in Figure 8.7 (b) & (c). It shows that, while the  $\text{sp}^2 - \text{sp}^2$  torsional strain is again large for the complexed bonds, the  $\text{sp}^3 - \text{sp}^2$  torsion angles do not match in this case. Nevertheless it has been possible to perform semi-quantitative strain-energy calculations which explain why epoxidation of humulene gives > 95% of the C(7)-C(8) monoxide<sup>(214)</sup>.

#### ii) Reactivity in Medium-Ring Olefins.

It is now well established that trans double bonds in medium-ring olefins are more reactive than their acyclic counterparts<sup>(215)</sup>, and this has been ascribed to steric strain. Hitherto it has been difficult to define the types of strain that occur, and to estimate their relative importance, due to the lack of accurate structural data to accompany the experimental results. The X-ray studies of humulene and germacatriene, as their silver nitrate adducts,

have provided such data.

Before the parameters discussed above can be used in arguments concerning reactivity two questions must be considered :

1) Are the ring conformations found in the solid silver nitrate adducts an accurate reflection of those adopted in solution just prior to reaction?

2) Does the complexing of a double bond with a silver ion induce changes in hybridisation, with consequent changes in bond-lengths and angles?

The first question has been answered at some length in this Thesis. The obvious chemical similarities between the crystal conformations of both germacatriene and humulene and their respective cyclisation products is shown in Figure 8.3, and in structural formulae 7.II, 7.III. Further evidence is also cited in Chap. 7, as refs. 165-167.

The answer to the second question lies in the discussion given above (Sect. 8.4 (v)), where the bonding of  $\text{Ag}^+$  to the olefinic bonds was shown to be weak compared to similar platinum complexes. The bond lengths and valence angles are not significantly altered in comparison with parameters for uncomplexed bonds.

It would seem logical for the silver ion to complex those bonds which have the greatest chemical reactivity;

since the bond formed is weak, the conformation present in solution is then 'frozen' in the crystal structure. This type of argument is not, however, general, and must depend on the type of complex formed, and the strength of the metal-olefin bond.

In an elegant analysis of the reactions of various olefins with diimide Garbisch *et. al.*<sup>(216)</sup> have had remarkable success in predicting relative reaction rates by resolving the steric strain ( $E_s$ ) about each reactive bond into, *inter alia*, bond-angle and  $sp^3$ - $sp^2$  torsional contributions ( $E_\theta$ ) and ( $E_\phi$ ), and comparing these in starting materials and products. Following this approach the strain-energy differences ( $\Delta E_s$ ) between the C(3)-C(4) and C(7)-C(8) bonds of humulene, and the C(4)-C(5) and C(8)-C(9) bonds of germacatriene, have been estimated. Inclusion of the di- and tetra-substituted double bonds (C(10)-C(11) in humulene, C(1)-C(11) in germacatriene) in the calculation is difficult, due to differences in the inductive effects of substituents, which would make comparison of their strain-energies with those for the trisubstituted bonds rather unreliable.

The data for germacatriene are the simplest to compute, since values of ( $\theta$ ) and ( $\phi$ ) match closely for both double bonds; other factors, such as non-bonded interactions between reagent and substrate, entropies of activation, and nucleo-

philicities should also match closely. Thus only the values of ( $\tau$ ) differ, and while the  $sp^2$ - $sp^2$  torsional strain was thought by Garbisch<sup>(216)</sup> to make a negligible contribution in the cases he considered, it is obviously of paramount importance here. A reliable estimate of ( $E_s$ ) for each bond may therefore be obtained by computing ( $E_\tau$ ). The latter is given by :

$$E_\tau = 8\tau^2 \text{ cal mole}^{-1} \dots\dots\dots 8.1;$$

a formula derived for ethylene by Herzberg<sup>(217)</sup>. Since we are concerned with the strain in the ring, it is correct to use the complements of the angles  $\tau_{3(4,5)6}^*$  ( $= -167^\circ$ , whence  $E_\tau = 1.35 \text{ kcal mole}^{-1}$ ) and  $\tau_{2(8,9)10}^\wedge$  ( $= -159.7^\circ$ ,  $E_\tau = 3.30 \text{ kcal mole}^{-1}$ ), in estimating the strain due to the out-of-plane twisting<sup>^</sup>. Thus  $\Delta E_s (= \Delta E_\tau)$  is given as  $1.95 \text{ kcal mole}^{-1}$ . Any reaction in which this strain can be relieved in the transition state should lead to a higher reactivity for the C(8)-C(9) double bond.

Epoxidation should be a suitable reaction for detecting differences in transition state activation energies ( $\Delta\Delta F^\ddagger$ ), since  $\pi$ - $\pi$  transannular interactions between the double bonds

\* The meaning of this nomenclature is given in Appendix II.

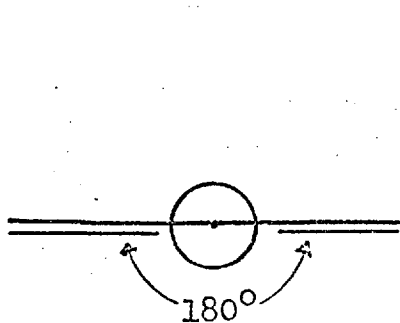
^ Any bond for which  $\tau = \pm 180^\circ$  obviously has  $E_\tau = 0$ , thus the complements of these angles give the correct  $E_\tau$ 's. The complements are shown in Figure 8.6. (b).



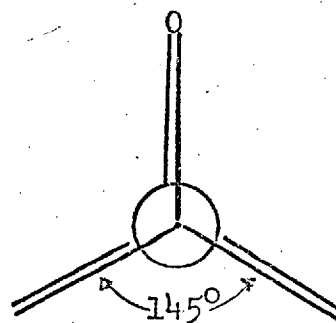
would be expected to be unimportant in the transition state. Further, it involves a minimal geometric change, as shown in Figure 8.8 (a) & (b) (projections down the C=C bond before and after epoxidation), in which the projected angle decreases from  $180^\circ$  to ca.  $145^\circ$ . The epoxidation of germacatriene (Fig. 5.6. p. 86) gave the 8-9 and 4-5 monoxides in the ratio 70:30, implying that the rate of reaction at the bond C(8)-C(9) is more than twice that at the C(4)-C(5) bond. We may therefore use the equation developed by Garbisch<sup>(216)</sup> :

$$-RT \ln(k_1/k_2) = \Delta \Delta F^{\ddagger} \dots\dots\dots 8.2,$$

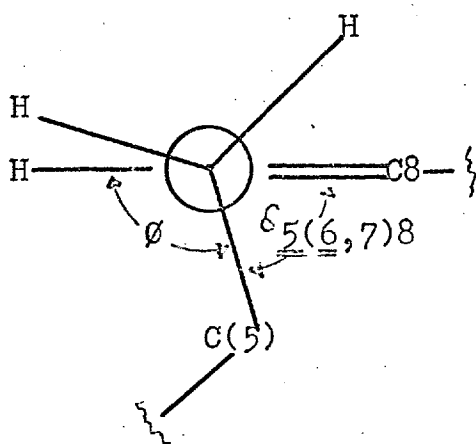
where (R) is the gas constant ( $1.99 \text{ cal deg}^{-1} \text{ mole}^{-1}$ ), (T) is the absolute temperature (taken as  $298^\circ\text{K}$ ), and  $(k_1/k_2)$  is the ratio of the reaction rate constants (taken as 70:30). The value of  $\Delta \Delta F^{\ddagger}$  given is ca.  $0.5 \text{ kcal mole}^{-1}$ , so that approximately  $\frac{1}{4}$  of the torsional strain-energy difference is relieved in the transition state. This result in itself is interesting, since Garbisch<sup>(216)</sup> only obtained good agreement of observed and calculated rate constants for the diimide reduction of medium ring olefins, by assuming that the transition state occurred somewhat further along the reaction co-ordinate between reactants and products. The high reactivity of the strained trisubstituted double bonds is clear from the isolation of only a trace of the 1-11 oxide.



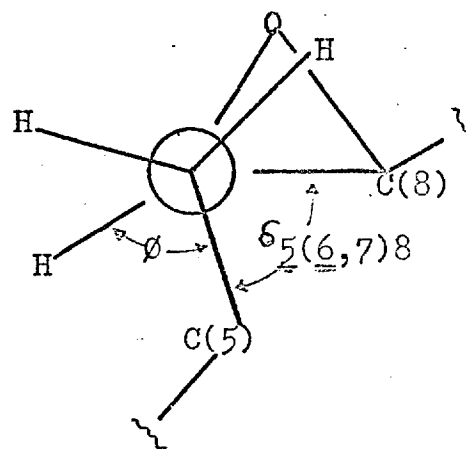
(a)



(b)



(c)



(d)

Figure 8.8.

The epoxidation of humulene is reported<sup>(214)</sup> to give >95% of the 7-8 monoxide, this corresponds to a  $\Delta\Delta F^\ddagger$  of  $\geq 1.7$  kcal mole<sup>-1</sup>. The relevant sp<sup>2</sup>-sp<sup>2</sup> torsion angles are  $\tau_{\underline{2}(\underline{3},4)5}$  and  $\tau_{\underline{6}(\underline{7},8)9}$ , and their complements (see Fig. 8.7 (c)) give  $E_\tau = 0.45$  kcal mole<sup>-1</sup> for bond C(3)-C(4), and  $E_\tau = 2.65$  kcal mole<sup>-1</sup> for C(7)-C(8); thus  $\Delta E_\tau$  is 2.2 kcal mole<sup>-1</sup>. If we assume that  $\frac{1}{4}$  of this energy difference is relieved in the transition state (cf. above), a value of 0.55 kcal mole<sup>-1</sup> is obtained for  $\Delta\Delta F^\ddagger$ , which is too small to account for the difference in reactivity. However, as noted above, the sp<sup>3</sup>-sp<sup>2</sup> torsion angles for the two bonds differ appreciably in humulene. The previous model for epoxidation is extended in Figure 8.8 (c) & (d), which show projections down the C(6)-C(7) bond before and after reaction; the sp<sup>3</sup>-sp<sup>2</sup> torsion angle  $\theta$  ( $=\delta_{\underline{5}(\underline{6},7)H}$ ) is effectively reduced by ca. 35°. This picture of epoxidation, involving only a twisting about the double bond, with little change in the remainder of the molecule, is reasonable, at least in the early stages of reaction, since C-C-C bond angles are similar in olefins and epoxides, and there are only slight changes in bond lengths. The twisting already present in the double bonds of germacra-triene and humulene makes this simple picture even more probable. The description implies that  $\delta_{\underline{5}(\underline{6},7)8}$  remains unchanged after reaction; however, this does not mean that

this is the angle to be used in estimating the torsional strain ( $E_\theta$ ) in Fig. 8.8 (d), as it would describe the dihedral angle only if the C-C bond of the oxide were a straight line, rather than the 'bent bond' (196) generally accepted in three-membered rings. Thus  $\theta$ , the only angle to change, is a better estimate of torsion angles.

Table 8.11 shows the strain energies ( $E_\theta$ ) about the relevant  $sp^3-sp^2$  bonds in humulene, compared with the values estimated for the epoxides, where  $\theta$  is reduced by ca.  $35^\circ$ . The results indicate that epoxidation decreases this type of strain by  $\sim 1.1$  kcal mole $^{-1}$  for bond C(7)-C(8), but increases it by  $\sim 1.9$  kcal mole $^{-1}$  for bond C(3)-C(4). The combination of  $sp^3-sp^2$  and  $sp^2-sp^2$  torsional strains gives a value of 5.1 kcal mole $^{-1}$  for  $\Delta E_s$ ; if again we assume that  $\frac{1}{4}$  of  $\Delta E_s$  is relieved in the transition state, a value of ca. 1.25 kcal mole $^{-1}$  is obtained for  $\Delta\Delta F^\ddagger$ . This value does not wholly account for the reported disparity in reaction rates, but indicates (216,218) that the proportion of the 7-8 monoxide is at least  $> 87\%$ .

These energy estimates must be regarded as, at best, semi-quantitative; nevertheless it is gratifying that the results obtained from the X-ray data agree with experiment within an order of magnitude. The errors are due to the assumptions made in the calculations, which may be listed as follows :

TABLE 8.11.

sp<sup>3</sup> - sp<sup>2</sup> Torsional Strain Energies, ( $E_{\emptyset}$ )<sup>†</sup>, in kcal mole<sup>-1</sup>,  
in Humulene and its Monoxides<sup>\*</sup>.

<u>Humulene.</u>			<u>Monoxides.</u>		
Bond	$\emptyset$	$E_{\emptyset}$	Bond	$\emptyset$	$E_{\emptyset}$
C(2)-C(3)	54°	0.02	C(2)-C(3)	19°	1.2
C(4)-C(5)	71	0.16	C(4)-C(5)	36	0.9
C(6)-C(7)	103	0.65	C(6)-C(7)	68	0.1
C(8)-C(9)	85	0.74	C(8)-C(9)	50	0.2

† The angle  $\emptyset$  is defined in Fig. 8.8 (c) & (d); values for humulene were computed from the X-ray results<sup>(128)</sup> using MOJO, values for the monoxides were estimated from models.

\* sp<sup>3</sup> - sp<sup>2</sup> torsional potential functions have the general form :  $ES = K(1 + \cos 3\delta)$  for angle ( $\delta$ ), if the three substituents on the sp<sup>3</sup> atom are identical. Though this is not true in this work, the function probably yields reasonable estimates, in view of the limited range of  $\emptyset$  ( $= \delta$ ) achievable. K is the half-height of the potential barrier; values of 2K for relevant compounds are : propene<sup>(219)</sup> : 2.0 kcal mole<sup>-1</sup>; isobutene<sup>(220)</sup> : 2.2;

TABLE 8.11 (contd.)

cis-butene<sup>(221)</sup>: 0.8; propene oxide<sup>(222)</sup>: 2.6; 2,3-cis-butylene oxide<sup>(223)</sup>: 1.6. As it is well established that the rotational barrier is considerably lower for cis-1,2-disubstituted olefins than for the corresponding trans-compounds<sup>(221)</sup>, extrapolation to trisubstituted olefins would suggest the use of two different values of K, viz: 1.0 kcal mole<sup>-1</sup> when the alkyl group is cis to hydrogen, and 0.4 when cis to another alkyl group; the appropriate values for epoxides would be 1.3 and 0.8 respectively. The torsional potential function for sp<sup>3</sup> - sp<sup>3</sup> strain-energy calculations is similar to that described above, it will be discussed in Appendix III.

- i) that the relief of strain energy in going from reactants to products follows a straight line graph;
- ii) that the relief of  $sp^2$ - $sp^2$  and  $sp^3$ - $sp^2$  torsional strain in humulene follows a graph having the same slope as that for germacatriene;
- iii) that the transition state for both types of strain in humulene has the same reaction co-ordinate, i.e.  $\frac{1}{2}$ , as in germacatriene.

All of the above assumptions have been made, since there is no relevant experimental evidence in the literature. Further, the quality of the X-ray data does not lead to high precision in the energy calculations, for instance a change of  $+1^\circ$  in  $\tau_{3(4,5)6}$  for germacatriene (i.e. from  $-167^\circ$  to  $-166^\circ$ ) gives a value of  $E_\tau$  of  $1.57 \text{ kcal mole}^{-1}$ , a difference of  $+0.22 \text{ kcal mole}^{-1}$ . If errors in the estimation of the ratios of the various products are also taken into account (at least  $\pm 2\%$ ), the results obtained must be regarded in a favourable light.

The calculations do give some idea of the order of magnitude of the strain energies about the double bonds, and also of the energetics of the epoxidation reactions. They also illustrate the importance of the contribution made by the  $sp^2$ - $sp^2$  torsional strain to the high reactivity of medium-ring trans-olefins; in certain cases, e.g. germacatriene, this contribution may be much larger than that

of the more familiar  $sp^3$ - $sp^2$  torsional strain. The very basic assumption that the crystal conformations adopted in the silver nitrate adducts are very similar to those adopted just prior to reaction in solution, is, in effect, proven as a corollary to the work described above.

The Author would like to make a special acknowledgement to Dr. J. K. Sutherland at this point, for providing the basic ideas behind this work, and for some lengthy and helpful discussion. He is also grateful for permission to quote experimental results obtained by Dr. Sutherland and Mr. E. D. Brown.

It should be noted that in the original note published on this topic<sup>(136)</sup>, values for the dihedral angles were computed from atomic co-ordinates which were not fully refined. The values used in the discussion above were obtained from the data of Table 8.2, and all strain-energy estimates have been recomputed. The value of the ratio of germacatriene monoxides ( 8-9 : 4-5 ) has also recently been obtained to greater precision (70:30) than that quoted in the paper and also in the review, Chapter 5, where the ratio 65:35 was cited.



## CHAPTER 9.

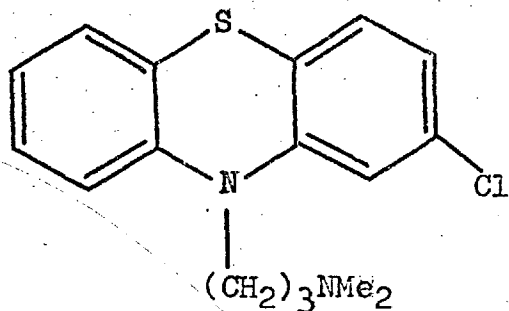
### The Crystal and Molecular Structure of

2,3,4,4a,9,9a-hexahydro-2-methyl-9-phenyl-1H-indeno [2,1-c]  
pyridine hydrobromide :  $C_{19}H_{22}NBr$ .

#### 9.1. Chemical Introduction.

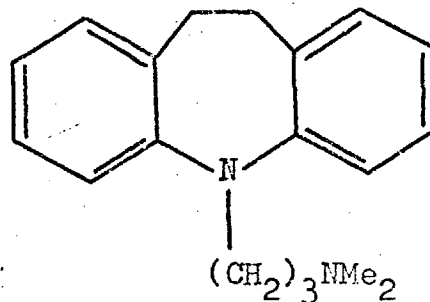
The anti-depressant properties of the anti-histamine drugs<sup>(224)</sup> were noted early in their clinical use. Minor structural modification has led to enhancement of the anti-depressant activity, at the expense of the anti-histamine function, in certain cases. For example chlorpromazine (9.I)<sup>(225)</sup>, a clinical anti-histamine<sup>(226)</sup>, and also the first drug effective in the treatment of schizophrenia<sup>(227)</sup>, can be modified to give imipramine (9.II)<sup>(228)</sup>, which has been found to have strong anti-depressant properties<sup>(229)</sup>, but which is only weakly anti-histaminic.<sup>(230)</sup>

Following these ideas, Leeming et. al.<sup>(231)</sup> have effected similar modifications of the well known anti-histamine phenindamine (tetrahydro-indeno-pyridine (9.III)<sup>(232)</sup>,



9.I. Chlorpromazine.

(marketed as the hydrochloride Largactil<sup>(226)</sup>)



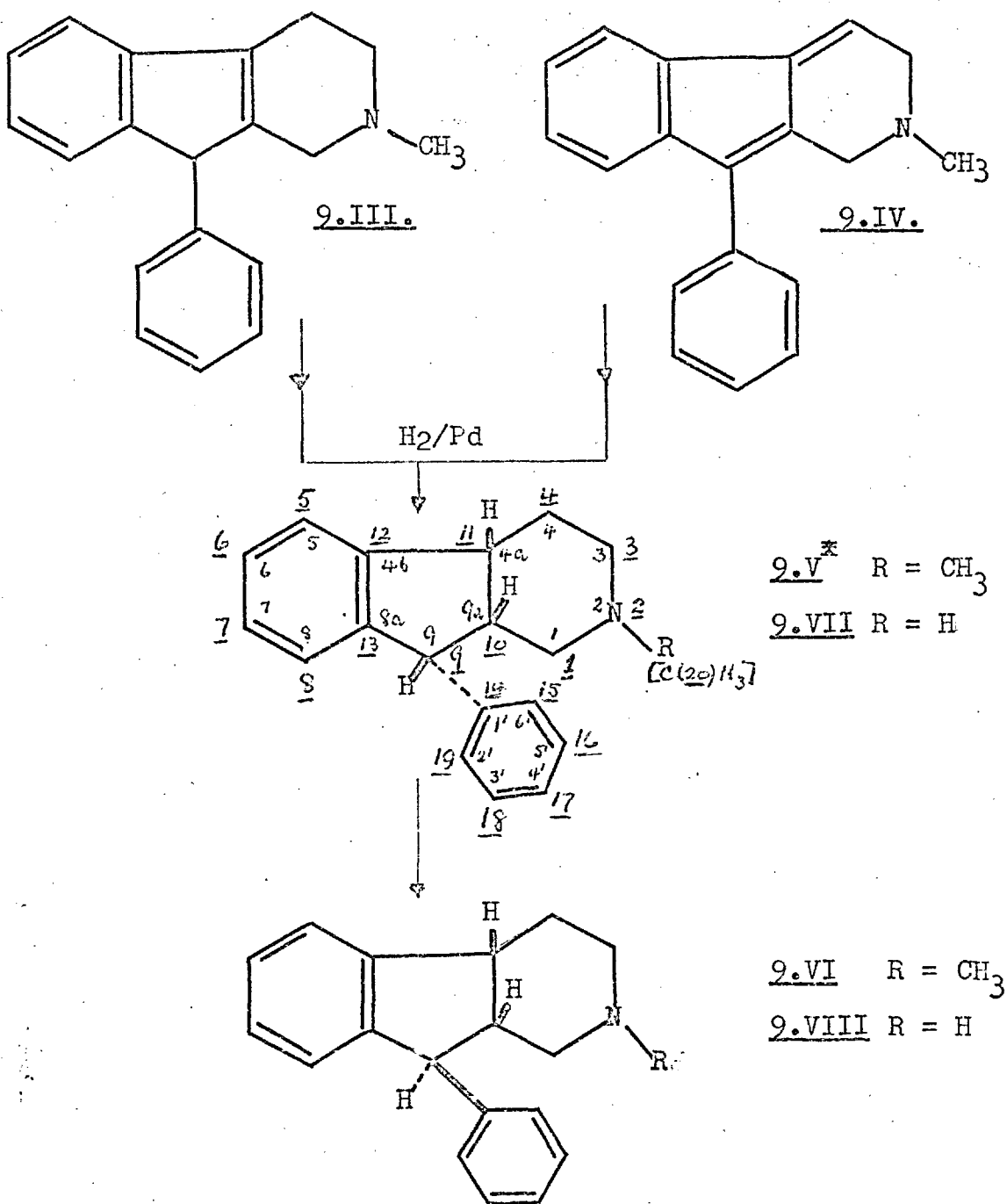
9.II. Imipramine.

(marketed as the hydrochloride Tofranil<sup>(230)</sup>)

marketed as the tartrate dihydrate Thephorin<sup>(233)</sup>). Catalytic hydrogenation of (9.III), and of the dihydro-1H-indeno [2,1-c] pyridine (9.IV)<sup>(234)</sup>, gives the compound (9.V), which can be irreversibly isomerized to (9.VI) using KOH in butanol. The corresponding demethylated derivatives (9.VII) & (9.VIII) were also obtained.

Correlation of n.m.r. evidence with deuteration studies indicated that, although both (9.V) and (9.VI) contain three asymmetric centres, they are epimeric at C(9) only, the stereochemistry at 9a, 4a, remaining unchanged. The all-cis stereochemistry shown for (9.V) was proposed<sup>(231)</sup> since :

i) It is well established that hydrogenation of double bonds at catalyst surfaces usually gives the product with the incoming hydrogens attached to the same face of the



\* This compound was eventually chosen for a full X-ray study, the numbering shown inside the ring is the chemically correct system, that shown outside is used in this work for computational convenience.

molecule<sup>(235)</sup>;

ii) There is a precedent for such a cis-hydrogenation in the synthesis of the closely related 3:4-cyclopentanopiperidine<sup>(236)</sup>.

Furthermore a study<sup>(231)</sup> of Dreiding and CPK solid models showed that the all-cis stereochemistry leaves the C(9) proton of (9.V) in a very exposed position; in the thermodynamically more stable epimer (9.VI) this proton is highly hindered. This would explain both the ready epimerization and deuteration at this position in (9.V).

The n.m.r. spectra were, however, somewhat ambiguous, and in parallel with further chemical work (and pharmacological studies to ascertain the anti-depressant properties), all four compounds (9.V → 9.VIII) have been studied by the X-ray method. Samples of the crystalline hydrobromides were supplied by Dr. P. R. Leeming of the Pfizer Co. (U.K.) Ltd. Since all four are related chemically (by the well established epimerization), the crystal structure of any one compound would suffice to establish the stereochemistry of a possibly important new group of pharmaceuticals.

## 9.2. Preliminary X-ray Studies.

Oscillation and Weissenberg photographs of the hydrobromides were taken using a Unicam X-ray goniometer and Ni<sup>2+</sup> filtered CuK<sub>α</sub>-radiation. The crystal data obtained are set out in Table 9.1. The cell dimensions quoted are visual

estimates only, and have not been refined by computer.

All four samples were completely stable to X-irradiation over a period of about four days each, during which the crystal data were obtained. The crystals of the more stable epimer (9.VI), and of its demethylated analogue (9.VIII), were excellent, giving full intensity records of any one layer after  $\sim 36$  hours. The crystals of the other parent epimer (9.V) were good, but its demethylated analogue was only poorly crystalline, being rather glassy; even the best specimens gave split diffraction spots, indicative of twinning, or more probably split crystals.

Although no measurements of optical rotation had been made the symmetry of the space groups, given in Table 9.1, shows the racemic nature of the compounds as supplied. Thus each cell contains equal numbers of D and L molecules. The only other point of interest is the rough similarity in the cell dimensions of the (9.V) and (9.VII) hydrobromides; the only difference is the doubling-up in the b-direction to accommodate the extra four molecules.

Dreiding models of the proposed stereochemistries of (9.V) and (9.VI) were made up. The former appeared the most interesting, purely on steric grounds, and a full three-dimensional X-ray analysis of this compound (which rejoices under the systematic name: 2,3,4,4a,9,9a-hexahydro-2-methyl-9-phenyl-1H-indeno[2,1-c]pyridine hydrobromide, hereinafter

TABLE 9.1.

Crystal Data for the Hydrobromides.

Compound	9.V:HBr	9.VII:HBr	9.VI:HBr	9.VIII:HBr
Formula	$C_{19}H_{22}NBr$	$C_{18}H_{20}NBr$	$C_{19}H_{22}NBr$	$C_{18}H_{20}NBr$
Habit	Laths*	Laths	Prisms	Rhombs
System	Monoclinic	Orthorhombic	Monoclinic	Monoclinic
$M$ ( $C^{12}=12.0$ )	344.3	330.3	344.3	330.3
$a$ (Å)	9.85	8.90	11.05	8.90
$b$ (Å)	15.05	30.40	7.45	10.15
$c$ (Å)	11.60	11.60	19.30	18.35
$\beta$ °	105.50	90.00	94.00	110.00
$V$ (Å <sup>3</sup> )	1648	3077	1583	1549
$D_x$ (g.cm <sup>-3</sup> )	1.38	1.39	1.41	1.40
$D_c$ (g.cm <sup>-3</sup> )	1.39	1.42	1.44	1.42
$Z$	4	8	4	4
$\mu$ (cm <sup>-1</sup> )	36.8	37.9	38.2	37.7
Space Group	$P2_1/c$	Pcan	$P2_1/c$	$P2_1/c$
(Int Tab No.)	(14)	(60)	(14)	(14)
Crystallinity	Good	Poor	Excellent	Excellent

called PIPH) was undertaken for three reasons :

- i) to check the proposed stereochemistry;
- ii) to examine the effect of overcrowding if the all-cis stereochemistry was confirmed;
- iii) to study the molecular geometry of the fused-ring heterocyclic system.

A fourth, and non-chemical, reason was to provide a lengthy test, involving the measurement of some 2800 intensities, for the Siemens automatic single-crystal diffractometer, which had recently been installed in the laboratory.

### 9.3. Experimental : The Siemens Automatic Single-Crystal Diffractometer.

The Siemens Automatische Einkristalle Diffraktometer (AED) is a four-circle instrument, designed according to the principles of the Eulerian cradle (see Figure 9.1). The position of any reflection,  $hkl$ , is defined by the three Eulerian angles:  $\theta_{hkl}$ ,  $\phi_{hkl}$ ,  $\chi_{hkl}$ , which can be computed<sup>(237)</sup> from the lattice parameters, radiation wavelength, and Miller indices. The instrument in use in this laboratory operates in the off-line mode; setting angles, together with other necessary data which will be mentioned below, are input to the machine via five-hole paper tape, the computation and preparation of which is performed by the ATLAS program SEKO (written by P. G. H. Troughton). The tape consists

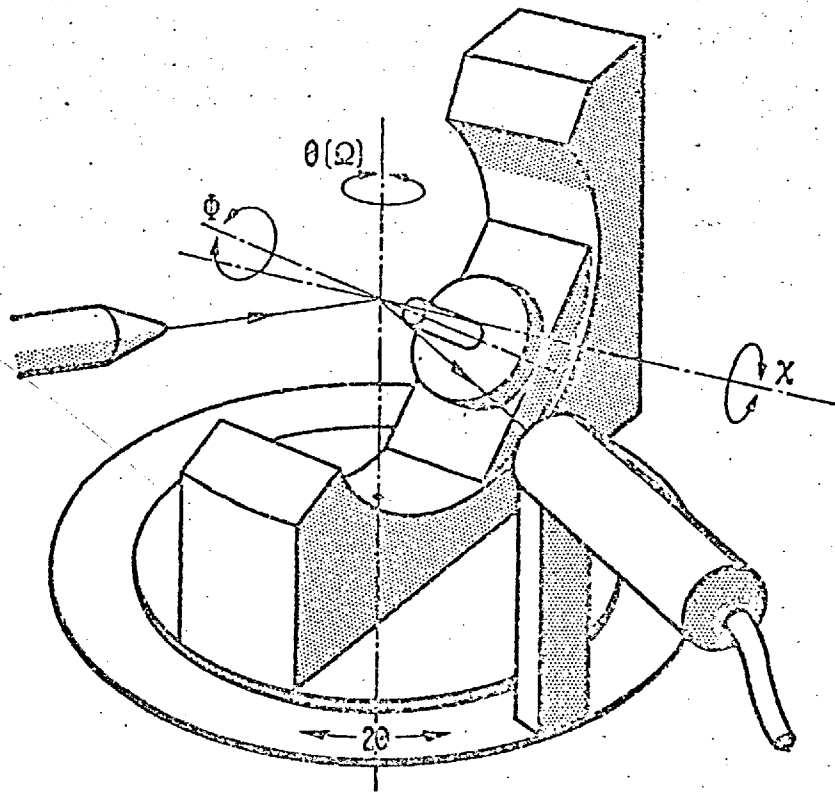


Figure 9.1. The Eulerian Cradle of the AED

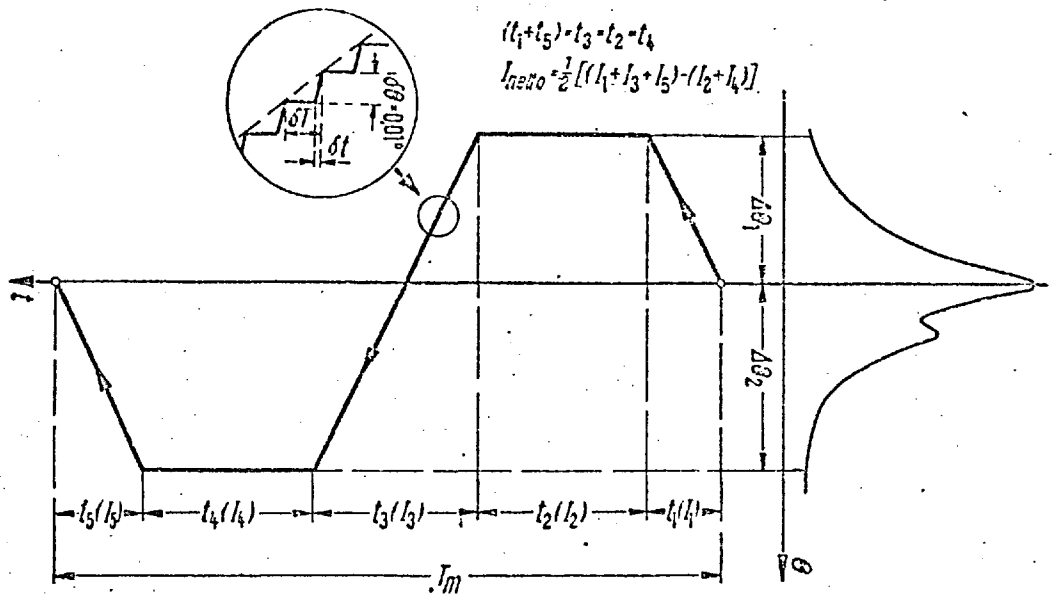


Figure 9.2. Schema of the five-point measurement technique (the values  $\Delta\theta_1$  and  $\Delta\theta_2$  are explained in the text).



basically of a series of commands to the pulse motors, which drive the circles in steps of  $0.01^\circ$ , and a command to start the measuring sequence (or perform various checks). The intensities of the diffracted beams are measured by scintillation counter, mounted on the  $\theta$ -circle, and kept at a constant temperature using cooling water. The recorded counts are passed, via a photomultiplier and pulse-height analyser, to the output tape. The X-rays are generated by a Siemens KRISTALLOFLEX 4 unit; in this work  $\text{CuK}\alpha$ -radiation was used, and the unit was run at 45 kV. and 16 mA. The mode of use of the machine, and some further instrumental points of interest, are exemplified in the description of the data-collection process for PIPH.

Crystals of PIPH are colourless laths, with  $[100]$  prominent, elongated along  $\underline{c}$ . A suitable specimen, of dimensions<sup>\*</sup> 0.61 x 0.20 x 0.14 mm, was mounted on a quartz fibre using Araldite, and set to rotate about the  $\underline{c}$ -axis on a Stöbe Weissenberg camera. A photograph of the  $hk0$ -layer was taken to check the suitability of the crystal. It was transferred to the diffractometer and, using the visually estimated cell dimensions together with some visually estimated relative intensities, it was possible to locate the reciprocal axes  $\underline{a}^*$ ,  $\underline{b}^*$ ,  $\underline{c}^*$ ; the former was set

---

\* A fuller description of the crystal morphology and dimensions is given in Sect. 9.4, where the application of an absorption correction is described.

to coincide with the  $\theta = 0^\circ$  position (thus  $b^*$  occurred at  $\theta = 90^\circ$ ). The setting angles for some 50 general reflections were then computed (SEKO) using the rough cell data. The values were set manually, and optimum  $\theta$ -values were obtained for some 30  $\text{CuK}\alpha_1$  peaks. The accurate cell parameters are listed below, and were obtained by the least-squares technique (CEDI).

### Crystal Data.

2,3,4,4a,9,9a-hexahydro-2-methyl-9-phenyl-1H-indeno [2,1-c] pyridine hydrobromide (PIPH) .....  $\text{C}_{19}\text{H}_{22}\text{NBr}$ .  
 Monoclinic (Laue symmetry 2/m): Space group  $\text{P2}_1/\text{c}(\text{C}_{2h}^5, \text{No. 14})$

$$\begin{aligned} \underline{a} &= 9.853 \pm 0.002 \text{ \AA}; & \underline{b} &= 15.099 \pm 0.002 \text{ \AA}; \\ \underline{c} &= 11.682 \pm 0.004 \text{ \AA}; & \underline{\beta} &= 105.81^\circ \pm 0.030^\circ; \\ \underline{V} &= 1672 \text{ \AA}^3; & \underline{D}_x &= 1.38 \pm 0.03 \text{ g. cm}^{-3}; \\ \underline{D}_c &= 1.367 \text{ g. cm}^{-3} & \text{for } \underline{Z} &= 4 \text{ molecules per cell}; \\ \underline{\mu} &= 36.220 \text{ cm}^{-1} \text{ for CuK}\alpha\text{-radiation } (\nu_{\text{K}\alpha_1} = 1.54051); \\ \underline{M} &= 344.3 \text{ (on the standard } \text{C}^{12} = 12.00); \\ \underline{F}(000) &= 712 \text{ electrons.} \end{aligned}$$

Using the above data, a steering tape was computed (SEKO) for a quadrant of the Cu-sphere, to a maximum  $\theta$ -value of  $65^\circ$ ; the 0.8 mm diameter collimator was used for data collection to compass the very anisotropic shape of the crystal. A five-point measuring technique was used to obtain the average intensity of each peak above the background

level; the scanning method is illustrated in Figure 9.2, which also shows how the net intensity is obtained from the five measurements. The values of the scanning limits  $\Delta\theta_1$ ,  $\Delta\theta_2$ , on either side of the peak maxima were obtained by scanning some representative reflections with  $\theta$ -values in the range  $8^\circ \rightarrow 70^\circ$ ; this information was input to SEKO in the form of a scan table, the correct values for each  $hkl$  were then obtained by interpolation.

A coupled  $\omega:2\theta$  scan ( $\omega = \theta$ ) was used throughout; the machine then approximates, as nearly as possible, a constant count per reflection device (as recommended by Killean<sup>(238)</sup>) except for the weakest intensities. This is effected by the automatic selection of measuring times: a maximum time ( $\tau_{\max}$ ) is selected by the user for each step, i.e.  $0.01^\circ$  of scan, and in this experiment 0.6 sec/step was chosen; should any reflection be too strong to fall within the range of maximum counter accuracy ( $\tau$ ) is successively reduced to 0.24, 0.12, and 0.06 sec/step. Reflections which are still too strong to be measured at  $\tau_{\min}$  are further reduced in intensity by the introduction of one of five attenuators, whose permeability to X-rays decrease in the approximate ratios: 100:45:21:9.5:4.5:2. The selection of measuring time, and the introduction of attenuators (if required), is carried out automatically before each five-point measurement; the exact attenuation factors for this machine were determined

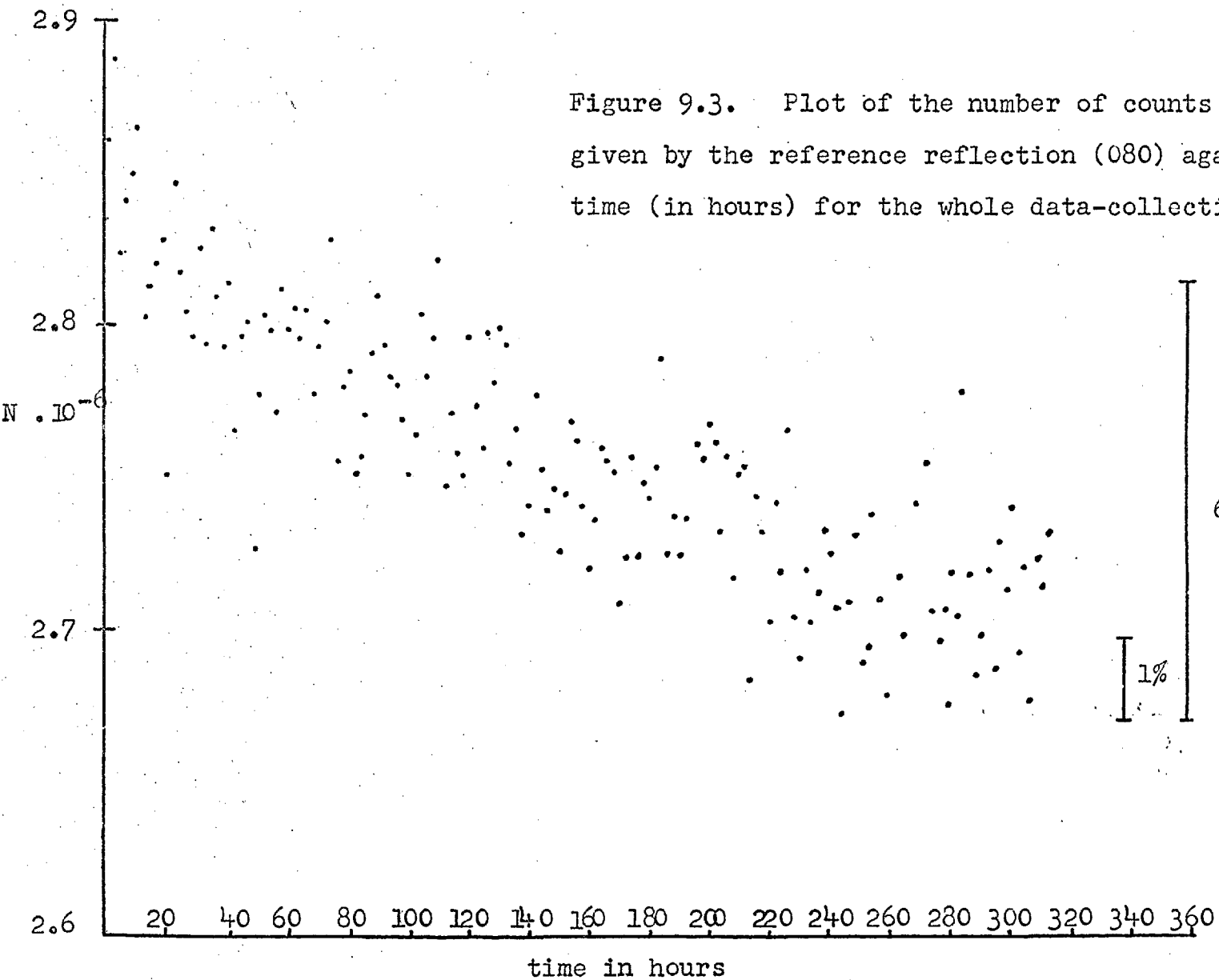
soon after its arrival, and were used in the final processing of the output tape.

A check was kept on the stability of the instrument, the setting of the crystal, and the accuracy of the setting angles actually used, in the following manner :

i) A strong reflection (080) was chosen as a 'reference', and measured once in every twenty reflections, i.e. once every two hours. This enabled a 'scale-factor' for each batch to be computed during processing, thus nullifying any instabilities, such as fluctuations in X-ray output or counter efficiency. A plot of the number of counts (N) given by this reflection against time is shown in Figure 9.3. It can be seen that, although most values lie within a band of width  $\sim 3\sigma$ , there is a gradual decline of  $\sim 5\%$  over the two-week period. This was almost certainly due to decreased efficiency of the Cu-target, and deposition of tungsten on the tube windows; the collection of only one other set of data was possible with this particular tube, and following this a complete  $\theta$ -scan from  $0^\circ \rightarrow 70^\circ$  for the  $h00$  reflections of a glucose monohydrate crystal revealed peaks due to both Fe- and W-radiations. Some of the observed decline could also have been due to radiation damage, but, in the light of the above evidence, the contribution from this source was probably minimal.

ii) A check on the crystal setting was provided by the

Figure 9.3. Plot of the number of counts (N) given by the reference reflection (080) against time (in hours) for the whole data-collection period.



data from 'kontrol' reflections, obtained after each batch of 100 five-point measurements. The reflections 700,  $\bar{7}00$ , 0100,  $0\bar{1}00$ , and 004, were chosen to check both goniometer arcs. The reflections were scanned with :

- a) full aperture, i.e. normal setting, (count  $N_T$ );
- b) insertion of a horizontal half-shutter into the aperture ( $N_H$ );
- c) insertion of a vertical half-shutter ( $N_V$ ).

It is experimentally very difficult to keep  $N_H = N_V$ , and  $N_H + N_V = N_T$  for any reflection. However an effective check is obtained by noting the ratio  $N_H/N_V$  which should stay reasonably constant for any hkl; also the ratios  $N_H/N_T$ ,  $N_V/N_T$  should remain constant and equal for reflections hkl,  $\bar{h}\bar{k}\bar{l}$ , if the crystal remains set. These values were checked periodically and minor adjustments made to the goniometer arcs if necessary.

iii) After every 40 five-point measurements a check was carried out on the angle circles by moving them by  $-\theta_{hkl}$ ,  $-\phi_{hkl}$ , and  $-\chi_{hkl}$ , where hkl was the last reflection measured. Digitizers were then brought into play to check that all circles were then in the zero position; all digitizer checks were successful in this experiment. If a circle is in error by  $\leq +0.2^\circ$  this is automatically corrected, but for larger errors the machine simply stops.

Exactly 3000 reflections were counted, and the five

measurements for each, plus the data for reference and kontrol reflections, were written to the output tape. This was processed using the ATLAS program SODI (F. G. H. Troughton) : the values of the raw intensities were evaluated using the formula quoted in Fig. 9.2, the  $L_p^{-1}$  correction applied, and the data (on a common arbitrary scale) written to ATLAS magtape and also output on cards in X-RAY '63 format. Of the possible 2873 independent reflections, 2396 had intensities significantly greater than background. The discrepancy between the number of independent reflections and the total measured is due to the inclusion of the  $\bar{h}k0$  reflections (equivalent to the  $hk0$ ). This was caused by a small programming error, but inadvertently provided a further check on the accuracy of the whole diffractometer experiment, since the data from the  $hk0$  zone were spread evenly over the whole data-collection period. A comparison of  $F^2(hk0)$  and  $F^2(\bar{h}k0)$  is given in Table 9.2; an 'agreement factor' of the form :

$$R' = \frac{2 \sum |F^2(hk0) - F^2(\bar{h}k0)|}{\sum F^2(hk0) + \sum F^2(\bar{h}k0)}$$

had a value of only 0.0116. The low value is a reflection not only of the reproducibility of the machine, but also of the very regular cross-section of the crystal (see Figure 9.3A on page 252); although absorption corrections have been neglected in deriving  $R'$ , the regularity of the cross-section gives an almost identical correction for any pair of reflections

TABLE 9.2.

PIPH : Comparison of  $F^2(hk0)$  and  $F^2(\bar{h}k0)$

The format is :

		*	h	†			
		k	$F^2(hk0)$	$F^2(\bar{h}k0)$	$F^2(hk0)$	$F^2(\bar{h}k0)$	$F^2(hk0) - F^2(\bar{h}k0)$
*	10	0			*	8	0
0	429.03	425.82	3.21	0	289.80	288.36	1.44
1	19.63	15.33	4.60	1	433.77	427.13	6.64
2	27.33	35.85	-8.52	2	9.53	9.25	0.28
3	55.02	58.20	-3.18	3	124.15	124.24	-0.09
4	93.42	95.01	-1.59	4	10.04	9.70	0.34
5	49.30	41.06	8.24	5	47.20	49.48	-2.28
6	65.11	55.88	9.23	6	33.90	35.26	-1.36
*	9	0		7	469.91	472.61	-2.70
0	61.11	69.08	-7.97	8	46.18	55.09	-8.81
1	229.84	227.53	2.31	9	16.50	24.81	-8.31
2	49.17	47.21	1.96	10	8.48	8.20	0.28
3	394.97	389.35	5.62	11	99.51	103.73	-4.22
4	155.29	169.48	-14.19	12	39.47	40.14	-0.67
5	154.79	154.85	-0.06	*	7	0	
6	94.50	95.31	-0.81	0	1283.98	1284.47	-0.49
7	95.96	107.48	-11.52	1	8.33	7.97	0.35
8				2	8.50	8.18	0.32
9	111.46	108.06	3.40	3	293.81	300.07	-6.26
				4	1215.77	1219.76	-3.99
				5	448.61	449.38	-0.77



Table 9.2. (Contd.)

※	7	0	(contd)	※	5	0	
6	22.85	30.32	-7.47	0	228.81	210.30	18.51
7	778.60	773.63	4.97	1	751.12	737.42	13.70
8	204.47	211.70	-7.27	2	274.13	266.23	7.90
9	10.21	17.20	-6.99	3	1163.53	1165.99	-2.46
10	21.25	20.25	1.00	4	213.84	217.15	-4.31
11	8.61	8.66	0.05	5	985.43	993.47	-8.04
12	194.42	207.59	-13.17	6	326.61	330.10	-3.49
13	7.18	6.84	0.34	7	1385.47	1392.61	-7.14
※	6	0		8	231.33	226.47	4.86
0	243.33	235.00	8.33	9	163.88	174.63	-10.75
1	25.39	21.45	4.94	10	226.38	225.08	1.30
2	47.43	44.22	3.21	11	229.66	229.22	0.44
3	339.22	338.14	1.08	12	255.84	258.74	-2.90
4	1319.44	1318.12	1.32	13	11.15	20.83	-9.68
5	199.60	197.69	1.91	14			
6	485.18	477.28	7.90	15	30.60	28.01	2.59
7	8.51	8.29	0.22	※	4	0	
8	763.92	794.09	-30.17	0	392.33	373.81	18.52
9	162.64	172.09	-9.45	1	248.59	241.13	7.46
10	184.17	187.23	-3.06	2	195.86	198.94	3.08
11	36.84	38.74	-1.90	3	1999.11	2014.13	-15.02
12	9.07	14.68	-5.61	4	4953.81	4965.52	-11.71
13	12.86	14.68	-1.82	5	663.06	660.19	2.87
14	11.30	9.27	2.03	6	452.29	443.67	8.62

Table 9.2 (Contd.)

* 4 0	* 3 0 (Contd.)
7 1831.64 1845.33 -13.69	13 32.22 30.09 2.13
8 753.31 770.06 -16.75	14 143.22 147.35 -4.13
9 8.02 7.99 0.03	15 137.95 137.83 0.12
10 322.93 330.18 -7.25	16 7.66 7.48 0.18
11 477.91 481.39 -3.48	17 6.44 6.15 0.29
12 10.12 9.65 0.47	* 2 0
13 241.97 228.34 13.63	0 1781.08 1790.06 -8.98
14 228.34 214.56 13.78	1 7068.67 7042.25 26.42
15 37.90 36.00 1.90	2 4499.66 4397.88 1.78
16 21.29 31.43 -10.14	3 100.78 101.13 -0.35
* 3 0	4 626.23 605.88 20.35
0 2756.75 2710.12 46.63	5 1023.48 1039.64 -16.16
1 1477.96 1470.36 7.60	6 187.83 192.60 -4.77
2 223.91 211.14 12.77	7 353.52 344.86 8.66
3 1382.12 1341.08 41.04	8 162.26 163.06 -0.80
4 1814.98 1794.73 20.25	9 234.70 248.18 13.48
5 2444.96 2371.77 73.19	10 38.13 32.08 6.05
6 5.63 5.38 0.25	11 1325.37 1314.33 11.04
7 1598.98 1607.62 -8.64	12 12.00 9.93 2.07
8 925.47 909.66 15.81	13 9.40 9.71 -0.31
9 82.57 86.53 -3.96	14 162.24 161.10 1.14
10 1217.32 1233.32 -16.00	15 51.12 57.76 -6.64
11 123.66 111.54 12.12	16 8.21 8.19 0.02
12 177.23 190.38 -13.15	17 6.84 6.66 0.18

Table 9.2 (concluded).

* 1	0		* 1	0 (contd.)
0	52.42	51.26	1.16	9 75.89 74.24 1.65
1	6589.51	6653.58	-64.07	10 40.62 32.80 7.82
2	748.97	739.96	9.01	11 2123.40 2125.14 -1.74
3	17311.76	17279.77	31.99	12 10.01 9.20 0.81
4	77.66	80.02	-2.36	13 215.53 225.84 -10.31
5	522.40	520.06	2.34	14 332.46 335.81 -3.35
6	511.82	508.60	3.22	15 359.90 364.78 -4.88
7	681.28	675.57	5.71	16 22.58 17.77 4.81
8	159.28	164.16	-4.88	17 46.79 51.56 -4.77

#### 9.4. Structure Solution and Refinement.

The position of the bromine ion was obtained from the Harker sections ( $\underline{x}, \frac{1}{2}, \underline{z}; 0, \underline{y}, \frac{1}{2}$ ) of a three-dimensional Patterson map, computed using FOURR. Structure factors were calculated (FC) using the phase angles (0 or  $\pi$ ) indicated by this position, together with an estimated  $\underline{B}$ -factor of  $3.0 \text{ \AA}^2$ . The data with intensities significantly greater than background were placed on an absolute scale by using the totals  $\sum |F_o|$  and  $\sum |F_c|$ ;  $R$  was 0.437. The first electron-density map (FOURR, in which, inadvertently, no structure factor rejection test was applied) revealed the positions of all 21 non-hydrogen atoms. The co-ordinates were optimized using Booth's method<sup>(161)</sup>, and used to construct a bead model

which showed chemically sensible geometry.

It was gratifying that the complete structure emerged so clearly from this one map, especially since no Fourier coefficients were either rejected or weighted down. The ratio ( $\underline{r}$ ) equal to  $(\sum z_H^2 / \sum z_L^2)^{\frac{1}{2}}$  is 1.32 in this case, tolerably close to Lipson and Cochran's suggested optimum value for ( $\underline{r}^2$ ) of unity<sup>(29)</sup> (see Eq. 2.17). The later, and somewhat more precise, analysis of Sim<sup>(239)</sup> suggests that ca. 83% of the signs predicted by the Br<sup>-</sup> position should be correct at this value of ( $\underline{r}$ ). This result is compared with similar ones for humulene bromohydrin and germacatriene : AgNO<sub>3</sub> in Table 9.3. It would appear that the ease of structure solution is not directly correlated with the value of ( $\underline{r}$ ), nor with the value of the initial  $\underline{R}$ -factor obtained.

TABLE 9.3.

Compound	$\sum z_H^2$	$\sum z_L^2$	$\underline{r}$	No. of maps to give the structure.	$\underline{R}$ of 1st map	% signs correct Sim(239)
PIPH	1296	742	1.32	1	0.437	83%
Humulene bromohydrin	1225	629	1.40	2	0.427	86½%
Germacra- triene:AgNO <sub>3</sub>	2209	805	1.66	3	0.346	89%

While the presence of a very heavy atom in a general position (e.g. Ag in the germacatriene complex) contributes substantially to all reflections, and thus tends to increase the former ( $\underline{r}$ ), and reduce the latter ( $\underline{R}$ ), it does require great accuracy in the measurement of the intensity data to avoid the swamping of the light-atom contribution. It was this latter factor which made the structure solution so straightforward in the case of PIPH.

For the refinement process the block-diagonal least-squares program BLOKLS was used throughout, except where specifically stated. Only the 'observed' data were used, and no weighting scheme (i.e.  $w = 1$  for all data) was employed the overall scale-factor ( $k$ ) was varied during all cycles. The designation of run numbers used in previous chapters is adhered to (see p. 95 for definitions), together with the following additional designations :

MR, As for runs of type M, but with the hydrogen atom positional parameters free to refine;

MH, As above, but with non-hydrogen atom parameters fixed.

Runs of type M and MH were alternated during the early stages to reduce the computing time over those of type MR, which required the variation of 256 parameters. The results of all runs are given in Table 9.4 on page 255.

The optimum positional parameters from the electron-

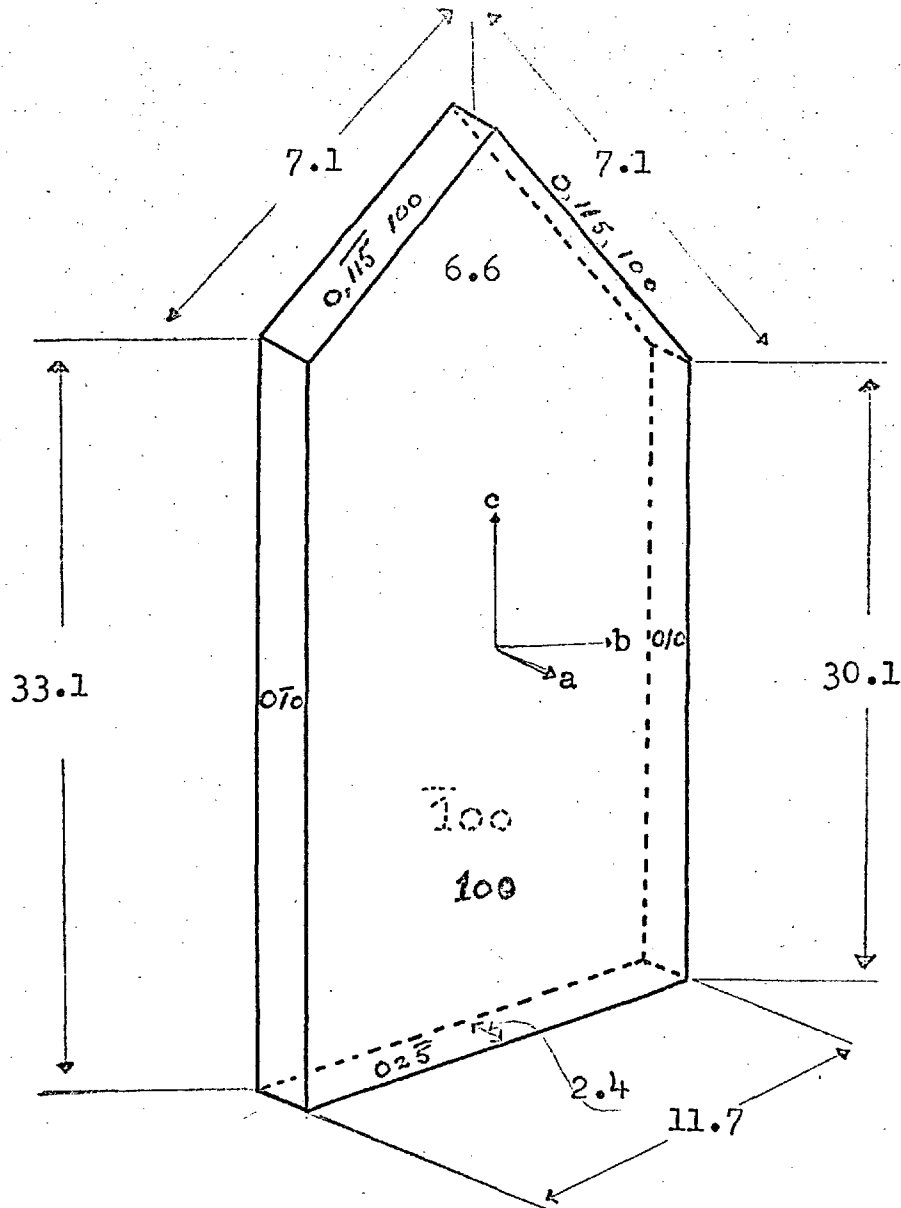
density map, together with estimated  $B$ -factors, were initially varied for six cycles (run I1), when  $R$  fell to 0.151. Scattering factors<sup>(19)</sup> appropriate to  $\text{Br}^{-1}$  and  $\text{N}^{+1}$  were employed. A difference map, using  $(F_o - F_c)$  as Fourier coefficients, showed no spurious features, but indicated some anisotropy, especially for the  $\text{Br}^{-}$  ion. The anisotropic thermal parameters were therefore computed ( $\beta_{ij}$ 's in the equation quoted in Table 6.5. p.103), and four cycles (run A1) reduced  $R$  to 0.086. Parameter shifts for  $\text{Br}^{-}$  and  $\text{N}^{+}$  remained high, and these two atoms only were refined for two cycles of full-matrix least-squares (ORFLS), other parameters being fixed.

A bond-length and valence-angle calculation (BONDLA) following run A3 showed chemically sensible geometry. Hydrogen atom positions calculated at this stage agreed with some tentative values from the difference map. They were included in further refinement at the calculated positions, with  $B$ -factors  $0.5\text{\AA}^2$  more than the final value for the atom to which they were bonded. An attempt to refine the  $B$ -factors (run MR1) failed, and they were fixed for all other runs. Refinement continued slowly (see Table 9.4), and after run M4 all parameter shifts for the non-hydrogen atoms were less than 0.2 of the corresponding estimated standard deviation. An interesting feature of these runs was the movement of H(20) (see the numbering scheme in the pull-out

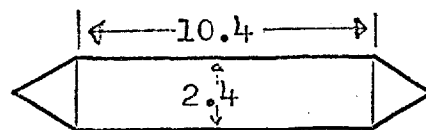
diagram bound with the end-papers) towards the  $N^+$  ion. This effect recurred later and is discussed below and in Sect.9.5; the atom was set back to its calculated position for run M4.

At this stage an absorption correction was applied using a program kindly supplied by Dr. B. J. Brandt of the University of Stockholm. It is modelled on the vector method outlined, and initially programmed, by Coppens et al<sup>(240)</sup>. The program (ABS0) was amended and altered by F. G. H. Troughton for use on both the IBM 7090 and ATLAS computers. The basic data required are the Miller indices of the crystal faces, and their perpendicular distances from an arbitrary origin within the crystal; this enables the program to set up a three-dimensional grid of sampling points. Figure 9.3(A) shows the relevant data, and also the crystal dimensions, as obtained using the microscope attachment to the AED. The morphology input is slightly idealized, as shown by the inset drawing of the crystal cross-section, but the designation of the boundary planes  $010$ ,  $0\bar{1}0$ , introduces only very minor errors.

A variety of grid sizes were tried using a sample batch of data, and one of  $6 \times 6 \times 6$  chosen as the smallest possible without significant loss of accuracy. The correction factors varied by  $\sim 1.5\%$  when the size was increased to  $10 \times 10 \times 10$ . Although the magnitude of  $(\mu)$  is small ( $36.22 \text{ cm}^{-1}$ ), the very anisotropic shape of the crystal gave a wide variation in



(Dimensions are given in AED microscope divisions:



1 div = 0.001714 cm.)

( Inset)

Figure 9.3(A). PIPH : Crystal Morphology and dimensions used in the application of absorption correction. The inset shows the actual cross-section. Both diagrams are exaggerated for clarity.



values of  $(\mu t)$ , where  $(t)$  is the thickness of crystal traversed by the X-ray beam. The 2396 'observed' data were processed in an average time of 1.09 sec/reflection on the IBM machine.

Refinement continued smoothly to  $R = 0.038$  (run MR5). Bond-length and valence-angle calculations during this period showed much improved standard deviations, reflecting the improvement in  $\sum (|F_o| - |F_c|)^2$ . At this stage the data deck was examined and two reflections (130, 221) were omitted for suspected extinction; two further reflections which had been duplicated were also corrected.

Following run MR6 it was noted that H(20) had again refined towards  $N^+$ , to a separation of only 0.476 Å. The  $N^+$ , and to a lesser extent  $Br^-$ , were showing oscillatory motion which was preventing successful convergence. A difference map was computed, using only non-hydrogen atom contributions to  $F_c$ . A rather diffuse peak of height  $0.4e^-$  was noted at  $\sim 0.6$  Å from  $N^+$ , but the resolution was very poor compared with other hydrogen peaks. The position adopted by H(20) in the refinement was almost certainly a node point of electron density due to the lone pair of  $N^+$ , and some bonding density directed towards  $Br^-$ . These points are more fully discussed in the next section.

The position of the proton was obviously not detectable by the X-ray experiment, and it was decided to try to obtain

convergence by removing H(20) and redefining the valence state of nitrogen as  $N^0$ . For run M5 the scale-factor (k),  $Br^-$  and  $N^0$  only were refined using ORFLS. The scheme was successful and following run MR7 all shifts for non-hydrogen atom parameters were less than 0.15 of their respective estimated standard deviations; some hydrogen parameter shifts were a little higher.

An analysis of the data (DELSIG) showed that  $\frac{(|F_o| - |F_c|)^2}{\text{AVE}}$  was almost constant over the most populated ranges of  $|F_o|$ . A weighting scheme of the Hughes<sup>(51)</sup> type was not, therefore, applicable; some attempts were made to use weights based on the standard deviation of each measurement, but it was not possible to pursue this work due to lack of computer time.

Refinement was, therefore, concluded at run MR7; the final positions and anisotropic temperature factors for the non-hydrogen atoms are shown in Tables 9.5, 9.6, while the refined hydrogen positions are shown in Table 9.7. These values were used to compute the structure factors listed in Table 9.8, for which an  $R$ -factor of 0.035 was obtained over the 2392 'observed' reflections not affected by extinction.

A similar structure factor calculation was performed for the 'unobserved' data, and the results (Table 9.9) show that, in general, the calculated values are less than those measured. However the reflections  $\bar{2},0,10$ ;  $\bar{2},0,12$ ;  $\bar{1},0,6$ ;  $\bar{1},0,8$ ;  $\bar{1},0,10$ ;  $\bar{1},0,12$ ; show surprising disagreement. This

was eventually traced to a programming error (now corrected): since  $\gamma$  for these reflections became  $> 90^\circ$ , a value not attainable on the AED, the equivalent reflections  $10\bar{1}$ ,  $20\bar{1}$ , should have been studied instead; however this switch was incorrectly programmed, and a value of  $180 - \gamma^\circ$  was set, leaving the machine to explore a blank area of reciprocal space. It was fortunate that only 6 reflections were so affected!

TABLE 9.4.

PIPH: The Refinement Process.

Run	Cycles	R	$\sum( F_o  -  F_c )^2$	max S/E	ave S/E
11	6	0.151	41860	3.9338	0.2277
A1	4	0.086	18400	5.7896	0.3380
A2 <sup>a</sup>	2	0.080	17060	0.3988	0.1220
A3	2	0.077	16410	1.1557	0.1048
M1	3	0.061	9573	0.7817	0.0725
MR1 <sup>b</sup>	2	0.058	8082	2.0704	0.2650
MR2 <sup>c</sup>	2	0.058	8138	1.6156	0.1232
M2	2	0.057	8026	0.2812	0.0465
MH1	2	0.057	8004	0.2530	0.0421
M3	2	0.057	8002	0.1767	0.0125

Absorption Correction Applied.

Table 9.4 (contd.)

Run	Cycles	R	$\sum ( F_o  -  F_c )^2$	max S/E	ave S/E
M4	4	0.050	6198	37.4632 <sup>d</sup>	1.4480
MR3 <sup>e</sup>	2	0.041	4114	2.4561	0.4062
MR4 <sup>f</sup>	2	0.038	3449	1.6586	0.1203
MR5	2	0.038	3391	1.3617	0.0684
MR6	2	0.035	2770	1.7229	0.1272
M5 <sup>g</sup>	2	0.035	2808	0.6085	0.1289
MR7 <sup>h</sup>	3	0.0353	2792	0.2467	0.0617

a) Scale-factor (k), Br<sup>-</sup>, & N<sup>+</sup>, only refined using ORFLS.

b) k, C(16), C(17), C(18), & C(20), plus all hydrogen parameters refined.

c) Hydrogen B-factors set back and fixed; hydrogen positions together with k, & C(17) refined.

d) The high shift is due to scale-factor adjustment.

e) All shifts damped by a factor of 0.6 for this run only.

f) Dispersion correction introduced using  $f_{Br}^i = -0.9$ ,  
 $f_{Br}^n = 1.5$  (ref. 59).

g) k, Br<sup>-</sup>, & N<sup>o</sup>, only refined using ORFLS, H(20) removed, and all other parameters fixed.

h) H(20) omitted.

TABLE 9.5.

PIPH : Final Atomic Co-ordinates for the Non-Hydrogen Atoms,  
as Fractions of the Cell Edges, together with their Estimated  
Standard Deviations.

Atom	$\bar{x}$	$\frac{\sigma}{\bar{x}}$	$\bar{y}$	$\frac{\sigma}{\bar{y}}$	$\bar{z}$	$\frac{\sigma}{\bar{z}}$
Br	0.15327	0.00005	0.38727	0.00003	-0.55468	0.00003
C(1)	0.25447	0.00036	0.29738	0.00023	-0.22910	0.00030
N(2)	0.11316	0.00029	0.31338	0.00019	-0.31627	0.00025
C(3)	0.03116	0.00036	0.37890	0.00028	-0.26531	0.00033
C(4)	0.10613	0.00039	0.46663	0.00026	-0.25155	0.00033
C(5)	0.20427	0.00038	0.48839	0.00025	0.02985	0.00034
C(6)	0.24945	0.00042	0.47413	0.00027	0.15154	0.00035
C(7)	0.36722	0.00044	0.42385	0.00027	0.20009	0.00033
C(8)	0.44327	0.00038	0.38590	0.00024	0.12823	0.00031
C(9)	0.46669	0.00033	0.37161	0.00021	-0.09029	0.00029
C(10)	0.34228	0.00033	0.38194	0.00022	-0.20521	0.00028
C(11)	0.25779	0.00034	0.46072	0.00022	-0.17475	0.00030
C(12)	0.27930	0.00033	0.45007	0.00021	-0.04239	0.00029
C(13)	0.39820	0.00033	0.39916	0.00021	0.00620	0.00028
C(14)	0.54683	0.00034	0.28535	0.00023	-0.07511	0.00031
C(15)	0.51382	0.00043	0.21452	0.00025	-0.01130	0.00038
C(16)	0.59401	0.00052	0.13598	0.00027	0.00262	0.00041
C(17)	0.70561	0.00049	0.12926	0.00032	-0.04910	0.00044
C(18)	0.73644	0.00044	0.19828	0.00032	-0.11364	0.00045
C(19)	0.65845	0.00039	0.27651	0.00028	-0.12677	0.00037
C(20)	0.03511	0.00046	0.22815	0.00029	-0.34909	0.00038

TABLE 9.6.

PIPH : Final Anisotropic Temperature Factors ( $\beta_{ij}$ ) for the  
Non-Hydrogen Atoms.

Atom	$\beta_{11}$	$\beta_{22}$	$\beta_{33}$	$\beta_{12}$	$\beta_{13}$	$\beta_{23}$
Br	0.01527	0.00569	0.00609	0.00283	0.00285	0.00052
C(1)	0.00848	0.00330	0.00573	0.00053	-0.00034	0.00017
N(2)	0.00834	0.00332	0.00563	0.00026	-0.00096	0.00009
C(3)	0.00704	0.00561	0.00751	0.00079	-0.00023	-0.00015
C(4)	0.00946	0.00429	0.00706	0.00218	-0.00020	0.00025
C(5)	0.00874	0.00370	0.00872	-0.00049	0.00295	-0.00072
C(6)	0.01279	0.00495	0.00790	-0.00218	0.00506	-0.00312
C(7)	0.01444	0.00455	0.00600	-0.00237	0.00241	0.00001
C(8)	0.01026	0.00306	0.00683	-0.00112	0.00005	0.00074
C(9)	0.00631	0.00290	0.00666	-0.00002	0.00088	0.00004
C(10)	0.00761	0.00304	0.00545	0.00053	0.00157	0.00051
C(11)	0.00783	0.00269	0.00641	0.00073	0.00109	0.00070
C(12)	0.00704	0.00262	0.00631	-0.00039	0.00113	-0.00018
C(13)	0.00726	0.00226	0.00604	-0.00057	0.00062	-0.00001
C(14)	0.00644	0.00318	0.00737	0.00064	-0.00073	-0.00073
C(15)	0.01167	0.00332	0.00986	0.00081	-0.00049	-0.00016
C(16)	0.01929	0.00323	0.01085	0.00169	-0.00300	-0.00020
C(17)	0.01425	0.00576	0.01362	0.00470	-0.00567	-0.00375
C(18)	0.00968	0.00662	0.01413	0.00266	-0.00008	-0.00389
C(19)	0.00839	0.00515	0.01012	0.00064	0.00066	-0.00218
C(20)	0.01386	0.00474	0.00888	-0.00172	-0.00297	0.00011

TABLE 9.7.

PIPH : Refined Hydrogen Atom Positions, in Fractional Coordinates, with their Estimated Standard Deviations ( $\sigma$ ).

The numerical designation of hydrogen atoms is made up of the number of the C or N atom to which they are bonded, together with one other number starting from zero; thus H(202) is the third hydrogen bonded to C(20).

Atom	$\bar{x}$	$\sigma_{\bar{x}}$	$\bar{y}$	$\sigma_{\bar{y}}$	$\bar{z}$	$\sigma_{\bar{z}}$
H(10)	0.2336	0.0043	0.2702	0.0028	-0.1660	0.0037
H(11)	0.2983	0.0043	0.2533	0.0028	-0.2673	0.0036
H(20)	This atom was not accurately definable (see Sect.9.5)					
H(30)	0.0201	0.0047	0.3525	0.0030	-0.1899	0.0039
H(31)	-0.0634	0.0046	0.3842	0.0030	-0.3221	0.0038
H(40)	0.0580	0.0046	0.5054	0.0031	-0.2191	0.0039
H(41)	0.1079	0.0047	0.4879	0.0031	-0.3260	0.0039
H(50)	0.1258	0.0044	0.5249	0.0029	0.0005	0.0038
H(60)	0.1967	0.0046	0.4933	0.0031	0.2058	0.0039
H(70)	0.3976	0.0046	0.4143	0.0030	0.2788	0.0039
H(80)	0.5264	0.0044	0.3497	0.0029	0.1629	0.0037
H(90)	0.5289	0.0043	0.4116	0.0027	-0.0986	0.0036
H(100)	0.3771	0.0042	0.3954	0.0028	-0.2739	0.0036
H(110)	0.3011	0.0043	0.5145	0.0028	-0.1886	0.0036
H(150)	0.4309	0.0047	0.2174	0.0031	0.0172	0.0040
H(160)	0.5703	0.0051	0.0879	0.0033	0.0444	0.0043

Table 9.7 (contd.)

---

H(170)	0.7650	0.0053	0.0745	0.0034	-0.0415	0.0044
H(180)	0.8148	0.0052	0.1954	0.0034	-0.1552	0.0044
H(190)	0.6762	0.0048	0.3211	0.0031	-0.1706	0.0040
H(200)	0.0908	0.0050	0.1969	0.0032	-0.3890	0.0042
H(201)	-0.0608	0.0050	0.2442	0.0033	-0.4033	0.0042
H(202)	0.0352	0.0050	0.1971	0.0032	-0.2741	0.0043

---



TABLE 9.8.

PIPH : Final Observed and Calculated Structure Factors for those Reflections with Intensities Significantly Greater Than the Background Level.

The format of the table is :

	H,	K,	L,
L	$10 F_o $		$10F_c$

The reflections omitted for suspected extinction were :

h	k	l	$10 F_o $	$10F_c$	$\sin\theta/\lambda$
1	3	0	152.51	-162.50	0.11248
2	2	0	158.56	-174.70	0.14159

-11,0,L	6	36	-43	-3,8,L	1	-8,6,L	-355
0 45 47	7	90	98	2 146 -151	2	341	71
6 186 198	8	73	-36	3 159 170	3	68	123
				4 199 -206	4	117	131
-11,1,L		-10,7,L		5 114 129	7	120	169
3 85 93	1	48	-52	6 108 -109	9	164	191
4 43 -50	2	95	131	7 105 115	10	84	-88
5 77 83	3	73	-76	8 44 45	11	142	158
7 50 60	4	110	120				
	5	43	-44	-9,9,L			
-11,2,L	6	61	71	1 167 -183		-8,7,L	-190
1 127 -137				2 83 92	2	180	-70
3 213 -224		-10,8,L		3 129 -136	3	73	-79
4 69 73	1	41	41	4 53 -54	4	72	147
5 31 -19	3	81	82		6	141	-72
6 32 43	4	32	31		7	72	69
				-9,10,L	8	70	159
-11,3,L		-9,0,L		1 31 45	10	146	
2 54 -66	2	317	-333	2 54 -66			
3 63 -68	4	309	-320	3 63 68		-8,8,L	-105
4 60 64	6	179	-197	4 79 -92	1	100	40
5 74 -73	8	80	84	5 76 -74	2	38	-54
7 101 -107	10	160	169		3	56	-196
				-9,11,L	4	196	-36
-11,4,L		-9,1,L		2 43 -51	5	49	-92
1 33 -35	1	103	-111	4 40 -47	6	90	119
3 51 -51	2	77	-78		7	105	-133
6 91 -104	3	133	-142	-8,0,L	8	127	156
	6	171	-176	2 350 -359	9	137	-42
-11,5,L	8	181	-193	4 287 -299	10	39	
2 77 82	9	54	57	6 226 -231			
3 126 -143	10	50	-59	8 243 -258		-8,9,L	-195
4 69 78	11	145	155	12 147 156	3	186	-222
5 149 -163					5	212	126
		-9,2,L		-8,1,L	6	122	-174
-10,0,L	2	113	-120	2 214 220	7	167	
2 84 92	3	49	44	3 65 -79			
4 159 172	5	173	-180	4 117 117		-8,10,L	111
6 152 172	7	172	-182	5 258 -271	1	104	-135
8 188 204	8	53	58	6 72 -76	2	131	138
	9	63	-74	7 110 -117	3	142	-93
-10,1,L	11	50	-63	9 80 -85	4	87	-77
1 75 -70				9 63 65	6	71	-81
2 178 -191		-9,3,L		10 131 -133	7	87	
3 276 -278	1	94	100	11 45 59			
4 85 -89	2	67	-74	12 69 -77		-8,11,L	-65
5 36 42	3	146	153		1	51	164
6 93 -93	4	225	-238	-8,2,L	2	163	-110
7 58 64	6	144	-152	1 156 165	3	98	54
9 61 63	7	59	62	2 102 -105	4	52	
	8	212	-226	3 142 150			
-10,2,L	9	43	-35	4 126 -135		-8,12,L	69
1 36 24				6 64 -76	1	69	49
2 56 49		-9,4,L		7 261 -279	3	48	49
3 159 -177	1	75	77	8 86 -97	4	50	-81
4 111 111	2	330	338	9 195 -211	5	76	51
5 88 -97	3	134	126	11 151 -163	6	48	
6 35 -20	4	263	269	12 52 51			
7 99 -104	5	90	-101		-8,3,L	-7,0,L	272
8 97 102	8	44	-38	1 81 -80	2	282	-109
	9	34	30	2 248 261	4	88	-334
-10,3,L	10	167	-171	3 263 269	6	330	-311
2 111 -124				4 161 166	8	291	-213
3 70 68		-9,5,L		5 180 130	10	205	
4 109 -112	1	79	95	6 81 -81			
6 157 -162	2	90	-97	7 208 209		-7,1,L	195
7 73 -78	3	48	54	8 153 -161	1	193	229
9 32 19	5	144	153	9 52 51	2	217	266
	6	85	82	10 230 -242	4	255	-130
-10,4,L	7	39	-42		5	128	129
1 75 -81	9	101	-114		6	131	-349
2 66 65				-8,4,L	7	333	-199
5 50 -58	1	174	-179	1 111 117	9	191	-150
6 96 -104	2	63	63	2 81 -63	10	147	-53
3 99 -104	3	42	45	3 197 -197	11	59	-164
	4	109	191	4 138 154			
-10,5,L	5	88	91	5 89 -91		-7,2,L	364
1 82 94	7	181	137	6 163 173	1	347	523
3 43 46	8	57	-65	7 92 -91	3	511	-80
5 39 -35	9	71	82	8 201 211	4	77	356
6 60 58				9 62 -69	5	350	89
7 94 -100		-9,7,L		10 37 -87	7	93	-86
8 49 53	2	87	-84		9	83	-77
	3	40	-40	-8,5,L	10	71	-209
-10,6,L	4	96	105	1 197 208	11	200	78
1 57 62	5	109	-96	3 377 392	12	71	
3 128 132	6	137	149	4 170 -179			
4 78 -84	8	129	134	5 297 316			
5 154 -164				6 45 51			
				7 145 152			
				10 81 84			

-7,3,L  
 2 328 336  
 3 59 67  
 4 326 336  
 5 42 -45  
 6 97 102  
 7 194 200  
 9 171 171  
 10 127 -124  
 11 59 48  
 12 159 -169

-7,4,L  
 1 125 129  
 2 197 -199  
 4 123 116  
 5 173 187  
 6 310 311  
 8 158 161  
 9 135 -142  
 10 162 174  
 12 92 80

-7,5,L  
 1 447 -461  
 4 192 -188  
 7 369 391  
 8 40 -43  
 9 235 252  
 10 60 53  
 12 65 46

-7,6,L  
 1 172 -180  
 2 186 -184  
 3 503 -513  
 4 93 98  
 5 470 -477  
 6 162 177  
 7 245 -261  
 8 80 81  
 9 65 57  
 10 106 120  
 11 88 93

-7,7,L  
 1 372 394  
 2 66 46  
 3 263 265  
 4 215 -231  
 5 54 64  
 6 102 -115  
 7 127 -120  
 8 62 69  
 9 113 -108  
 10 225 238  
 11 99 -94

-7,8,L  
 1 222 -223  
 2 124 133  
 3 241 -252  
 6 155 -158  
 7 47 47  
 8 107 -106  
 9 51 -43  
 10 95 -101

-7,9,L  
 1 226 232  
 3 49 -44  
 4 159 155  
 5 46 -56  
 6 75 77  
 7 174 -182  
 8 115 117  
 9 206 -216  
 10 72 89

-7,10,L  
 1 115 119  
 2 51 -63  
 3 93 94  
 4 98 -95  
 5 137 143  
 6 179 -189  
 7 95 102  
 8 128 -113  
 9 83 -85

-7,11,L  
 2 149 149  
 3 45 -52  
 4 178 197  
 5 64 -54  
 -7,12,L  
 1 119 140  
 2 164 -171  
 3 136 152  
 5 78 90  
 7 38 45

-7,13,L  
 1 43 -30  
 3 73 -74  
 5 48 48  
 6 69 -73

-7,14,L  
 3 57 -64

-6,0,L  
 2 542 578  
 4 346 363  
 6 39 41  
 8 268 -266  
 10 158 -173  
 12 264 -276

-6,1,L  
 1 343 348  
 2 191 175  
 3 239 253  
 4 340 342  
 6 285 282  
 7 147 -146  
 8 249 260  
 9 298 -308  
 10 45 55  
 11 256 -263  
 13 111 -100

-6,2,L  
 1 82 -78  
 2 190 197  
 3 234 231  
 4 178 173  
 5 319 333  
 6 51 28  
 7 440 456  
 8 50 -56  
 9 203 212  
 11 150 -140  
 13 96 -102

-6,3,L  
 1 181 -185  
 3 379 -388  
 4 490 500  
 5 250 -255  
 6 427 447  
 7 60 71  
 8 180 195  
 10 135 141  
 11 164 164  
 12 137 -145  
 13 97 70

-6,4,L  
 1 106 103  
 2 158 -171  
 3 120 135  
 4 312 -322  
 5 107 121  
 6 52 47  
 7 59 71  
 8 424 437  
 9 80 -79  
 10 336 358  
 12 175 193

-6,5,L  
 1 620 -628  
 3 279 -285  
 4 141 -134  
 6 209 -219  
 8 134 -141  
 9 132 134  
 10 54 53

11 177 188  
 -6,6,L  
 1 199 199  
 2 145 -152  
 3 208 -212  
 4 81 72  
 5 93 -93  
 6 47 35  
 7 164 -178  
 8 155 164  
 9 189 -192  
 10 136 145  
 11 59 25

-6,7,L  
 1 79 80  
 2 86 -92  
 3 142 -139  
 4 471 -483  
 5 98 -93  
 6 433 -456  
 7 105 98  
 8 133 -136  
 10 44 -48

-6,8,L  
 1 87 90  
 2 230 239  
 3 157 -171  
 4 235 234  
 5 222 -236  
 6 57 -57  
 7 193 -204  
 8 185 -182  
 9 61 -69  
 10 168 -178  
 11 109 102

-6,9,L  
 1 385 392  
 2 64 -69  
 3 308 324  
 5 155 160  
 6 58 50  
 7 80 -76  
 8 51 -44  
 9 168 -181  
 11 153 -165

-6,10,L  
 1 116 -124  
 2 115 121  
 4 89 100  
 5 220 233  
 7 165 167  
 8 161 -168  
 9 128 134  
 10 106 -118

-6,11,L  
 2 181 195  
 3 49 61  
 4 215 225  
 5 64 -66  
 6 221 232  
 7 50 -51  
 8 173 183  
 9 58 58

-6,12,L  
 1 46 -39  
 2 143 -144  
 3 47 42  
 4 134 -134  
 5 112 119  
 7 85 92  
 8 44 47

-6,13,L  
 1 225 -237  
 2 167 175  
 3 101 -118  
 4 62 64  
 5 41 -40  
 6 65 74  
 -6,14,L  
 1 62 -68  
 2 93 -98

4 118 -126  
 5 39 -42  
 6 59 68  
 -6,15,L  
 1 100 -117  
 2 44 43  
 3 46 -46  
 -5,0,L  
 2 668 693  
 4 888 890  
 6 483 487  
 8 264 269  
 10 108 -58  
 12 304 -320

-5,1,L  
 1 190 203  
 2 626 -623  
 3 368 393  
 4 308 -288  
 5 485 498  
 6 146 158  
 7 182 185  
 8 436 446  
 9 107 -104  
 10 54 66  
 11 174 -186  
 12 98 101  
 13 120 -124

-5,2,L  
 1 688 -702  
 2 172 173  
 3 209 -230  
 5 280 276  
 6 53 60  
 7 324 337  
 9 380 407  
 10 120 115  
 11 257 265  
 12 96 -96

-5,3,L  
 1 97 -105  
 2 275 -297  
 3 374 -372  
 4 159 -162  
 5 316 -306  
 6 73 85  
 8 362 380  
 9 147 -151  
 10 183 202  
 11 166 165  
 12 112 131  
 13 78 76

-5,4,L  
 1 99 -101  
 2 333 -346  
 3 84 -91  
 4 583 -602  
 5 316 307  
 6 513 -523  
 7 88 100  
 8 180 -187  
 9 315 318  
 12 162 166

-5,5,L  
 1 281 -291  
 2 111 123  
 3 457 -452  
 5 557 -554  
 6 60 55  
 7 223 -245  
 8 267 -269  
 9 93 94  
 10 205 -183  
 11 232 243  
 12 64 -98

-5,6,L  
 1 512 527  
 2 76 -50  
 3 363 375  
 4 152 -173  
 5 202 -198







9	1,2,L	321	335	4	166	171	3	562	592	2	130	136
10		119	-122	5	181	181	4	128	87	3	368	376
				7	43	43	5	913	947	4	327	339
				11	174	-185	7	481	484	5	261	255
	1,3,L						8	205	213	6	212	215
1		313	-321		1,10,L		9	55	46	8	271	279
2		243	221	0		71	10	149	162	9	173	-171
3		140	-174	1		74		129	129			
4		334	345	2		91						
5		124	-134	3		110		2,2,L		0	2,9,L	173
6		336	362	4		207		793	-769	1	173	-170
7		146	151	5		236		486	-449	2	60	-63
8		516	531	6		110		980	-908	3	38	-36
9		97	106	7		306		194	-169	4	242	256
10		159	177	8		180		668	-652	5	152	-155
11		167	180	9		40		149	-130	6	516	522
				10		89		341	359	7	342	351
								169	173	8	94	-36
	1,4,L							315	329	9	126	130
0		99	48		1,11,L			243	251			
1		67	-96	0		521					2,10,L	70
2		977	-970	1		123				0	70	-76
3		160	-161	2		75		2,3,L		1	329	-344
4		679	-775	3		82		115	-155	2	175	-171
5		318	309	4		87		636	592	3	359	-372
6		81	-87	5		322		731	-803	4	282	286
7		320	324	6		130		330	-331	5	163	-161
8		164	170	7		230		691	-683	6	240	243
10		268	286	8		232		694	-688	7	129	145
11		131	125	9		40		88	-85	8	90	93
12		189	218					168	185	9	101	105
					1,12,L			196	-195	10	60	54
				0		35		349	365			
	1,5,L			1		233		93	91		2,11,L	414
0		256	-242	2		65		71	95	0	414	-437
1		1166	-1208	3		76				1	134	-130
2		99	-95	4		130		2,4,L		2	319	-341
3		553	-578	5		138		285	-249	3	42	-45
4		378	-368	6		144		553	-558	4	81	-82
5		533	-544	7		225		128	-148	5	61	-68
6		204	-209	8		61		59	49	6	71	77
7		104	-102	9		133		555	-584	7	94	-105
8		219	-223					57	-62	8	220	223
9		66	84		1,13,L			546	-553	9	74	75
11		250	255	0		167		83	88			
				1		124		490	-501		2,12,L	39
				3		229		59	-29	0	39	23
	1,6,L			4		76		122	121	1	356	-367
0		254	188	5		136		88	106	2	190	-200
1		517	514							3	150	-146
2		462	-460		1,14,L					4	235	-247
3		35	-50	0		209		2,5,L		5	63	-66
4		229	-241	2		247		365	351	8	142	-153
5		426	-443	4		221		163	158			
6		141	-142	5		99		335	342			
7		463	-463	6		73		258	-285		2,13,L	39
8		76	-65					254	251	2	39	53
9		217	-230		1,15,L			404	-421	3	93	-94
10		164	165	0		219		97	90	4	73	-71
11		150	-152	1		113		295	-312	5	299	-316
				3		192		246	-254	6	60	55
	1,7,L			4		137		79	68	7	105	-115
0		293	326	5		126				8	86	94
1		144	134	6		42		2,6,L				
2		208	216					155	-125		2,14,L	147
3		73	91		1,16,L			1233	1250	0	147	143
4		224	-235	0		55		379	-340	1	172	183
5		54	59	1		84		443	449	2	37	46
6		473	-492	2		75		78	-87	3	45	37
7		43	46	4		66		231	227	4	194	-202
8		348	-366	5		79		317	-330	6	48	-50
9		45	40	6				35	-93	7	116	-123
10		75	-73		1,17,L			185	-193			
11		72	-76	0		81		133	-144		2,15,L	83
				1		122		211	-223	0	83	95
				2		69				2	181	189
	1,8,L			3		57		2,7,L		3	45	51
0		142	160					212	272	4	103	113
1		277	252		2,8,L			230	220	5	60	65
2		402	421	0		553		816	825	6	43	47
3		30	-19	2		499		124	125			
4		289	302	4		922		176	176		2,16,L	112
5		226	-227	6		374		195	112	1	116	112
6		64	53	8		443		142	-142	2	73	-71
7		131	-131	10		130		160	161			
8		176	-185	12		71		156	-193		2,17,L	63
9		247	-253					194	-110	2	63	53
10		290	-311					222	-236			
					2,9,L							
0		98	-98								3,0,L	67
1		536	557	0		1065		2,8,L		0	67	-700
2		29	12	1		158		144	121	2	1166	-1190
3		625	640	2		1064		193	213			





	5,1,L		1	320	335	6,5,L		7	73	-73	
6	273	-291	2	115	-126	0	174	-167			
10	88	-103	4	132	-126	1	121	-138	7,2,L		
			5	120	-25	2	259	-258	2	150	142
	5,2,L		6	146	-152	3	131	-137	3	138	143
0	202	193	7	50	-50	4	49	41	5	129	135
1	947	963				5	159	159	7	96	106
2	168	175		5,11,L		6	131	-138			
3	207	221	0	183	175	7	113	117		7,3,L	
4	35	30	2	225	238				0	201	-211
5	168	-177	4	51	46		6,6,L		1	247	-250
6	65	63	5	81	-93	0	275	-285	2	88	83
7	74	-77	6	90	-94	3	505	-527	3	112	-114
9	257	-268	7	38	-36	4	47	-56	4	185	194
						5	126	-141	5	98	97
	5,3,L			5,12,L		6	77	78	6	322	335
0	425	442	0	195	217	7	57	-60	7	72	72
1	210	205	1	222	237	8	89	91	8	145	161
2	119	149	2	174	171						
3	181	184	3	63	61		6,7,L			7,4,L	
4	171	175	4	138	152	1	175	-128	0	412	-418
5	293	305	5	45	43	2	463	-478	1	121	-119
6	154	-159	6	51	61	3	67	-69	2	502	-515
8	173	-178				4	123	-130	4	157	-170
10	126	-137		5,13,L		5	101	-103	5	58	-69
			0	41	50	6	108	-118	6	50	-48
	5,4,L		1	53	46	7	35	-45			
0	-186	-173	2	48	54					7,5,L	
1	198	207	3	151	149		6,8,L		0	252	252
2	322	341	4	102	111	0	350	364	2	80	-78
3	294	249	5	156	157	1	91	-100	3	263	-279
4	122	131				2	121	-115	4	81	-87
5	106	113		5,14,L		3	113	-123	5	42	-60
6	276	295	1	83	-95	4	78	-74	6	68	-69
8	50	-50	4	69	71	5	156	-166	7	102	126
9	78	-82				6	185	-188			
				5,15,L						7,6,L	
	5,5,L		0	69	-68		6,9,L		0	57	-68
0	393	-346	1	63	-60	0	160	167	1	193	-190
1	39	-26	2	34	-49	1	135	142	2	104	-112
2	131	-130				2	95	103	3	88	-87
3	376	387		6,0,L		3	119	123	4	132	-136
4	94	93	0	183	215	5	130	-133	5	121	-136
5	352	342	2	189	191	6	100	-97	6	83	-83
6	59	-61	4	120	-130	7	103	-113	7	104	-113
7	238	249	6	325	-314						
8	67	67	8	254	-262		6,10,L			7,7,L	
						0	170	181	0	337	350
	5,6,L		0	59	66	1	72	70	2	146	-145
0	223	-213	1	456	456	2	205	216	3	85	91
1	148	-166	2	282	286	3	185	200	4	165	-166
2	173	171	3	98	88	4	49	47	6	154	-163
3	430	-442	4	156	162	5	89	100			
4	131	129	5	38	-32	6	40	-42		7,8,L	
5	323	334	6	88	103				0	173	174
6	116	113	9	130	-139		6,11,L		1	59	63
7	230	252				0	76	79	2	155	156
8	94	102		6,2,L		1	83	96	4	99	103
9	203	219	0	81	-61	2	143	150	5	80	-79
			1	253	253	4	85	82			
	5,7,L		2	108	-90					7,9,L	
0	455	-470	3	309	325		6,12,L		1	215	230
2	231	-247	4	44	-45	1	113	120	2	45	45
3	229	-233	5	418	441	2	45	-45	3	212	234
4	290	-291	6	242	-247	3	162	166	4	39	32
7	41	45	7	128	136	4	55	62			
8	216	229	8	77	-77	5	158	168		7,10,L	
9	135	150	9	80	-93				0	56	59
							6,13,L		1	93	92
	5,8,L		0	221	227	0	45	-50	2	98	109
0	184	176	2	469	478	1	131	-137	3	128	131
1	160	-172	3	154	-157				5	45	50
2	248	-265	4	131	150		6,14,L				
3	174	-182	5	212	218	0	41	-41		7,11,L	
5	60	61	6	112	106	2	74	-86	2	41	33
6	177	-186	7	119	124				3	45	45
7	46	-43	8	41	-31		7,0,L		4	191	197
			9	79	81	0	415	424			
	5,9,L					2	380	390		7,12,L	
0	155	-152		6,4,L		4	98	113	0	168	-182
1	147	-148	0	443	-456	5	60	-65	1	34	-51
2	117	-120	3	240	237	8	144	-152	2	82	-81
3	309	-322	4	139	133					7,13,L	
4	43	35	5	75	33		7,1,L		1	113	-122
5	325	-333	6	310	315					8,0,L	
6	140	-151	7	44	55	1	329	347			
7	145	-150	8	133	146	2	73	56			
						3	183	179			
	5,10,L					4	283	307			
0	182	167				5	87	94	0	195	196
						5	194	207	2	84	70

4	8,0,L	296	312	0	9,2,L	79	-82
6		187	209	1		239	-244
	8,1,L			3		220	-237
0		239	-242	4		70	70
1		87	85	5		99	-112
2		118	-128		9,3,L		
3		132	138	0		226	-232
5		46	48	1		166	175
	8,2,L			2		191	-198
1		188	-211	3		78	-76
5		104	92	4		138	-156
6		40	36	5		74	-84
	8,3,L				9,4,L		
0		128	-144	0		142	158
1		169	-170	4		71	-70
2		145	-154		9,5,L		
3		54	-47	0		142	139
4		75	-85	1		38	40
5		34	-33	2		132	141
	8,4,L			3		111	-105
1		70	-77	4		60	66
2		100	-104		9,6,L		
3		50	-46	0		111	128
4		140	-152	1		136	130
	8,5,L			2		66	77
0		79	-79	3		65	76
2		76	-75	4		44	58
3		193	-202		9,7,L		
5		118	-117	0		112	120
6		57	-53	2		60	71
	8,6,L				9,8,L		
0		67	72	1		80	87
1		194	206	2		59	61
2		79	-81		9,9,L		
4		157	-165	0		121	-125
5		121	-122	1		157	-178
	8,7,L			2		44	-43
0		253	265		9,10,L		
1		73	72	0		33	-42
2		90	99		10,0,L		
3		90	104	0		233	-242
4		76	85	2		64	-72
5		66	72		10,1,L		
	8,8,L			0		50	-39
0		79	-79	1		86	-94
1		56	56	2		87	-87
2		77	81	3		64	-72
3		70	79		10,2,L		
4		119	129	0		59	64
	8,9,L			1		62	-53
0		47	61	3		69	-55
1		126	125		10,3,L		
2		113	121	0		83	73
3		119	119	2		59	69
4		80	83	3		35	-29
	8,10,L				10,4,L		
1		101	-104	0		109	116
3		40	27	2		42	44
	8,11,L				10,5,L		
0		117	-126	0		79	75
1		33	-45	1		164	175
2		69	-72		10,6,L		
	8,12,L			0		91	99
0		73	-77				
	9,0,L						
0		88	-107				
2		124	-143				
4		43	25				
	9,1,L						
0		172	-177				
1		118	-133				
3		57	56				
4		81	-90				
5		98	99				

TABLE 9.9.

PIPH : Observed and Calculated Structure Factors for those  
Reflections with Intensities not Significantly Greater than  
the Background Level.

The format is exactly as in the previous table (9.8).





3	2,16,L	32	14	4	5,1,L	33	11	8	7,1,L	29	16	1	10,3,L	31	0
4		31	1	9		34	-8								
0	2,17,L	31	5	8	5,2,L	36	-12	4	7,2,L	36	50	1	10,4,L	31	9
1		31	17	10		42	3	6		35	32				
								8		29	6	2	10,5,L	28	4
8	3,1,L	37	-16	7	5,3,L	37	-21	3	7,4,L	36	9		10,6,L	29	-30
				9		33	-4	7		31	-25	1			
7	3,2,L	36	-20	7	5,4,L	37	-32	1	7,5,L	36	-16	0	10,7,L	29	-17
7	3,3,L	37	-1	9	5,5,L	32	-2	1	7,7,L	37	12				
								5		33	-0				
0	3,6,L	27	17	1	5,7,L	34	16		7,8,L	36	11				
3	3,7,L	30	12	5		38	-22	3		30	-12				
				6		38	26	6							
2	3,9,L	32	7	4	5,8,L	39	-19	0	7,9,L	38	-49				
4		35	-41	8		32	-20	5		31	22				
5		36	14												
8		38	32		5,9,L	30	-28		7,10,L	32	6				
4	3,10,L	36	-5		5,10,L	38	14	0	7,11,L	35	-11				
7		37	-26	3				1		35	17				
5	3,11,L	37	-9	1	5,11,L	37	-10		7,12,L	30	19				
				3		39	50	3							
2	3,13,L	30	-11		5,14,L	35	-14	0	7,13,L	32	-11				
3		37	17	0		35	-14								
5		38	-14	2		35	-18								
				3		33	-16		8,1,L	35	-25				
	3,14,L	36	7	7	6,1,L	35	-26	4		31	12				
				8		33	14								
	3,15,L	34	22						8,2,L	35	-11				
					6,3,L	32	-5	0		36	-1				
	3,16,L	33	-18	1				2		36	27				
					6,4,L	33	31	3		35	-11				
	3,17,L	31	-34	1		34	20	4							
				2					8,3,L	30	4				
	4,2,L	37	-17		6,5,L	32	41								
11		51	-30	8					8,4,L	36	30				
										33	3				
					6,6,L	35	-6			29	-17				
	4,6,L	38	28	1		36	-10								
10		45	-5	2					8,5,L	36	-10				
					6,7,L	36	9			34	10				
	4,8,L	30	-34	0		29	-2		4						
				8											
	4,9,L	33	-13		6,8,L	31	-24		3	35	9				
0		37	-35	7											
4		35	-23		6,9,L	36	-0		0	34	-17				
8				4					2	31	28				
	4,11,L	39	30		6,11,L	36	48								
		35	-24	3		31	14		2	35	20				
				5											
	4,12,L	38	-36		6,12,L	38	-3		2						
				0											
	4,13,L	36	41		6,13,L	33	-29		1	35	19				
				2		31	6		2	34	-22				
	4,14,L	36	29	3					3	32	-0				
		35	41		6,14,L	32	3								
				1					1	33	-30				
	4,15,L	34	3		7,1,L	33	-11		3	29	21				
		33	-19	0											
					7,2,L	34	37								
	4,16,L	31	-23	0		34	-41								
				1					2	30	1				

## 9.5. Discussion.

### i) Accuracy of the Determination.

The standard deviations shown in Tables 9.5, 9.7, are probably low estimates, since they were obtained from block-diagonal least-squares approximations. This is also true of the  $\sigma$ -values obtained for the bond lengths and valence angles shown in Tables 9.10, 9.11. In general the respective  $\langle \sigma \rangle$ -values obtained here are better, by a factor of two, than those obtained by a similar process for humulene bromohydrin (cf. Tables 7.2, 7.6, 7.7), while the  $\underline{R}$ -factor is better by a factor of three. However a meaningful comparison is difficult, since the weighting schemes used in each case were different, and this plays an important part in determining the magnitude of  $\langle \sigma \rangle$ . Thus it is not possible to predict the type of relationship to be found between improvements in  $\underline{R}$  and  $\langle \sigma \rangle$ -values.

The most interesting point to arise from the refinement was the large drop in  $\underline{R}$  ( $\sim 2\%$  in 5.7%, an improvement of 35%) due to the absorption correction. As pointed out above, the anisotropic crystal-shape gave wide variations in  $\mu t$ , and the results obtained show the danger of ignoring absorption corrections, even when  $\mu$  is relatively low, unless the crystal shape is very nearly isotropic. It appears better to apply a rough correction than none at all.

The general accuracy of the data, obtained over a long (~2 weeks) collection period, was encouraging, especially since this was one of the first jobs of any length performed on this machine. It would have been possible to attain higher accuracy in the determination if the crystal had not been so anisotropic in shape, requiring the use of the 0.8mm collimator to encompass the lengths of the needle. A shorter crystal and smaller collimator would have reduced the background scattering, and probably increased the number of 'observed' reflections.

The accuracy of the initial data contributed in no small way to the speed of structure solution, a breakdown of the times is interesting in comparison with the photographic method. The data-collection process took exactly 322 hours (i.e. a rate of 9.32 useful reflections per hour). Data processing and structure solution took a further week, while one more week was required to reduce  $R$  to 0.086. Since this experiment formed part of an intensive series of trials of the AED, and was especially chosen because structure solution was expected to be straightforward, it can only be said that the machine gave an excellent response.

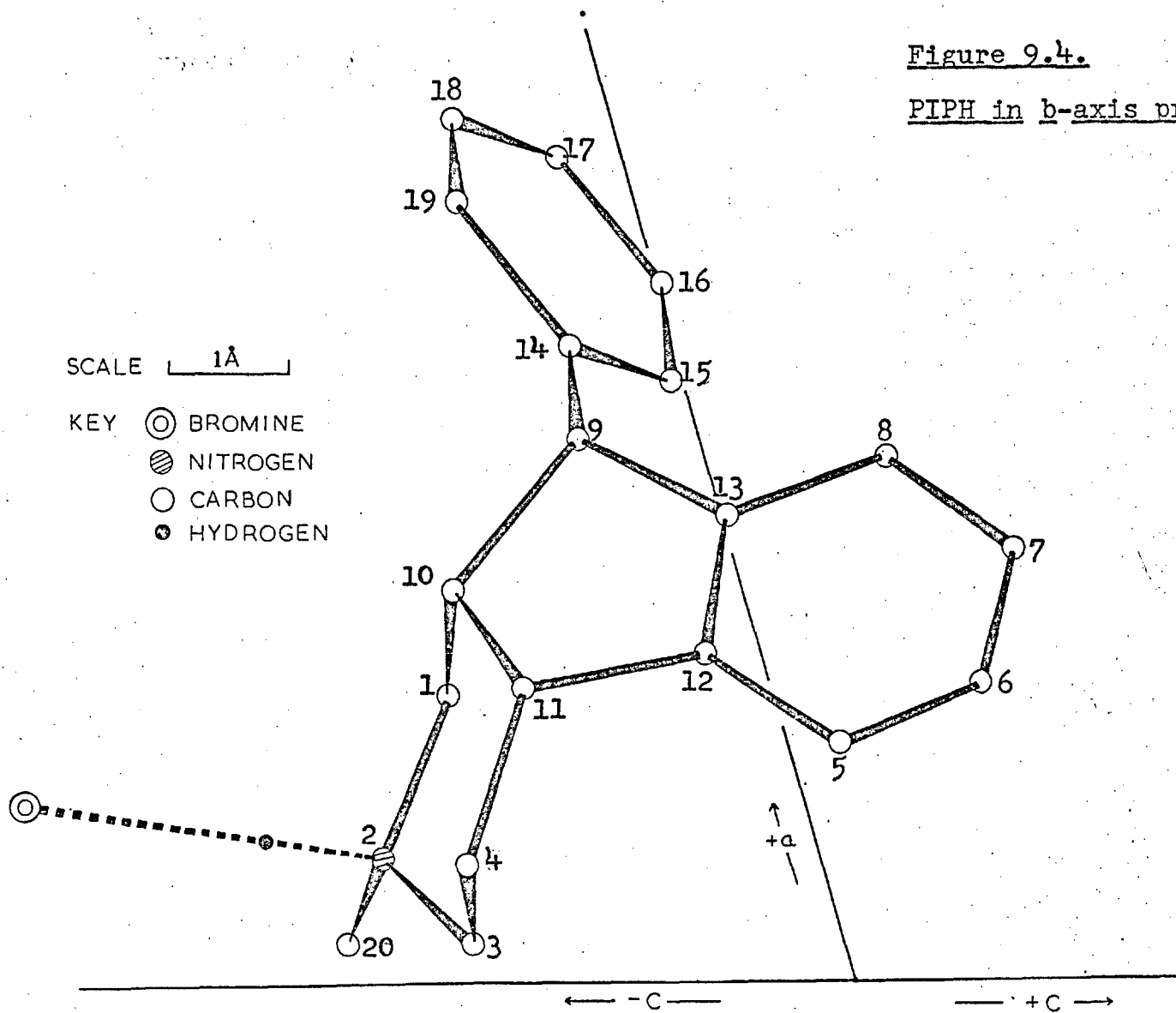
ii) Stereochemistry, Conformation and Molecular Geometry.

In the ensuing discussion the numbering adopted in the crystallographic study will be adhered to throughout. The



Figure 9.4.

PIPH in b-axis projection.



b-axis projection of one molecule (Figure 9.4) shows that the three protons at C(9), C(10), C(11), are all cis; the proposed stereochemistry<sup>(231)</sup> is therefore confirmed, and is shown correctly in 9.V (p.231).

The bond lengths and valence angles in Tables 9.10, 9.11, have been subdivided into two groups : those involving only C and N, and those involving hydrogens. The former are shown for clarity in figure 9.5. The average  $C_{sp^3}-C_{sp^3}$  and  $C-C_{aromatic}$  distances are  $1.531 \pm 0.005$  and  $1.513 \pm 0.005 \text{ \AA}$  respectively, not significantly different from the accepted averages of 1.537 and  $1.505 \text{ \AA}$ <sup>(153)</sup>. The average C-N<sub>quaternar</sub> distance of  $1.499 \pm 0.005 \text{ \AA}$  is a little higher than the cited average ( $1.479 \text{ \AA}$ <sup>(153)</sup>), but comparable averages have<sup>(241)</sup> been found in the structures of DL-betaprodine hydrobromide and hydrochloride<sup>(242)</sup> ( $1.495 \text{ \AA}$  in each case), piperazine hydrochloride<sup>(243)</sup> ( $1.50 \text{ \AA}$ ), and also in the piperidine rings of certain alkaloids<sup>(244)</sup>.

The carbon atoms of both benzene rings are closely coplanar, average deviations ( $\langle |d| \rangle$ ) from the mean planes being  $0.0022 \text{ \AA}$  for the C(5,6,7,8,12,13) ring, and  $0.0043 \text{ \AA}$  for the phenyl side-chain. The discrepancy is due to the higher thermal motion possible in the latter ring, which also accounts for the increased values of  $\sigma_x$ ,  $\sigma_y$ ,  $\sigma_z$ , for C(15)  $\rightarrow$  C(19) (see Table 9.5). Inclusion of hydrogen atoms in the calculation of the mean planes increases the

TABLE 9.10.

PIPH : Intramolecular bonded distances (r) in Å, together with their estimated standard deviations ( $\sigma_r$ )

a) Bonds not involving hydrogen atoms.

Atoms	$\bar{r}$	$\sigma_r$	Atoms	$\bar{r}$	$\sigma_r$
C(1) - N(2)	1.504	0.004	C(9) - C(13)	1.521	0.005
C(1) - C(10)	1.525	0.005	C(9) - C(14)	1.508	0.005
N(2) - C(3)	1.499	0.005	C(10) - C(11)	1.548	0.005
N(2) - C(20)	1.495	0.005	C(11) - C(12)	1.511	0.005
C(3) - C(4)	1.504	0.006	C(12) - C(13)	1.387	0.004
C(4) - C(11)	1.522	0.005	C(14) - C(15)	1.392	0.006
C(5) - C(6)	1.386	0.005	C(14) - C(19)	1.398	0.006
C(5) - C(12)	1.390	0.006	C(15) - C(16)	1.410	0.006
C(6) - C(7)	1.373	0.006	C(16) - C(17)	1.395	0.008
C(7) - C(8)	1.392	0.006	C(17) - C(18)	1.368	0.007
C(8) - C(13)	1.387	0.005	C(18) - C(19)	1.395	0.006
C(9) - C(10)	1.560	0.004			

Table 9.10 (contd.)

b) Bonds involving hydrogen atoms.

The bond lengths are given in groups, classified according to the degree of substitution of the carbon atom; the average  $\bar{r}$  in each group is compared with the spectroscopic average<sup>(153)</sup>

C(aromatic)-H.

C(5) - H(50)	0.93	0.04
C(6) - H(60)	0.97	0.05
C(7) - H(70)	0.90	0.04
C(8) - H(80)	0.98	0.04
C(15)- H(150)	0.96	0.05
C(16)- H(160)	0.94	0.05
C(17)- H(170)	1.00	0.05
C(18)- H(180)	1.02	0.06
C(19)- H(190)	0.89	0.05

$$\langle \bar{r} \rangle = 0.99 \text{ \AA}$$

$$\text{Spect. Ave.} = 1.084 \text{ \AA}$$

C(methyl)-H.

C(20)- H(200)	0.94	0.05
C(20)- H(201)	1.01	0.04
C(20)- H(202)	0.99	0.05

$$\langle \bar{r} \rangle = 0.98 \text{ \AA}$$

$$\text{Spect. Ave.} = 1.096 \text{ \AA}$$

C(disubstituted)-H.

C(1) - H(10)	0.91	0.05
C(1) - H(11)	0.97	0.05
C(3) - H(30)	1.00	0.05
C(3) - H(31)	0.99	0.04
C(4) - H(40)	0.90	0.05
C(4) - H(41)	0.93	0.05

$$\langle \bar{r} \rangle = 0.95 \text{ \AA}$$

$$\text{Spect. Ave} = 1.073 \text{ \AA}$$

C(trisubstituted)-H.

C(9) - H(10)	0.88	0.04
C(10)- H(100)	0.98	0.05
C(11)- H(110)	0.95	0.04

$$\langle \bar{r} \rangle = 0.94 \text{ \AA}$$

$$\text{Spect. Ave} = 1.070 \text{ \AA}$$

TABLE 9.11.

PIPH : Valence angles ( $\theta$ )<sup>o</sup> in the asymmetric unit, together with their estimated standard deviations ( $\sigma$ )<sup>o</sup>

a) Angles not involving hydrogen atoms.

End	-Apex	-End	$\theta$	$\sigma$	End	-Apex	-End	$\theta$	$\sigma$
C(1)	-N(2)	-C(3)	109.7	0.3	C(1)	-N(2)	-C(20)	110.6	0.3
C(1)	-C(10)	-C(9)	110.3	0.3	C(1)	-C(10)	-C(11)	111.8	0.3
N(2)	-C(1)	-C(10)	111.3	0.3	N(2)	-C(3)	-C(4)	108.8	0.3
C(3)	-N(2)	-C(20)	112.0	0.3	C(3)	-C(4)	-C(11)	112.7	0.3
C(4)	-C(11)	-C(10)	114.4	0.3	C(4)	-C(11)	-C(12)	116.8	0.3
C(5)	-C(6)	-C(7)	120.6	0.4	C(5)	-C(12)	-C(11)	128.8	0.3
C(5)	-C(12)	-C(13)	120.8	0.3	C(6)	-C(5)	-C(12)	118.9	0.3
C(6)	-C(7)	-C(8)	120.8	0.4	C(7)	-C(8)	-C(13)	119.1	0.3
C(8)	-C(13)	-C(9)	129.8	0.3	C(8)	-C(13)	-C(12)	119.9	0.3
C(9)	-C(10)	-C(11)	103.0	0.3	C(9)	-C(13)	-C(12)	110.1	0.3
C(9)	-C(14)	-C(15)	122.4	0.4	C(9)	-C(14)	-C(19)	118.7	0.3
C(10)	-C(9)	-C(13)	102.0	0.3	C(10)	-C(9)	-C(14)	116.8	0.3
C(10)	-C(11)	-C(12)	102.7	0.3	C(11)	-C(12)	-C(13)	110.2	0.3
C(13)	-C(9)	-C(14)	118.2	0.3	C(14)	-C(15)	-C(16)	120.2	0.4
C(14)	-C(19)	-C(18)	120.5	0.4	C(15)	-C(14)	-C(19)	119.0	0.4
C(15)	-C(16)	-C(17)	119.6	0.4	C(16)	-C(17)	-C(18)	120.2	0.4
C(17)	-C(18)	-C(19)	120.5	0.5					

Table 9.11 (contd.)b) Angles involving hydrogen atoms.

C(1) -C(10)-H(100)	109.4	2.4	N(2) -C(1) -H(10)	104.3	2.4
N(2) -C(1) -H(11)	104.2	2.2	N(2) -C(3) -H(30)	106.7	2.7
N(2) -C(3) -H(31)	107.4	2.8	N(2) -C(20)-H(200)	103.4	3.0
N(2) -C(20)-H(201)	106.3	2.8	N(2) -C(20)-H(202)	107.6	2.7
C(3) -C(4) -H(40)	108.5	3.0	C(3) -C(4) -H(41)	109.7	2.7
C(4) -C(3) -H(30)	115.2	2.5	C(4) -C(3) -H(31)	110.3	2.7
C(4) -C(11)-H(110)	105.3	2.2	C(5) -C(6) -H(60)	123.1	2.4
C(6) -C(5) -H(50)	118.1	2.9	C(6) -C(7) -H(70)	121.4	3.1
C(7) -C(6) -H(60)	116.1	2.5	C(7) -C(8) -H(80)	120.6	2.7
C(8) -C(7) -H(70)	117.9	3.1	C(9) -C(10)-H(100)	111.0	2.2
C(10)-C(1) -H(10)	118.0	2.5	C(10)-C(1) -H(11)	111.0	2.6
C(10)-C(9) -H(90)	104.1	2.41	C(10)-C(11)-H(110)	108.8	2.8
C(11)-C(4) -H(40)	109.6	2.5	C(11)-C(4) -H(41)	107.8	2.7
C(11)-C(10)-H(100)	111.1	2.5	C(12)-C(5) -H(50)	123.1	2.9
C(12)-C(11)-H(110)	108.7	2.4	C(13)-C(8) -H(80)	120.4	2.7
C(13)-C(9) -H(90)	110.8	2.9	C(14)-C(9) -H(90)	104.2	2.7
C(14)-C(15)-H(150)	119.7	2.7	C(14)-C(19)-H(190)	118.5	3.2
C(15)-C(16)-H(160)	119.9	3.2	C(16)-C(15)-H(150)	119.9	2.8
C(16)-C(17)-H(170)	122.1	3.3	C(17)-C(16)-H(160)	120.4	3.3
C(17)-C(18)-H(180)	122.8	2.9	C(18)-C(17)-H(170)	117.7	3.3
C(18)-C(19)-H(190)	121.0	3.2	C(19)-C(18)-H(180)	116.8	2.9
H(10)-C(1) -H(11)	106.8	3.8	H(30)-C(3) -H(31)	108.3	3.8

Table 9.11 (contd.)

H(40)-C(4) -H(41)	108.4	4.1	H(200)-C(20)-H(201)	112.5	4.0
H(200)-C(20)-H(202)	109.9	4.2	H(201)-C(20)-H(202)	116.1	4.1

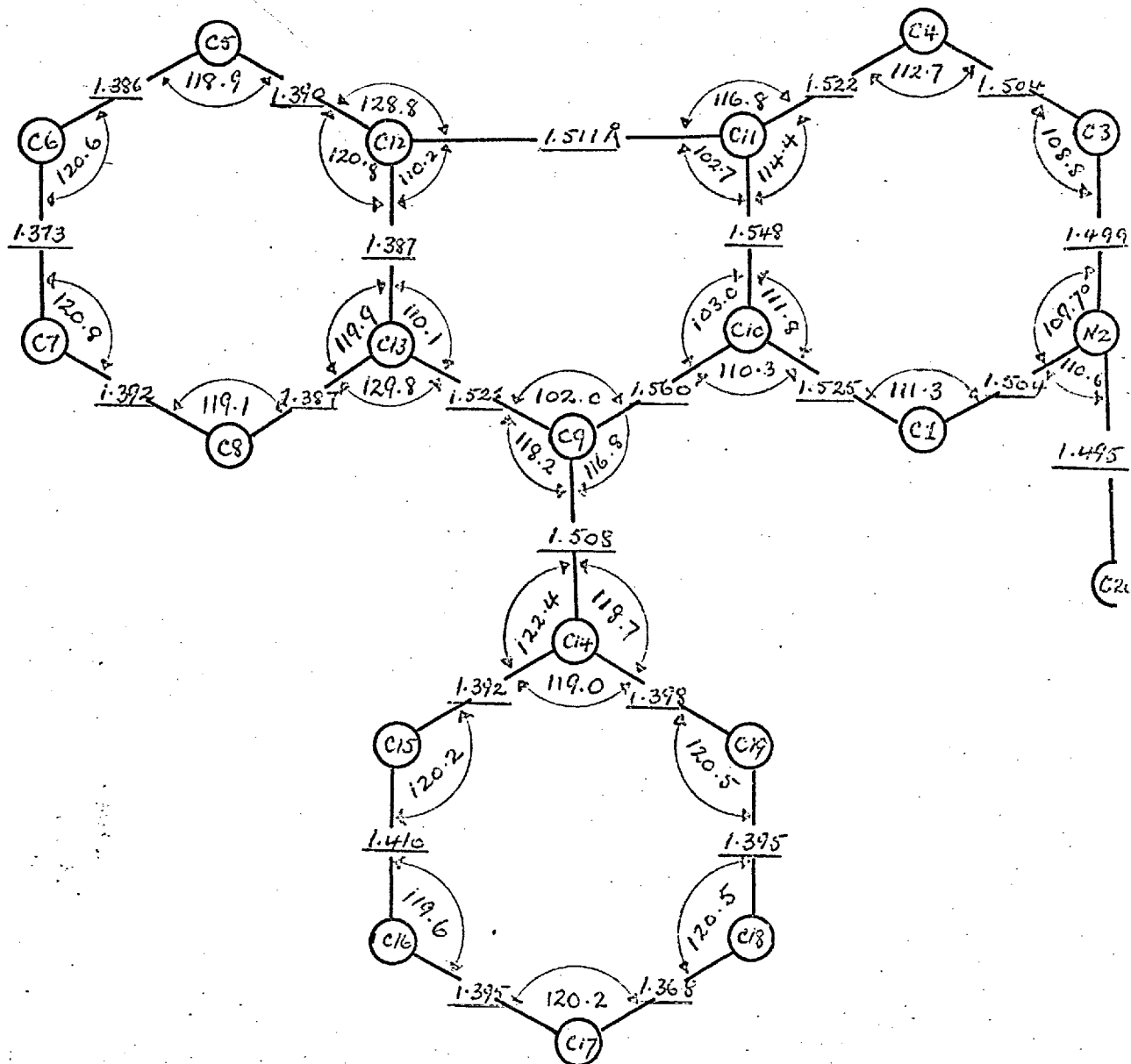


Figure 9.5. Diagrammatic representation of bond lengths and valence angles.

$\langle |d| \rangle$ -values ~~of~~<sup>to</sup> 0.021 and 0.024 Å respectively. In both rings the average C-C distances (1.386 Å in the fused ring, 1.393 Å in the phenyl group), and the average C-C-C angles (120.0° in each case), agree well with expected values.

The five-membered ring C(9) → C(13) adopts the envelope conformation<sup>(245)</sup>, frequently found in cyclopentanes<sup>\*</sup>; atoms C(9,11,12,13) are strictly coplanar ( $\langle |d| \rangle = 0.00068$  Å), with C(10) 0.545 Å above the mean plane. This conformation ideally has  $\underline{C}_s$  symmetry, and minimum-energy calculations by Pitzer et al.<sup>(246)</sup> and Hendrickson<sup>(158,247)</sup> have given theoretical optimum values for  $sp^3$ - $sp^3$  torsion angles ( $\omega$ ), and valence angles ( $\theta$ ). These values are compared with those obtained experimentally in this work in Table 9.12. It can be seen that the ring in this structure deviates surprisingly little from the ideal  $\underline{C}_s$ -form; the major distortions from the preferred conformation are at  $\omega_1$ ,  $\omega_5$ , and at  $\theta_3$ ,  $\theta_4$ , due to the fusion of two six-membered rings.

The heterocyclic ring adopts the chair conformation, but is again slightly distorted from the symmetrical minimum-energy form for cyclohexane by the ring fusion, and also by the substitution of nitrogen for carbon at position 2.

---

\* This ring is not strictly cyclopentanoid, since it contains two atoms, C(12), C(13), common to the benzene ring, which are not true  $sp^3$  hybrids. Nor is it a cyclopentene.

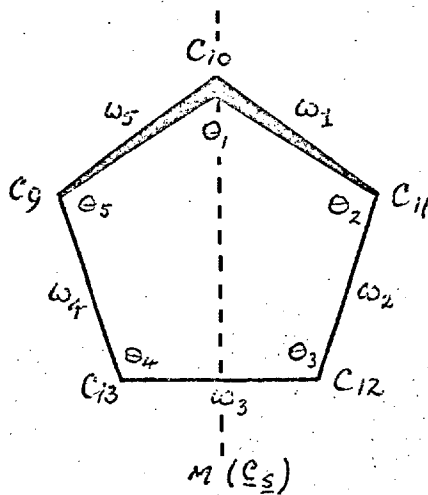


TABLE 9.12.

Comparison of torsion angles ( $\omega$ ) and valence angles ( $\theta$ ) for the five-membered ring in PIPH with values predicted from minimum-energy calculations for the  $C_s$ -form of cyclopentane.

Parameter	This work	Pitzer <sup>(246)</sup>	Hendrickson <sup>(158, 247)</sup>
$\omega_1$	32.82°	46.1°	41.7°
$\omega_2$	-21.02	-28.6	-25.9
$\omega_3$	-0.16	0.0	0.0
$\omega_4$	21.04	28.6	25.9
$\omega_5$	-32.71	-46.1	-41.7
$\theta_1$	102.99	100.4	101.7
$\theta_2$	102.66	102.4	103.6
$\theta_3$	110.19	105.6	106.0
$\theta_4$	110.13	105.6	106.0
$\theta_5$	101.96	102.4	103.6

The parameters involved are shown below :



Hendrickson<sup>(159)</sup> predicts all valence angles as  $111.6^\circ$  and all  $\omega$ -values as  $54.4^\circ$  in cyclohexane. In this work the former vary from  $108.75^\circ \rightarrow 114.38^\circ$  but average to  $111.45^\circ$ , the latter vary from  $41.90^\circ \rightarrow 65.03^\circ$  and average to  $53.66^\circ$ .

The high accuracy of the intensity data allowed a complete refinement of all hydrogen atoms (except H(20), the reason for this will be discussed below). The relatively large drop in  $R$ -factor and  $\sum(|F_o| - |F_c|)^2$  between runs A3 and MR2 can be largely attributed to this factor. The positions obtained are obviously not so well defined as those for C, N, and Br, and have  $\sigma$ -values some 10 times greater than those for the heavier atoms. The successful refinement of the methyl hydrogens, H(200-202), was no doubt due to their proximity to the hydrogens attached to C(1) and C(3), and to some bonding density in the sense N  $\rightarrow$  Br. To minimize the H-H non-bonded repulsions the substituents at N(2) and C(20) have adopted the staggered conformation, as can be seen from the Newman projection<sup>(213)</sup> (Figure 9.6) down the bond C(20)-N(2). The relevant H-H and C-H non-bonded contacts are also shown.

The C-H bond lengths (Table 9.10(b)) are rather short: the overall average of  $0.95 \text{ \AA}$  is some  $0.13 \text{ \AA}$  less than values obtained spectroscopically, or by electron- and neutron-diffraction studies. This effect has been noted in previous X-ray structure determinations<sup>(248)</sup> and has been ascribed to

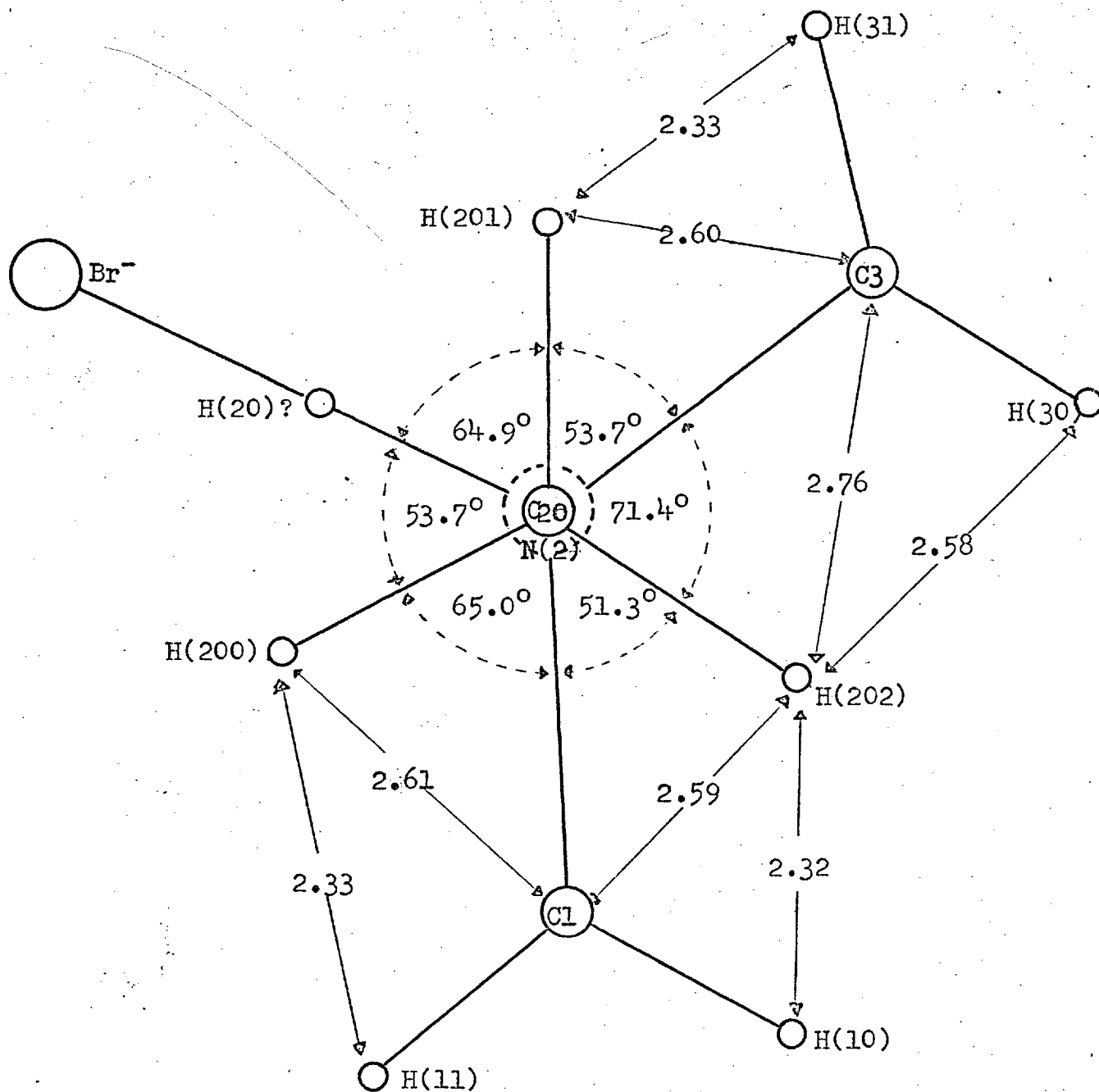


Figure 9.6. PIPH : Newman projection down the bond C(20)-N(2) showing the staggered conformation of the substituents.

'pulling' of the hydrogen K-electron density towards the heavier atom during bond formation. Vainshtein<sup>(249)</sup> has pointed out that, in a bond A—H, the nuclear position obtained for hydrogen from a difference map represents the centre of gravity of the hydrogen electron density  $\rho_H$ , and the bonding density  $\rho_{AH}$ ; refinement, using scattering factors pertinent to a spherical atom, will simply optimize this position. For such a light atom as hydrogen the resultant foreshortening of  $r_{AH}$  is serious; Tomlie<sup>(250)</sup> has shown that the magnitude of the observed shift in the electron-density maximum (ca. 0.13 Å) is consistent with valence-bond calculations.

In the case of a general bond A—B, where both A and B are of comparable size, and both contain a filled K-shell, the effect is not so serious. However Dawson<sup>(251)</sup> has predicted a shortening of all terminal bonds, in an X-ray determination, of ca. 0.01 Å, since the distortion of the electron-density about the terminal atom is not counteracted by distortion in other directions, as it would be if the atom were multiply substituted. Nevertheless Coppens and Coulson<sup>(252)</sup>, while agreeing with the general conclusion, have shown that the degree of hybridisation of atoms A and B must be taken into account in certain cases, and predict a slight lengthening in the particular case of an N—O bond in a nitro-group.

Thus, while the C-H distances obtained here are in good agreement with other X-ray results, they do not represent the true inter-nuclear separations. In retrospect it would have been better to have calculated hydrogen positions at a bonding distance of ca. 0.95 Å for the other three structures described in this Thesis; these positions would then have given a better estimate of the electron-density maxima.

The C-H distances shown in the Table have been grouped according to the degree of substitution, and differing hybridisation states, of the carbon atoms. In general the trend of  $\langle r_{C-H} \rangle$ -values follows that obtained spectroscopically<sup>(153)</sup> (the comparison can be seen in the Table), but further discussion would be profitless in view of the high  $\delta_r$ -values obtained in this work. It should be noted that comparison of C-H distances obtained by the X-ray and electron diffraction methods is doubly invalid, since Ibers<sup>(253)</sup> has estimated that values obtained by the latter method are some 0.03 Å longer than the inter-nuclear distance.

The bond angles involving hydrogen atoms are not significantly different from expected values (see Table 9.11(b)). This is reasonable since, although the  $r_{C-H}$ -values are foreshortened, the vector sense of the C-H bond remains unchanged.

In Figure 9.4 it can be seen that a hydrogen bond is postulated between nitrogen and bromine; the valence angles:

$$\text{C(1)-N(2)-Br} = 110.03^\circ,$$

$$\text{C(3)-N(2)-Br} = 109.34^\circ,$$

$$\text{C(20)-N(2)-Br} = 105.07^\circ,$$

show that  $\text{Br}^-$  is tetrahedrally disposed to N(2), and this supports the proposition. Similar results have been reported for other quaternary amine hydrobromides, and the N-Br distance in the present work (3.124 Å) is somewhat shorter than other values quoted, viz: 3.17 Å in 19-propylthevinol hydrobromide<sup>(254)</sup> and in strychnine hydrobromide dihydrate<sup>(255)</sup>, 3.26 Å in (+)-hetisine hydrobromide<sup>(256)</sup>, and 3.38 Å in 11-amino-undecanoic acid hydrobromide hexahydrate<sup>(257)</sup>.

The difficulty encountered (p.253) in the refinement of the hydrogen atom of this bond, H(20), is explicable using the type of argument given above. One would expect the K-electron of hydrogen to be more strongly attracted towards  $\text{N}^+$ , than towards a neutral atom, e.g. carbon. The peak seen in the difference map must have represented the centre of gravity of  $\rho_{\text{H}}$  and the electron density due to the lone-pair of nitrogen. The failure to attain convergence using  $\text{N}^+$ ,  $\text{H}^0$ , was almost certainly due to the use of spherically-symmetric scattering factors for these atoms. The relative success obtained by redefining  $\text{N}^+$  as  $\text{N}^0$ , and removing H(20), was possibly fortuitous, but probably gave a slightly better estimate of the electron-density distribution about nitrogen. It would have been preferable to employ the aspherical

scattering factors derived by Dawson<sup>(258)</sup> for quaternary ( $sp^3$ ) nitrogen, but time did not permit the additional programming and computation involved.

iii) Molecular Overcrowding.

The Dreiding model of the all-cis stereochemistry, made prior to structure solution, showed that the phenyl side-chain must twist about the bond C(9)-C(14) in order to minimize H-H and C-H interactions with the fused indeno-pyridine system. This has been confirmed by the X-ray study (see Figs. 9.4, 9.8): the angle between the mean planes through the phenyl group and the fused ring system being  $73^\circ$ . The closest contacts between the fused ring system and the hydrogens H(150) and H(190), which are bonded to the nearest 'corners' of the phenyl side-chain, are given below :

H(150)-H(10)	2.56 Å	H(190)-H(90)	2.33 Å
H(150)-H(80)	2.63	H(190)-H(100)	3.08
H(150)-C(13)	2.76	H(190)-C(9)	2.62
H(150)-C(9)	2.71		

If we take the van der Waals radii of hydrogen and carbon as 1.2 and 2.0 Å respectively<sup>(210)</sup>, then no distance given above is significantly shorter than the appropriate radial sum. Thus, the position adopted by the phenyl side-chain is completely explicable in terms of the minimization of

non-bonded interactions between the two ring systems.

iv) Molecular Packing.

The molecular packing, projected down the  $a$ -axis, is shown in Figure 9.7, in which molecules have been identified by Roman numerals. The 'zig-zag' formation of  $\text{Br}^-$  ions at any one level in  $x$  (e.g.  $\text{Br}_{\text{II}}$ ,  $\text{Br}_{\text{III}}$ ,  $\text{Br}_{\text{IV}}$ ), is important in stabilizing the molecular arrangement. If we take the van der Waals radius of hydrogen as  $1.2 \text{ \AA}$ , and the ionic radius of  $\text{Br}^-$  as  $1.95 \text{ \AA}^{(210)}$ , then their sum ( $3.15 \text{ \AA}$ ) is comparable with the distances given below :

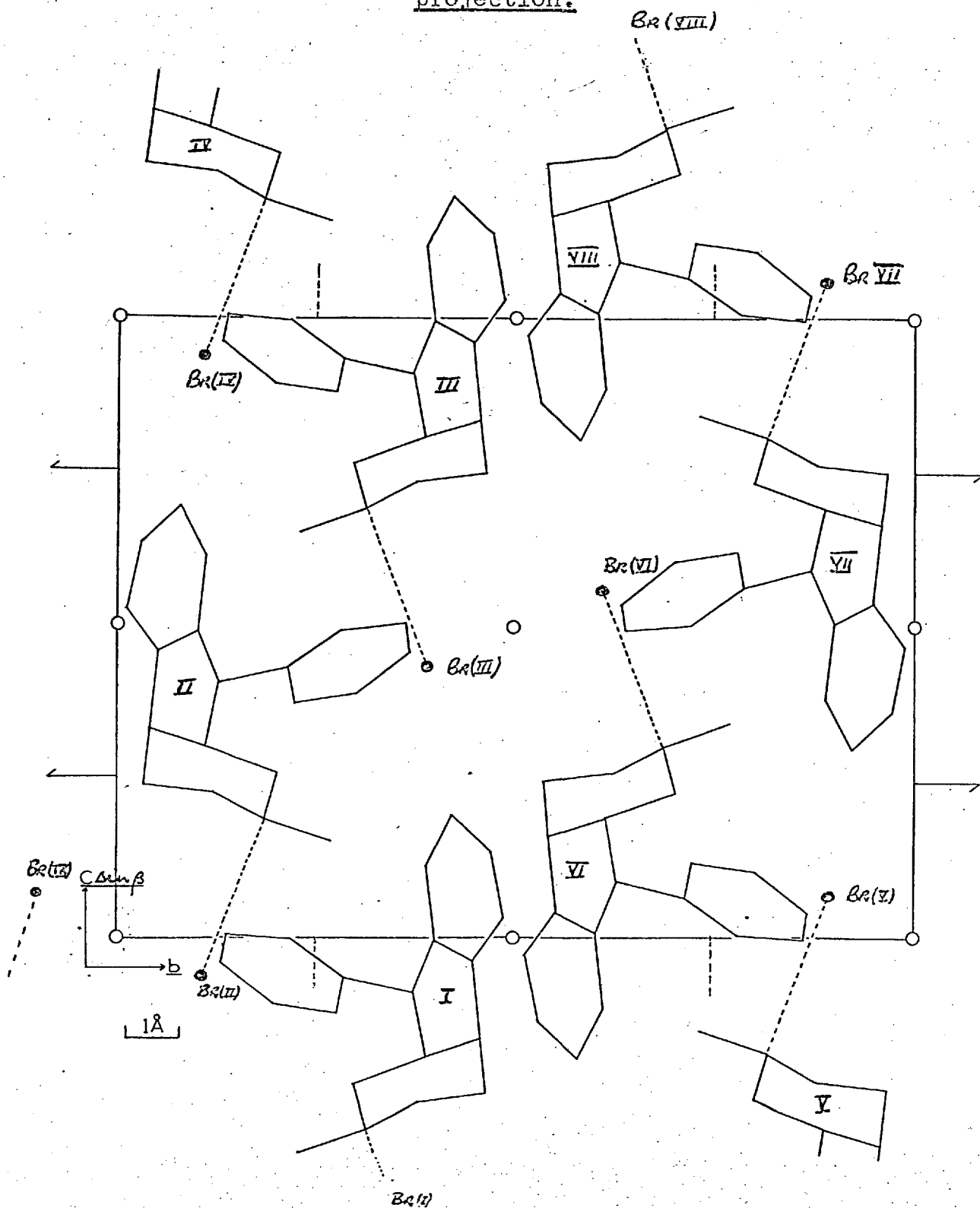
$\text{Br}_{\text{III}}$	-	$\text{H}(10)_{\text{II}}$	2.92 $\text{ \AA}$	
	-	$\text{H}(202)_{\text{II}}$	2.81	N.B. (a) represents the translationally-equivalent molecule to (II) in the cell below, i.e. with co-ordinates : $x_{\text{II}}-1, y_{\text{II}}, z_{\text{II}}$ .
	-	$\text{H}(150)_{\text{II}}$	3.07	
	-	$\text{H}(60)_{\text{I}}$	3.35	
	-	$\text{H}(70)_{\text{I}}$	3.50	
$\text{Br}_{\text{IX}}$	-	$\text{H}(170)_{\text{I}}$	3.07	
	-	$\text{H}(40)_{\text{IIa}}$	3.31	
	-	$\text{H}(41)_{\text{IIa}}$	3.19	

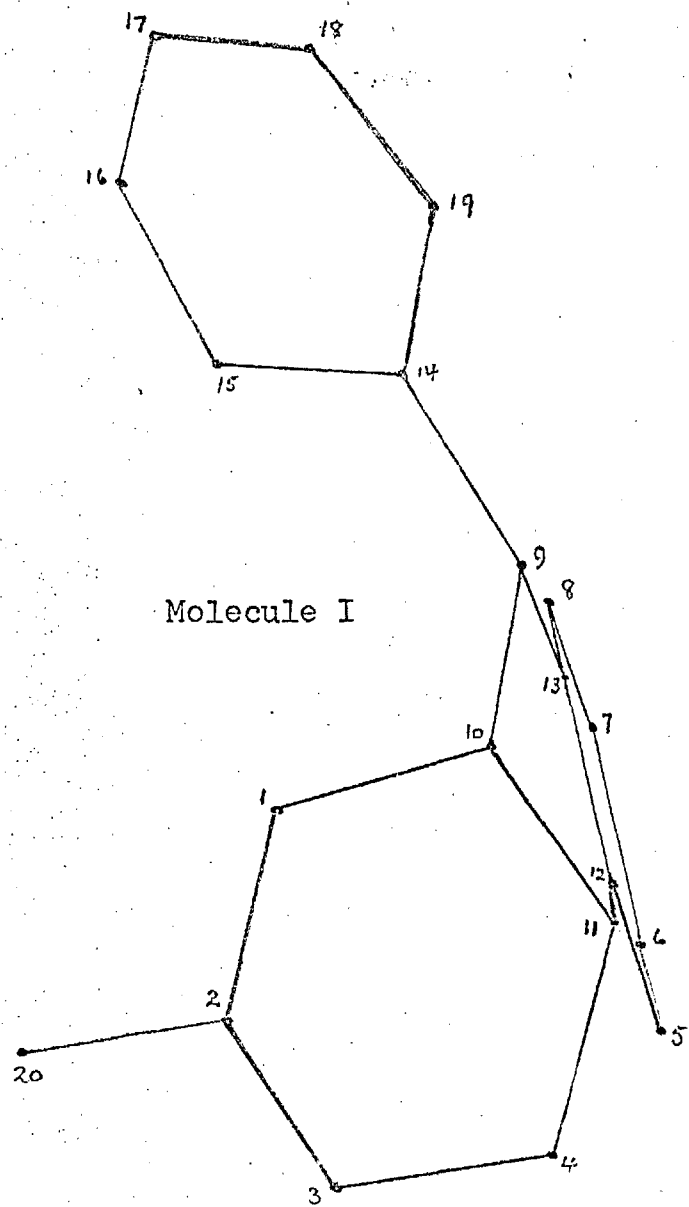
The above values, taken together with the strong hydrogen bond ( $\text{Br}_{\text{N}}-\text{N}(2)_{\text{N}}$ ) in any molecule, shows the effect of  $\text{Br}^-$  in 'cementing' together the organic moieties.

Additional stability is provided by the close approach of pairs of molecules (e.g. I and VI) across centres of



Figure 9.7. PIPH : The Molecular Packing in a-axis projection.





$\odot \bar{1}$

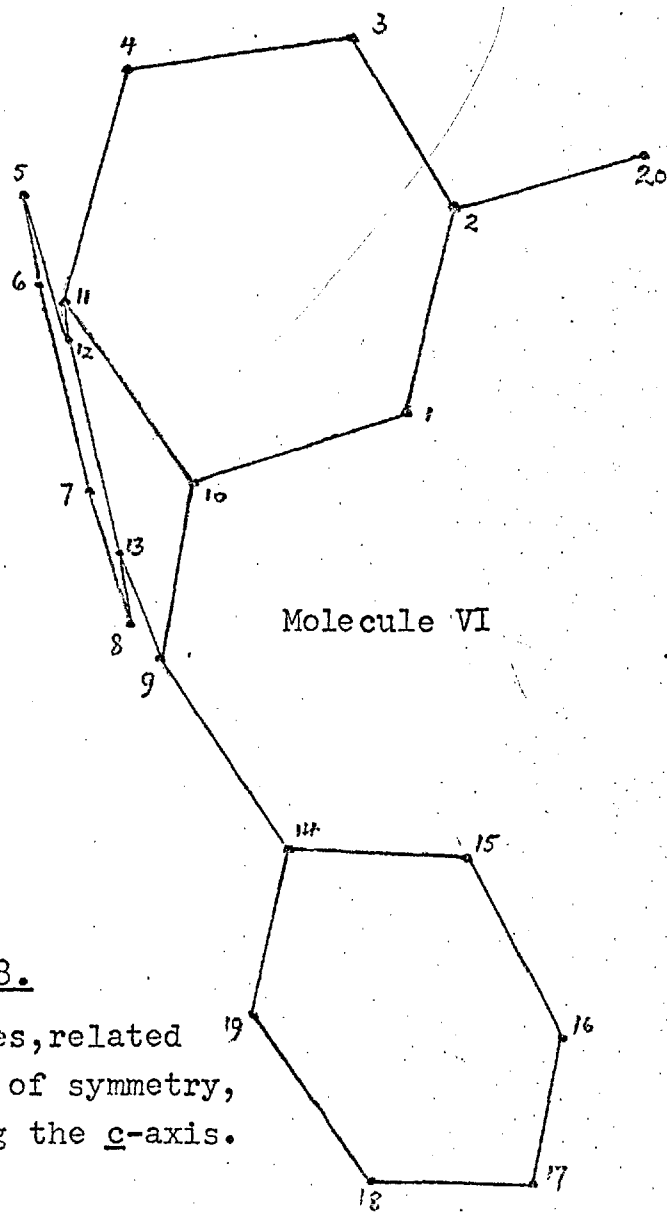


Figure 9.8.

Two molecules, related by a centre of symmetry, viewed along the  $c$ -axis.

symmetry. This is shown schematically in Figure 9.8, which shows the arrangement of any two centrosymmetrically related molecules as viewed along  $c$ . The planes of the two indene portions are parallel, and the closest C-C contacts are :

C(9) <sub>VI</sub> - C(5) <sub>I</sub>	3.773 Å	C(9) <sub>VI</sub> - C(8) <sub>I</sub>	3.821 Å
- C(6) <sub>I</sub>	3.854	- C(12) <sub>I</sub>	3.715
- C(7) <sub>I</sub>	3.874	- C(13) <sub>I</sub>	3.742

The three cis protons of molecule I, i.e. H(90, 100, 110)<sub>I</sub>, protrude into this gap opposite the fused benzene ring of molecule VI. The closest contact is then between H(110)<sub>I</sub> and H(80)<sub>VI</sub> at 2.62 Å, a distance only slightly greater than twice the van der Waals radius of hydrogen (2.4 Å). Since all contacts occur twice, i.e. C(5)<sub>I</sub>-C(9)<sub>VI</sub> = C(9)<sub>I</sub>-C(5)<sub>VI</sub>, the stability introduced by this interaction is high.

#### v) Conclusion.

It only remains to report that PIPH was found to be very active as an antagonist of tetrabenazine-induced sedation in rats<sup>(259)</sup>, but its high toxicity (common to all four compounds) precluded its use as a clinical anti-depressant. A suggestion that it be marketed as an exceptionally humane rodent exterminator (happy-rat?) was not well received.

APPENDIX I.

Reference Lists of Organic Structures whose Absolute  
Configurations have been determined by X-ray Methods.

Reprinted from Chemical Communications 1966, 838; 1968, 308.

## APPENDIX II

### The Uses of a Connectivity or Bonding Array in Molecular Geometry Calculations.

#### II.1 Introduction.

The calculation of the various geometrical characteristics of a molecule or crystal structure is lengthy, but mathematically trivial. Computer programs for this task require either the calculation of all possible interatomic distances less than a specified limit<sup>(260)</sup>, a process easy to use but wasteful of computer time (and requiring the user to sift a large volume of output), or the calculation of specified distances, a process wasteful of the user's time and prone to mistakes and omissions. The process to be described here is a compromise, ensuring an exhaustive search over one asymmetric unit (or indeed any portion of the total structure specified by the user). Needless calculations are avoided, and input and output are cut to a minimum.

The process was devised originally for the computation of dihedral angles, but is ideally suited for the quick and efficient checking of bond lengths and valence angles during structure refinement. It utilizes a connectivity or bonding array, an extension of an idea suggested by Mooers<sup>(261)</sup>, and developed by other workers<sup>(262)</sup> as an important topographical tool. In particular the array in its present form (see Sect. II.2 below) has been employed by Penny<sup>(263)</sup> in the recognition of certain ring systems in larger chemical units by a computer procedure. The work described below, however, represents the first use of such an array for a purely scientific purpose. Some ideas on the link-up of this work with the topographical studies are set out in Sect. II.6.

The basic theory developed is described in Sections II.2,3,4. The actual program, MOJO, lags a little behind the theory (since both are 'living' entities), and incorporates some adaptations; it will be described in Sect. II.5.

### II.2. The Connectivity or Bonding Array.

The fractional co-ordinates,  $x$ ,  $y$ ,  $z$ , and possibly their standard deviations,  $\sigma_x$ ,  $\sigma_y$ ,  $\sigma_z$ , for the  $N$  atoms in an asymmetric unit are input to the computer, together with an alphanumeric atom identifier (e.g. C24). They may then be referred to by this identifier, or, more simply, by their position ( $1 \rightarrow N$ ) in the input list. An  $N \times N$  square is

is then cleared to zero in computer store, and the connectivity or bonding information is read in. This requires  $N$  lines of input, one for each atom treated, each a string of digits of the form :

$$i \quad j_1 \quad j_2 \quad j_3 \quad j_4 \quad * \quad \dots\dots\dots \text{II.1}$$

indicating that the atom numbered  $i$  in the input list is bonded to those numbered  $j_1, j_2, j_3, j_4$ ; any convenient non-numeric character may be used to terminate each line.

To set up the array (B), the cells  $j_{1,2,3,4}$  on the  $i$ 'th row have unity added into them; the resultant array should be symmetric (i.e. elements  $b_{ij}$  should match  $b_{ji}$ ), and all cells should contain zero or unity only. Before proceeding these two requirements should be checked : a non-symmetric array indicates incorrect, or incomplete input of bonding information, while entries  $>1$  indicate unwanted duplicates (this is the reason for adding unity to the cells rather than just setting them to 1). Other checks may also be added if required, e.g. the number of entries per row or column for carbon atoms should be  $\leq 4$ . An array (B) made up of single-bit locations is compact, but it is then unsafe to add unity to denote each bond, since duplication would cause errors.

Figure II.1(a) shows the structure of humulene bromohydrin (Chapter 7); both the chemical numbering and atomic designations are given, together with their possible reference numbers in an input positions list. Input of bonding

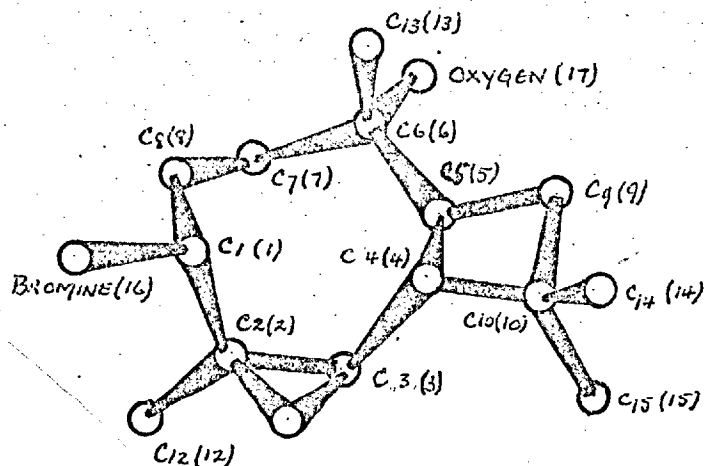


Figure II.1 (a) The structure of humulene bromohydrin, showing the chemical numbering, and the possible reference numbers of the atoms in an input positions list are given in brackets.

<u>i</u>	<u>j<sub>1</sub></u>	<u>j<sub>2</sub></u>	<u>j<sub>3</sub></u>	<u>j<sub>4</sub></u>	
1	2	8	16	*	
2	1	3	12	11	*
3	2	11	4	*	
4	3	5	10	*	
5	4	6	9	*	
6	5	7	13	17	*
7	6	8	*		
8	7	1	*		
9	5	10	*		
10	4	9	14	15	*
11	2	3	*		
12	2	*			
13	6	*			
14	10	*			
15	10	*			
16	1	*			
17	6	*			

Figure II.1(b). Input of bonding information: each atom (i) is bonded to atoms j<sub>1</sub>, j<sub>2</sub>, j<sub>3</sub>, etc.



		values of j, l.																
		1	2	3	4	5	6	7	8	9	10	11	12	13	14	15	16	17
C(1)	1		1						1									1
C(2)	2	1		1								1	1					
C(3)	3		1		1							1						
C(4)	4			1		1					1							
C(5)	5				1		1			1								
C(6)	6					1		1						1				1
C(7)	7						1		1									
C(8)	8	1						1										
C(9)	9					1					1							
C(10)	10				1					1					1	1		
C(11)	11		1	1														
C(12)	12		1															
C(13)	13						1											
C(14)	14										1							
C(15)	15										1							
Br	16	1																
O	17						1											

Figure II.1 (c). The bonding array (B) (heavily outlined) for humulene bromohydrin. Both reference numbers and atomic designations are given for clarity.

information is shown in Figure II.1(b), in the form of statements similar to Eq<sup>n</sup>. II.1 above. Part (c) of the Figure shows the resultant array (B), in which both types of atomic designation are given for clarity.

### II.3. The Systematic Calculation of Bond Lengths, Valence Angles, and Direction Cosines.

The position of the i'th atom is defined by the vector :

$$\vec{r}_i = x_i \vec{a} + y_i \vec{b} + z_i \vec{c} \dots\dots\dots \text{II.2,}$$

where  $\vec{a}$ ,  $\vec{b}$ ,  $\vec{c}$ , are the unit-cell vectors. The vector  $\vec{r}_{ij}$  between two atoms is simply the difference between two vectors,  $\vec{r}_i$ ,  $\vec{r}_j$ , of type II.2 :

$$\vec{r}_{ij} = \Delta x_{ij} \vec{a} + \Delta y_{ij} \vec{b} + \Delta z_{ij} \vec{c} \dots\dots\dots \text{II.3,}$$

where  $\Delta x_{ij}$  equals  $x_i - x_j$ , with similar expressions for  $y$  &  $z$ .

The square of the magnitude of the bond length  $|r_{ij}|$  is given by the scalar product of Eq. II.3 with itself :

$$\begin{aligned} |r_{ij}|^2 = \vec{r}_{ij} \cdot \vec{r}_{ij} &= x_{ij}^2 a^2 + y_{ij}^2 b^2 + z_{ij}^2 c^2 \\ &+ 2ab x_{ij} y_{ij} + 2bc y_{ij} z_{ij} \\ &+ 2ac x_{ij} z_{ij} \dots\dots\dots \text{II.4.} \end{aligned}$$

The direction cosines of the bond,  $l_{ij}$ ,  $m_{ij}$ ,  $n_{ij}$ , referred to axes  $a$ ,  $b$ ,  $c$ , are given by :

$$(l, m, n)_{ij} = \frac{(a\Delta x, b\Delta y, c\Delta z)_{ij}}{|r_{ij}|} \dots\dots\dots \text{II.5.}$$

An ordered and complete sequence of bond lengths and direction cosines can be obtained by working systematically through the bonding array, reading along each row (i) and using equations II.4, II.5, for each cell (j) containing unity. Only the upper right triangular half of the array need be scanned for this purpose: use of the whole array produces each bonded distance twice over. The bond lengths and direction cosines are output, and also stored in similar triangular arrays (R, L, M, N); it should be noted that the full arrays L, M, N, are anti-symmetric (i.e.  $m_{ij} = -m_{ji}$ ); due allowance must be made for this sign reversal when using these half arrays to read the direction cosines of bonds in the lower triangular half (i.e. for vector  $r_{ji}$ ).

Valence angles,  $\theta_{ijk}$ , are calculated from :

$$\cos\theta_{ijk} = \frac{\vec{r}_{ij} \cdot \vec{r}_{jk}}{|\vec{r}_{ij}| |\vec{r}_{jk}|} \dots\dots\dots \text{II.6.}$$

All angles occurring at atom (j) can be evaluated together by reading down column (j) to locate the first entry (i), and then reading on down the column to identify the possible values of (k).  $\cos\theta_{ijk}$  is computed and output for each indicated combination of ijk. The next (i) is selected by moving down the column, and is combined with all (k's) indicated lower down the same column, thus avoiding duplicates  $\theta_{jki}$ . The process is repeated until all permitted combinations (ik) are exhausted for atom (j), scanning is then

transferred to the next column,  $j + 1$ . In every case  $\cos\theta_{ijk}$  is stored, together with the integers  $i, j, k$ , for use in the calculation of dihedral angles.

#### II.4. The Systematic Calculation of Dihedral (Torsion) Angles.

An attempt will first be made to define and generalize the nomenclature for dihedral, or torsion, angles. Reference to Figure II.2(a) shows two groups of atoms, ABC bonded to D, and FGH bonded to E, which is below the plane of the paper. The Newman projection<sup>(213)</sup> down the bond  $D \rightarrow E$  is shown in Figure II.2(b).

The dihedral or torsion angle ( $\omega$ ) is the angle between, say, the projections of CD and EF on a plane perpendicular to the bond DE. Thus we may define the angle as :

$$\omega_{\underline{\underline{C}}(\underline{\underline{D}}, \underline{\underline{E}})\underline{\underline{F}}} = x^\circ \dots\dots\dots \text{II.7.}$$

Other more general dihedral angles, of use in certain contexts can be described analogously. Thus the angle between the projections of AD and CD on the plane perpendicular to DE may be written :

$$\omega_{\underline{\underline{A}}(\underline{\underline{D}}, \underline{\underline{E}})\underline{\underline{C}}} = x^\circ \dots\dots\dots \text{II.8.}$$

Similarly the angle between  $\text{proj}(GE)$ ,  $\text{proj}(EF)$ , as seen from viewing point D is :

$$\omega_{\underline{\underline{G}}(\underline{\underline{D}}, \underline{\underline{E}})\underline{\underline{F}}} = x^\circ \dots\dots\dots \text{II.9.}$$

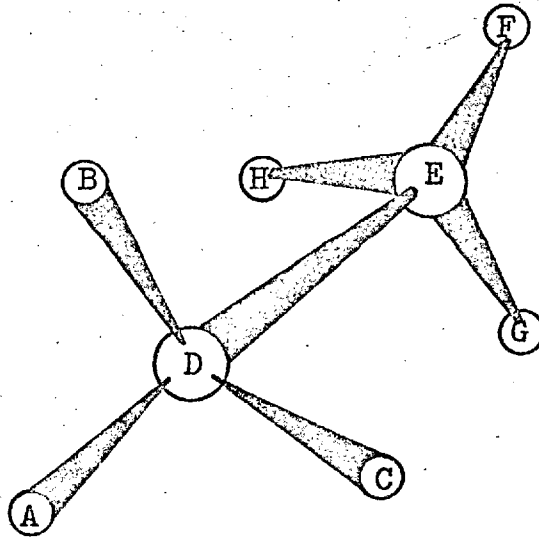


Figure II.2(a)

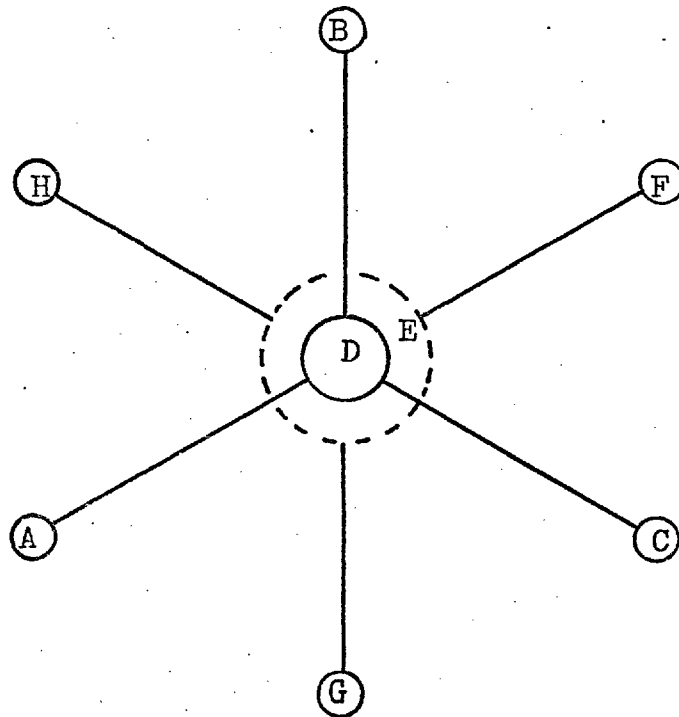


Figure II.2(b)

The atoms in brackets indicate the direction of view down the bond, i.e. from D to E; atoms which are doubly underlined in the above equations should be printed in Clarendon type, they represent atoms of the nearer group in the viewing direction. For ordinary dihedral angles, representing twist or torsion about the bond DE (Eq. II.7) the first quoted atom is a member of the nearer group, and the last of the farther group. For the more general dihedral angles they are both of the nearer group (Eq. II.8), or both of the farther group (Eq. II.9). Furthermore it is often imperative to distinguish between  $sp^3-sp^3$ ,  $sp^3-sp^2$ , and  $sp^2-sp^2$  torsion angles in an organic structure (see Sect. 8.5), where the hybridisation states referred to are those of atoms D and E respectively. This was effected in Section 8.5 by reserving the symbol ( $\omega$ ) for the first mentioned, and referring to the other two as ( $\delta$ ) and ( $\zeta$ ) respectively. General adoption of this type of nomenclature saves the reader from continually referring to the structural formula.

In all cases the sense of rotation is defined in terms of the movement required to rotate the first mentioned bond (CD in Eq. II.7, AD in 8, GE in 9) to overlie the projection of the second bond (EF, DC, EF, respectively). Clockwise rotation of the first-quoted bond is taken as positive, anti-clockwise rotation is taken as negative. Thus, with reference to Figure II.2(b), we may write :

$$\omega_{\underline{\underline{A}}(\underline{\underline{D}},\underline{\underline{E}})H} = +60^\circ \dots\dots\dots \text{II.7(a)}$$

$$\omega_{\underline{\underline{A}}(\underline{\underline{D}},\underline{\underline{E}})G} = -60^\circ \dots\dots\dots \text{II.7(b)}$$

$$\omega_{\underline{\underline{A}}(\underline{\underline{D}},\underline{\underline{E}})\underline{\underline{B}}} = +120^\circ \dots\dots\dots \text{II.8(a)}$$

$$\omega_{\underline{\underline{G}}(\underline{\underline{D}},\underline{\underline{E}})F} = -120^\circ \dots\dots\dots \text{II.9(a)}$$

Figure II.3(a) shows the relationship between the three bond vectors involved, i.e.  $\vec{r}_1$ ,  $\vec{r}_2$ ,  $\vec{r}_3$ , represent bonds CD, DE, EF, in Eq. II.7, or AD, DE, DC, in 8, or GE, DE, EF, in 9. Figure II.3(b) shows the vectors in relation to a spherical triangle<sup>(264, 265)</sup>, whence we may write :

$$\cos(\omega) = \frac{\cos(\widehat{r_1 r_3}) - \cos(\widehat{r_1 r_2})\cos(\widehat{r_2 r_3})}{\sin(\widehat{r_1 r_2})\sin(\widehat{r_2 r_3})} \dots \text{II.10,}$$

where :  $\widehat{r_1 r_2}$  and  $\widehat{r_2 r_3}$  are the valence angles :

$\theta_{CDE}$  and  $\theta_{DEF}$  in Eq. II.7,

$\theta_{ADE}$  and  $\theta_{CDE}$  in Eq. II.8,

and  $\theta_{GED}$  and  $\theta_{FED}$  in Eq. II.9.

and :  $\widehat{r_1 r_3}$  is the angle between  $r_1$ ,  $r_3$  in each case.

The angles  $\omega_{i(j,k)l}$  can be evaluated, and systematically output in a convenient order, using the bonding array as follows. For a given viewing bond DE, identified by unity in cell  $b_{jk}$ , look backward and forward along row ( $j$ ) to identify possible ( $i$ 's), and up and down column ( $k$ ) to identify possible ( $l$ 's). Equation II.10 is then evaluated for all combinations of :

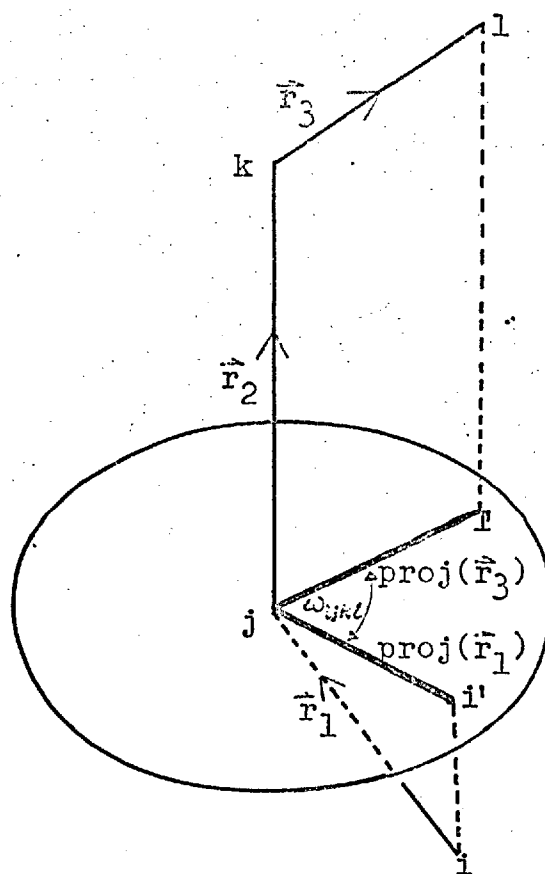


Figure II.3(a) Definition of the dihedral angle  $\omega_{ijkl}$  where  $(ijkl)$  are (for example) ADEF in Eq. II.7.

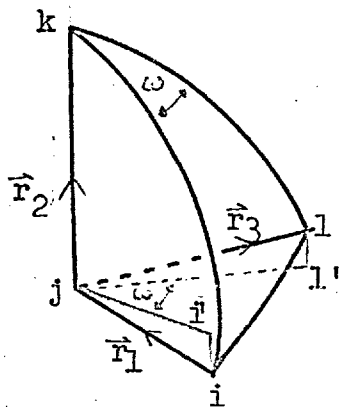


Figure II.3(b) The vectors in relation to a spherical triangle.

The angle  $\omega_{ijkl}$  (=angle  $\widehat{i' j l'}$ ) is the angle  $\widehat{ikl}$  of the triangle i.e. the angle between the planes  $ijk, ljk$ ; the 'sides' of the triangle are the valence angles  $(\widehat{r_1 r_2})$ ,  $(\widehat{r_2 r_3})$ , and the angle  $(\widehat{r_1 r_3})$ , whence Eq. II.10 can be

derived from the cosine formulae for spherical triangles.



- (i)  $i, l$  ( $i \neq l$ ) cf. Eq. II.7,
- (ii)  $i, i'$  ( $i \neq i'$ ) cf. Eq. II.8,
- (iii)  $l, l'$  ( $l \neq l'$ ) cf. Eq. II.9,

for any given combination of  $jk$ . This process is repeated systematically for all bonds ( $jk$ ) specified in the upper right triangular half of array (B), this avoids duplication since  $\omega_{ijkl}$  is equivalent to  $\omega_{lkji}$  in both magnitude and sign. The sines and cosines of  $\widehat{r_1 r_2}$ ,  $\widehat{r_2 r_3}$ , required by Eq. II.10, can be obtained from the previously stored valence angles.  $\text{Cos}(\widehat{r_1 r_3})$  can be obtained using :

$$\cos(\widehat{r_1 r_3}) = \cos(\widehat{r_{ij} r_{kl}}) = \frac{\vec{r}_{ij} \cdot \vec{r}_{kl}}{|\vec{r}_{ij}| |\vec{r}_{kl}|} \dots\dots\dots \text{II.11}$$

The sign of the rotation is given by the sign of the determinant  $V$  :

$$V = \begin{vmatrix} l_{ij} & m_{ij} & n_{ij} \\ l_{jk} & m_{jk} & n_{jk} \\ l_{kl} & m_{kl} & n_{kl} \end{vmatrix} \dots\dots\dots \text{II.12},$$

which gives the volume of the parallelepipedon defined by the vectors  $\vec{r}_1, \vec{r}_2, \vec{r}_3$ .

## II.5. The Program MOJO.

The theory developed above is given in its most general mathematical form. In the program MOJO, written in 1967 EXCHLF for the University of London ATLAS computer, several adaptations have been made. A brief description of these, and also the input and output, together with a flow chart, forms the subject matter of this section.

Although vector methods afford both mathematical simplicity and generality, the use of orthogonalized Ångstrom coordinates, while being just as general, reduces the geometrical manipulation to simple Cartesian terms. Furthermore they are useful in the preparation of crystal drawings. If we take a perfectly general triclinic lattice, with cell parameters  $\underline{a}$ ,  $\underline{b}$ ,  $\underline{c}$ ,  $\alpha$ ,  $\beta$ ,  $\gamma$ , then we may define three orthogonal unit vectors I, J, K, such that :

I is parallel to  $\underline{a}$ ,

J is perpendicular to the  $\underline{a}$ - $\underline{c}$  plane,

K is perpendicular to  $\underline{a}$  in the  $\underline{a}$ - $\underline{c}$  plane,

whence, by using spherical triangles<sup>(264,265)</sup>, we may express the lengths of the orthogonal axes as :

$$A = \underline{a}I$$

$$B = \underline{b}\cos\gamma I + \underline{b}\sin\gamma J \quad \dots\dots\dots \text{II.13}$$

$$C = \underline{c}\cos\beta I - \underline{c}\sin\beta\cos\alpha J + \underline{c}\sin\beta\sin\alpha K$$

or, in matrix notation :

$$(A) = (\beta)(I) \dots\dots\dots \text{II.14,}$$

where the orthogonalization matrix ( $\beta$ ) obviously has the form:

$$(\beta) = \begin{pmatrix} \underline{a} & 0 & 0 \\ \underline{b}\cos\gamma & \underline{b}\sin\gamma & 0 \\ \underline{c}\cos\beta & -\underline{c}\sin\beta\cos\alpha^* & \underline{c}\sin\beta\sin\alpha^* \end{pmatrix} \dots\dots\dots \text{II.15}$$

The determinant of this matrix gives the cell volume (V).

The matrix is quite general, and its complexity is obviously reduced for systems of higher symmetry than triclinic.

If the fractional co-ordinates of the atoms in the real cell ( $\underline{x}$ ,  $\underline{y}$ ,  $\underline{z}$ ) are provided, then the orthogonal Angstrom co-ordinates ( $\underline{X}$ ,  $\underline{Y}$ ,  $\underline{Z}$ ) are given by an expression similar to Eq. II.14, viz :

$$(\underline{X}) = (\beta)(\underline{x}) \dots\dots\dots \text{II.16}$$

We may now rewrite Eqs. II.4,5,6, in terms of  $\underline{X}$ ,  $\underline{Y}$ ,  $\underline{Z}$ , as follows<sup>(266)</sup>:

$$R_{ij}^2 = \Delta X_{ij}^2 + \Delta Y_{ij}^2 + \Delta Z_{ij}^2 \dots\dots\dots \text{II.17}$$

$$(L, M, N)_{ij} = \frac{(\Delta X, \Delta Y, \Delta Z)_{ij}}{|R_{ij}|} \dots\dots\dots \text{II.18}$$

$$\cos\theta_{ijk} = L_{ij}L_{jk} + M_{ij}M_{jk} + N_{ij}N_{jk} \dots\dots\dots \text{II.19}$$

Thus, as can be seen from Figure II.4, the initial operation in MOJO is to read in the cell data, set up the ( $\beta$ )-matrix, and compute (and output) the orthogonal co-ordinates from the input positions list. The bonding information is read in (see Fig. II.1(b)) and the array (B) set up and checked.

The present program does not, at present, incorporate standard deviation formulae; nor does it obtain the valence angles and dihedral angles from the array (B) in quite the same manner as described above. Referring again to Figure II.1(c), the former are obtained by reading across the rows (i) and finding possible values for (j), as in the bond-length calculation; values of (k) are then found by reading down column (j) to avoid duplication. The dihedral angles are found by an extension of this method: once the value of (j) has been found the (k) values are obtained by scanning column (j) completely, but omitting the value  $k = j$ ; the k'th row is then similarly scanned for values of (l), but omitting  $l = k$ . This early method has two drawbacks:

- i) All dihedral angles are produced twice over, i.e. both  $\omega_{ijkl}$  and  $\omega_{lkji}$  are obtained;
- ii) The more general dihedral angles, exemplified by Eqs. II.8, II.9, are not obtained.

It is hoped to incorporate the newer theory described in Sections II.3, II.4, in the near future.

Other routines have also been included in the program, using the initial orthogonalized co-ordinate list:

- i) Cyclobutane ring analysis: the positions of the four ring atoms in the input positions list are specified ( $N_{1-4}$ ). The routine then evaluates criteria (c) and (d) of Figure 7.5 (p. 165).

- ii) Specified (single) bond lengths, valence angles, or

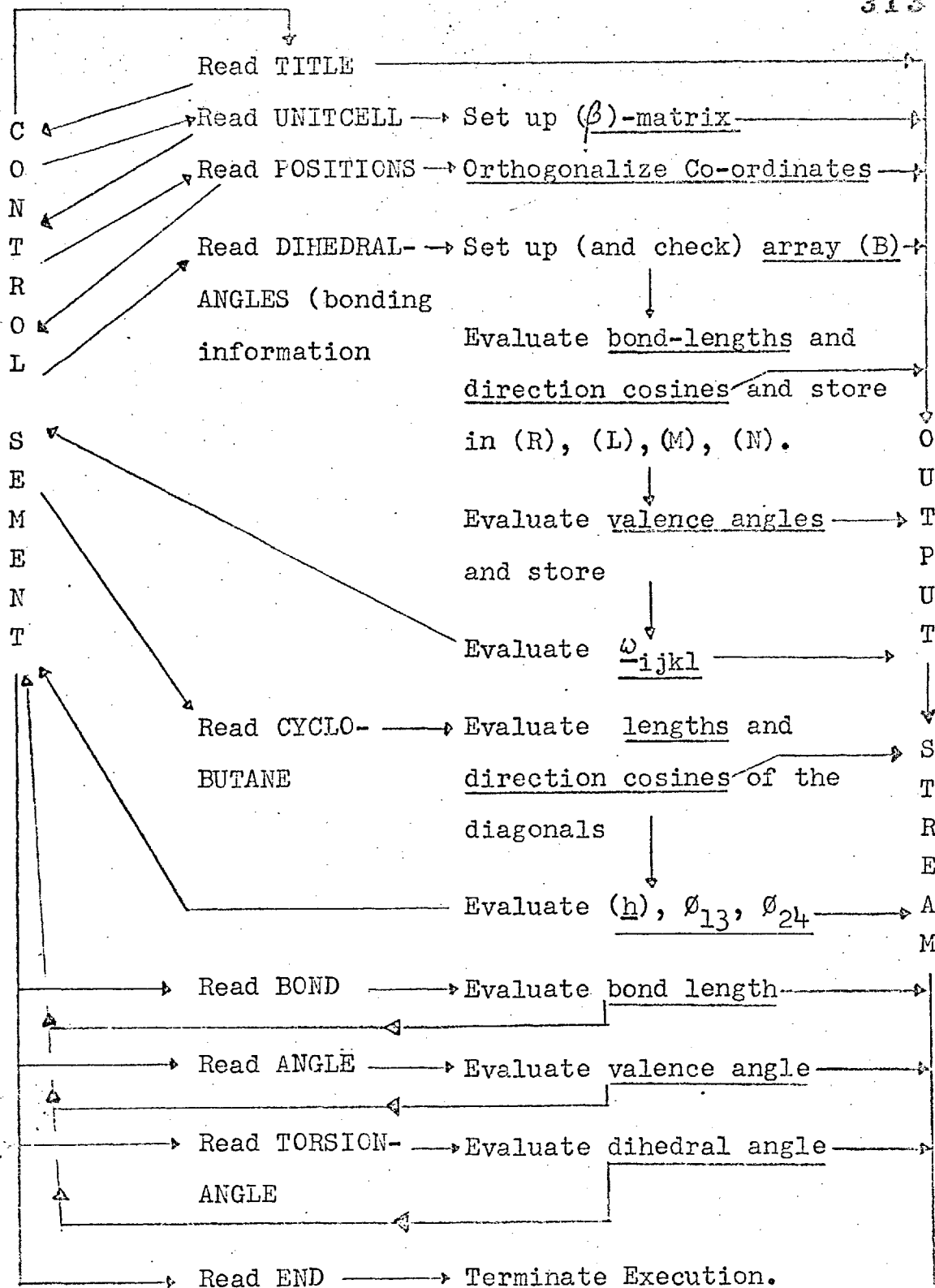


Figure II.4. Flow chart of the program MOJO.

dihedral angles, may be computed by specifying two, three, or four values of N.

All the data required in a particular run are input under one word directives (as in all ATSYS programs); those used here are :

TITLE : followed by one line of information to be output;

UNITCELL : followed by  $a$ ,  $b$ ,  $c$ ,  $\alpha$ ,  $\beta$ ,  $\gamma$ ;

POSITIONS : followed by N lines of information of the form:

CA23     $x$      $y$      $z$

where N is the total number of atoms input, the list is terminated with an asterisk.

DIHEDRALANGLES : followed by a number (n) (which must be  $\leq N$ ) and (n) lines of information similar to Figure II.1(b). This directive turns on the bonding array calculations.

CYCLOBUTANE : followed by four numbers as described above. Specific functions are requested under the self-explanatory directives : BOND, ANGLE, TORSIONANGLE. A flow chart is given as Figure II.4.

## II.6. Further uses of Bonding Array Theory.

The use of the above program, incorporated as a routine in both least-squares and general molecular geometry programs, has possibilities. In the former it would provide a quick and systematic check on the chemical sensibility of the structure being refined, and could be called in automatically at the end of each run. In the latter it would provide an

ordered output listing, for one asymmetric unit, of bond-length and valence angles; a similar ordered list of intramolecular non-bonded distances can be obtained by reading across rows (i) and avoiding all cells (j) which contain unity, again only the upper right triangular half of (B) need be used.

On a more philosophical plane, the bonding array would appear to have important uses in the field of information storage and retrieval, as applied to crystallographic structural data. At present the information listed under any one compound is limited to the name(s) of author(s) and the literature reference. Inclusion of a list of orthogonalized co-ordinates, and the bonding information, would permit a search program, incorporating the bonding array routine, to provide a complete listing of the basic molecular geometry, in addition to the literature reference, for a specified compound. Far more extensive information could be output by the search program if the bonding array was used to recognize particular ring systems within a larger chemical unit. Thus if a naphthalene nucleus or a cyclobutane ring were found they could be checked for planarity; for larger saturated carbocycles it should be possible to actually define the conformation adopted from the geometry obtained.

This is, however, not the correct place to expand these ideas further. Nevertheless, with the present explosion in

the quantity of structural information appearing in the literature, largely due to the ever increasing use of automatic diffractometers, a satisfactory means of storage and retrieval is of importance to the crystallographer. It is the author's opinion that a computer procedure very similar to the bonding array will provide the ultimate answer, for organic molecules at any rate. The time when one may tell a computer to provide structural data and references for, say, all eight membered carbocycles having the boat-chair conformation, may not be far off. The task of the would-be reference-hunter and/or Thesis-writer will then be considerably less burdensome!



APPENDIX III.Minimum-Energy Calculations.

Since the work of Pitzer et. al. (267) on ethane, many workers have attempted to predict preferred conformations on the basis of detailed energy calculations. While this is not the place for a full review of the various methods employed, and the results obtained, it is pertinent to give a brief description of the approach for small- and medium-ring saturated carbocycles, since numerous comparisons have been made in this Thesis between parameters obtained crystallographically, and those obtained from minimum-energy calculations. In general the results obtained by various groups of workers are very similar; however since the work of Hendrickson (158,159,247) was chosen for comparison with the X-ray data, mainly due to the completeness of his studies, ranging from simple alkanes to cyclodecanes, his papers have largely been used in the compilation of this Appendix.

A particular n-membered ring conformation may be defined by the (n) values of the C-C-C valence angles ( $\theta$ ), and the (n)  $sp^3-sp^3$  torsion angles ( $\omega$ ). The assumption is made that bond lengths remain invariant, since the energy required to distort a bond from its optimum length is very much more severe than the strain energies mentioned below. A reduction in the number of parameters is effected by the assumption of only symmetrical forms (except in the case of the cyclopentanes<sup>(247)</sup>); this is reasonable since the calculations of Wiberg<sup>(171)</sup>, which proceed through unsymmetrical forms, result in symmetrical minima only. The strain-energy content of a particular conformation may be subdivided into :

i) Bond angle bending strain ( $\underline{E}_\theta$ ) which is the energy associated with the distortion of a single bond-angle from the optimum. The function used, derived from spectroscopic results, gives :

$$\underline{E}_\theta = K_\theta (\theta - \theta_0)^2 \dots\dots\dots \text{III.1}$$

where, initially<sup>(247)</sup>, the value of  $\theta_0$  was taken as the tetrahedral value ( $109.28^\circ$ ). More recent hybridisation studies have shown that  $\theta_0$  at a methylene carbon is more nearly  $112^\circ$ , and this value was used in later work<sup>(159)</sup>. the value of  $K_\theta$  used with the new value of  $\theta_0$  was  $0.0230 \text{ kcal mole}^{-1}$ .

ii) Torsional Strain ( $E_{\omega}$ ), the function used to calculate the strain-energy, due to twist of substituents about a single bond, has the form :

$$E_{\omega} = \frac{1}{2}K_{\omega}(1 + \cos 3\omega) \dots\dots\dots \text{III.2}$$

in which  $K_{\omega}$  is the height of the potential barrier to rotation in ethylene (i.e. the energy difference between staggered and eclipsed conformations). Hendrickson<sup>(159)</sup> has pointed out that, since non-bonded interactions make up a small, but real, portion of this barrier,  $K_{\omega}$  should be *less* than the quoted value of 2.8 kcal mole<sup>-1</sup>, and he has derived a value of 2.65 kcal mole<sup>-1</sup> to exclude the van der Waals forces. Although the general form of the above expression is not well founded theoretically, considerable success has attended its use (see the work of Garbisch<sup>(216)</sup>, who used a similar expression to estimate  $sp^3$ - $sp^2$  torsional strain).

iii) Energy due to non-bonded interactions. Any pair of non-bonded atoms, at inter-nuclear distance ( $r$ ), possesses a mutual interaction, which is partially repulsive and partially attractive. The form of the expression for  $E_{NB}$  is one of the most problematical in this work, it has the general form :

$$E_{NB} = Be^{-\mu r} - A/r^6 \dots\dots\dots \text{III.3}$$

and while values of the attractive constant ( $A$ ) are known the constants  $B$  and  $\mu$  are difficult to evaluate experimentally

Hendrickson has chosen to make them parameters in the minimization procedure (see below) for both H-H and C-C interactions, the geometric mean of the values obtained was used to estimate the C-H interactions.

The energy minimization is carried out by computer : from a given starting conformation each independent angular parameter, plus  $B$  and  $\mu$ , is varied by  $1^\circ$  in turn, and values of  $\underline{E}_O$ ,  $\underline{E}_\omega$ , and  $\underline{E}_{NB}$  (taken over all atoms in the ring), are computed to give the total strain energy  $\underline{E}_T$ . A checking routine is included to ensure that the angles used in each calculation give a closed ring, since this was not the case with some of the cyclopentanes<sup>(247)</sup>.

The comparisons carried out by Hendrickson, using data from X-ray and electron-diffraction work, and from other sources, show that, despite the problematical nature of some of the functions used, the geometrical parameters obtained are in good agreement with experimentally determined values.

References.

1. R. Hooke, *Micrographia : or some Physiological Descriptions of Minute Bodies made by Magnifying Glasses. With Observations and Inquiries thereupon.* London, 1667. ( Alembic Club Reprint No. 5 ).
2. C. Huygens, *Traité de la lumière.* Leiden, 1690.
3. R. J. Haüy, *Traité de Minéralogie.* Paris, 1801.  
R. J. Haüy, *Essai d'une théorie sur la structure des cristaux appliquée a plusieurs genres des substances cristallisées.* Paris, 1874.
4. N. Steno, *De Solido intra Solidum Naturaliter Contento Dissertationis Prodromus.* Florence, 1669.
5. W. H. Miller, *A Treatise on Crystallography.*  
Cambridge, 1839.
6. M. A. Bravais, *Memoire sur les systèmes formés par des points distribués régulièrement sur un plan ou dans l'espace.* J. école polytech., (Paris), Cahier 33,  
Tome XIX (1850).
7. E. S. Fedorov, *An attempt to express by means of an abbreviated sign the symbols of all equal directions of a given sub-division of a symmetry system.*  
*Trans Imperial St. Petersburg Min. Soc., 1887, 23, 99.*
8. W. Barlow, *Nature, 1883, 29, 186 & 205.*
9. A. Schoenflies, *Krystallsysteme und Krystallstruktur.*  
Teubner, Leipzig, 1891.

10. A. Sommerfeld, Z. Physik., 1900, 2, 55.
11. W. Friedrich, P. Knipping, and M. von Laue,  
Proc. Bavarian Acad. Sci., 1913, 303.
12. M. von Laue, Ibid., 363.
13. W. L. Bragg, Proc. Camb. Phil. Soc., 1913, 17, 43.
14. P. Niggli, Geometrische Kristallographie des  
Diskontinuums. Gebrüder Borntraeger, Leipzig, 1919.
15. I. Waller, Ann. Physik., 1927, 83, 153.
16. P. P. Ewald, Z. Physik., 1913, 14, 465 & 1038.  
P. P. Ewald, Zeit. f. Krist., 1921, 56, 129.  
Willard Gibbs, Vector Analysis, (ca. 1884) reprinted  
in his collected works, 1928.
17. S. C. Nyburg, X-Ray Analysis of Organic Structures.  
Academic Press, New York & London, 1961. Section  
3.9. and references therein.
18. M. Renninger, Z. Physik., 1937, 106, 141.
19. International Tables for X-Ray Crystallography,  
3 volumes, The Kynoch Press, Birmingham, 1952, 1959, 1962.
20. H. T. Evans Jr., and M. G. Ekstein, Acta. Cryst.,  
1952, 5, 540.
21. A. Claasen, Phil. Mag., 1930, 2, 57.
22. D. Rogers and R. H. Moffett, Acta. Cryst., 1956,  
2, 1037.
23. G. Albrecht, Rev. Sci. Instrum., 1939, 10, 221.
24. C. G. Darwin, Phil. Mag., 1922, 43, 800.

25. W. L. Bragg, Proc. Roy. Soc., 1929, A123, 537.
26. A. L. Patterson, Phys. Rev., 1934, 46, 372.  
Z. Krist., 1935, 90, 517.
27. D. Harker, J. Chem. Phys., 1936, 4, 381.
28. J. M. Robertson and I. Woodward, J. Chem. Soc.,  
1940, 36; See also : J. M. Robertson, Ibid.,  
1935, 615; 1936, 1195; J. M. Robertson and  
I. Woodward, Ibid., 1937, 219.
29. H. Lipson and W. Cochran, The Crystalline State :  
Vol. III, The Determination of Crystal Structures.  
Bell, London, 1957, p.207.
30. M. M. Woolfson, Acta. Cryst., 1956, 2, 804.
31. G. A. Sim, Acta. Cryst., 1959, 12, 813; Ibid.,  
1960, 13, 511.
32. C. Bokhoven, J. C. Schoone, and J. M. Bijvoet,  
Proc. K. Ned. Acad. Wetenschap., 1949, 52, 120;  
Acta. Cryst., 1951, 4, 275.
33. D. W. Green, V. M. Ingram, and M. F. Perutz,  
Proc. Roy. Soc., 1954, A225, 287.
34. C. E. Nordmann and Nakatsu, J. Amer. Chem. Soc.,  
1963, 85, 353; C. E. Nordmann, Transactions of the  
American Crystallographic Association, 1966, 2, 29.
35. W. Hoppe, Acta. Cryst., 1957, 10, 750.
36. M. J. Buerger, Vector Space and its Application in  
Crystal Structure Investigation. Wiley, New York, 1959.

37. A.D. Mighell, and R.A. Jacobsen, Acta. Cryst., 1963, 16, 443.
38. H. Lipson and C. A. Taylor, Fourier Transforms in X-Ray Analysis. Bell, London, 1958.
39. H. Lipson and C. A. Taylor, Optical Transforms. Bell, London, 1961.
40. D. Harker and J. S. Kasper, Acta. Cryst., 1948, 1, 70.
41. J. Karle and H. Hauptmann, Acta. Cryst., 1950, 3, 181.
42. D. Sayre, Acta. Cryst., 1952, 5, 60.
43. W. Cochran, Acta. Cryst., 1952, 5, 65.
44. W. H. Zachariasen, Acta. Cryst., 1952, 5, 68.
45. D. F. Grant, R. G. Howells and D. Rogers, Acta. Cryst., 1957, 10, 489.
46. M.M. Woolfson, Acta. Cryst., 1957, 10, 116.
47. H. Hauptmann and J. Karle, Solution of the Phase Problem, I. The Centrosymmetric Crystal. A. C. A. Monograph No. 3. Wilmington: The Letter Shop.
48. I. L. Karle and J. Karle, Acta. Cryst., 1964, 17, 835. Ibid., 1966, 21, 860.
49. I. L. Karle and J. Karle, Acta. Cryst., 1966, 21, 849.
50. A. M. Legendre, Nouvelles méthodes pour la détermination des orbites des comètes. Courcier, Paris, 1806, p. 72.
51. E. W. Hughes, J. Amer. Chem. Soc., 1941, 63, 1737.



52. L. Sohncke, Entwicklung einer Theorie der Kristallstruktur. Leipzig, 1879.
53. G. Friedel, Comptes Rendus, 1913, 157, 1533.
54. M. von Laue, Ann. Phys. Leipzig, 1916, 50, 433.
55. H. Hönl, Zeit. Phys., 1933, 84, 1.
56. D. Coster, K. S. Knol, and J. A. Frins, Zeit. Phys., 1930, 63, 345.
57. J. M. Bijvoet, Proc. K. Ned. Acad. Wetenschap, 1949, 52, 313.
58. S. W. Peterson, Nature, 1955, 176, 395.
59. C. H. Dauben and D. H. Templeton, Acta. Cryst., 1955, 8, 841.
60. A. F. Peerdemann and J. M. Bijvoet, Acta. Cryst., 1956, 9, 1012.
61. A. F. Peerdemann, A. J. Van Bommel, and J. M. Bijvoet, Proc. K. Ned. Acad. Wetenschap, 1951, 54, 16.
62. J. M. Bijvoet, Endeavour, 1955, XIV, 71.
63. see : Y. Okaya and R. Pepinsky, in Computing Methods and the Phase Problem, eds. J. M. Robertson, R. Pepinsky and J. C. Speakman. Pergamon Press, Oxford, 1961. p. 273 et. seq.
64. G. N. Ramachandran and S. Raman, Current Sci. (India), 1956, 25, 348. See also : Advanced Methods of Crystallography, ed. G. N. Ramachandran, Academic Press London, New York, 1964. Chapters 2 & 3 ( pp. 25 & 67 )

65. J. A. Ibers and W. C. Hamilton, *Acta. Cryst.*, 1964, 17, 781.
66. W. C. Hamilton, *Acta. Cryst.*, 1965, 18, 502.
67. R. Parasarathy and R. E. Davis, *Acta. Cryst.*, 1967, 23, 1049.
68. S. C. Abrahams, P. B. Jamieson, and J. L. Bernstein, *J. Chem. Phys.*, 1967, 47, 4034.
69. R. Pepinsky, *Record Chem. Progress*, 1956, 17, 145.
70. A. McL. Mathieson, *Acta. Cryst.*, 1956, 2, 317.
71. R. Hine and D. Rogers, *Chem. and Ind.*, 1956, 1428.  
see also : R. Hine, *Acta. Cryst.*, 1962, 15, 635.
72. F. H. Allen and D. Rogers, *Chem. Comm.*, 1966, 838.
73. F. H. Allen, S. Neidle, and D. Rogers, *Chem. Comm.*, 1968, 308.
74. A. de Vries, *Nature*, 1958, 181, 1193.
75. J. M. Robertson, *J. Sci. Instr.*, 1943, 20, 175.
76. M. G. B. Drew, Ph. D. Thesis, University of London, 1966.
77. A. D. Booth, *Fourier Techniques in Organic Structure Analysis*, Cambridge University Press, 1948.
78. D. W. J. Cruickshank in reference 63, p. 32 et. seq.
79. J. S. Rollett, in *Computing Methods in Crystallography*, Pergamon Press, Oxford, 1964. p. 42.
80. W. R. Busing, K. O. Martin, and H. A. Levy, Oak Ridge National Laboratory Report ORNL-TM-229, 1961.

81. D. W. J. Cruickshank in ref 19.
82. F. R. Ahmed and D. W. J. Cruickshank, *Acta. Cryst.*, 1953, 6, 385.
83. S. F. Darlow, *Acta. Cryst.*, 1960, 13, 683.
84. J. S. Rollett, ref 79, chapter 6.
85. V. Schomaker, J. Waser, R. E. Marsh, and G. Bergman, *Acta. Cryst.*, 1959, 12, 600.
86. A. J. C. Wilson, *Nature*, 1942, 150, 152.
87. D. Rogers, ref 79, chapter 16.
88. J. S. Rollett, W. C. Hamilton, and R. A. Sparkes, *Acta. Cryst.*, 1965, 18, 129.
89. O. Wallach, *Annalen*, 1887, 238, 78; 239, 49.
90. For an interesting review see : 'The History of the Isoprene Rule', L. Ruzicka, *Proc. Chem. Soc.*, 1959, 341.
91. J. W. Cornforth, *Chem. in Britain*, 1968, 4, 102.  
see also : D. H. R. Barton and P. de Mayo, ref 132,  
for a modern definition of 'terpene'.
92. L. Ruzicka, A. Eschenmosser, and H. Heusser, *Experientia*, 1953, 9, 357.  
L. Ruzicka, A. Eschenmosser, O. Jeger, and D. Arrigoni,  
*Helv. Chim. Acta.*, 1955, 38, 1890.
93. D. E. Wolf, C. H. Hoffman, P. E. Aldrich, H.R. Skeggs,  
L. D. Wright, and K. Folkers, *J. Amer. Chem. Soc.*,  
1956, 78, 4499; 1957, 79, 1486.  
K. Folkers et. al., in the CIBA Foundation

- Symposium : Biosynthesis of Terpenes and Sterols,  
Ed. G. Wolstenholme and M O'Connor, Churchill,  
London, 1959.
94. G. Popjak and J. W. Cornforth, in Advances in  
Entomology, Ed. G. Nord, Interscience, New York,  
1960, 22, 281.
- J. D. Brodie, G. Wasson and J. W. Porter,  
J. Biol. Chem., 1963, 238, 1294.
95. S. Chaykin, J. Law, A. H. Phillips, T. T. Tchen,  
and K. Bloch, Proc. Nat. Acad. Sci., (U.S.A.)  
1958, 44, 998.
96. F. Lynen, H. Eggerer, U. Henning, I. Kessel ,  
Angew. Chem., 1958, 70, 738.
97. F. Lynen, B. W. Agranoff, H. Eggerer, U. Henning,  
and E. M. Moslein, Angew. Chem., 1959, 71, 657.
98. B. W. Agranoff, H. Eggerer, U. Henning and F. Lynen,  
J. Amer. Chem. Soc., 1959, 81, 1254.
99. Idem., J. Biol. Chem., 1960, 235, 326.
100. R. B. Clayton, Quart. Rev., 1965, 19, 168 & 201.
101. J. B. Hendrickson, Tetrahedron, 1959, 7, 82.
102. W. Parker, J. S. Roberts, and R. Ramage,  
Quart. Rev., 1967, 21, 331.
103. Sir John Simonsen and L. N. Owen, The Terpenes,  
Vol. II, University Press, Cambridge, 1949. P.373  
et. seq.

104. J. B. Dumas, Ann. Chim., 1833, (ii), 48, 430;  
Annalen, 1833, 6, 245.
105. J. Brecht, Ber. 1893, 26, 3047.
106. G. Komppa, Ber. 1903, 36, 4332; Annalen, 1909,  
370, 225.
107. W. H. Perkin and J. F. Thorpe, J. Chem. Soc.,  
1904, 85, 146; 1906, 89, 799.
107. I. L. Finar, Organic Chemistry Vol. II : Stereo-  
Chemistry and the Chemistry of Natural Products,  
Longmans, London, 1964.
108. W. Hüchel, J. prakt. Chem., 1941, 157, 225.
109. A. J. Birch, Ann. Rep. Prog. Chem., 1950, 47, p.192.
- 110a. A. Fredga and J. K. Miettinen, Acta. Chim. Scand.,  
1947, 1, 371.
- 110b. J. Porath, Arkiv. Kemi., 1949-1950, 1, 385 & 525.
111. A. Fredga, Tetrahedron, 1960, 8, 126.
112. E. L. Eliel, Stereochemistry of Carbon Compounds,  
McGraw Hill, New York 1962, p. 106.
113. O. Wallach, Annalen, 1909, 369, 63.
114. A. Fredga, Arkiv. Kemi. Min. Geol., 1942, 15B, No.23.
115. Correlation with the absolute configuration of  
Ergoflavin : A. T. McPhail, G. A. Sim, J.D.M.Asher,  
J. M. Robertson and J. V. Silverton,  
J. Chem. Soc. (B), 1966, 18.

116. E. J. Eisenbraun, F. Burian, J. Osiecki, and C. Djerassi, *J. Amer. Chem. Soc.*, 1960, 82, 3476.  
C. Djerassi, J. Osiecki, and E. J. Eisenbraun, *Ibid.*, 1961, 83, 4433.
117. M. R. Cox, H. P. Koch, W. B. Whalley, M. B. Hursthouse, and D. Rogers, *Chem. Comm.* 1967, 212.
118. R. B. Woodward, Sir Robert Robinson Memorial Lecture : 'Recent Advances in Natural Product Chemistry'; Chemical Society Anniversary Meeting, Birmingham, 1964.
119. K. Freudenberg and W. Lwowski, (experimental appendix by H. Hohmann), *Annalen*, 1955, 594, 76.
120. A. C. Chapman, *J. Chem. Soc.*, 1895, 54, 780.
121. G. R. Clemo and J. O. Harris, *J. Chem. Soc.*, 1951, 22; 1952, 665.
122. F. Sorm, M. Streibl, V. Jarolim, L. Novotny, L. Dolejs, and V. Herout, *Coll. Czech. Chem. Comm.*, 1954, 19, 570.
123. E. Deussen, *J. prakt. Chem.*, 1911, 83, 483.
124. D. H. R. Barton and A. Nickon, *J. Chem. Soc.*, 1954, 4665.
125. J. M. Robertson and G. Todd, *J. Chem. Soc.*, 1955, 1254.
126. P. Clark and G. R. Ramage, *J. Chem. Soc.*, 1954, 4345.

127. M. D. Sutherland and O. J. Waters, Austral. J. Chem., 1961, 14, 596.
128. A. T. McPhail and G. A. Sim, Chem. and Ind., 1964, 976. Idem., J. Chem. Soc. (B), 1966, 112.
129. J. A. Hartsuck and I. C. Paul, Chem. and Ind., 1964, 977.
130. J. M. Greenwood, J. K. Sutherland and A. Torre, Chem. Comm., 1965, 410.
131. F. H. Allen and D. Rogers, Chem. Comm., 1966, 582; Idem., J. Chem. Soc., Submitted for publication.
132. D. H. R. Barton and P. de Mayo, Quart. Rev., 1957, 11, 189.
133. E. D. Brown, M. D. Solomon, J. K. Sutherland, and A. Torre, Chem. Comm., 1967, 112.
134. F. H. Allen and D. Rogers, Chem. Comm., 1967, 588.
135. E. D. Brown and J. K. Sutherland, Private Communication.
136. F. H. Allen, E. D. Brown, D. Rogers, and J. K. Sutherland, Chem. Comm., 1967, 1116.
137. D. A. Brueckner, T. A. Hamor, J. M. Robertson, and G. A. Sim, J. Chem. Soc., 1962, 799.
138. W. von Auwers, Ber. 1899, 22, 605.
139. J. Forster, J. Chem. Soc., 1899, 58, 1141.  
P. Ginnings and W. Noyes, J. Amer. Chem. Soc., 1922, 44, 2567.

140. M. Keller, Chem. Z., 1880, 4, 156.
141. F. S. Kipping and W. J. Pope, J. Chem. Soc., 1893, 63, 576.
142. E. H. Wiebenga and C. J. Krom., Rec. Trav. Chim., 1946, 65, 663.
143. Ref 19, Vol I.
144. J. E. Baldwin, private communication.
145. Similar assumptions that the atomic positions in isomorphous compounds correspond very closely have been made by (inter alia) : A. Cox and T. Jeffrey, Nature, 1939, 143, 894;  
J. M. Bijvoet and E. H. Wiebenga, Naturwiss., 1944, 32, 45.
146. E. C. Lingafelter and J. Donohue, Acta. Cryst., 1966, 20, 321.
147. F. H. Allen and D. Rogers, Chem. Comm., 1966, 837.
148. T. Norin, Acta. Chem. Scand., 1962, 17, 640.
149. M. G. Northolt and J. H. Palm, Rec. Trav. Chim., 1966, 85, 143.
150. J. A. Wunderlich, Acta. Cryst., 1967, 23, 846.
151. P. P. Williams, Chem. and Ind., 1964, 1583.
152. G. Ferguson, C. J. Fritchie, J. M. Robertson, and G. A. Sim, J. Chem. Soc., 1961, 1976.



153. L.E. Sutton (Ed.) : Tables of Interatomic Distances and Configuration in Molecules and Ions. The Chemical Society Special Publication No. 18, (First Supplement), London 1965.
154. G. A. Sim, J. Chem. Soc., 1965, 5974.
155. A. C. MacDonald and J. Trotter, Acta. Cryst., 1965, 19, 456.
156. A. C. MacDonald and J. Trotter, Acta. Cryst., 1965, 18, 243.
157. S. Abrahamsson and B. Nilsson, J. Org. Chem., 1966, 31, 3631.
158. J. B. Hendrickson, J. Amer. Chem. Soc., 1964, 86, 4854.
159. J. B. Hendrickson, J. Amer. Chem. Soc., 1967, 89, 7036.
160. C. W. Bunn, Chemical Crystallography, Oxford University Press, Oxford, 1961; p. 256.
161. A. D. Booth, Fourier Techniques in Organic Structure Analysis, Cambridge University Press, 1948.
162. J. D. Roberts and R. H. Mazur, J. Amer. Chem. Soc., 1951, 73, 2509.
163. M. D. Solomon, Ph. D. Thesis Univ. London, 1967.
164. S. Dev, J. E. Anderson, V. Cornier, N. P. Damodaran, and J. D. Roberts, J. Amer. Chem. Soc., 1968, 90, 1246.
165. R. B. Jackson and W. E. Streib, J. Amer. Chem. Soc., 1967, 89, 2539.

166. W. R. Roth, P. Goebel, R. L. Sass, R. B. Turner, and A. P. Yu, *J. Amer. Chem. Soc.*, 1964, 86, 3178.
167. G. Allegra and J. W. Bassi, *Atti. Acad. Nat. Lincei Rend., Classe. Sci. fis., Mat. Nat.*, 1962, 33, 72.
168. M. Huber, *Acta. Cryst.*, 1957, 10, 129.
169. J. A. Wunderlich and W. N. Lipscomb, *Tetrahedron*, 1960, 11, 219.
170. E. L. Eliel, M. L. Allinger, S. J. Angyal, and G. A. Morrison, *Conformational Analysis*, Interscience, New York, 1965. Page 210, and references cited there.
171. K. Wiberg, *J. Amer. Chem. Soc.*, 1967, 89, 1070.
172. M. Bixon and S. Lifson, *Tetrahedron*, 1967, 23, 769.
173. J. D. Dunitz and A. Mugnoli, *Chem. Comm.*, 1966, 166. M. Dobler, J. D. Dunitz, and A. Mugnoli, *Helv. Chim. Acta.*, 1966, 49, 2492.
174. F. Groth, *Acta. Chim. Scand.*, 1965, 19, 1497.
175. M. Shiro, T. Sato, H. Koyama, Y. Maki, K. Nakanishi, and S. Uyeo, *Chem. Comm.*, 1966, 97.
176. J. D. Dunitz and V. Prelog, *Angew. Chem.*, 1960, 72, 896. H. C. Mez, *Dissertation*, E. T. H. Zurich, 1961.
177. G. Ferguson, D. D. MacNichol, W. Oberhansli, R. A. Raphael, and J. A. Zabkiewicz, *Chem. Comm.* 1968, 103.
178. H. E. Bellis and E. J. Slowinski, *Spectrochim. Acta.*, 1959, 15, 1102.

179. J. A. Hamilton, A. T. McPhail, and G. A. Sim,  
J. Chem. Soc., 1962, 708.
180. D. Rogers and Mazhar-ul-Haque, Proc. Chem. Soc.,  
1963, 371; Mazhar-ul-Haque, Ph. D. Thesis, Univ.  
London, 1963.
181. R. F. Bryan and J. D. Dunitz, Helv. Chim. Acta.,  
1960, 43, 3.
182. E. Huber-Buser and J. D. Dunitz, Helv. Chim. Acta.,  
1961, 44, 2027.
183. E. Huber-Buser and J. D. Dunitz, Helv. Chim. Acta.,  
1960, 43, 760.
184. I. J. Karle and J. Karle, Acta. Cryst., 1966, 19, 555.
185. T. B. Owen and J. L. Hoard, Acta. Cryst., 1951, 4, 172.
186. J. D. Dunitz and V. Schomaker, J. Chem. Phys.,  
1952, 20, 1703.
187. T. N. Margulis, Acta. Cryst., 1965, 18, 742.
188. S. H. Bauer and J. Y. Beach, J. Amer. Chem. Soc.,  
1942, 64, 1142.
189. W. Shand, V. Schomaker, and J. R. Fisher, J. Amer.  
Chem. Soc., 1944, 66, 636.
190. H. P. Lemaire and R. L. Livingstone, J. Amer. Chem.  
Soc., 1952, 74, 5732.
191. W. N. Lipscomb and V. Schomaker, J. Chem. Phys.,  
1946, 14, 475.
192. J. D. Dunitz, Acta. Cryst., 1949, 2, 1.

193. A. Almennigen, O. Bastiansen and P. N. Skancke,  
Acta. Chim. Scand., 1961, 15, 711
194. G. W. Rathjens Jr., N. K. Freeman, W. D. Gwinn, and  
K. S. Pitzer, J. Amer. Chem. Soc., 1953, 75, 5634.
195. J. B. Hendrickson, J. Amer. Chem. Soc., 1961, 83, 4537.
196. C. A. Coulson and W. E. Moffitt, Phil. Mag., 1949,  
1, 40 (Seventh Series); C. A. Coulson, Valence,  
Oxford University Press, 1963.
197. H. G. Smith and R. E. Rundle, J. Amer. Chem. Soc.,  
1958, 80, 5075.
198. F. S. Matthews and W. N. Lipscomb, J. Phys. Chem.,  
1959, 63, 845.
199. J. S. McKechnie, M. G. Newton, and I. C. Paul,  
J. Amer. Chem. Soc., 1967, 89, 4819.
200. L. Helmholtz and R. Levine, J. Amer. Chem. Soc.,  
1942, 64, 354.
201. N. C. Baenziger, H. L. Haight, R. Alexander, and  
J. R. Doyle, Inorg. Chem., 1966, 5, 1399.
202. J. S. McKechnie and I. C. Paul, Chem. Comm. 1968, 44.
203. F. A. Cotton and J. G. Bergmann, J. Amer. Chem. Soc.,  
1964, 86, 2941.
204. D. Grdenic, Quart. Rev., 1965, 19, 303.
205. S. C. Nyburg and J. Hilton, Acta. Cryst., 1959, 12, 116.
206. M. J. S. Dewar, Bull. Soc. Chim. Fr. 1951, 18, C79.
207. J. Chatt and L. A. Duncanson, J. Chem. Soc., 1953, 2939.

208. J. A. Wunderlich and D. P. Mellor, *Acta. Cryst.*, 1954, 2, 130; Idem, *Ibid.*, 1955, 8, 57.
209. P. R. H. Alderman, P. G. Owston, and J. M. Rowe, *Acta. Cryst.*, 1960, 13, 149.
210. L. Pauling, *The Nature of the Chemical Bond*, Cornell University Press, Ithaca, New York, 1960.
211. N. C. Baenziger, H. L. Haight, and J. R. Doyle, *Inorg. Chem.*, 1964, 3, 1535.
212. N. C. Baenziger, G. F. Richards, and J. R. Doyle, *Inorg. Chem.*, 1964, 3, 1529.
213. M. S. Newman, *J. Chem. Educ.*, 1955, 32, 344.
214. F. Sorm, M. Streibl, J. Pliva, and V. Herout, *Coll. Czech. Chem. Comm.*, 1951, 16, 639; S. K. Ramaswani, and S. C. Bhattacharyya, *Tetrahedron*, 1962, 18, 575; J. M. Greenwood, and J. K. Sutherland, Unpublished.
215. V. Prelog, K. Schenker, and W. Kung, *Helv. Chim. Acta.*, 1953, 36, 471; V. Prelog, K. Schenker, and H. H. Gunthardt, *Ibid.*, 1952 35, 1602. A. Aebi, D.H.R. Barton, and A. S. Lindsay, *J. Chem. Soc.*, 1953, 3124.
216. E. W. Garbisch, S. M. Schildcrout, D. B. Patterson, and C. M. Sprecher, *J. Amer. Chem. Soc.*, 1965, 87, 2932.
217. F. Herzberg, *Infrared and Raman Spectra of Polyatomic Molecules*, D. Van Nostrand Co. Inc., New York, 1945, p. 183.
218. Ref 170, p. 12.

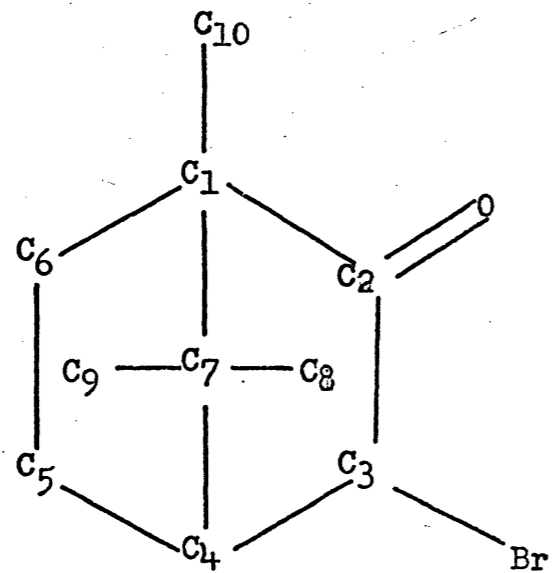
219. D. R. Lide and E.E. Mann, J. Chem. Phys., 1957, 27, 868;  
D. R. Herschbach and L. C. Krisher, Ibid., 1958, 28, 728.
220. V. W. Laurie, J. Chem. Phys., 1961, 34, 1516.
221. R. A. Beaudet, J. Chem. Phys., 1964, 40, 2705.
222. J. D. Swalen and D. R. Herschbach, J. Chem. Phys.,  
1958, 29, 761.
223. M. L. Sage, J. Chem. Phys., 1961, 35, 142.
224. For an interesting review of the anti-histamine drugs  
see : B. Idson, Chem. Rev., 1950, 47, 307.
225. Société des usines chimique Rhône-Poulenc : Brit. Pat.  
716205, 716206, 716269 (1954) - per Chem. Abs. 1956,  
30, columns 1930, 1931.
226. a) Martindales 'Extra Pharmacopoeia', 25th Edition  
(Ed. R. G. Todd), Pharmaceutical Press, London,  
1967, p. 367.
- b) British Pharmacopoeia, General Medical Council,  
Pharmaceutical Press, London 1958, p. 162.
227. See (inter alia) : M. Fink, R. Shaw, G. E. Cross, and  
F. S. Coleman, J. Amer. Med. Ass., 1958, 166, 1846.  
F. J. Ayd Jr., Ibid., 1963, 184, 51.
228. F. Häfliger and W. Schindler, U.S. Pat., 2,554,736 (1951)  
W. Schindler and F. Häfliger, Helv. Chim. Acta.,  
1954, 37, 472.
229. See (inter alia) : H. Azima, Canad. Med. Ass. J.,  
1959, 80, 535; M. Straker, Ibid., 1959, 80, 546;  
J. R. B. Ball and L. G. Kiloh, Brit. Med J., ii/1959, 105

230. Ref. 226 (a), p. 1046.
231. P. R. Leeming and A. L. Ham, Paper given to the Chemical Society Heterocyclic Group, London 1968.  
Idem., J. Med. Chem., Submitted for publication.
232. J. T. Plati and W. Wenner, J. Org. Chem., 1950, 15, 259.
233. Ref. 226 (a), p. 1199; Ref. 226 (b), p. 476.
234. J. T. Plati and W. Wenner, J. Org. Chem., 1955, 20, 1412.
235. R. L. Augustine, 'Catalytic Hydrogenation', Edward Arnold, London, 1965, chapter 4.
236. G. G. Ayerst and K. Schofield, J. Chem. Soc., 1958, 4097.
237. U. W. Arndt and B. T. M. Willis, 'Single Crystal Diffractometry', Cambridge Univ. Press, 1966.
238. R. C. G. Killean, Acta. Cryst., 1967, 23, 54.
239. G. A. Sim, in ref 63, p. 206.
240. P. Coppens, J. Leiserowitz and D. Rabinovich, Acta. Cryst., 1965, 18, 1035.
241. F. R. Ahmed, W. H. Barnes and L. di M. Masironi, Acta. Cryst., 1963, 16, 237.
242. F. R. Ahmed and W. H. Barnes, Acta. Cryst., 1963, 16, 1249.
243. C. Rerat, Acta. Cryst., 1960, 13, 459.
244. See refs. 254, 255, below.
245. F. V. Brutcher, T. Roberts, S. J. Barr, and N. Pearson, J. Amer. Chem. Soc., 1959, 81, 4915.
246. K. S. Pitzer and W. E. Donath, J. Amer. Chem. Soc., 1959, 81, 3213.

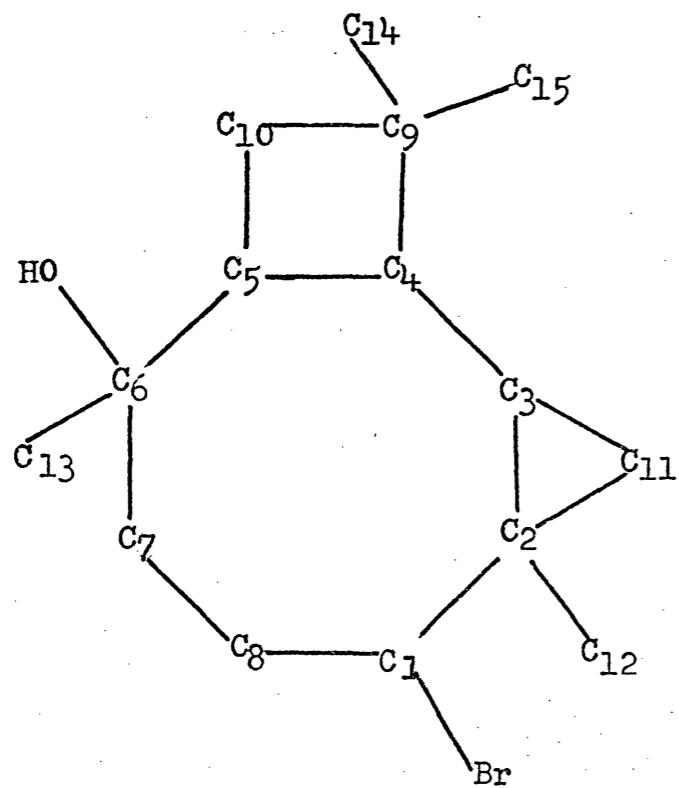
247. J. B. Hendrickson, J. Amer. Chem. Soc., 1961, 83, 4537; Addendum : Idem., Ibid., 1963, 85, 4059.
248. See for example : R. E. Marsh, Acta. Cryst., 1958, 11, 654.
249. B. K. Vainshtein in 'Advances in Structure Research by Diffraction Methods', Vol I, (Ed. R. Brill) Interscience, London, 1964, p. 173.
250. Y. Tomiie, J. Phys. Soc. Jap., 1958, 13, 1030.
251. B. Dawson, Aust. J. Chem., 1965, 18, 595.
252. P. Coppens and C. A. Coulson, Acta. Cryst., 1967, 23, 718.
253. J. A. Ibers, Acta. Cryst., 1961, 14, 853.
254. J. H. Van den Hende and N. R. Nelson, J. Amer. Chem. Soc., 1967, 89, 2901.
255. A. F. Peerdemann, Acta. Cryst., 1956, 2, 824.
256. M. Przybylska, Acta. Cryst., 1963, 16, 871.
257. G. A. Sim, Acta. Cryst., 1955, 8, 833.
258. B. Dawson, Acta. Cryst., 1964, 17, 997.
259. P. R. Leeming, Private Communication.
260. J. S. Rollett, in ref 79, p.25.
261. C. Mooers, 'Zator Tech.Bull.' No. 59, Zator Co., Boston, 1959-cited in ref 262.
262. M. F. Lynch, Endeavour, 1968, XXVII, 68; and additional references cited therein.
263. R. H. Penny, J. Chem. Documentation, 1965, 5, 113.
264. J. S. Rollett, ref. 79, p.14.



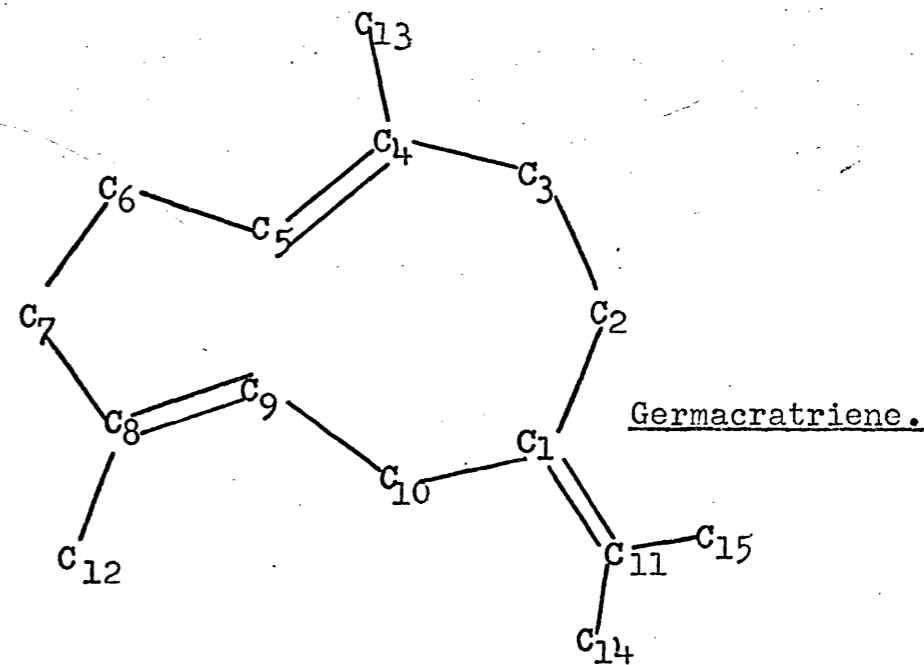
265. J. Blakey, University Mathematics, Blackie, 1966, p.508.
266. Ref. 19, Vol II, p52 et seq.
267. J. D. Kemp and K. S. Pitzer, J. Chem Phys., 1936,4,749.



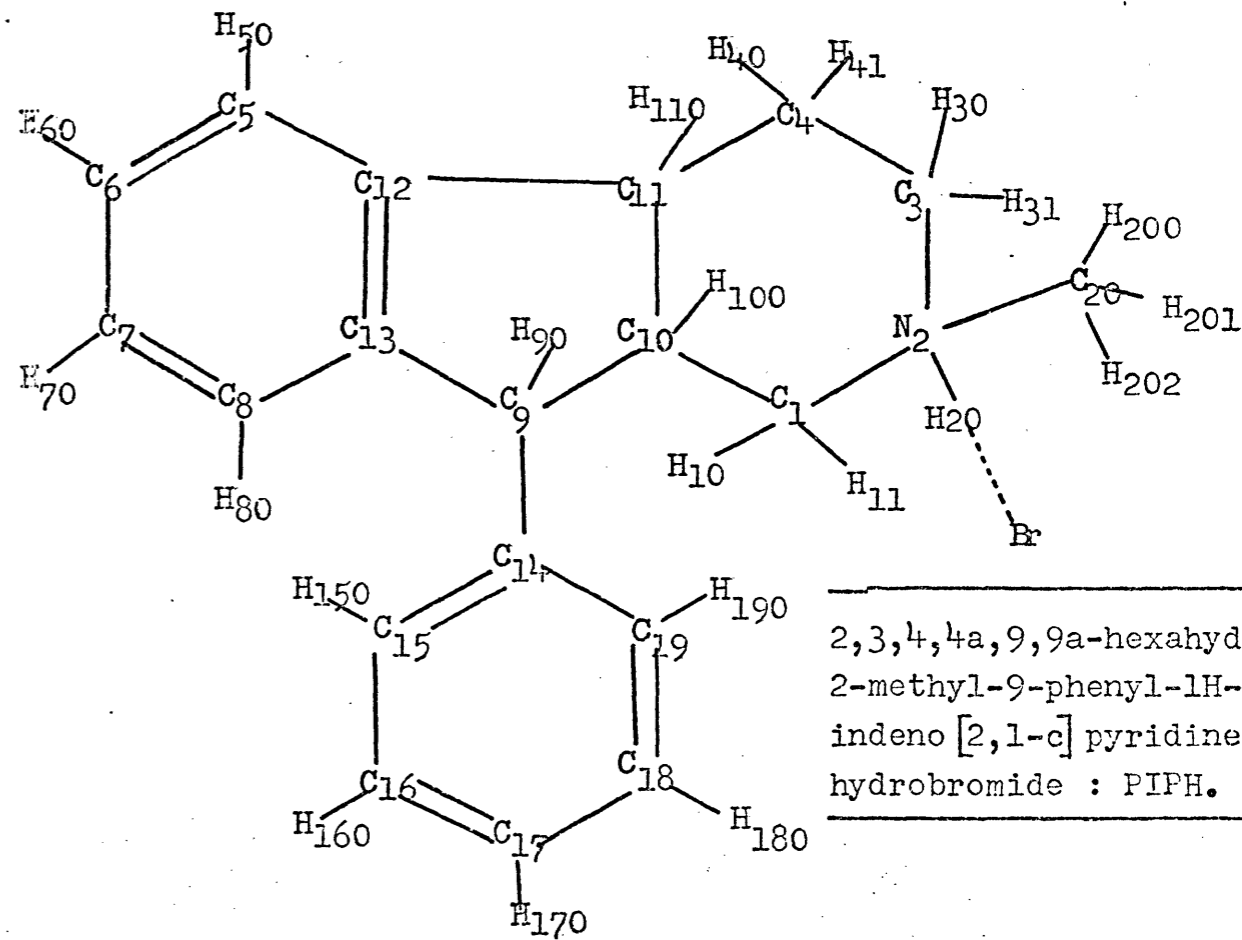
(+)-3-bromocamphor.



Humulene Bromohydrin.



Germacatriene.



2,3,4,4a,9,9a-hexahydro-2-methyl-9-phenyl-1H-indeno[2,1-c]pyridine hydrobromide : PIPH.

**A Reference List of Organic Structures whose Absolute Configurations  
have been determined by X-Ray Fluorescence**

By F. H. ALLEN and D. ROGERS

*(Chemistry Department, Imperial College, London, S.W.7)*

*Reprinted from* CHEMICAL COMMUNICATIONS, 1966,

THE CHEMICAL SOCIETY  
BURLINGTON HOUSE, LONDON, W.1

## A Reference List of Organic Structures whose Absolute Configurations have been determined by X-Ray Fluorescence

By F. H. ALLEN and D. ROGERS

(Chemistry Department, Imperial College, London, S.W.7)

DETERMINATIONS of absolute configurations by Bijvoet's X-ray fluorescence technique<sup>1</sup> are now appearing frequently in the press, but in rather scattered journals. Most are for organic substances, so the following list has been compiled, and groups them under five headings for the convenience of organic chemists. There are 54 entries, more than half of which have appeared in the last three years. They are confined to determinations based on X-ray fluorescence, the fluorescing atom and the radiation being quoted. The list is believed to be comprehensive up to the end of 1965, but we would be grateful if users or crystallographers would advise us of errors or omissions. If the list

is found useful we propose to issue supplements and corrigenda, and an attempt will be made in later lists to include assignments involving internal comparisons with reference centres<sup>2,3</sup> if the latter are quite reliable.

It is gratifying to note that more and more authors are determining the absolute configuration whenever possible, but attention is drawn in an accompanying Communication<sup>4</sup> to the possibility of resurrecting old structure determinations from the literature and getting their absolute configurations with comparatively little effort. We hope the list will indicate to crystallographers areas where reference compounds are still needed.

### (1) Simple Molecules and Amino-Acids.

Compound	Fluorescent atom	Radiation used	Reference
L-Aspartic acid as cobaltous salt	Co	Cu	T. Doyne, R. Pepinsky, and T. Watanabe, <i>Acta Cryst.</i> , 1957, <b>10</b> , 438.
D-(+)-Barium uridine-5'-phosphate	Ba and P	Cu	E. Shefter and K. N. Trueblood, <i>Acta Cryst.</i> , 1965, <b>18</b> , 1067.
Biotin as bis- <i>p</i> -bromoanilide of CO <sub>2</sub> -biotin	Br	Cu	J. Trotter and J. A. Hamilton, <i>Biochemistry</i> , 1966, <b>5</b> , 713.
Hirsutic acid as <i>p</i> -bromophenacyl ester	Br	Cu	F. W. Comer and J. Trotter, <i>J. Chem. Soc. (B)</i> , 1966, 11.
D-Isocitric acid as (1) Rb salt (2) K salt	Rb K	Mo Cr, Cu	A. L. Patterson, C. K. Johnson, D. Van der Helm, and J. A. Minkin, <i>J. Amer. Chem. Soc.</i> , 1962, <b>84</b> , 309.
D(-)-Isoleucine as hydrated hydrobromide	Br	Cu	J. Trommel and J. M. Bijvoet, <i>Acta Cryst.</i> , 1954, <b>7</b> , 703.
L-Lysine as hydrochloride dihydrate	Cl	Cu	S. Raman, <i>Z. Krist.</i> , 1959, <b>111</b> , 301.
D-Methadone as hydrobromide	Br	Cu	A. W. Hanson and F. R. Ahmed, <i>Acta Cryst.</i> , 1958, <b>11</b> , 724.
(+)-Benzylmethylphenylpropylphosphonium bromide	Br	Mo	A. F. Peerdemann, J. P. C. Holst, L. Horner, and H. Winkler, <i>Tetrahedron Letters</i> ; 1965, 811.
(+)-Methylsuccinic acid	See Section 5 under Ergoflavin.		
(-)-Methyl- $\alpha$ -naphthylphenylsilane	Si	Co, Cu	T. Ashida, R. Pepinsky, and Y. Okaya, <i>Acta Cryst.</i> , 1963, <b>16</b> , (supplement), A48, abstract 5.8.
Tartaric acid as (1) Na, Rb salt	Rb	Zr	A. F. Peerdemann, A. J. Van Bommel, and J. M. Bijvoet, <i>Proc., k. ned. Akad. Wetenschap</i> , 1951, <b>B54</b> , 16.
(2) Rb, H salt	Rb	Zr	A. J. Van Bommel, and J. M. Bijvoet, <i>Acta Cryst.</i> , 1958, <b>11</b> , 61.
L-Tyrosine as hydrochloride	Cl	Cu	R. Parasarathy, <i>Acta Cryst.</i> , 1962, <b>15</b> , 41.

Compound	Fluorescent atom	Radiation used	Reference
<b>(2) Terpenoids.</b>			
(+)-3-Bromocamphor	Br	Mo	M. G. Northolt and J. H. Palm, <i>Rec. Trav. chim.</i> , 1966, <b>85</b> , 143.
	Br	Cu	F. H. Allen and D. Rogers, preceding Communication.
(+)-Camphor as oxime hydrobromide	Br	Cu	H. A. J. Oonk, Ph.D. Thesis, Utrecht, 1965.
Cascarillin as deacetylcascarillin acetal iodoacetate	I	Cu	C. E. McEachan, A. T. McPhail, and G. A. Sim, <i>J. Chem. Soc. (B)</i> , 1966, <b>633</b> .
Clerodin as bromolactone	Br	Cu	I. C. Paul, G. A. Sim, T. A. Hamor, and J. M. Robertson, <i>J. Chem. Soc.</i> , 1962, <b>4133</b> .
Davallol as iodoacetate	I	Cu	Yow-Cam Oh and E. N. Maslen, <i>Acta Cryst.</i> , 1966, <b>20</b> , 852.
Enmein as acetyl-bromoacetyl dihydro-compound	Br	Cu	M. Natsume and Y. Iitaka, <i>Acta Cryst.</i> , 1966, <b>20</b> , 197.
Ophiobolin as bromomethoxy-derivative	Br	Cu	S. Nozoc, M. Morisaki, K. Tsuda, Y. Iitaka, S. Tamura, K. Ishibashi, and M. Shirasaka, <i>J. Amer. Chem. Soc.</i> , 1965, <b>87</b> , 4968.
Picrotoxinin as $\alpha_1$ -bromo-compound	Br	Cu	B. M. Craven, <i>Acta Cryst.</i> , 1962, <b>15</b> , 387.
Simarolide as <i>m</i> -iodobenzoate and 4-iodo-3-nitrobenzoate (both needed)	I	Cu	W. A. C. Brown and G. A. Sim, <i>Proc. Chem. Soc.</i> , 1964, 293.
Swietenine as <i>p</i> -iodobenzoate of destigloylswietenine	I	Cu	A. T. McPhail and G. A. Sim, <i>Tetrahedron Letters</i> , 1964, 2599; <i>J. Chem. Soc. (B)</i> , 1966, 318.
Bromoisotenulin	Br	Cu	D. Rogers and Mazhar-ul-Haque, <i>Proc. Chem. Soc.</i> , 1963, 92.
$\alpha$ -Bromoisotutin	Br	Cu	B. M. Craven, <i>Acta Cryst.</i> , 1964, <b>17</b> , 396.
Verrucaric acid as <i>p</i> -iodobenzoate	I	Cu	A. T. McPhail and G. A. Sim, <i>Chem. Comm.</i> , 1965, 350.
<b>(3) Alkaloids.</b>			
Aspidospermine as <i>N</i> (a)-acetyl-7-ethyl-5-desethylaspidospermine <i>N</i> (b)-methiodide	I	Cu	A. Camerman, N. Camerman, and J. Trotter, <i>Acta Cryst.</i> , 1965, <b>19</b> , 314.
(+)-Demethanolaconinone as hydriodide trihydrate	I	Cu	M. Przybylska, <i>Acta Cryst.</i> , 1961, <b>14</b> , 429.
Bulbocapnine as methiodide	I	Cu	T. Ashida, R. Pepinsky, and Y. Okaya, <i>Acta Cryst.</i> , 1963, <b>16</b> , (supplement) A48, abstract 5.8.
Cleavamine as methiodide	I	Cu	N. Camerman and J. Trotter, <i>Acta Cryst.</i> , 1964, <b>17</b> , 384.
Codeine as hydrobromide dihydrate	Br	Cu	G. Kartha, F. R. Ahmed, and W. H. Barnes, <i>Acta Cryst.</i> , 1962, <b>15</b> , 326.
Cucurbitine as perchlorate	Cl	Cu	Hai-Fu Fan and Cheng-Chung Lin, <i>Wu Li Hsueh Pao</i> , 1965, <b>21</b> , 253.
Echitamine as iodide	I	Cu	H. Manohar and S. Ramaseshan, <i>Tetrahedron Letters</i> , 1961, 814.
Ephedrine as hydrochloride	Cl	Cu	G. N. Ramachandran and S. Raman, <i>Current Sci.</i> , 1956, <b>25</b> , 348.
Erythroidine as hydrobromide of dihydro-compound	Br	Cu	A. W. Hanson, <i>Proc. Chem. Soc.</i> , 1963, 52.
Galanthamine as methiodide	I	Cu	D. Rogers and D. J. Williams, <i>Proc. Chem. Soc.</i> , 1964, 357.
Gelsemicine as hydriodide of <i>N</i> -methyl compound	I	Cu	M. Przybylska, <i>Acta Cryst.</i> , 1962, <b>15</b> , 326.
Gliotoxin (also establishes sporidesmin in conjunction with circular dichroism data)	S	Cu	A. F. Beecham, J. Fridrichsons, and A. McL. Mathieson, <i>Tetrahedron Letters</i> , 1966, 3131.

Compound	Fluorescent atom	Radiation used	Reference
(+)-Hetsine as hydrobromide	Br	Cu	M. Przybylska, <i>Acta Cryst.</i> , 1963, <b>16</b> , 871.
Himbacine as hydrobromide	Br	Cu	J. Fridrichsons and A. McL. Mathieson, <i>Acta Cryst.</i> , 1962, <b>15</b> , 119.
Jacobine as bromohydrin	Br	Cu	J. Fridrichsons, A. McL. Mathieson, and D. J. Sutor, <i>Acta Cryst.</i> , 1963, <b>16</b> , 1075.
Leurocristine (vincristine) as methiodide (also establishes vincalkeboblantine)	I	Cu	J. W. Moncrieff and W. N. Lipscomb, <i>J. Amer. Chem. Soc.</i> , 1965, <b>87</b> , 4963.
Lucidusculine as hydriodide	I	Cu	A. Yoshino and Y. Iitaka, <i>Acta Cryst.</i> , 1966, <b>21</b> , 57.
(+)-Des(oxymethylene)lycoctonine as hydriodide monohydrate	I	Cu	M. Przybylska and L. Marion, <i>Canad. J. Chem.</i> , 1959, <b>37</b> , 1843.
Methyl melaleucate iodoacetate	I	Cu	S. R. Hall and E. N. Maslen, <i>Acta Cryst.</i> , 1965, <b>18</b> , 265.
Securine as hydrobromide dihydrate	Br	Cu	S. Imado, M. Shiro, and Z. Horii, <i>Chem. and Ind.</i> , 1964, 1691.
Strychnine as hydrobromide	Br	Cu	A. F. Peerdemann, <i>Acta Cryst.</i> , 1956, <b>9</b> , 824.
Thelepogine as methiodide	I	Cu	J. Fridrichsons and A. McL. Mathieson, <i>Acta Cryst.</i> , 1963, <b>16</b> , 206.
<b>(4) Steroids.</b>			
Lanostane as 3 $\beta$ -acetoxy-7 $\alpha$ ,11 $\alpha$ -dibromolanostane 8 $\alpha$ ,9 $\alpha$ -epoxide	Br	Cu	J. K. Fawcett and J. Trotter, <i>J. Chem. Soc. (B)</i> , 1966, 174.
<b>(5) Miscellaneous large molecules and mould metabolites.</b>			
Duclauxin as monobromo-compound	Br	Cu	Y. Ogihara, Y. Iitaka, and S. Shibata, <i>Tetrahedron Letters</i> , 1965, 1289.
Ergoflavin as tetra- <i>O</i> -methyl di- <i>p</i> -iodobenzoate [also establishes (+)-methylsuccinic acid]	I	Cu	A. T. McPhail, G. A. Sim, J. D. M. Asher, J. M. Robertson, and J. V. Silverton, <i>J. Chem. Soc. (B)</i> , 1966, 18.
Factor VIa, C <sub>46</sub> H <sub>86</sub> O <sub>9</sub> N <sub>11</sub> Co, 11H <sub>2</sub> O	Co	Cu	D. Dale, D. C. Hodgkin, and K. Venkatesan. In: "Crystallography and Crystal Imperfection," (ed. G. N. Ramachandran), Academic Press, London, 1963.
Ferrichrome "A", C <sub>41</sub> H <sub>58</sub> N <sub>9</sub> O <sub>20</sub> Fe, 4H <sub>2</sub> O	Fe	Cu	A. Zalkin, J. D. Forrester, and D. H. Templeton, <i>Science</i> , 1964, <b>146</b> , 261.
Dibromoleucodrin	Br	Cu	R. D. Diamond and D. Rogers, <i>Proc. Chem. Soc.</i> , 1964, 63.

(Received, October 7th, 1966; Com. 759.)

<sup>1</sup> J. M. Bijvoet, *Endeavour*, 1955, **14**, 71.

<sup>2</sup> A. McL. Mathieson, *Acta Cryst.*, 1956, **9**, 317.

<sup>3</sup> R. Hine and D. Rogers, *Chem. and Ind.*, 1956, 1428.

<sup>4</sup> F. H. Allen and D. Rogers, preceding Communication.

**A Reference List of Organic Structures whose Absolute Configurations  
have been determined by X-ray Methods. Part 2**

By F. H. ALLEN, S. NEIDLE, and D. ROGERS\*

*(Chemical Crystallography Laboratory, Imperial College, London, S.W.7)*

*Reprinted from* CHEMICAL COMMUNICATIONS, 1968

**THE CHEMICAL SOCIETY**  
BURLINGTON HOUSE, LONDON, W.1

## A Reference List of Organic Structures whose Absolute Configurations have been determined by X-ray Methods. Part 2

By F. H. ALLEN, S. NEIDLE, and D. ROGERS\*

(Chemical Crystallography Laboratory, Imperial College, London, S.W.7)

Part 1 of this list (F. H. Allen and D. Rogers, *Chem. Comm.*, 1966, 838) contained 54 entries.

This supplement, believed to be complete to the end of 1967, contains 40 new entries.

### 1. Using the Anomalous Dispersion Method

Compound	Fluorescent atom	Radiation used	Reference
(1) <i>Amino-acids</i>			
(+)-2-Benzylglutamic acid as hydrobromide dihydrate	Br	Cu	T. Ashida, Y. Sasada, and M. Kakudo, <i>Bull. Chem. Soc. Japan</i> , 1967, 40, 476.
(+)-2-Methyl-2-isopropylglutaric acid	Rb	Cu	M. R. Cox, H. P. Koch, W. B. Whalley, M. B. Hursthouse, and D. Rogers, <i>Chem. Comm.</i> , 1967, 212.
(+)-2-Methyl-2-isopropylsuccinic acid as Rb salt			
Cucurbitine as perchlorate (erroneously included under alkaloids in the first list)	Cl	Cu	Fan Hai-Fu and Lin Cheng-Chiung, <i>Acta Phys. Sinica</i> , 1965, 21, 253.
(2) <i>Terpenoids</i>			
Ginkgolide A as mono- <i>p</i> -bromobenzoate	Br	Cu	N. Sakabe, S. Takada, and K. Okabe, <i>Chem. Comm.</i> , 1967, 259.
Caryophyllene iodonitrosite	I	Mo	D. M. Hawley, J. S. Roberts, G. Ferguson, and A. L. Porte, <i>Chem. Comm.</i> , 1967, 942.
Pseudoclovene A as mono- <i>p</i> -bromobenzene sulphonate ester	Br	Cu	G. Ferguson, D. M. Hawley, T. F. W. McKillop, J. Martin, W. Parker, and P. Doyle, <i>Chem. Comm.</i> , 1967, 1123.
Laurinterol as acetate (also establishes aplysin)	Br	Mo	A. F. Cameron, G. Ferguson, and J. M. Robertson, <i>Chem. Comm.</i> , 1967, 271.
Desmotroposantonin as 2-bromo-( $\alpha$ )- $\beta$ -compound	Br	Cu	A. T. McPhail, B. Rimmer, J. M. Robertson, and G. A. Sims, <i>J. Chem. Soc. (B)</i> , 1967, 101.
Beyerol as monoethylidene iodoacetate derivative	I	Cu	A. M. O'Connell and E. N. Maslen, <i>Acta Cryst.</i> , 1966, 21, 744.
Caesalpin as <i>p</i> -bromobenzoate	Br	Mo	A. Balmain, K. Bjamer, J. D. Connolly, and G. Ferguson, <i>Tetrahedron Letters</i> , 1967, 5027.
Gibberellic acid as methyl bromogibberellate	Br	Cu	F. McCapra, A. T. McPhail, A. I. Scott, G. A. Sim, and D. W. Young, <i>J. Chem. Soc. (C)</i> , 1966, 1577.



Compound	Fluorescent atom	Radiation used	Reference
(2) <i>Terpenoids—continued</i>			
Taxa-4(16),11-diene-5 $\alpha$ ,9 $\alpha$ ,10 $\beta$ ,13 $\alpha$ -tetraol as dihydro-anhydroisopropylidene derivative	Br	Cu	K. Bjamer, G. Ferguson, and J. M. Robertson, <i>J. Chem. Soc. (B)</i> , 1967, 1272.
(+)-Camphor—see Retusamine below			
(3) <i>Sugar Derivatives</i>			
Aristeromycin as hydrobromide	Br	Cu(?)	T. Kishi, M. Muroi, T. Kusaka, M. Nishikawa, K. Kamiya, and K. Mizuno, <i>Chem. Comm.</i> , 1967, 852.
Showdomycin as isopropylidene- <i>N</i> -methylbisdeoxycycloshowdomycin hydrobromide	Br	Mo(?)	Y. Tsukuda, Y. Nakagawa, H. Kano, T. Sato, M. Shiro, and H. Koyama, <i>Chem. Comm.</i> , 1967, 975.
Formycin as monohydrobromide monohydrate	Br	Cu	G. Koyama, K. Maeda, H. Umezawa, and Y. Iitaka, <i>Tetrahedron Letters</i> , 1966, 597.
$\alpha$ -D-Glucosamine as hydrochloride	Cl	Cu	G. N. Ramachandran, R. Chandrasekaran and K. S. Chandrasekaran, <i>Biochim. Biophys. Acta.</i> , 1967, <b>148</b> , 317.
Ethyl 1-thio- $\alpha$ -D-glucofuranoside	S	Cu	R. Parthasarathy and R. E. Davis, <i>Acta Cryst.</i> , 1967, <b>23</b> , 1049.
(4) <i>Alkaloids</i>			
Tuberostemonine as methobromide dihydrate	Br	Cu	H. Harada, H. Irie, N. Masaki, K. Osaki, and S. Uyeo, <i>Chem. Comm.</i> , 1967, 460.
Quinidine as (-)-1,1'-dimethylferrocene-3-carboxylic acid	Fe	Cu	O. L. Carter, A. T. McPhail, and G. A. Sim, <i>J. Chem. Soc. (A)</i> , 1967, 365.
Buxenine-G as dihydroiodide	I	Cu(?)	R. T. Puckett, G. A. Sim, E. Abushanab, and S. M. Kupchan, <i>Tetrahedron Letters</i> , 1966, 3815.
Corymine as hydrobromide monohydrate	Br	Cu	C. W. L. Bevan, M. B. Patel, A. H. Rees, D. R. Harris, M. L. Marshak, and H. H. Mills, <i>Chem. and Ind.</i> , 1965, 603.
Gliotoxin (also establishes sporidesmin)	S	Cu	J. Fridrichsons and A. McL. Mathieson, <i>Acta Cryst.</i> , 1967, <b>23</b> , 439.
19-Propylthevinol as hydrobromide (also establishes morphine series)	Br	Cu	J. H. Van den Hende and N. R. Nelson, <i>J. Amer. Chem. Soc.</i> , 1967, <b>89</b> , 2901.
Mitomycin A as <i>N</i> - <i>p</i> -bromobenzene-sulphonyl compound	Br,S	Cu	A. Tulinsky and J. H. Van den Hende, <i>J. Amer. Chem. Soc.</i> , 1967, <b>89</b> , 2905.
Haplophytine as dihydrobromide	Br	Cu	I. D. Rae, M. Rosenberger, A. G. Szabo, C. R. Willis, P. Yates, D. E. Zacharias, G. A. Jeffrey, B. Douglas, J. L. Kirkpatrick, and J. A. Weisbach, <i>J. Amer. Chem. Soc.</i> , 1967, <b>89</b> , 3061.
Retusamine as $\alpha'$ -bromo-D-camphor- <i>trans</i> - <i>n</i> -sulphonate monohydrate [also establishes absolute configuration of (+)-camphor]	Br	Cu	J. A. Wunderlich, <i>Acta Cryst.</i> , 1967, <b>23</b> , 846.
(5) <i>Steroids</i>			
Cholestane as 2 $\alpha$ ,3 $\beta$ -dibromo-5 $\alpha$ -compound	Br	Cu	E. Van Heijkoop, H. J. Geise, and C. Romers, <i>Rec. Trav. chim.</i> , 1965, <b>83</b> , 1626.
17 $\alpha$ $\beta$ - <i>p</i> -Bromobenzenesulphonyloxy-17 $\alpha$ -methyl-19-nor-9 $\beta$ ,10 $\alpha$ -D-homoandrost-4-en-3-one	Br,S	Cu	R. T. Puckett, G. A. Sim, A. D. Cross, and J. B. Siddall, <i>J. Chem. Soc. (B)</i> , 1967, 783.
17 $\beta$ -Bromoacetoxy-9 $\beta$ ,10 $\alpha$ -androst-4-en-3-one	Br	Cu	W. E. Oberhänslı and J. M. Robertson, <i>Helv. Chim. Acta</i> , 1967, <b>50</b> , 53.
(6) <i>Miscellaneous large molecules and mould metabolites (antibiotics)</i>			
Erythromycin A as hydriodide dihydrate	I	Cu	D. R. Harris, S. G. McGeachin, and H. H. Mills, <i>Tetrahedron Letters</i> , 1965, 679.
Siccanin as <i>p</i> -bromobenzene sulphonate	Br	Cu	K. Hirai, S. Nozoe, K. Tsuda, Y. Iitaka, K. Ishibashi, and M. Shirasaka, <i>Tetrahedron Letters</i> , 1967, 2177.
Ryridomycin as dihydrobromide	Br	Cu	G. Koyama, Y. Iitaka, K. Maeda, and H. Umezawa, <i>Tetrahedron Letters</i> , 1967, 3587.

## 2. By Internal Comparison with a Reference Centre

<i>Compound</i>	<i>Internal comparison centre</i>	<i>Reference</i>
(+)-S-Methyl-L-cysteine S-oxide	L <sub>6</sub> -Amino-acid	R. Hine and D. Rogers, <i>Chem. and Ind.</i> , 1956, 1428; R. Hine, <i>Acta Cryst.</i> , 1962, 15, 635.
(-)-Menthyl (-)-p-iodobenzenesulphinate	(-)-Menthyl group	E. B. Fleischer, M. Axelrod, M. Green, and K. Mislow, <i>J. Amer. Chem. Soc.</i> , 1964, 86, 3395.
(-)-Iberin as a thiourea (also establishes all naturally derived sulphoxide mustard oils)	(+)-R-Phenylethyl-amine	K. K. Cheung, A. Kjaer, and G. A. Sim, <i>Chem. Comm.</i> , 1965, 100.
Cycloalliin hydrochloride monohydrate	L-Amino acid (from a natural source)	K. J. Palmer and K. S. Leed, <i>Acta Cryst.</i> , 1966, 20, 790.
Monotropein as Rb salt	D-Glucose unit	N. Masaki, M. Hirabayashi, K. Fuji, K. Osaki, and H. Inouye, <i>Tetrahedron Letters</i> , 1967, 2367.

## 3. By External Correlation with a Related Compound

1,2-O-Aminoisopropylidene- $\alpha$ -D-glucopyranose hydriodide	Derived from D-glucose	J. Trotter and J. K. Fawcett, <i>Acta Cryst.</i> , 1966, 21, 366.
Triol Q as p-iodobenzoate	Correlation with rose-nonolactone	G. Ferguson, J. W. B. Fulke, and R. McCrindle, <i>Chem. Comm.</i> , 1966, 691.
Bromoambrosin	Correlation with analogous compound, parthenin	M. T. Emerson, W. Herz, C. N. Caughlan, and R. W. Witters, <i>Tetrahedron Letters</i> , 1966, 6151.

(Received, January 17th, 1968; Com. 064.)